

Mechanisms of Aluminium Toxicity, Tolerance and Amelioration in Wheat

Tim Werhett

B. Agr. Sc. (Hons)

University of Tasmania, Australia

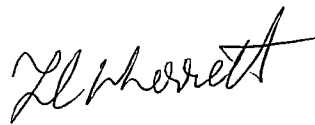
Submitted in fulfilment of the requirements for
the Degree of Doctor of Philosophy

October 2006



DECLARATION

This thesis contains no material that has been accepted for the award of any other degree or diploma in any tertiary institution and to the best of my knowledge contains no material previously published or written by any other person, except where due reference is made in the text of this thesis.

A handwritten signature in black ink, appearing to read 'Tim Wherrett', with a stylized, cursive script.

Tim Wherrett

This Thesis may be made available for loan and limited copying in accordance with the *Copyright Act* 1968.

A handwritten signature in black ink, appearing to read 'Tim Wherrett', with a stylized, cursive script.

Tim Wherrett

University of Tasmania

Hobart, 6th October 2006

Abstract

Acid soil stress, particularly aluminium (Al) toxicity, is one of the biggest constraints to food production worldwide, particularly in tropical developing countries. Despite decades of extensive research both our knowledge of the mechanisms of Al tolerance and toxicity and consequently our management strategies are very limited. The aim of this project was to deepen understanding of the physiology of Al toxicity, tolerance and amelioration, which may later lead to more sustainable management of acid soils. Because many different genes with diverse actions confer Al stress tolerance, significant genotypic variation exists between species and cultivars. This project specifically examines two near isogenic cultivars of wheat (*Triticum aestivum*), ET8 (Al-tolerant) and ES8 (Al-sensitive), that differ at a single genetic locus that confers Al tolerance.

It is generally thought that the mechanism conferring Al tolerance to ET8 is restricted to Al induced malate efflux from the root apex. Consequently the most commonly reported difference between ET8 and ES8 genotypes is root elongation in the presence of Al. Other aspects of root morphology are less studied. In this work, a significant difference in root hair growth was found between Al-exposed ET8 and ES8 varieties. It is suggested that this differential tolerance was either expressed directly at the root hairs or remotely from the root tip via hormone production or retention of malate in the cell wall. The higher tolerance of ET8 root hairs was also reflected in nutrient acquisition; this effect was not attributed to changes in the root hair surface area between cultivars, implying greater tolerance of nutrient acquisition in ET8.

Application of external ameliorants had significant effects on root, shoot and root hair growth. Ca, Mg and silicate all increased root length significantly and there was

no interaction observed with cultivar (ET8 or ES8) suggesting that the mechanism of amelioration is identical in each cultivar and is not associated with enhanced malate efflux. This was further confirmed by measuring Ca^{2+} and K^+ fluxes at the root apex. Ca and Mg both significantly increased root hair surface area in the presence and absence of Al. In comparison, silicate reduced root hair density in ET8 in the presence of Al and completely abolished root hair development in ES8 with or without Al. Amelioration by Mg and Ca appears general to the whole root and is probably associated with reduced membrane binding of Al^{3+} , whereas amelioration by silicate seems to be restricted to the apex.

Examining the Al-induced malate tolerance mechanism more closely, the hypothesis that Al-activated malate and other ionic fluxes would induce changes in the membrane potential (V_m) and that these responses would differ between ET8 and ES8 was examined. Within minutes of exposing wheat roots to 50 μM AlCl_3 , a significant depolarisation was measured in the elongation zone of the ET8 genotype, but not in ES8. Underlying ionic mechanisms that may be responsible for these changes in V_m were investigated by measuring real-time fluxes of Cl^- , H^+ and K^+ at the root apices of wheat seedlings. Addition of 50 μM AlCl_3 to the bathing solution stimulated an increase in K^+ efflux and H^+ influx in ET8 but not in ES8. The differences between the genotypes were sustained for 24 h and were observed only at the elongating zone and not the meristematic zone. After 24 h Al^{3+} increased Cl^- influx in ET8, but inhibited ES8 influx in a dose dependent manner. These results provide the first real time kinetics of K^+ flux kinetics from intact roots showing K^+ efflux to charge balance malate efflux in tolerant, but not sensitive cultivars and that this is maintained even after 24 hours exposure. It is also suggested that Cl^- may play

a significant role in both charge balance and maintenance of cell turgor in longer term tolerance of Al.

Disrupted Ca^{2+} homeostasis has been often suggested as a primary mechanism of aluminium toxicity, with reports showing that Al induces a greater increase in cytosolic Ca^{2+} in ES8 than ET8. It is unknown whether this cultivar difference is a result of Al-malate complexing or a direct difference in ET8 versus ES8 Ca^{2+} signalling in response to Al. In this work, patch-clamp experiments revealed that ET8 and ES8 wheat cultivars differed significantly in slow vacuolar (SV) channel properties. The SV channel density was about 35% lower in ET8 than ES8 and was not altered by 24hr aluminium pre-treatment. Al^{3+} at the vacuolar side reduced the inward (cytosol-directed) current through single open SV channels, suggesting Al^{3+} enters the pore and is permeable. In ET8, but not ES8, stabilisation of the closed states of SV by Al^{3+} was observed. SV channel activity was significantly increased in Al pre-treated vacuoles of ES8 by some unknown low molecular weight compound. Taken together, this data suggests that the observed differences in SV channel properties between ET8 and ES8 may be responsible for some the differences observed in Al disruption of Ca^{2+} homeostasis and may have significant benefits for Al tolerance in ET8.

The precise signalling pathway involved in Al induced elevation of cytoplasmic Ca^{+} remains unknown, with a large number of second messengers and channels from endomembranes and the plasma membrane being suggested. In order to determine a possible signalling pathway underlying Al stress signalling, the capacity of SV channel to mediate vacuolar Ca release and the effect of a number of second messengers on vacuolar Ca^{2+} fluxes were studied in a model system, red beet vacuoles. It was found that at the measured natural intravacuolar activity of K^{+} , Na^{+} ,

Ca^{2+} and Mg^{2+} the SV channel becomes insensitive to intravacuolar Ca^{2+} changes, but still responds to cytosolic Ca^{2+} and Mg^{2+} . Ca^{2+} efflux observed in Ca free solutions was enhanced by exogenous Ca^{2+} and blocked by Zn^{2+} , suggesting that SV mediates the majority of the observed Ca^{2+} efflux. The effect of 26 different combinations of common second messengers and other molecules implied in Al toxicity or Ca^{2+} signalling on Ca^{2+} efflux are reported. In similar experiments using wheat cultivars ET8 and ES8, significantly larger efflux from vacuoles was observed in ES8 confirming the earlier patch observation of higher ES8 SV density and the possible involvement of SV density in Ca^{2+} homeostasis. Higher efflux in ES8 than ET8 was also observed in all second messenger treatments. The importance of SV channel density in Al tolerance was conclusively demonstrated by growth experiments of *Arabidopsis* mutants over and under expressing the SV channel. Mutants under expressing the SV channel (*tpc 1-2*) had a better relative root growth in the presence of Al than wild type (Columbia) and over expressing mutants (TPC1 5-6 and TPC1 10-21).

In its entirety this project raises serious questions about the validity of the assumption that the difference between ET8 and ES8 is simply associated with an Al-induced plasma membrane channel that mediates malate efflux. Rather it is suggested that the Alt1 locus encodes a number of genes associated with a more complex suite of tolerance mechanisms. Furthermore this thesis provides significant new knowledge of the physiological mechanisms by which ET8 and ES8 differ in Al tolerance, malate and K^{+} release and Ca^{2+} homeostasis.

Publications from this thesis

Journal Articles

Wherrett T, Shabala S, Pottosin I (2005) Different properties of SV channels in root vacuoles from near isogenic Al-tolerant and Al-sensitive wheat cultivars *FEBS Letters* **579**(30):6890-689

Wherrett T, Ryan PR, Delhaize E and Shabala S (2005) Effect of aluminium on membrane potential and ion fluxes at the apices of wheat roots *Functional Plant Biology* **32**(3):199-208

Conference Presentations

Wherrett T, Pottosin I and Shabala S Wheat cultivars differ in SV channel properties and response to aluminium – Alt-1 locus codes for more than just plasma membrane malate channel, Combio 2004, the 44th annual meeting of the Australian Society of Plant Scientists Inc. in Perth, Western Australia, 26th-30th Sept 2004

Wherrett T, Ryan P, Delhaize E and Shabala S Effect of aluminium on membrane potential and ion fluxes at the apices of wheat roots of contrasting aluminium tolerance, Combio 2004, the 44th annual meeting of the Australian Society of Plant Scientists Inc. in Perth, Western Australia, 26th-30th Sept 2004

Acknowledgements

During the course of this project I was supported by the Cuthbertson Research Scholarship. Many thanks to the Cuthbertson family who continue to personally support the development of research students in Agriculture, Forestry and Fisheries.

Many people have been significant in me reaching this final point of submitting a doctoral thesis, my thanks and appreciation is deep to all.

I must particularly mention:

Dr Sergey Shabala for excellent supervision, passion for research, ongoing support of project running costs and travel and allowing me the freedom to travel and take time off as needed.

Professor Igor Potossin for extensive help and input into patch clamp experimentation and analysis and particularly for the many wonderful days travelling in Mexico taking photos, eating great food and drinking good beer and ponche. Los portales is definitely the best restaurant in the world!

Dr Peter Ryan and Dr Steve Wilson for their supervision and advice when necessary.

Professor Jesus Muniz for generously accommodating us in Comala, Mexico.

Dr Yuda Hariadi for all the laughs and practical jokes, wouldn't have made it without you. To the rest of the lab and office for all the good times talking, eating etc.

To the countless friends and who encouraged me to persevere and not quit when it got so boring!!!

But more than anyone, thanks to my beautiful wife Emma who had to put up with my complaints and procrastination for too many years without wavering in her love.

Table of Contents

<i>List of Figures</i>	15
<i>List of Tables</i>	18
<i>Introduction</i>	19
Chapter 1: Literature Review	22
1.1 Soil acidity and aluminium toxicity	22
1.2 Mechanisms of toxicity	23
1.2.1 <i>Symptoms and region of toxicity</i>	24
1.2.2 <i>Possible extracellular targets</i>	26
1.2.3 <i>Possible intracellular targets</i>	33
1.3 Mechanisms of tolerance	45
1.3.1 <i>Cell wall properties</i>	45
1.3.2 <i>Alterations in rhizosphere pH</i>	46
1.3.3 <i>Antioxidants</i>	47
1.3.4 <i>Phosphorus exudation</i>	47
1.3.5 <i>Root Cap</i>	48
1.3.6 <i>Vacuolar Sequestering</i>	49
1.3.7 <i>Organic acids</i>	50
1.3.8 <i>Unidentified mechanisms</i>	52
1.4 ET8 and ES8	53
1.4.1 <i>Genetics</i>	54
1.4.2 <i>Characteristics of the plasma membrane malate channel</i>	55
1.4.3 <i>Malate exudation as a tolerance mechanism in ET8</i>	56
1.4.4 <i>Ca²⁺ homeostasis in response to Al in ET8 and ES8</i>	58
1.5 Amelioration of Al toxicity	61

1.5.1	<i>Lime</i>	61
1.5.2	<i>Cation amelioration</i>	62
1.5.3	<i>Silicon</i>	62
1.5.4	<i>Organic materials</i>	64
1.6	Conclusions	65
 Chapter 2: General Materials and Methods		66
2.1	Experimental Solutions	66
2.2	Plant materials	67
2.3	Isolation of protoplasts from wheat	67
2.4	Vacuole Immobilisation	68
2.5	Microelectrode Ion Flux Estimation (MIFE™)	68
2.5.1	<i>Background theory</i>	68
2.5.2	<i>MIFE setup</i>	71
2.5.3	<i>Microelectrode fabrication</i>	74
2.5.4	<i>Microelectrode calibration and characteristics</i>	76
2.6	Patch Clamp	77
2.6.1	<i>The gigohm seal</i>	78
2.6.2	<i>Patch configurations</i>	79
2.6.3	<i>Junction potentials and pipette offset</i>	81
2.6.4	<i>Capacitance and series resistance</i>	81
2.6.5	<i>Data acquisition</i>	82
2.6.6	<i>Data analysis</i>	83
 Chapter 3: Morphological responses to Al³⁺ and amelioration by Ca²⁺, Mg²⁺ and silicate		85

3.1	Introduction	85
3.2	Materials and methods	87
3.2.1	<i>Morphological changes of ET8 and ES8 with exposure to Al from germination and amelioration by Ca, Mg and silicate.....</i>	87
3.2.2	<i>Malate measurement.....</i>	88
3.2.3	<i>Effect of low silicate levels on growth and fluxes from the elongation zone in ES8</i>	89
3.2.4	<i>Root hair morphology and nutrient acquisition after 24 hr exposure to Al</i>	89
3.3	Results.....	90
3.3.1	<i>Effects of Al exposure, cultivar and amelioration by Ca^{2+}, Mg^{2+} and silicate on wheat root and shoot characteristics</i>	90
3.3.2	<i>Effects of Al exposure, cultivar and amelioration by Ca^{2+}, Mg^{2+} and silicate on root hair morphology.....</i>	99
3.3.3	<i>Effects of 24 hr Al exposure on root hair morphology and fluxes from the root hair zone in ET8 and ES8</i>	107
3.4	Discussion	110
3.4.1	<i>Effects of Al exposure, cultivar and amelioration by Ca^{2+}, Mg^{2+} and silicate on wheat root and shoot characteristics</i>	110
3.4.2	<i>Amelioration by Ca^{2+}, Mg^{2+} and silicate.....</i>	111
3.4.3	<i>Interaction of Al and cultivar on wheat root hair development</i>	113
 Chapter 4: Effect of Al^{3+} on membrane potential and ion fluxes at the root apex		
4.1	Introduction	116
4.2	Materials and Methods.....	118

4.2.1	<i>Plant materials.....</i>	118
4.2.2	<i>Spatial distribution of malate efflux in ET8.....</i>	119
4.2.3	<i>Effects of Al on membrane potential.....</i>	119
4.2.4	<i>Non-invasive ion flux measurements</i>	120
4.2.5	<i>Short-term effects of Al on ion fluxes.....</i>	120
4.2.6	<i>Long-term effects of Al on ion fluxes</i>	121
4.2.7	<i>Effect of exogenous malate on K⁺ fluxes</i>	121
4.3	Results	122
4.3.1	<i>Effect of Al on root growth and malate efflux.....</i>	122
4.3.2	<i>Effect of Al on root-cell V_m.....</i>	124
4.3.3	<i>Effect of Al on net ion fluxes.....</i>	126
4.3.4	<i>Effect of exogenous malate on K⁺ fluxes</i>	132
4.4	Discussion	132
4.4.1	<i>Membrane potential and malate efflux.....</i>	132
4.4.2	<i>Al effects on root fluxes.....</i>	134
 Chapter 5: Effect of Al³⁺ on slow vacuolar channels and their involvement in Al induced [Ca²⁺]_{cyt} elevation		
5.1	Introduction	139
5.2	Materials and Methods.....	140
5.2.1	<i>Plant material and isolation of vacuoles</i>	140
5.2.2	<i>Experimental solutions</i>	141
5.2.3	<i>Patch-clamp protocols and analyses</i>	141
5.3	Results.....	142
5.3.1	<i>Direct effects of Al on SV channels in ET8 and ES8</i>	142
5.3.2	<i>Long-term effects of Al on SV channel in ET8 and ES8</i>	147

5.4	Discussion	149
5.4.1	<i>Genetics of ET8 and ES8</i>	<i>149</i>
5.4.2	<i>SV channel properties in ET8 and ES8</i>	<i>149</i>
5.4.3	<i>SV channels, Ca²⁺ signalling and Al tolerance</i>	<i>150</i>
5.4.4	<i>Possible signalling pathway</i>	<i>153</i>
5.4.5	<i>Impact of SV channel properties on Al tolerance.....</i>	<i>153</i>
Chapter 6:	Second messengers and Ca²⁺ signalling in Al toxicity and tolerance	156
6.1	Introduction	156
6.2	Materials and Methods.....	158
6.2.1	<i>Plant material and vacuole isolation.....</i>	<i>158</i>
6.2.2	<i>Intravacuolar ion activities and concentration</i>	<i>159</i>
6.2.3	<i>Vacuolar Ca fluxes</i>	<i>162</i>
6.2.4	<i>Patch clamp</i>	<i>164</i>
6.2.5	<i>Arabidopsis morphology.....</i>	<i>165</i>
6.3	Results.....	167
6.3.1	<i>Intravacuolar ionic composition.....</i>	<i>167</i>
6.3.2	<i>SV activity under native vacuolar ion activities</i>	<i>169</i>
6.3.3	<i>Ca²⁺ currents in red beet vacuoles</i>	<i>172</i>
6.3.4	<i>Ca²⁺ currents in ET8 and ES8 wheat vacuoles</i>	<i>178</i>
6.3.5	<i>Effects of second messengers on red beet SV activity.....</i>	<i>179</i>
6.3.6	<i>Growth experiments of Arabidopsis mutants.....</i>	<i>180</i>
6.4	Discussion	183
6.4.1	<i>Capacity of SV to mediate Ca²⁺ flux at physiological potentials</i>	<i>183</i>
6.4.2	<i>Screening elicitors of vacuolar Ca²⁺ flux with red beet vacuoles</i>	<i>184</i>

6.4.3	<i>Vacuolar Ca^{2+} fluxes in ET8 and ES8</i>	187
6.4.4	<i>SV channel density affects tolerance to Al</i>	188
Chapter 7: General Discussion		189
References		195
Appendix 1: Solutions for Protoplast isolation		236
Appendix 2: Correction of intravacuolar ion activities for liquid junction potential and V_m		237
Appendix 3: Calculations to correct for individual vacuole size		238

List of Figures

Figure 1.1. A model for Al^{3+} activated malate efflux from wheat roots	57
Figure 1.2. A model for Al^{3+} induced $[\text{Ca}^{2+}]_{\text{cyt}}$ elevation..	60
Figure 2.1. Microelectrode Ion Flux Estimation (MIFE™) - basic principles.....	70
Figure 2.2. MIFE setup for measuring root fluxes.	72
Figure 2.3. MIFE setup for measuring vacuoles on the right hand side. Patch clamp setup on the left hand side..	73
Figure 2.4. Patch clamp configurations.	79
Figure 3.1. Effect of Al and amelioration by low concentrations of silicate from germination on root and shoot growth in ES8.....	97
Figure 3.2. Effect of Al and amelioration by low concentrations of silicate from germination on Ca^{2+} and K^{+} fluxes from the elongation zone in ES8.....	98
Figure 3.3. Root hair length and density measured in the mature root hair zone following a 24 h treatment with different Al^{3+} concentrations.....	108
Figure 3.4. Net ion fluxes measured mature root hair zone following a 24 h treatment with different Al^{3+} concentrations.	109
Figure 4.1. Effect of Al^{3+} on root growth of ET8 and ES8 wheat lines.	122
Figure 4.2. Spatial distribution of malate efflux from the terminal 3.0mm of ET8 apices in response to addition of $50\mu\text{M}$ Al^{3+}	123
Figure 4.3. Average response of V_m to Al measured at the elongation zone in ET8 and ES8.....	125
Figure 4.4. Transient response of ion fluxes to Al measured at the elongation zone	128

Figure 4.5. Transient responses of ion fluxes to Al measured at the root meristem.	129
Figure 4.6. Net ion fluxes measured at the elongation zone following a 24 h treatment with different Al^{3+} concentrations.	130
Figure 4.7. Net ion fluxes measured at the root meristem following a 24 h treatment with different Al^{3+} concentrations.	131
Figure 5.1. Effect of Al on the activation of SV currents.....	143
Figure 5.2. Modulation of the SV channel voltage dependence by vacuolar Al^{3+} in ET8 and ES8.	144
Figure 5.3. Effect of Al^{3+} on deactivation kinetics of SV currents.....	145
Figure 5.4 Effect of Al^{3+} on single channel I/V curve from ES8	146
Figure 5.5 Long term (24 h) effects of 14 μM free Al^{3+} on SV channels in ET8 and ES8 plants.	148
Figure 6.1. Red beet vacuolar Ca^{2+} fluxes in response to changing bath Ca^{2+} concentration.	168
Figure 6.2. Effect of vacuolar Na^{+} on the SV channel voltage dependence at 0 μM CaCl_2 and 500 μM CaCl_2	170
Figure 6.3. Modulation of the SV channel voltage dependence by cytosolic Ca^{2+} and Mg^{2+} in vacuole attached and outside out configurations.	171
Figure 6.4. Ca^{2+} efflux induced by low bath Ca^{2+} concentrations and calmodulin (CaM) in red beet vacuoles.....	174
Figure 6.5. Ca^{2+} efflux induced by bath Mg^{2+} in red beet vacuoles.	174

Figure 6.6. Ca^{2+} efflux induced by bath cAMP alone and in combination with calmodulin (CaM) and ATP in red beet vacuoles.	175
Figure 6.7. Ca^{2+} efflux induced by bath ABA alone and in combination with inositol triphosphate (IP_3) in red beet vacuoles.	176
Figure 6.8. Ca^{2+} efflux induced by bath ATP alone and in combination with calmodulin (CaM) in red beet vacuoles.....	177
Figure 6.9. Ca^{2+} efflux in ET8 and ES8 induced by bath ABA, IP_3 and cAMP.	178
Figure 6.10. Representative traces of large outside out vacuole showing inhibition of SV currents and increase of leak by 1 mM H_2O_2	179
Figure 6.11. Effect of Al on root length in <i>Arabidopsis</i> wildtype Columbia (Col-0) and TPC-1 under expressor (<i>tpc 1-2</i>) and over expressors (TPC1 5-6 and TPC1 10-21).....	181
Figure 7.1. Proposed model of response of ET8 and ES8 apical root cells to Al exposure.....	192

List of Tables

Table 2.1. Commercially available liquid ionophores (LIX) and the appropriate backfilling solutions used for preparation of ion selective microelectrodes.	76
Table 3.1. Effect of Al exposure and amelioration on root length in wheat.....	91
Table 3.2. Effect of Al exposure and cultivar on shoot length in wheat.	92
Table 3.3. Effect of ameliorant on shoot length in wheat.....	92
Table 3.4. Effect of ameliorant and cultivar on root to shoot ratio in wheat.....	93
Table 3.5. Effect of Al exposure, amelioration and cultivar on root diameter at the meristem, elongation zone and mature zone in wheat.....	95
Table 3.6. Effect of Al exposure, amelioration and cultivar on root hair length in wheat.....	100
Table 3.7. Effect of ameliorant on root hair diameter in wheat.....	101
Table 3.8. Effect of Al exposure and amelioration on root hair density in wheat.....	102
Table 3.9. Effect of ameliorant and cultivar on root hair density in wheat.	103
Table 3.10. Effect of ameliorant on length of the root hair zone in wheat.....	104
Table 3.11. Effect of Al exposure, amelioration and cultivar on total root hair surface area in wheat.	106
Table 6.1. Effect of various compounds on Ca^{2+} flux from SV vacuoles.	173

Introduction

Soil acidity is one of the biggest problems limiting food production world wide. It is estimated that 30% of the world's soils are acidic (von Uexkull and Mutert, 1995). Of the soils currently used for food production a large proportion are acidic and a further 40% of potentially arable lands are acidic (Kochian, 1995). In the tropics approximately 75% of soils are acidic and in many soils crop plants cannot be grown because the pH is too low. In Australia alone, 33 million hectares of agricultural land are highly acidic and a further 55 million hectares are at risk (CSIRO, 2004). Soil acidity has been identified as the most serious land degradation issue for Australia with an estimated \$1 billion in lost production every year (CSIRO, 2004).

Current technology to manage acid soils is essentially limited to soil liming and plant breeding. Application of lime is effective in elevating the pH in the topsoil however it is of limited use in treating subsoil acidity. Liming is also very expensive and machinery intensive, so it is of limited use in addressing soil acidity in most developing countries. Alternate methods of soil amelioration must be discovered. Ca^{2+} , Mg^{2+} and silicon have all been shown to ameliorate acid soil toxicity, further work to understand the basic physiological basis and to enhance management is necessary.

A lot of natural variation in plant tolerance to soil acidity exists. Even in the most acidic soils there are many species (mostly non-crop) that are able to grow successfully. Therefore there is some scope to breed or engineer plants with higher tolerance to acid soils. However for long term sustainable management of agriculture on acid soils more sustainable management practises must be found. Despite decades of research into the mechanisms of plant toxicity, tolerance and amelioration in acid soils, our understanding remains quite limited. The greatest advances in our

understanding of plant physiology in acid soils have come in the last few years in a relatively restricted number of plant species. In order to sustainably manage acid soils it is essential to gain a greater understanding of the underlying physiological mechanisms.

This thesis approaches the problem of acid soils, particularly Al toxicity, by examining the physiology of two near isogenic cultivars of wheat that differ in Al tolerance at a single genetic locus (ET8 – Al tolerant; ES8 – Al sensitive). The first chapter summarises and presents the current literature addressing Al toxicity, tolerance and amelioration and provides a detailed examination of the mechanisms thought to be operating in ET8 and ES8. Chapter 2 outlines the major experimental techniques employed. The experimental chapters follow a progression of increasing detail of the physiological response to Al before finally returning to morphological experiments utilising *Arabidopsis* mutants. The first experimental chapter (chapter 3) examines the morphological differences between ET8 and ES8 and the effects of ameliorants on morphology. A brief examination of the basis of root hair tolerance is included before subsequent chapters focus predominantly on the physiology of tolerance at the root tip. Chapter 4 examines the physiological mechanisms of Al induced malate release from the root apices. Chapters 6 and 7 examine the differences in Al induced alterations in Ca^{2+} homeostasis between ET8 and ES8 and their relationship to toxicity and tolerance.

The specific aims of this study were:

- To clarify the mechanisms involved in Al induced malate release from ET8. Particularly the effect of Al on membrane potential and ion fluxes associated with malate release. It aimed to establish the ions most likely to be responsible for charge balance, which enables sustained malate efflux.

Introduction

- To examine morphological differences between ET8 and ES8. Particularly the differences in morphology that can be observed when elongation rate is equally inhibited. A specific interest was also taken in possible
- To study the amelioration of Al by Ca^{2+} , Mg^{2+} and SiO_4^- .
- To examine the physiological differences between ET8 and ES8 which that lead to the Al induced differences observed in Ca^{2+} homeostasis. Specifically to identify: the source of Ca^{2+} , transporters and second messengers involved in $[\text{Ca}^{2+}]_{\text{cyt}}$ elevation after Al exposure.

Over all this study aimed to extend our understanding of the physiology of Al toxicity, tolerance and amelioration in the hope that this information can be used to improve the sustainable management of acid soils.

Chapter 1: Literature Review

1.1 Soil acidity and aluminium toxicity

Soil acidification is a natural process in soils whereby soil water causes leaching of basic cations, which are replaced by H^+ ions. Consequently soils in high rainfall areas and older soils exhibit greater acidity. A number of other processes also contribute to soil acidification including nitrogen fixation by legumes (Bolan *et al.*, 1991; Coventry and Slattery, 1991; Dolling, 1995; Shen *et al.*, 2004b); use of ammonia and amide containing fertilisers (Moody and Aitken, 1997; Zoysa *et al.*, 1998; Tang *et al.*, 2000); imbalances in nitrogen, carbon and carbon cycles (Ridley *et al.*, 1990; Goulding *et al.*, 1998; Mannion, 1998); atmospheric acidification (Schuurkes, 1986; Alcamo and Bartnicki, 1988; Galloway, 1989) and excess plant cation uptake (Shen *et al.*, 2004b).

The major constraints to plant growth in acid soils are H^+ , Al^{3+} and Mn^{2+} toxicity and Ca^{2+} , Mg^{2+} , K^+ , phosphorus and molybdenum deficiency (Marschner, 1991). The relative importance of each constraint is dependent upon the plant species, genotype and soil involved, though generally aluminium toxicity is considered to be the most significant of these constraints.

Aluminium (Al) is one of the most abundant elements in the earth's crust however it is mostly incorporated in insoluble aluminosilicates and oxides. As the pH decreases below 5, Al becomes increasingly soluble. The toxicity of various Al species remains somewhat unclear due to its highly complex speciation even in the most basic solutions (Kinraide, 1991). Al^{3+} and polynuclear hydroxy-Al complexes (such as Al_{13} , $AlO_4Al_{12}(OH)_{24}(H_2O)_{12}^{7+}$) and Al-fluoride complexes have been clearly demonstrated as rhizotoxic, whilst Al-sulphate, Al-hydroxide, Al-phosphate and Al-organic acid

complexes do not appear to be rhizotoxic (Kinraide, 1991, 1997; Takita *et al.*, 1999; Matsumoto, 2000; Suwalsky *et al.*, 2002). Because of the complex speciation of Al, extreme care must be taken in the preparation of experimental solutions to avoid the formation of insoluble complexes and unexpected species that may be highly toxic (such as Al_{13}). Many experiments published in the literature must be treated with caution because many have not taken appropriate care in selecting or controlling pH, have adjusted pH with strong alkalis or have included other compounds that complex Al. Maximal Al toxicity is often observed at around pH 4.2-4.3 (Kinraide, 1993; Taylor *et al.*, 2000). Al speciation and toxicity is further complicated by the myriad of complexes which Al forms with other compounds in solution. Even the ionic strength of solutions has a large impact on the activity of Al^{3+} and toxicity. The importance of nutrient solutions is reflected in results from tropical grass genus *Brachiaria*, Al stress or low nutrient stress alone doesn't show any difference between species, but under conditions of Al and nutrient stress, similar to that experienced in acid soils, differences were observed between species (Wenzl *et al.*, 2003).

1.2 Mechanisms of toxicity

Despite decades of research, the primary mechanism of Al toxicity remains unclear. Numerous intracellular and extracellular targets have been suggested, but problems associated with determining Al speciation, detecting Al transport across membranes, Al localisation and separating the timing of events have made it very difficult to distinguish cause from effect. The other problem in determining the mechanism of toxicity is that there are a great diversity of experiments with different species, cultivars and experimental conditions that point to a wide variety of toxicities. But there are no unifying experiments with a controlled set of experimental conditions and

a single species and cultivar to analyse the timing and importance of all proposed toxicities. Such an experiment would be very long and exhaustive, but would allow a more objective analysis of Al toxicity for that cultivar and species at least.

1.2.1 Symptoms and region of toxicity

In most plant species Al toxicity is primarily observed in the root system although it does induce stomatal closing and altered gene expression in the shoots, presumably via root to shoot signalling (Sivaguru *et al.*, 2003a). In these plant species Al is localised in the root. Al accumulators, such as tea and buckwheat, are the exception, they actively take up and translocate Al to the leaves where it is sequestered in the vacuoles (Ma *et al.*, 1998; Shen *et al.*, 2002; Watanabe and Osaki, 2002).

The most dramatic and obvious symptom of Al toxicity is inhibition of root growth. Micromolar concentrations of Al have been shown to inhibit cell elongation within minutes of exposure in solution culture (Blamey *et al.*, 2004) which is followed by inhibition of cell division after longer periods. Exposure to low pH alone initially enhances root elongation (Blamey *et al.*, 2004). Experiments by Ryan *et al.* (1993) using split chambers demonstrated that inhibition of root elongation by Al is only observed if exposure occurs in the terminal 3mm of the root tip. Al exposure in the mature root zone doesn't inhibit root growth. Further work in maize has suggested that sensitivity occurs specifically at the distal transition zone (Kollmeier *et al.*, 2000). Yet even within the root apex there is a diverse response, with adjacent cells differing in sensitivity to Al (Ciamporova, 2000).

Because of the focus on root elongation there has been relatively little research on the effect of Al on root hairs and nutrient acquisition. Al also decreases root hair elongation and disrupts basic physiology such as Ca^{2+} homeostasis (Jones *et al.*,

1995). As far as I am aware there have been no studies looking at whether differences in root hair responses are linked to Al tolerance. Al toxicity also reduces shoot growth and induces deficiency in most other nutrients, particularly Mg^{2+} and Ca^{2+} (Cocker *et al.*, 1997; Mariano and Keltjens, 2005). However, it has not been established if these deficiencies are induced because of reduced root elongation and therefore surface area for nutrient uptake, or if Al actually disrupts the uptake or transport mechanisms for these nutrients.

Both intracellular and extracellular targets for Al toxicity have been suggested. Toxicity is highly correlated to Al^{3+} membrane activity at the root membrane surface as calculated by a Gouy-Chapman-Stern model (Ryan *et al.*, 1994) and early inhibition of root elongation is rapidly reversed upon solution change (Lazof and Holland, 1999). This has prompted many to suggest that the primary lesion is extracellular or an intracellular lesion that is signalled by apoplastic Al. WAK1 is a trans plasma membrane cell wall associated receptor kinase whose expression is enhanced by Al and has been suggested as a possible positive signal transducer because higher expression enhances tolerance (Sivaguru *et al.*, 2003a). Numerous experiments have suggested that Al can rapidly cross the plasma membrane, though the majority remains in the cell wall (Vitarello and Haug, 1996; Marienfeld *et al.*, 2000). This has led to the suggestion that the primary lesion may actually arise due to direct intracellular interactions of Al. The difficulty with many of these experiments is that they may not have adequately accounted for the entire cell-bound fraction when estimating transmembrane Al fluxes. In the giant algal cells of *Chara corallina*, where surgical excision of the cell wall and plasma membrane is possible it has been shown that transmembrane fluxes are commonly over estimated and that even after 95% of total Al was desorbed there was still over 20 times more Al in the cell wall than

intracellularly (Rengel and Reid, 1997; Taylor *et al.*, 2000). Despite the over estimate of transmembrane fluxes, very low fluxes are observed almost immediately after Al exposure confirming that intracellular lesions could be involved in early stages of toxicity (Rengel and Reid, 1997; Taylor *et al.*, 2000).

It is somewhat simplistic to only look for one primary lesion, more likely there are a number of toxic effects of Al which occur almost simultaneously. The challenge is determine which early observations following Al exposure are causes and which are effects of Al toxicity. A major problem in determining this is that whilst many hypotheses have been developed from different experiments and plant materials, all hypotheses have not been examined in a single plant species or consistent experimental protocols. The use of tolerant and sensitive cultivars of the same species, are useful to determine what is not important in toxicity if the response is the same in both genotypes. However if the response is different the same problem of distinguishing cause from effect remains and the difference can be either due to differences in toxicity, mechanisms of tolerance, or some unrelated difference. The major extracellular and intracellular toxicities addressed by the literature are discussed.

1.2.2 Possible extracellular targets

Changes in cell wall properties

Almost immediately after introduction to solution culture Al binds very strongly to the cell wall. Experiments in *Chara corallina* with Al radioisotopes showed that over 95% of Al taken up was localised in the cell wall (Rengel and Reid, 1997; Taylor *et al.*, 2000). Changes in cell wall elastic properties, ion concentrations, enzymes,

protein composition have all been observed in response to Al and implicated in toxicity (Ryan *et al.*, 1994; Tabuchi and Matsumoto, 2001; Wehr *et al.*, 2003).

The high valency of Al^{3+} means that it rapidly binds at cation exchange sites in the cell wall and displaces other cations such as Ca^{2+} (Ryan *et al.*, 1994). Decreased cell wall extensibility due to cross binding of pectates has been implied in reduced root elongation (Horst, 1995). Al concentrations that inhibited sensitive (Scout 66), but not resistant (Atlas 66) cultivars of wheat, decreased mechanical extensibility of the cell wall in both cultivars, but were significantly lower in Scout (Tabuchi and Matsumoto, 2001). Al exposure also increased hemicellulose deposition in Scout, but not Atlas. The authors suggest that cell wall thickening and rigidity contributes to the inhibition of wheat roots (Tabuchi and Matsumoto, 2001). However the effect of Al^{3+} must be more specific than solely valency and cell wall binding because different toxicity and effects are observed with lanthanides and other multivalent cations (Ryan *et al.*, 1995a; Kataoka *et al.*, 2002b; Kinraide *et al.*, 2004). Low pH alone increases cell wall extensibility (Ktitorova and Skobeleva, 1999). No studies were found indicating that cell wall extensibility was significantly lower in sensitive compared with tolerant cultivars within a species suggesting that whilst extensibility may influence elongation rate it is not the most important primary mechanism of toxicity and it doesn't explain the cellular disruption observed during Al toxicity.

Maize roots pre-treated with 150mM NaCl for 5 days to increase the pectin content of the cell walls accumulated more Al in their root apices and were more sensitive to Al than control plants (Horst *et al.*, 1999). It has been suggested that such changes in cell wall composition might actually modulate the concentration of Al or other ions at the plasma membrane surface and that this might modulate toxicity (Wehr *et al.*, 2003). However a recent study has suggested that whilst cell wall

composition effects subtle variations on the ion concentrations at the plasma membrane surface, the effect of the cell wall on toxicity is very slight (Kinraide, 2004). In five species (rice, maize, pea wheat and sorghum) no correlation was found between CEC and Al tolerance (Ishikawa *et al.*, 2001). Clearly more experiments are needed to resolve this issue.

Al inhibits pectin hydrolysis which is a key component of cell wall loosening and extension; although no differences have been observed between tolerant and sensitive plants suggesting that this is not the primary mechanism of toxicity (Wehr *et al.*, 2003).

Another early hypothesis was that Al displacement of Ca from the cell wall was the primary mechanism of toxicity. Al causes rapid and significant displacement of Ca^{2+} from the cell wall cation exchange sites and pectates and Al toxicity can be relieved by application of Ca^{2+} (Ryan and Kochian, 1993; Kinraide *et al.*, 1994). It was thought that this caused toxicity by reduced plasma membrane Ca^{2+} concentrations. However later experiments demonstrated that in near isogenic wheat cultivars, sensitive lines were inhibited by low concentrations of Al that did not significantly displace Ca^{2+} from the apoplast (Ryan *et al.*, 1997a) and toxicity is indifferent to the computed membrane-surface Ca^{2+} activity (Gouy-Chapman-Stern model) (Ryan *et al.*, 1994).

Plasma membrane integrity

Direct interaction of Al with the plasma membrane is a more likely site of initial Al perception and signal transduction which leads to toxicity and it has also been suggested as the site of primary toxicity. Al binds directly with the plasma membrane and it has been suggested that Al may directly disrupt the plasma membrane and it may also bind directly with enzyme metal binding sites. Toxicity is strongly

correlated with cell membrane surface Al^{3+} concentrations as calculated by a Gouy-Chapman-Stern model, but only poorly with Al^{3+} activities in the external medium (Kinraide *et al.*, 1992; Ryan *et al.*, 1994).

In barley, maize, pea, wheat, sorghum and rice (though there is some conflict amongst the papers) the plasma membrane was rapidly permeabilised when roots were transferred to Al free solution after short term (1hr) exposure to Al (Ishikawa *et al.*, 2001; Ishikawa *et al.*, 2003). However in soybean, lipid peroxidation was only enhanced after 32 hours of Al exposure and the Fe (III) reducing capacity of Fe deficient plants was enhanced by short term Al treatment, suggesting that membrane disruption is not the primary toxicity (Cakmak and Horst, 1991; Horst *et al.*, 1992).

Directly investigating the binding of Al to plasma membranes, Jones and Kochian (1997) found that Al has variable affinity for phospholipids. The highest affinity is for phosphatidylinositol-4,5-bisphosphate which is part of the signal transduction of IP_3 based Ca^{2+} signalling (Jones and Kochian, 1995; Pina-Chable and Hernandez-Sotomayor, 2001). Significantly Al binding was reduced by citrate, malate and high concentrations of Ca^{2+} ($>1\text{mM}$) which all ameliorate Al toxicity (Jones and Kochian, 1997). Additionally they didn't observe any Al inhibition of metal dependent enzyme activities except for phospholipase A(2) suggesting Al doesn't exert toxicity through interaction with enzymatic catalytic metal binding sites, but may be via interaction with specific membrane lipids (Jones and Kochian, 1997).

Alteration of channel and transporter activity

Al binds strongly with the plasma membrane altering the surface charge and may also interact directly with protein channels and pumps. Aluminium also has the potential to affect the transmembrane potential (V_m) by directly interacting with the membrane to alter its structure and fluidity (Chen *et al.*, 1991), by blocking Ca^{2+} and

K⁺ channels (Ding *et al.*, 1993; Pineros and Tester, 1993; Gassmann and Schroeder, 1994) or by inhibiting the H⁺-ATPase in the plasma membrane (Ahn *et al.*, 2002). Direct binding and alteration of surface or transmembrane charge can significantly alter the activity of channels and pumps.

Although the effect of Al treatment on the V_m of root cells has been measured in a variety of species (Kinraide, 1988; Miyasaka *et al.*, 1989; Lindberg *et al.*, 1991; Olivetti *et al.*, 1995; Sasaki *et al.*, 1995; Lindberg and Strid, 1997; Papernik and Kochian, 1997; Takabatake and Shimmen, 1997; Pavlovkin and Mistrik, 1999) the results from these are not consistent with one another. Changes in both the membrane surface potential and membrane potential will have a significant effect on ion fluxes through alteration in channel open probability (Kinraide, 2001). The involvement of changes in ionic fluxes on membrane potential and vice versa needs to be studied more fully.

Plasma membrane Ca²⁺ flux

A lot of early studies examined the inhibition of Ca²⁺ uptake and its role in toxicity (Horst, 1995). Early studies with ion selective microelectrodes showed that application of Al³⁺ rapidly inhibited Ca²⁺ uptake at the root apex and that this was highly correlated with Al toxicity (Huang *et al.*, 1992; Ryan and Kochian, 1993). It was suggested that Al-Ca interactions were consistent with competitive inhibition by Al and it was suggested that the ability of Ca²⁺ transport systems to resist disruption by Al may be a tolerance mechanism (Huang *et al.*, 1992; Rengel *et al.*, 1995). However the evidence against this hypothesis is overwhelming. Al can inhibit root growth without affecting net Ca influx and addition of ameliorating cations restores root growth, but significantly reduces Ca²⁺ influx (Ryan and Kochian, 1993; Ryan *et al.*, 1994). Similarly in root hairs, inhibition of root hair growth has been observed

without affecting Ca^{2+} flux (Jones *et al.*, 1995). Poor correlation between Al^{3+} and La^{3+} inhibition of Ca^{2+} influx and elongation in *Chara corallina* also suggest that inhibition of Ca^{2+} uptake is not the primary cause of toxicity (Reid *et al.*, 1995). Al actually blocks a voltage gated Ca^{2+} channel equally well in plasmalemma vesicles from both tolerance (Atlas 66) and sensitive (Scout 66) wheat suggesting that the differential sensitivity of Ca^{2+} influx to Al is probably due to a reduction in the apoplastic Al by tolerance mechanisms in the resistant cultivar (Huang *et al.*, 1995; Huang *et al.*, 1996). Furthermore cytosolic calcium ($[\text{Ca}^{2+}]_{\text{cyt}}$) is elevated, rather than decreased, in sensitive compared with tolerant species (Zhang and Rengel, 1999).

Plasma membrane H^{+} -ATPase

Al has been shown to inhibit of H^{+} ATPase in many species (Sasaki *et al.*, 1995; Ahn *et al.*, 2001; Ahn *et al.*, 2002). Ahn *et al.* (2001) reported that in squash roots greatest inhibition of root elongation occurs in the central elongation zone and this inhibition corresponds with H^{+} -ATPase inhibition due to decreased surface negativity. Inhibition of H^{+} -ATPase in purified PM vesicles from the apex of squash roots occurs at the same time inhibition of root growth and *invitro* Al reduces H^{+} -ATPase activity in a dose dependent manner (Ahn *et al.*, 2002). Inhibition of H^{+} -ATPase after long exposure to Al was observed in barley and wheat (sensitive Scout 66 and tolerant Atlas 66) (Sasaki *et al.*, 1995). Vanadate, an inhibitor of H^{+} -ATPase, increased the K^{+} efflux whilst Al^{3+} inhibited the efflux suggesting that Al^{3+} affects multiple membrane proteins (Sasaki *et al.*, 1995). The activity of H^{+} -ATPase is important for pH homeostasis as a very large electrochemical gradient for H^{+} movement into the cytoplasm exists, reduced H^{+} -ATPase activity would be expected to cause acidification of the cytoplasm. At low external pH the pH of the cytoplasm decreases because of increased influx (Plieth *et al.*, 1999). In order to determine whether these

observations are as a result of toxicity or the primary cause, the response of H^+ fluxes and H^+ -ATPase activities to Al in tolerant and sensitive cultivars of the same species should be compared.

K^+ fluxes

At low pH, significant K^+ efflux occurs due to H^+ influx leading to plasmamembrane depolarisation and subsequent efflux via potassium outward rectifying channels (KOR). In most species examined, Al reduces net K^+ efflux (Horst *et al.*, 1992; Olivetti *et al.*, 1995; Sasaki *et al.*, 1995; Ahn *et al.*, 2002). This is caused by a reduction in efflux rather than an increase in uptake (Horst *et al.*, 1992). In patch clamp work Al has been shown to decrease the open probability and change the activation kinetics of a K^+ inward channel in root hairs and guard cells by an internal block (Liu and Luan, 2001). In wheat, Al induced or maintained K^+ efflux has been shown in tolerant, but not sensitive cultivars (Ryan *et al.*, 1995a; Sasaki *et al.*, 1995; Osawa and Matsumoto, 2002). It is proposed that this is related to the tolerance mechanism associated with organic acid efflux rather than a primary mechanism of toxicity.

Hormones

There is little research examining the effect of Al on plant hormones, although very rapid changes in hormone levels have been observed which precede inhibition of root elongation. After 5min of Al exposure levels of cytokinin nucleotides decline by 60-50% whilst the zeatin content increased six times (Massot *et al.*, 2002). The zeatin content increased throughout the measurement period and was eighty times higher after 150 min. The increase in zeatin was followed by production of ethylene which doubled after 15minutes and reached a maximum after 30mins. It is suggested that

ethylene is induced by the rapid increase in cytokinins and together they may contribute to inhibition either directly or indirectly (Massot *et al.*, 2002). Work in maize has suggested that ethylene is not involved in the signalling or tolerance mechanism (Gunse *et al.*, 2000).

Auxin has also been implicated in the signalling or toxic response to Al because exogenous application of indole-3-acetic acid (IAA) to the elongation zone, but not the meristem, significantly alleviated growth inhibition (Kollmeier *et al.*, 2000). Basipetal transport of exogenous IAA was significantly reduced by Al in the sensitive cultivar. It is suggested that auxin transport may mediate the Al signal between the distal transition zone and the elongation zone (Kollmeier *et al.*, 2000), though it could be equally well explained by Al inhibition of auxin signalling causing cessation of root growth.

1.2.3 Possible intracellular targets

Nucleus

It has been suggested that the binding of Al with chromatin in nucleus is responsible for the reduction in cell division, though there is some discrepancy in the data showing distribution of Al in the root tip and importantly in the meristem. In soybean, Kataoka and Nakanishi (2001) report observing trace amounts of Al in the nucleus of cells and in the middle tissue of the roots after just 15 minutes. In *Danthonia linkii*, an Australian perennial grass, Al accumulated in the nuclei of the root meristem after 24 hr exposure to Al (Crawford *et al.*, 1998). Al appeared to co-localise with phosphorus (Crawford *et al.*, 1998). However in wheat, *Microlaena stipoides* and *Vicia faba* and in both short and long term exposure (<24hrs), Al is localised mostly in the epidermal and outer cortical cells (Delhaize *et al.*, 1993a;

Horst, 1995; Crawford *et al.*, 1998; Marienfeld *et al.*, 2000; Ishikawa *et al.*, 2003). Even after 15 days, Al in *Vicia faba* was mostly localised on the root surface and in the cortical cell walls (Mangabeira *et al.*, 1999). It should be noted that in these negative observations above, except for *Microlaena stipoides*, no mention was made about the meristem and there was no indication of intracellular location.

Cytoskeleton

Al induces significant change in the structure and organisation of microtubules and actin microfilaments of the cytoskeleton, however significant differences in the observed effects of Al are reported. The most common observation is that Al causes disintegration and disorganisation of the microtubule cytoskeleton network in sensitive cells which is thought to cause the distinctive swelling of sensitive cells (Blancaflor *et al.*, 1998; Sivaguru *et al.*, 1999). Inhibition of root hairs by low Al concentrations caused tip swelling identical to that of microtubule inhibitors (Jones *et al.*, 1995). In *Arabidopsis* disintegration of cortical microtubules was observed after Al treatment, but not after lanthanum (Sivaguru *et al.*, 2003a)

Maximal sensitivity is observed in the distal transition zone (as for elongation sensitivity) and this area correlates with the maximum uptake and accumulation of Al along the root apex (Sivaguru *et al.*, 1999; Ciamporova, 2002). Studies, even in the same species, differ in the specific regions of cells affected by Al. Most studies in maize suggest maximal disorganisation occurs in the outer cells of the cortex, initially in the first cell layer and then with time affecting deeper layers (Sivaguru *et al.*, 1999). However another study, also in maize, showed that the microtubule disorganisation only occurred in the inner cortical cells of the elongation zone and that in the outer cortical cells and epidermis the orientation of microtubules remained even after chronic symptoms of Al toxicity (Blancaflor *et al.*, 1998). Al pre-treatment

blocked auxin induced reorientation and folding-induced depolymerization of microtubules in outer cortical cells and this Al induced stabilisation coincided with growth inhibition (Blancaflor *et al.*, 1998). Microtubule depolymerisation and membrane depolarisation by Al in *Arabidopsis* are prevented by Ca^{2+} channel blockers, 2-amino-5-phosphopentanoate (a specific antagonist of ionotropic glutamate receptors) and an antagonist of an aluminium gated anion channel (Sivaguru *et al.*, 2003b). Given that Ca^{2+} channel blockers prevent microtubule depolymerisation it seems that an alteration in Ca^{2+} homeostasis is more likely the primary toxicity, with changes in microtubule structure and organisation occurring secondarily. Al can also have severe effects on the cytoskeleton of meristematic cells. Al disturbs the organisation and function of mitotic apparatus, inhibits cells from entering mitosis, affects cell plate development and in the longer term inhibits chromatin condensation (Frantzios *et al.*, 2000, 2001).

ABA

ABA is a very important molecule signalling abiotic stress and most research has been in the area of stomatal control and water stress in leaves (MacRobbie, 1998; Wilkinson and Davies, 2002; Kuhn and Schroeder, 2003; Desikan *et al.*, 2004). However elevated ABA is also one of the early responses to Al (Kasai *et al.*, 1993; Shen *et al.*, 2004a). Exogenous Al and ABA both increased the ATP and PPi dependent H^+ pumping activities in tonoplast enriched membrane vesicles (Kasai *et al.*, 1993). ABA generation may actually form part of a tolerance mechanism because exogenous application of ABA increased the activity of citrate synthase and citrate efflux from soybean roots (Shen *et al.*, 2004a).

In guard cells ABA is responsible for signalling many processes that bear some resemblance to the observations in response to Al. As with Al in roots, ABA induces

an increase $[Ca^{2+}]_{cyt}$, opening of an anion channel, membrane depolarisation and K^{+} efflux (MacRobbie, 1998). This chain of events is activated by increased Ca^{2+} influx through a non selective cation channel and by unidentified channels and mechanisms from internal stores (MacRobbie, 1998). ABA does not activate the plasma membrane DACC (Pineros and Tester, 1997). However identical processes are clearly not happening in response to Al in roots and ABA in guard cells because higher $[Ca^{2+}]_{cyt}$ is observed in Al sensitive plants (Zhang and Rengel, 1999; Rengel and Zhang, 2003), whilst depolarisation, opening of an anion channel and K^{+} efflux are observed only in Al tolerant plants (Olivetti *et al.*, 1995; Ryan *et al.*, 1997b; Zhang *et al.*, 2001).

In guard cells ABA and ROS signalling are closely tied, ROS are actually rate limiting down stream second messengers in ABA signalling (Kwak *et al.*, 2003; Park *et al.*, 2003; Mori *et al.*, 2004). It should be noted that ABA and ROS may elicit different responses depending on the concentration and location, intracellular or extracellular. Therefore results from different experiments may not be directly comparable.

Reactive oxygen species

Reactive oxygen species (ROS) are unwanted by-products of aerobic respiration formed when O_2 is only partially reduced. They can be highly toxic to plant cells or can be utilised as signalling molecules depending on the circumstances (Vranova *et al.*, 2002; Scholz-Starke *et al.*, 2005). ROS production has been identified as an early response to Al (Boscolo *et al.*, 2003; Devi *et al.*, 2003; Kawano *et al.*, 2003; Tamas *et al.*, 2003; Yamamoto *et al.*, 2003; Tamas *et al.*, 2004). Al itself is not a transition metal so cannot catalyse redox reactions, however it is thought to bind to membranes and enhance the radical chain reactions mediated by Fe, thereby enhancing lipid peroxidation in phospholipid liposomes (Oteiza, 1994), soybean roots (Cakmak and

Horst, 1991), rice (Meriga *et al.*, 2004) and cultured tobacco cells (Ono *et al.*, 1995; Yamamoto *et al.*, 1997). In tobacco the production of ROS, respiration inhibition and depletion of ATP correlated well with loss of growth capacity, although this did not occur for 12 hours (Yamamoto *et al.*, 2002). In pea roots, peroxidation of lipids occurred without additional Fe and Al also triggered ROS production, respiration inhibition, and ATP depletion, which correlated with inhibition of root elongation after four hours (Yamamoto *et al.*, 2001; Yamamoto *et al.*, 2002). Simply given the length of time for these responses it seems unlikely that these long term changes are the primary mechanism of Al toxicity and it has been suggested they are significant not in inhibition of root elongation, but rather callose production (Yamamoto *et al.*, 2002).

A number of proposals for rapid ROS production by Al have been made including dysfunction of mitochondria (Yamamoto *et al.*, 2002), formation of a aluminium superoxide semi reduced radical ion (Exley, 2004) and activation of oxidising enzymes (Simonovicova *et al.*, 2004a, b). A couple of reports suggest ROS may have a direct influence on root elongation (Yamamoto *et al.*, 2003; Kobayashi *et al.*, 2004). However, data from maize suggests that oxidative stress does not cause the cessation in root growth because protein oxidation took place after the drop in root growth (Boscolo *et al.*, 2003). In *Arabidopsis* Al exposure induces gene expression, in both the short and longer term, of three genes encoding antioxidant enzymes that are induced by oxidative stress; further suggesting ROS production is significant in long term Al toxicity (Richards *et al.*, 1998).

ROS are capable of regulating activity of some channels and are necessary for polar cell growth as has been shown in root hairs. ROS activate a potassium outward rectifying channel (KORC) and a non selective cation channel (NSCC) in monocots,

dicots, C3 and C4 root hair tips, which conduct K^+ efflux and Ca^{2+} influx respectively (Demidchik *et al.*, 2003b). The importance of free radicals in root hair elongation was clear because quenching root ROS inhibited root elongation (Demidchik *et al.*, 2003b). The ROS essential for root hair elongation are produced by NADPH oxidase, and stimulate hyperpolarisation activated cation channels (HACC) in the root hair tip (Foreman *et al.*, 2003). Application of exogenous ROS to root hairs causes cessation of growth or non polar development, probably because of a breakdown in tip localised production of ROS (Jones *et al.*, 1998a; Foreman *et al.*, 2003). This class of HACCs have also been identified in guard cells (Hamilton *et al.*, 2000; Pei *et al.*, 2000), and root elongation zone epidermal cells (Kiegle *et al.*, 2000; Demidchik *et al.*, 2002; Demidchik *et al.*, 2003b; Foreman *et al.*, 2003). The similarity of polar growth in the elongation zone to the root hair zone (Demidchik *et al.*, 2002; Demidchik *et al.*, 2003b; Foreman *et al.*, 2003), coupled with the observation that Al causes swelling of root epidermal cells (Blancaflor *et al.*, 1998; Sivaguru *et al.*, 1999) suggests that one of the mechanisms of Al toxicity might be to disturb ROS balance and distribution.

Ca^{2+} homeostasis

Disrupted Ca^{2+} homeostasis the primary Al toxicity?

There exists large discrepancy and disagreement on Al effects on Ca^{2+} homeostasis and its involvement in Al toxicity. In many plant species where Al effects on Ca^{2+} homeostasis have been studied a rapid elevation of cytoplasmic Ca^{2+} is observed in response to Al and elevation is higher in sensitive cultivars of the same species (Jones *et al.*, 1998a; Zhang and Rengel, 1999; Ma *et al.*, 2002; Rengel and Zhang, 2003; Bhuja *et al.*, 2004). This has prompted many to postulate that disruption of Ca^{2+} homeostasis may be the primary Al toxicity (Rengel and Zhang, 2003). Cytoplasmic Ca^{2+} activities are tightly controlled in plants because the frequency,

amplitude and location of changes in $[Ca^{2+}]_{cyt}$ are used by plants to transmit a great number of signals into a variety of plant responses (Sanders *et al.*, 2002; Hetherington and Brownlee, 2004; Medvedev, 2005). Disruption of Ca^{2+} homeostasis could lead to very varied and serious disorders because signal encoding may be masked or disrupted. In near isogenic wheat cultivars greater $[Ca^{2+}]_{cyt}$ elevation is observed in sensitive wheat cultivars and this correlates well with inhibition of root growth (Zhang and Rengel, 1999). Correlation of growth inhibition and elevated $[Ca^{2+}]_{cyt}$ is also observed in rye (Navazio *et al.*, 2001). However, some studies have questioned whether $[Ca^{2+}]_{cyt}$ elevation is in fact necessary for toxicity because it has not always correlated with altered $[Ca^{2+}]_{cyt}$ (Jones *et al.*, 1998a; Plieth *et al.*, 1999). A lack of tight correlation between Al exposure, growth inhibition and altered $[Ca^{2+}]_{cyt}$ has been observed in the root hairs of wild type, sensitive and tolerant *Arabidopsis* species suggesting that altered Ca^{2+} homeostasis may not be a required event for Al toxicity (Jones *et al.*, 1998a). Recent work with *Arabidopsis* suggests that it is the maintenance of tip to base $[Ca^{2+}]_{cyt}$ gradient, rather than total $[Ca^{2+}]_{cyt}$, that is essential for tip growth in root hairs (Wymer *et al.*, 1997; Demidchik *et al.*, 2003b; Foreman *et al.*, 2003). Paradoxically Al induced elevation of root hair tip $[Ca^{2+}]_{cyt}$ occurs in sensitive, not tolerant mutants so clearly more work needs to occur to understand how this relates to root hair and root elongation (Jones *et al.*, 1998a). Other experiments have suggested that the elevation of $[Ca^{2+}]_{cyt}$ is actually a tolerance mechanism to low pH and that Al blocks this response and is therefore toxic (Plieth *et al.*, 1999).

The problem with establishing if alteration to Ca^{2+} homeostasis is the primary toxicity is that the temporal and spatial resolution of current techniques in whole roots does not allow rapid enough detection of elevation. Techniques to detect $[Ca^{2+}]_{cyt}$

changes in the time period of seconds rather than minutes are eagerly awaited. Many of the discrepancies observed in Al induced changes in $[Ca^{2+}]_{cyt}$ may be clarified once we are able to measure the time course and spatial changes of $[Ca^{2+}]_{cyt}$ and to decipher their meaning (Falcke, 2004; Sathyanarayanan and Poovaiah, 2004; Plieth, 2005). Data collected from isolated root cells should be treated with caution because there is a great diversity in responses of individual cells in roots.

Extracellular sources of Ca^{2+} for $[Ca^{2+}]_{cyt}$ elevation

Various sources for $[Ca]_{cyt}$ elevation have been postulated, the focus has particularly been on plasma membrane channels, even though an external source for elevated $[Ca^{2+}]_{cyt}$ is questionable because measurements of Ca^{2+} flux all indicate that Ca^{2+} flux is reduced by Al and that this is more severe in sensitive species (Huang *et al.*, 1992; Ryan and Kochian, 1993). The channels that have been implicated include the hyperpolarisation activated cation channel (HACC), depolarisation activated cation channel (DACC), non selective cation channel (NSCC) and a plant glutamate activated cation channel. Both HACC and DACC are inhibited by Al, though the HACCs are more sensitive (87% inhibition of hyperpolarisation-activated channels (Kiegle *et al.*, 2000) compared to 44% in depolarisation-activated (Pineros and Tester, 1995), leading to the suggestion that DACCs are the plasma membrane channels most likely to mediate Ca^{2+} influx (Rengel and Zhang, 2003). The direct effect of Al^{3+} on NSCCs was not found in the literature, but given that a significant proportion of Ca^{2+} uptake in the elongation zone is through NSCC (Demidchik *et al.*, 2002) and Al exposure reduces Ca^{2+} influx (Huang *et al.*, 1992; Ryan and Kochian, 1993) it is reasonable to suggest that Al may block NSCC.

Experiments in *Arabidopsis* have also suggested that Al induced Ca^{2+} signalling may involve a glutamate gated Ca channel, similar to those found in animal cells (Sivaguru *et al.*, 2003b). It is proposed that rapid Al induced efflux of a glutamate like ligand through an anion channel and the binding of this ligand to a glutamate receptor mediates influx of Ca^{2+} (Sivaguru *et al.*, 2003b). The obvious candidates for the 'glutamate like ligand' are organic acids such as malate, citrate and oxalate which are stimulated by Al. Another hypothesis is that because anion channels tend to have low selectivity, glutamate may leak through open channels activating Ca^{2+} permeable channels (Dennison and Spalding, 2000). However Al induced opening of anion channels and higher effluxes of organic acids are observed in tolerant species that exhibit lower increases in $[\text{Ca}^{2+}]_{\text{cyt}}$ (Rengel and Zhang, 2003). In *Arabidopsis* root protoplasts, glutamate activated a channel permeable equally to monovalent cations and partially to divalent cations (Demidchik *et al.*, 2004). Only inward currents, were analysed and these were sensitive to Gd^{3+} and La^{3+} suggesting they will also be sensitive to Al^{3+} , and consequently not involved in $[\text{Ca}^{2+}]_{\text{cyt}}$ elevation.

Intracellular sources of Ca^{2+} for $[\text{Ca}^{2+}]_{\text{cyt}}$ elevation

The other potential source of Ca^{2+} is from intracellular stores, the vacuoles or endoplasmic reticulum (ER). The known intracellular Ca^{2+} channels include, SV, Inositol-1,4,5-trisphosphate (IP_3) gated, cADPR gated and nicotinic acid adenine dinucleotide phosphate (NAADP) gated channels. IP_3 and cADPR gated channels are thought to be present in both the tonoplast and ER (Allen *et al.*, 1995; Muir *et al.*, 1997; Muir and Sanders, 1997; Martinec *et al.*, 2000; Navazio *et al.*, 2001). NAADP gated channels have only been observed in the ER (Navazio *et al.*, 2000).

cADPR channels observed in plants mediate Ca^{2+} release and demonstrate inhibition by ruthenium red, ryanodine activation and high affinity for cADPR similar to animal cells (Allen *et al.*, 1995; Muir and Sanders, 1996; Muir *et al.*, 1997). To my knowledge there is nothing in the literature about the possibility of cADPR channels being involved in the Al response or on the effect of Al on cADPR activity.

IP_3 channels have not been considered by most in Al induced $[\text{Ca}^{2+}]_{\text{cyt}}$ elevation because Al reduces IP_3 concentration through direct binding with IP_3 (Jorge *et al.*, 2001) and also binding with phospholipase C thereby disrupting the phosphoinositide signalling pathway (Jones and Kochian, 1995; Pina-Chable and Hernandez-Sotomayor, 2001). However a recent experiment with *Coffea arabica* L. suspension culture showed that whilst Al does cause a reduction in IP_3 after an extended time it is preceded by a spike in IP_3 and PLC activity after just one minute (Martinez-Estevez *et al.*, 2003). In the same experiment Al increased activities of phosphatidylinositol 4-kinase, phosphatidylinositol phosphate 5-kinase and diacylglycerol kinase (Martinez-Estevez *et al.*, 2003). This raises the possibility of Al having differential effects depending on the period of exposure. In the short term it may cause a transient increase in IP_3 leading to an initial influx of Ca^{2+} into the cytoplasm, which is further increased/sustained by CICR or other signals. There is some evidence to suggest that in plants as for animals IP_3 induced calcium release is dependent on $[\text{Ca}^{2+}]_{\text{cyt}}$. In animal studies concentrations of Ca^{2+} 1.2-4.0 nM alone inhibit the channel by about half maximal, while with IP_3 open probability increases (Mak *et al.*, 2003). Similarly in plants, IP_3 with Ca^{2+} increases open probability (Scanlon *et al.*, 1996; Taylor and Laude, 2002). It is thought in plants that IP_3 promotes Ca^{2+} to bind to a stimulatory site of the protein, whilst an accessory protein, potentially calmodulin, causes Ca^{2+} to bind to an inhibitory site (Taylor and Laude, 2002). Though it has also been noted that

Ca^{2+} increases the affinity of IP_3 binding to the receptor (Scanlon *et al.*, 1996). Physiological concentrations of ATP inhibit IP_3 by displacing it from the receptor (50% displacement at 241 μM) (Scanlon *et al.*, 1996). IP_3 does not stimulate the plasma membrane DACC (Pineros and Tester, 1997).

The phosphoinositol signalling pathway involves the catalysis of phosphatidylinositol by phospholipase C in IP_3 and diacylglycerol (DAG) (Mueller-Roeber and Pical, 2002; Ochocka and Pawelczyk, 2003). Interestingly in tolerant *Coffea Arabica* L. cell suspension cultures phospholipase C specific activity was maintained higher than sensitive lines (Martinez-Estevéz *et al.*, 2003). This may reflect either lower cytoplasmic Al concentrations or decreased sensitivity of phospholipase C and may potentially allow normal Ca^{2+} signalling.

NAADP channels have only recently been described and the effect of Al on them has not been examined. NAADP channels are insensitive to $[\text{Ca}^{2+}]_{\text{cyt}}$ and not inhibited by IP_3 or cADPR blockers (Navazio *et al.*, 2000).

The importance of SV channels in $[\text{Ca}^{2+}]_{\text{cyt}}$ elevation and possibly directly in response to Al has been demonstrated by recent experiments in tobacco suspension cultures and *Arabidopsis*. Elevation of $[\text{Ca}^{2+}]_{\text{cyt}}$ in response to ABA, H_2O_2 and Al was proportional to the expression of the *Arabidopsis* two pore channel gene (AtTPC1) in both species (Kawano *et al.*, 2003; Kawano *et al.*, 2004a; Peiter *et al.*, 2005). The double pore Ca channel encoded by TPC1 has been shown to be electrophysiologically identical to the SV channel (Peiter *et al.*, 2005). The elevation of $[\text{Ca}^{2+}]_{\text{cyt}}$ is reduced by superoxide scavengers and Ca^{2+} chelators suggesting that Al induced superoxide production stimulates the influx of Ca^{2+} (Kawano *et al.*, 2003). Whilst there are significant methodological issues with the Al treatments of Kawano and associates (discussed chapter 4) the involvement of SV in Al induced $[\text{Ca}^{2+}]_{\text{cyt}}$

elevation deserves more research particularly because it is the only channel that is thought to be involved in calcium induced calcium release (CICR) (Pottosin *et al.*, 1997; Bewell *et al.*, 1999; Pei *et al.*, 1999; Carpaneto *et al.*, 2001; Sanders *et al.*, 2002; Pottosin *et al.*, 2004).

The other possible source for alteration of $[Ca^{2+}]_{cyt}$ are active Ca^{2+} transporters that are responsible for pumping cytosolic Ca^{2+} back into the vacuole and ER or across the plasma membrane. Two distinct active Ca^{2+} transporters have been shown in wheat endomembranes from the root tips. One Ca^{2+} -ATPase, found in ER, was inhibited by vanadate and erythrosin B and had a pH optimum less than or equal to 6.8 (Olbe and Sommarin, 1991). The ER transporter share many similar characteristics with a plasma membrane Ca^{2+} -ATPase (Olbe and Sommarin, 1991). The other transporter was a H^+/Ca^{2+} antiport found in the tonoplast, completely inhibited by bafilomycin, activated by oxalate and with a pH optimum of 7.4 (Olbe *et al.*, 1997). A Ca^{2+} -ATPase is also present in the plasma membrane (Olbe and Sommarin, 1991).

Al may also have an effect on Ca^{2+} homeostasis through binding with other molecules involved in Ca response and signal generation such as calmodulin. Al in the cytoplasm was thought to alter the patterns of Ca^{2+} -calmodulin binding, inhibiting fully or partially the activation of calmodulin (Rengel, 1992). However in experiments with physiological concentrations of citrate, calmodulin, IP_3 , ATP, ADP, Al^{3+} and Mg^{2+} , Al bound with citrate and IP_3 , but not with calmodulin, suggesting it is not a primary target for Al toxicity (Jorge *et al.*, 2001).

1.3 Mechanisms of tolerance

Two major strategies are employed by plants to tolerate mineral toxicities, namely exclusion and internal detoxification. Exclusion is the Al tolerance mechanism most commonly observed in crop species and the one mainly considered here. Lower root concentrations of Al are commonly observed in tolerant cultivars (Delhaize *et al.*, 1993a; Samuels *et al.*, 1997; Kollmeier *et al.*, 2000; Ishikawa *et al.*, 2001). In a wide range of wheat cultivars, screening for Al tolerance using hydroponic experiments was well correlated with field trials in acid soils (Baier *et al.*, 1995). However combined physiological and genetic studies are required to actually understand the mechanism of tolerance and how these can be enhanced through management or breeding. A number of different tolerance mechanisms have been proposed and it is likely that in highly tolerant species a number of these and as yet undiscovered mechanisms are operating. Here the major tolerance mechanisms that have been suggested in the literature are discussed.

1.3.1 Cell wall properties

The cation exchange capacity (CEC) of the cell wall has often been implied in root tolerance mechanisms. The actual concentration of apoplastic Al bound in the cell wall is proportional to its CEC (Horst, 1995). Plants with lower CEC sometimes demonstrate higher tolerance to Al. Al tolerance due to low CEC is not mediated by the ability to maintain pectin hydrolysis, rather it seems more likely that it simply influences the actual concentration of Al and other ions (cations increased and anions decreased) at the plasma membrane surface (Wehr *et al.*, 2003). However a recent study has suggested that whilst there are subtle variations in the ion concentrations at the plasma membrane surface, the effect of the cell wall on toxicity is very slight

(Kinraide, 2004). In five species (rice, maize, pea wheat and sorghum) no correlation was found between CEC and Al tolerance (Ishikawa *et al.*, 2001). It seems unlikely that CEC has a large impact on tolerance.

1.3.2 Alterations in rhizosphere pH

A tolerance mechanism via elevated rhizosphere pH has been often suggested although there is a lack of very strong evidence. The effect of rhizosphere pH on Al toxicity is quite interesting. Clearly pH has a strong effect on the speciation of Al and therefore the concentration of various rhizotoxic species, however maximal toxicity is observed at about pH 4.2-4.4. There may be a number of reasons for this observation, at low pH it has been suggested that there is alleviation of Al toxicity because of competition with H^+ ions (Kinraide, 1993; Taylor *et al.*, 2000). Interestingly though, in *Chara corallina* there was no correlation observed between pH and cell wall accumulation of Al^{3+} (Taylor *et al.*, 2000), which is thought to control plasma membrane Al concentration and therefore toxicity. There was observed however maximal plasma membrane transport of Al^{3+} at pH 4.3 (Taylor *et al.*, 2000).

There is conflicting evidence from growth experiments. In Arabidopsis mutant *alr-104* the pH at the root tip was raised by 0.15 pH units compared with control (Degenhardt *et al.*, 1998). In strongly buffered experimental solutions there was no difference in tolerance between *alr-104* and wildtype, and an increase in pH from 4.4 to 4.5 significantly ameliorated growth (Degenhardt *et al.*, 1998). The authors suggest that in this mutant increased rhizosphere pH occurs due to a 2 fold higher influx of H^+ in the tolerant mutant. In wheat there is conflicting data. Miyasaka *et al.* (1989) claim changes in the rhizosphere around tolerant and sensitive wheat cultivars are the same and not affected by Al treatment. Whereas greater rhizosphere alkalisation is

observed in tolerant Atlas 66 than Sensitive Scout 66 wheat cultivars (Pellet *et al.*, 1997).

1.3.3 Antioxidants

In *Arabidopsis* Al exposure induces gene expression of antioxidant enzymes (Richards *et al.*, 1998). Application of exogenous antioxidants to Al tolerant and sensitive tobacco cell lines exposed to Al reduced production of ROS, inhibition of growth and depletion of ATP (Yamamoto *et al.*, 2002). Over expression of glutathione S-transferase and peroxidase genes conferred enhanced tolerance (Ezaki *et al.*, 2001). In tolerant and sensitive wheat cultivars Al induced ROS and antioxidant enzymes, of which catalase and glutathione-S-transferase were significantly higher in the tolerant cultivar (Darko *et al.*, 2004). In a tolerant tobacco cell line, citrate and manganese superoxide dismutase were not responsible for tolerance, however antioxidants ascorbate and glutathione levels were significantly higher, and maintained during Al exposure in the tolerant cell line (Devi *et al.*, 2003).

1.3.4 Phosphorus exudation

Phosphate exudation has the capacity to be involved in tolerance mechanisms as phosphate in solution will strongly bind Al. In wheat, tolerant cultivar Atlas 66 displays a higher constitutive exudation of phosphate than sensitive Scout 66 (Pellet *et al.*, 1997). No constitutive phosphorous exudation is observed in tolerant wheat cultivar ET3 suggesting phosphate exudation may contribute to the multigenic, higher tolerance of Atlas (Pellet *et al.*, 1996). Cell wall phosphate levels may also influence tolerance, as a significant difference in tolerance was observed between two cultivars of buckwheat associated with greater phosphate accumulation in the cell wall which bound Al (Zheng *et al.*, 2005). The cultivars did not differ in oxalate exudation,

changes rhizosphere pH or phosphate exudation, significant tolerance was observed associated with greater phosphate accumulation which bound Al in the cell wall (Zheng *et al.*, 2005).

1.3.5 Root Cap

The role of the root cap in Al tolerance has long been speculated. Particularly excretion of mucilage was thought to be involved in binding Al and reducing activity. However in maize it was shown that removal of the root cap did not affect Al sensitivity (Ryan *et al.*, 1993) and subsequently the involvement of the root cap was discounted. Recently the involvement of root cap sloughed cells in Al tolerance has been considered and the term root border cells (RBC) has been coined to describe them. RBC have not been considered in most studies of Al tolerance and toxicity because they do not undergo normal physiological development or presumably function in hydroponic solutions (Tamas *et al.*, 2005). However, recent experiments, utilising filter papers, have shown that the presence of RBC significantly increases tolerance to Al (Miyasaka and Hawes, 2001; Zhu *et al.*, 2003a; Tamas *et al.*, 2005). Al inhibits RBC production and initiates cell death which appears to be linked to ROS production (Pan *et al.*, 2001; Zhu *et al.*, 2003a; Tamas *et al.*, 2005). In snapbean tolerant cultivar Dade RBC are more tolerant to Al than sensitive cultivar Romano (Miyasaka and Hawes, 2001). The reason for higher tolerance of RBC may be because of release of organic acids from Dade or because of an inherent mechanism of tolerance, but irrespectively the maintenance of higher RBC density may contribute to the higher Al tolerance of Dade.

1.3.6 Vacuolar Sequestering

The involvement of vacuolar sequestering is well established in Al tolerance in accumulator species, however some interesting recent observations have suggested this may also be employed in a variety of ways as a tolerance mechanism in species which are generally considered to be Al excluders. A tolerant maize variety has been shown to only exhibit transient Al induced inhibition of elongation, haematoxylin staining, cell wall thickening and disturbance of cytosolic Ca^{2+} (Vázquez *et al.*, 1999). After 4 hrs of Al exposure, significant inhibition of elongation, deposition of solid Al-phosphate in the cell wall and Al in the vacuole was observed. After 24 hrs root elongation was restored, Al was not detected in the cell wall and higher vacuolar concentrations were measured. After 96 hrs Al precipitates were localised in the vacuoles and apoplast of maize roots (Vázquez, 2002). In *Chara corallina* avacuolate protoplasts demonstrated signs of saturation of Al uptake after 60 minutes, but vacuolar sequestering delayed saturation for up to 12-24 hrs (Taylor *et al.*, 2000), suggesting vacuolar sequestering may be able to lower cytoplasmic Al concentration. A longer term, Al inducible, increase in organic acid concentration has been observed in maize (Pineros *et al.*, 2002). However in a number of species no correlation between Al tolerance and internal concentration of citrate and malate has been found (Pellet *et al.*, 1995; Wenzl *et al.*, 2002a; Hayes and Ma, 2003; Mariano and Keltjens, 2004)

Significant diversity in the sensitivity of adjacent cells has also been observed in Maize roots. Within the cortex, cells with dark and shrunken cytoplasm occurred next to swollen cells with preserved organelles (Ciamporova, 2000). It has been suggested that these cells with shrunken protoplasm may hyper-accumulate Al to protect the

surrounding cells and activated lysogeny has been observed in tolerant, but not sensitive cultivars (Vázquez, 2002).

1.3.7 Organic acids

Many studies have described an Al-activated efflux of organic anions from the roots of a range of species and evidence from some of these indicate that organic anions can protect the plants from Al by chelating the harmful cations to form non-toxic complexes (Miyasaka *et al.*, 1991; Delhaize and Ryan, 1995; Larsen *et al.*, 1998; Ma and Miyasaka, 1998; Zheng *et al.*, 1998a, b; Yang *et al.*, 2000; Ma *et al.*, 2001; Pineros and Kochian, 2001; Ryan *et al.*, 2001; Yang *et al.*, 2001; Pineros *et al.*, 2002; Mariano and Keltjens, 2003; Peng *et al.*, 2003; Zhang *et al.*, 2003; Zhu *et al.*, 2003b). In *Arabidopsis*, quantitative trait loci (QTL) analysis of Al tolerance revealed two QTL that explain 40% of the variance of Al tolerance observed amongst recombinant inbred lines from Landsberg erecta (sensitive) and Columbia (tolerant) (Hoekenga *et al.*, 2003). These two QTL co-segregate with Al activated malate release though malate release itself explains about 95% of the variation in Al tolerance implying that the other unidentified QTL must also be involved in Al induced malate release (Hoekenga *et al.*, 2003). So it seems that in *Arabidopsis* at least that a number of genes underlie tolerance achieved through malate release. Similarly the greater tolerance of wheat cultivar Atlas 66 over some backcrossed lines seems in part to be because of greater malate efflux suggesting that also in wheat there may be multiple genes expressing Al activated malate release (Pellet *et al.*, 1997; Tang *et al.*, 2002).

Complexing of organic acid with Al has been shown to reduce a number of the mechanisms which may contribute to Al toxicity. Malate binding of Al increases the

hydrolysis of pectates, which is associated with cell wall loosening and expansion (Wehr *et al.*, 2003). Citrate and to a lesser extent malate, significantly reduced binding to phosphatidylinositol-4,5-bisphosphate which may be a key to signalling Al toxicity (Jones and Kochian, 1997). Interestingly there doesn't appear to be any direct relationship between Al induced organic acid exudation and reduced transmembrane Al flux (Rengel, 1996), though many report lower Al accumulation in the apex of tolerant plants (Delhaize *et al.*, 1993a; Kollmeier *et al.*, 2000; Ishikawa *et al.*, 2001). Actually, in *Chara corallina*, complexing ligands were shown to increase the flux of Al across the plasma membrane (Taylor *et al.*, 2000). Organic acids with higher numbers of carboxylic acid groups (such as citrate) chelate Al^{3+} more strongly (Kochian *et al.*, 2004). Exogenous application of malate ameliorates Al toxicity (Ryan *et al.*, 1995b).

Organic acid efflux may be immediate or occur after a time delay (Yang *et al.*, 2001; Pineros *et al.*, 2002). It is associated with Al activation of an organic acid permeable plasma membrane channel (Ryan *et al.*, 1997b; Pineros and Kochian, 2001; Zhang *et al.*, 2001) and continued synthesis of the organic acids are required (Basu *et al.*, 1994). The shoots seem to play an important role in long term efflux, because efflux is reduced by removal of the shoots (Yang *et al.*, 2000; Yang *et al.*, 2001). It is suggested that this is because *de novo* synthesis of organic acids requires a continued source of carbohydrates from the shoots. In wheat, Al induced or maintained K^+ efflux has been shown in tolerant, but not sensitive cultivars and it is proposed that this may account for charge balance (Ryan *et al.*, 1995a; Sasaki *et al.*, 1995; Osawa and Matsumoto, 2002). However in snapbean, which also has an organic acid induced tolerance mechanism, decreased K^+ efflux was observed in the tolerant, but not in the sensitive cultivar (Olivetti *et al.*, 1995). Wheat provides some of the

most compelling evidence for the hypothesis of tolerance via Al activated organic acid efflux since much of the data was collected on a pair of near-isogenic lines, ET3 and ES3, that differ in Al tolerance at a single genetic locus (Delhaize *et al.*, 1993a; Delhaize *et al.*, 1993b; Ryan *et al.*, 1995b, a).

Recently some doubt has been cast over exudation of organic acid as the main tolerance mechanism. In a study of diverse maize genotypes that incorporated both the range of Al resistance and differ significantly in their genetic background, it was shown that there was a clear correlation between tolerance and Al exclusion from the root tip, however there was poor correlation with exudation of citrate (Pineros *et al.*, 2005). In fact, one of the sensitive lines had the largest Al activated citrate exudation. This a very curious fact because the mechanism of tolerance by organic acid is hypothesised simply to be on the basis of citrate and malate binding, though this data suggests it may actually be more complex and clearly there are other important tolerance mechanisms working in maize roots. A number of other potential Al-resistance mechanisms were investigated, including release of other Al-chelating ligands, Al-induced alkalization of rhizosphere pH, changes in internal levels of Al-chelating compounds in the root, and Al translocation to the shoot, however no additional Al resistance mechanisms were identified (Pineros *et al.*, 2005).

1.3.8 Unidentified mechanisms

Signal grass (*Brachiaria decumbens* Stapf cv. Basilisk) is a tropical forage grass which has extremely high Al resistance, much greater than crop species such as wheat, triticale and maize, but this cannot be explained by organic acid or phosphate exudation or changes in rhizosphere pH (Wenzl *et al.*, 2001). Al accumulation in signal grass and in its close relative Al sensitive ruzigrass (*Brachiaria ruzizensis*

Germain and Evrard cv Common) is similar (Wenzl *et al.*, 2001). Similarly internal detoxification by organic acids cannot explain the differences between signal grass and ruzigrass because both accumulate high levels of citrate in the root tips in response to Al (Wenzl *et al.*, 2002a). There is a difference in malate synthesis, it being higher in signal grass, however it is not enough to account for the difference in tolerance (Wenzl *et al.*, 2002a). It should be noted that whilst ruzigrass is more sensitive than signal grass it is still highly resistant and the stimulation of internal citrate may contribute to that. The phosphorus content of the root apex was maintained in signal grass, but reduced by 70% in ruzigrass though this is thought to be a sign of toxicity rather than associated with the tolerance mechanism (Wenzl *et al.*, 2002b). These Brachiaria species provide interesting and important genetic material for further research.

1.4 ET8 and ES8

A large amount of the research on Al tolerance, specifically Al induced organic acid release, has been performed on four near isogenic wheat cultivars, ET8 and ET3 (tolerant) and ES8 and ES3 (sensitive). These cultivars have over 99% homology and differ in Al tolerance at a single, dominant genetic locus (designated Alt-1) (Delhaize *et al.*, 1993a; Delhaize *et al.*, 1993b; Ryan *et al.*, 1995b, a). They provide an ideal model system to study Al tolerance because it has been suggested that the high degree of homology means that most differences observed between the cultivars are related to the Alt-1 locus rather than other differences (Delhaize *et al.*, 1993a).

Aluminium rapidly activates a large and sustained efflux of malate from the root apices of the Al-tolerant ET3 (Delhaize *et al.*, 1993b; Ryan *et al.*, 1995a). This response shows a saturating dependence on external Al concentration whereas the

responses with several other trivalent cations tested (eg. La^{3+} and Ga^{3+}) were significantly smaller (Ryan *et al.*, 1995a; Kataoka *et al.*, 2002b). By contrast, the efflux of malate from the Al-sensitive ES3 genotype is small or absent. After short term exposure (10min and 1 hr) the Al concentration in the roots of ET3 is lower than ES8 (Delhaize *et al.*, 1993a).

1.4.1 Genetics

The near isogenic lines of wheat, ET3 and ES3 and ET8 and ES8 were bred through backcrossing progeny from Al tolerant Carazinho and Al sensitive Egret cultivars three and eight times respectively (Delhaize *et al.*, 1991; Delhaize *et al.*, 1993a). Analysis of the F2 population revealed that Al tolerance was inherited on a single dominant locus and that tolerance co-segregated with Al stimulated malate efflux (Delhaize *et al.*, 1993b). Recently the putative gene associated with Al-induced malate release in wheat was identified and isolated (Sasaki *et al.*, 2003; Sasaki *et al.*, 2004). The gene, designated *ALMT1*, encodes a membrane protein that facilitates an Al-activated malate efflux when expressed in tobacco, rice, barley and *Xenopus* oocytes (Delhaize *et al.*, 2004; Sasaki *et al.*, 2004). Tolerance was improved in transgenic plants and was attributed to the level of expression of *ALMT1* gene (Sasaki *et al.*, 2003; Delhaize *et al.*, 2004; Sasaki *et al.*, 2004). An *ALMT1* homolog identified in rye is also thought to be involved in organic acid exudation in this species (Fukuyama *et al.*, 2005). The protein coded by the *ALMT1* gene has been shown to be localised in the plasma membrane (Yamaguchi *et al.*, 2005). The clear identification of the *ALMT1* gene has meant that everyone has considered Alt-1 locus to only code for the malate permeable plasma membrane channel and not consider whether the Alt-1 locus may also include other genes related to Al tolerance.

1.4.2 Characteristics of the plasma membrane malate channel

The involvement of an anion channel in the release of malate was first implicated by studies that showed anion channel blockers decreased the Al induced malate release (Ryan *et al.*, 1995a). Patch clamp studies attempting to characterise this putative channel demonstrated that in whole cell configuration Al activated a large inward current immediately in 20% and after a delay of 10-90 min in another 30% of ET8 protoplasts (Ryan *et al.*, 1997b). Reversal potentials showed that this channel was selective for Cl^- over cations. The channel was not responsive to La^{3+} , was active as long as Al^{3+} was in the bath solution and was only observed in protoplasts from the root apex and not the mature region. Single channel recordings from whole cells demonstrated a strongly inward rectifying channel with a single channel conductance between 27 and 66ps. The channel could not be activated in outside out patches of ET8. However in maize an Al activated anion channel equivalent was observed in outside out patches, suggesting that, in maize at least, Al activates the anion channel by interacting directly with the channel protein itself or with an adjacent membrane-bound receptor (Pineros and Kochian, 2001). Later experiments in ET8 showed the channel is preferentially permeable to malate²⁻ over Cl^- ($P_{\text{malate}}/P_{\text{Cl}} = 2.6$) (Zhang *et al.*, 2001). Additionally, comparison of ET8 with ES8 showed that in ET8 the Al activated anion current occurs more frequently, the current density is higher, there is a shorter delay after Al addition and the current is maintained longer (Zhang *et al.*, 2001).

Stimulation of malate is accompanied by a stimulation of K^+ in experiments using excised root tips prompting the suggestion that K^+ efflux may be responsible for charge balancing malate (Ryan *et al.*, 1995a). No Al activation of K^+ channels was observed in the first patch clamp study of ET8, rather blockage of a potassium

outward rectifier in control patches was observed (Ryan *et al.*, 1997b). However in a later study when cAMP was included in the patch pipette Al^{3+} induced cation channels that were permeable to K^+ were discovered in ET8, but not in ES8 (Zhang *et al.*, 2001).

1.4.3 Malate exudation as a tolerance mechanism in ET8

A model to explain Al activated malate exudation has been proposed by Ryan *et al.* (2001) (Figure 1.1). In this model Al^{3+} activates the malate channel either 1) by directly binding to the channel, 2) interacting with an adjacent membrane bound receptor protein that activates the channel directly or 3) indirectly, perhaps via a distant membrane bound receptor protein and intermediate steps involving soluble compounds. Some of the malate release will be protonated, other will complex with Al^{3+} reducing its toxicity. It is not known how this complexing affects Al activation of the malate channel, although reduced malate efflux is observed from root tips if malate is included in the solution (Ryan *et al.*, 1995b). An Al induced K^+ outward rectifier requires cytosolic cAMP, and the resultant K^+ efflux, possibly along with other ion movements, are necessary for charge balancing malate. Coordination, if any, between the outward K^+ channel and the malate permeable channel is unknown.

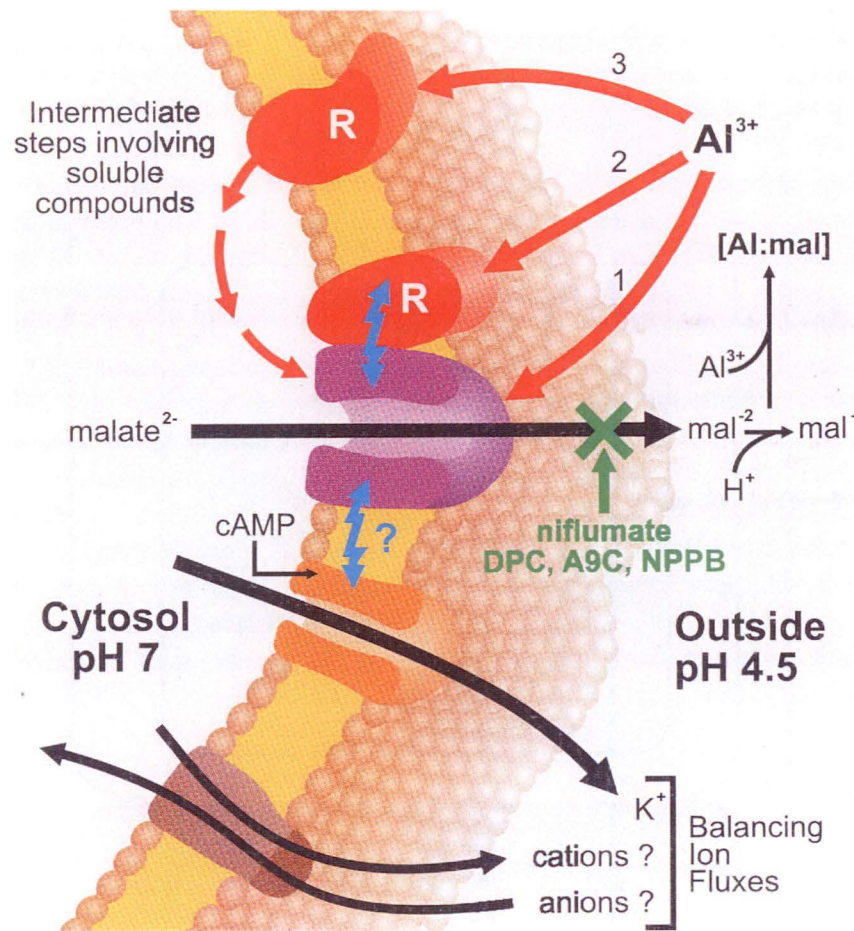


Figure 1.1. A model for Al^{3+} activated malate efflux from wheat roots. Reproduced from Ryan *et al.* (2001).

Unless there are two closely linked genes inherited on the Alt-1 locus, one for Al induced malate and one for Al induced K^+ , malate release must somehow signal K^+ release. It is possible that if a glutamate activated non selective cation channel is induced by malate then this could be responsible for the increase in K^+ efflux in ET8 (Sivaguru *et al.*, 2003b). As discussed previously it is most likely that this channel is blocked by Al. However an interesting prospect is that if Al physically blocks the channel, it may prevent Ca^{2+} influx, but still allow K^+ efflux which would provide a neat explanation of the connection between K^+ and malate fluxes. This can be simply

tested by seeing if malate can induce K^+ efflux in intact wheat roots. Osawa and Matsumoto (2002) have proposed that Al can trigger K^+ efflux in the Al-tolerant cultivar Atlas independently of malate release and, conversely, that K^+ efflux is not a requirement for Al-activated malate efflux. However their model was developed on the results from inhibitors that have non-specific interactions and no kinetics of either malate or K^+ efflux was measured, so it requires further validation. Clearly the mechanism of activation of the malate and K^+ channels and the nature of the balancing ion fluxes need to be investigated further.

1.4.4 Ca^{2+} homeostasis in response to Al in ET8 and ES8

In ET8 and ES8, as for other plants, Al induces an increase in $[Ca^{2+}]_{cyt}$. The elevation of $[Ca^{2+}]_{cyt}$ is faster, higher and sustained longer in ES8 than ET8 (Zhang and Rengel, 1999). The model of Al induced $[Ca^{2+}]_{cyt}$ elevation proposed by Rengel and Zhang(2003a) (2003) is outlined in Figure 1.2. In the absence of Al Ca^{2+} homeostasis is maintained by a balance of influx to the cytoplasm through hyperpolarisation activated channels (1) (HACC), depolarisation activated channels (2) (DACC), non selective cation channels (3) (NSCC), IP_3 channel (6), SV channel (4) and an endoplasmic reticulum Ca^{2+} channel (5) and efflux from the cytoplasm through a Ca^{2+} ATPase proteins in the plasma membrane (8) and the endoplasmic reticulum (7) and a Ca^{2+}/H^+ symporters in the tonoplast. Addition of Al inhibits the majority of HACC flux, and partially inhibits DACC. The effect on NSCC is unknown. It is proposed net Ca^{2+} flux through DACC increases because of Al induced membrane depolarisation, which would reduce flux through NSCC even if it is not blocked by Al. The elevation of $[Ca^{2+}]_{cyt}$ promotes further Ca^{2+} release from internal stores. Al movement across the plasma membrane is proposed to block IP_3 and

therefore inhibit IP₃ mediated Ca flux from the vacuole and endoplasmic reticulum. The effect of Al on the plasma membrane and endoplasmic reticulum Ca²⁺ ATPases and the vacuolar syporter are unknown. The authors propose that the difference in [Ca²⁺]_{cyt} between ET8 and ES8 in response to Al is simply that ET8 malate release reduces the activity of Al³⁺ eliciting the response. A lot of work is still required to determine the source of Ca²⁺ and the transporters involved, the nature of intracellular signals promoting Ca²⁺ release and the reasons for the differences between ET8 and ES8 [Ca²⁺]_{cyt}.

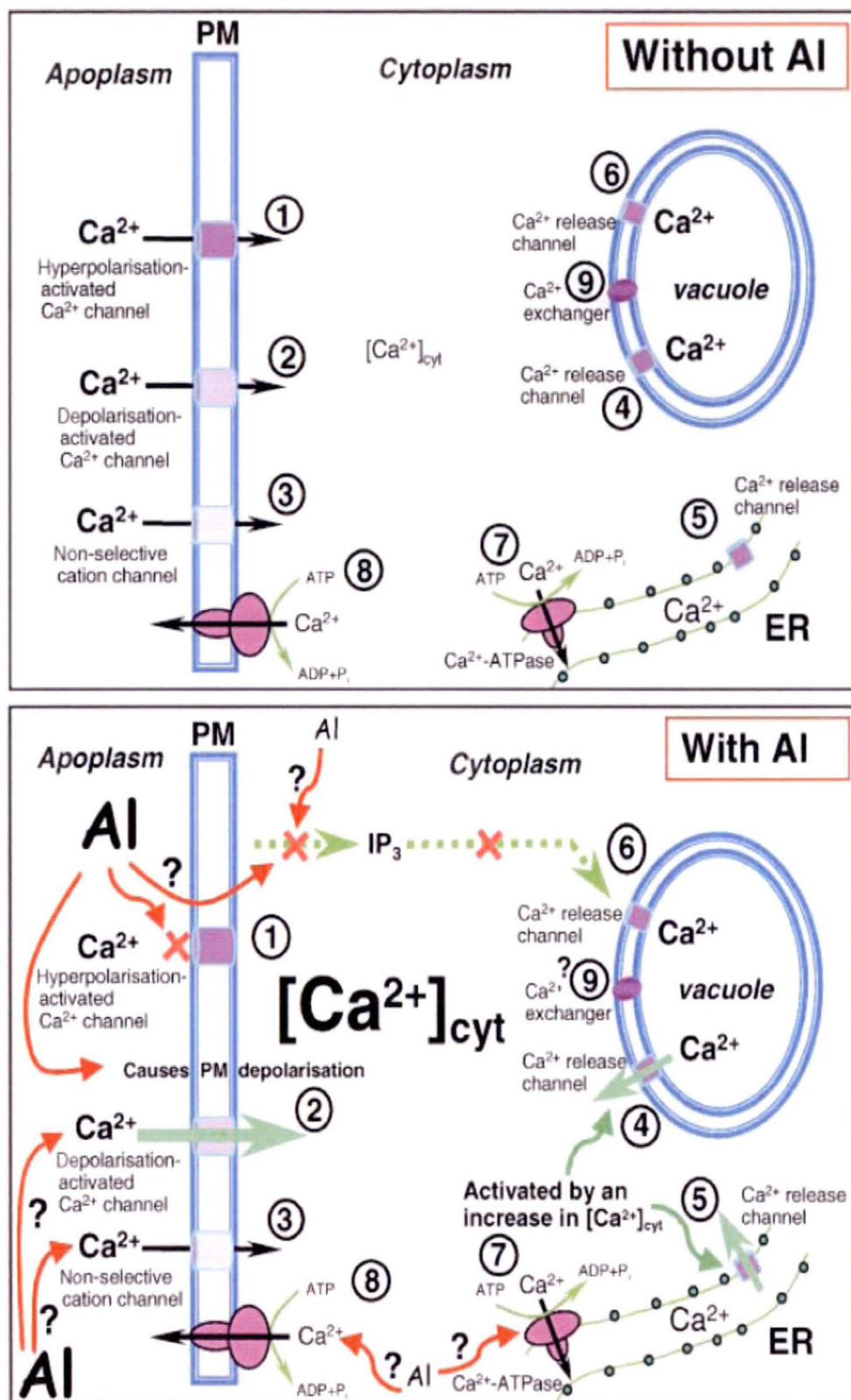


Figure 1.2. A model for Al^{3+} induced $[\text{Ca}^{2+}]_{\text{cyt}}$ elevation. Reproduced from (Rengel and Zhang, 2003).

1.5 Amelioration of Al toxicity

Irrespective of how tolerant a plant species is to soil acidity, plant breeding can never be the final solution. If the processes that first caused the problems with soil acidity are not addressed then the problems with acidity will continue to worsen until eventually the plant can no longer tolerate the stress. So it is necessary not only to consider how plants may be made more tolerant, but also how acid soils can be managed sustainably to either rectify the acidification or enable the plants to be grown in an acidic soil and to prevent further acidification. Specifically in regards to Al toxicity a number of different approaches to external amelioration exist.

1.5.1 Lime

The mechanism of amelioration by lime is very simple. Carbonate reacts with H^+ ions increasing the pH and thereby reducing the activity of Al^{3+} in the soil solution. Furthermore addition of lime or gypsum increases the concentration of Ca^{2+} and Mg^{2+} respectively which have further ameliorative effects (see below), as well as improving soil structure. Despite the efficacy of liming in raising soil pH there are a number of limitations which prevent it from being useful in all circumstances. Penetration of lime into the subsoil is quite limited, so highly effective amelioration is only observed to just below the depth that can be incorporated into the soil. Because of the need for heavy machinery and the expense of lime, liming is not a viable option in many developing countries where the money and resources may not be available. Additionally much subsistence farming occurs on land too steep to operate heavy machinery.

1.5.2 Cation amelioration

Most cations ameliorate Al toxicity and studies have shown that amelioration is generally effective in the following order $H^+ = Cat^{3+} > Cat^{2+} > Cat^{1+}$ (Kinraide *et al.*, 1992; Ryan *et al.*, 1994). Various reports have claimed that Ca^{2+} or Mg^{2+} may be slightly more effective than other divalent cations and H^+ is clearly more effective than other monovalent ions (Kinraide *et al.*, 1992). The discrepancies between different experiments may reflect different responses depending on experimental protocols, plant species and cultivars. It had been thought that amelioration by cations may be related to membrane surface activities of cations, and subsequently their uptake, however it was shown that toxicity is indifferent to the computed membrane surface Ca^{2+} activity (Ryan *et al.*, 1994). Rather it seems that amelioration by cations may be due to decreased membrane surface negativity and the consequent decrease in the membrane surface activity of Al^{3+} (Ryan *et al.*, 1994; Ryan *et al.*, 1997a; Yermiyahu *et al.*, 1997; Kinraide *et al.*, 2004). One specific effect may be reduced Al binding of phosphatidylinositol-4,5-bisphosphate by high concentrations of Ca^{2+} ($>1mM$) (Jones and Kochian, 1997). In soybean Mg^{2+} is more effective than Ca^{2+} and is associated with enhancement of Al activated citrate efflux and consequently lower Al accumulation (Silva *et al.*, 2001)

1.5.3 Silicon

Various mechanisms have been proposed for Al amelioration effected by silicon, from direct soil chemical interactions to *in planta* mechanisms. Silicon applied by itself has been variously reported to both increase and decrease cell wall and root elongation (Yang *et al.*, 1999; Hattori *et al.*, 2003), it also enhances shoot growth through increased extensibility (Hossain *et al.*, 2002). It has been suggested that

silicon will reduce free Al^{3+} activity in solution because it will interact to form aluminosilicates (Birchall, 1992; Exley *et al.*, 2002; Ryder *et al.*, 2003). Application of sodium silicate to soil ameliorated Al toxicity, altered mobile forms of Al and plant Al concentrations (Grenda and Badora, 2001). However silicon has been shown to be effective at concentrations that are not predicted to affect free Al^{3+} activity and do not affect plant Al uptake (Cocker *et al.*, 1997; Cocker *et al.*, 1998b, a). Amelioration by silicon appears to be highly complex, dependent on plant species and cultivar, material preparation, pH, $[\text{Al}^{3+}]$ and silicon concentration (Hodson and Evans, 1995; Cocker *et al.*, 1997; Cocker *et al.*, 1998b; Rahman *et al.*, 1998; Rahman *et al.*, 1999; Yang *et al.*, 1999; Liang *et al.*, 2001; Ryder *et al.*, 2003; Zsoldos *et al.*, 2003a; Zsoldos *et al.*, 2003b). In barley pot trials at low Al, silicon ameliorated root growth, but inhibited it at high Al (Liang *et al.*, 2001). In a number of studies silicon amelioration is not observed at low pH, but increases markedly at slightly higher pH (Cocker *et al.*, 1997; Cocker *et al.*, 1998b; Ryder *et al.*, 2003). It has been suggested that silicon may enhance the tolerance of some species by inducing root exudates, even in the absence of Al (Kidd *et al.*, 2001). In wheat and maize no effect of silicon on organic acid efflux was observed (Cocker *et al.*, 1998b; Kidd *et al.*, 2001). In maize, silicon pre-treatment increased phenolic exudation by up to 15 times (Kidd *et al.*, 2001). The role of flavonoid type phenolics in Al tolerance has not been previously considered and deserves further investigation to determine if this mechanism operates differently in tolerant and sensitive cultivars. In conifers (Hodson and Sangster, 1999) and *Faramea marginate* (Britez *et al.*, 2002) it is suggested that silicon may ameliorate Al *in planta* through co deposition with Al.

The effectiveness of silicon application in the field has been variable. The use of different silicon ameliorants on two andosols increased soil silicon in all treatments,

but amelioration was only observed in the treatment that increased soil pH (Morikawa and Saigusa, 2002). In rice paddies silicon fertilizer has been effective at ameliorating Al (Gu *et al.*, 1999; Hara *et al.*, 1999; Yang *et al.*, 1999). Similarly in wheat a calcium-silicon fertilizer ameliorated Al though it was most probably a combined effect (He and Jiang, 1999).

1.5.4 Organic materials

There is relatively little literature addressing the use of organic amendments to ameliorate Al toxicity. During decomposition of organic residues, a wide range of organic molecules are released. The most important of these for Al toxicity appear to be soluble humic compounds and low molecular weight aliphatic organic acids that can both complex Al^{3+} in the soil solution (Haynes and Mokolobate, 2001). During decomposition transient increases in soil pH can often occur, which may further decrease soluble Al by formation of insoluble hydroxy-Al complexes. Application of sodium humate to soil ameliorated Al toxicity and decreased mobile forms of Al and plant Al concentrations (Grenda and Badora, 2001). Several different sources of organic residue have been used successfully to alleviate Al and acid toxicity including crop residues (Kretzschmar *et al.*, 1991), manure and tree prunings (Wong *et al.*, 1995), waste paper pulp (Voundi Nkana *et al.*, 1998) and leaf litter ash (Noble *et al.*, 1996). In small scale subsistence farming the use of organic matter in food production is highly viable and has numerous side benefits such as an increase in soil fertility, reduced dependence on inorganic fertilisers, improved soil structure and improved soil water retention. The incorporation of organic matter in conventional agriculture should also be maximised for the many benefits it can confer.

1.6 Conclusions

There has been extensive research into the topic of soil acidity and specifically aluminium toxicity, tolerance and amelioration. Despite this we have quite limited understanding of the underlying physiology or good management strategies. The most detailed studies have been into the mechanisms of organic acid release from Al tolerant species and cultivars. Even in this area there remain many unanswered questions. The mechanism by which malate efflux is elicited is unknown. It is thought that K^+ efflux sustains malate efflux by charge balance though the kinetics of this haven't been shown, it hasn't been studied in intact roots and it hasn't been shown to be sustained over long periods. Some aspects of Al induced elevations in $[Ca^{2+}]_{cyt}$ have been elucidated, but many more questions about the channels and pathways involved remain, particularly in relation to the difference between tolerant and sensitive cultivars. The great interest in organic acid exudation as a tolerance mechanism has meant that other mechanisms, which may even be operating in the same plants, have been neglected. Most importantly, apart from a recent spate in genetic engineering, our increases in understanding of aluminium toxicity and tolerance have not yet lead to the development of more sustainable practises. This must surely be the end goal of all research. An understanding of basic physiology is one important piece of the pie, but should not be simply an aim in its self.

Chapter 2: General Materials and Methods

2.1 *Experimental Solutions*

Due to the complex speciation of Al, extreme care must be taken during solution preparation to ensure that the activity and speciation of the final solution is correct. Particularly the pH must be carefully controlled so that during preparation the solution is reduced to a pH just higher than the final prior to addition of the Al stock, any further adjustments of pH are then only done with HCl. If the pH was too low the solution was discarded and a new one made, because any adjustment of pH with a strong alkali may cause formation of both unknown and insoluble Al complexes. Al also forms many complexes with many common buffers and organic compounds, so these had to be carefully selected and the influence of Al complexes on the final Al^{3+} activity taken into consideration. AlCl_3 stock solution was made by adding $\text{AlCl}_3 \cdot 6\text{H}_2\text{O}$ to 0.1 mM HCl to make a final AlCl_3 concentration of 10-20 mM.

For most experiments the basic plant growth solution was 0.1mM CaNO_3 , 0.1 mM MgSO_4 , 0.1 mM KCl and 0.1 mM NH_4NO_3 adjusted to pH 4.0 with HCl. This was chosen to mimic the low concentration of basic cations in acidic soils and to provide a solution in which signal to noise ratio was optimised for measurement of ion fluxes. In some circumstances, such as examining the effect of ameliorants on Al toxicity, the solution was simplified to 200 μM CaCl_2 because root elongation sometimes varied inexplicably from experiment to experiment when using the basic growth solution in combination with NaSiO_4 in particular.

2.2 Plant materials

The majority of experiments were performed on the two near isogenic wheat cultivars ET8 (Al tolerant) and ES8 (Al sensitive). The genetics of these two cultivars was outlined in the previous chapter. Seed was kindly provided by Dr. Peter Ryan, CSIRO Plant Industry (Canberra). For experiments on signalling of vacuolar Ca^{2+} release fresh red beets, *Beta vulgaris*, were bought from a local market for the preliminary experiments because vacuolar isolation is very simple. To examine the effects of SV channel density on Al tolerance, *Arabidopsis thaliana* mutants over expressing (TPC1 5-6 and TPC1 10-21) and under expressing (*tpc 1-2*) SV were generously provided by Dr Frans Maathius (York University, UK).

2.3 Isolation of protoplasts from wheat

Wheat (*Triticum aestivum* L.) seedlings of cultivars ET8 and ES8 were germinated in a floating mesh on aerated 500mL solutions of 0.2mM CaCl_2 , pH 4.5. After 4-5 days, protoplasts were isolated from the terminal 2-3mm of roots of 27 different plants as has been described previously (Schachtman *et al.*, 1991). A series of solutions: A, cellulase-pectolyase and gradients 1, 2 & 3 were prepared and stored in the freezer (see appendix 1 for details). Solutions for isolation were removed from the freezer and thawed, then kept on ice. The terminal 2-3 mm of the wheat roots were removed with a razor in a drop of solution A and were chopped to a fine pulp. The chopped tips were washed into a small beaker with 5 mL of cellulase-pectolyase. The beaker covered in aluminium foil and transferred to a 30°C shaking incubator where it was gently shaken for 3 ¼ hours. After digestion the solution was filtered through two layers of muslin into a 15 mL falcon tube. The beaker was rinsed with solution A and then muslin was gently squeezed to release all protoplasts. The falcon tube was then

centrifuged at 60g for 5min at 4°C. The supernatant was transferred to another falcon tube leaving approximately 0.5 mL in the original tube. The pellet was gently resuspended with a plastic pipette and 5 mL of ice cold, 0.2µm filtered gradient 3 was added. Very carefully 2 mL of ice cold, 0.2 µm filtered gradient 2 was layered on top of gradient 3 and then 1 mL of ice cold, 0.2µm filtered gradient 1 was layered on top of gradient 2. This was centrifuged for 5min at 200g and 4°C. The start up acceleration was low and no brake was used on the centrifuge so that the gradients were not disturbed. A new plastic Pasteur pipette was used to carefully aspirate off all of gradient 1 and 1 mL of gradient 2. This was transferred to a new 15 mL Falcon tube and 5mL of ice cold, 0.2 µm filtered Gradient 1 was added. This was centrifuged for 5 min at 60g and 4°C. The supernatant was discarded and the pellet was carefully resuspended in 250-500 µL of the remaining solution and kept on ice ready for use.

2.4 Vacuole Immobilisation

For experiments measuring the fluxes or channel activities of vacuoles, clean glass was critical so that freshly released vacuoles spontaneously attached to the base of the measuring chamber. The measuring chamber consisted of a cut glass microscope slide which was attached to a plastic Teflon™ ring with Sylguard™. The glass was cleaned before use with 99% ethanol, rinsed in distilled water and then dried with compressed air.

2.5 Microelectrode Ion Flux Estimation (MIFE™)

2.5.1 Background theory

A detailed review of the theory of MIFE was published recently (Newman, 2001), so here I will just cover the most pertinent details. MIFE works on the principle that in

living cells acquire and release ions from the surrounding solutions and consequently ionic concentration gradients form. If the net movement of an ion is uptake, its concentration close to the surface will be lower than that further away. *Vice versa*, if the net movement of an ion is out of a tissue, then there will be an electrochemical potential gradient directed away from the cell or tissue surface (Figure 2.1). The crux of MIFE is an ion selective microelectrode that can be used to measure the electrochemical gradient of a specific ion in solution adjacent to the tissue of interest. Ion selectivity is achieved by filling a glass microelectrode with a liquid ion exchange resin (LIX, also called an ionophore) which creates a voltage, dependent on the specific ion it measures. The microelectrode is moved in a slow square wave pattern between two positions (position 1, x and position 2, $x + \Delta x$) the sample surface (normally a 5 sec cycle with approximately 0.75 sec moving between each position) and electrode voltage is recorded at each position (Figure 2.1).

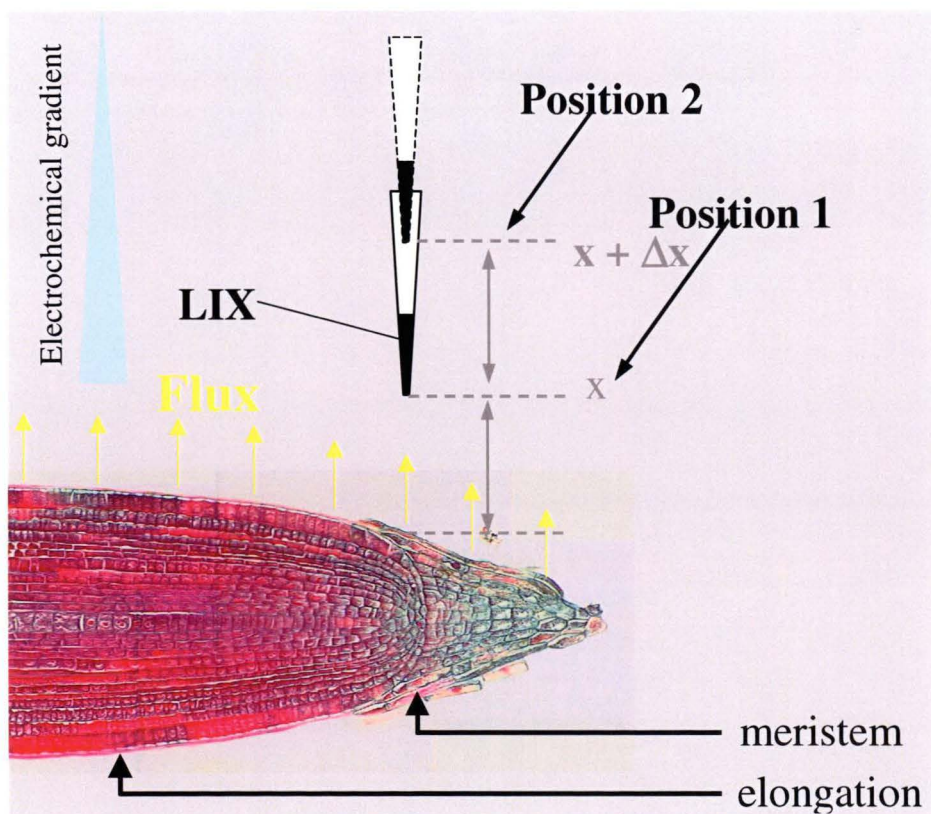


Figure 2.1. Microelectrode Ion Flux Estimation (MIFE™) - basic principles

The net flux of specific ions can then be calculated from the measured voltage gradient near the surface. For calculations it is assumed that convection and water uptake are negligibly small and unstirred layer conditions are met so that the concentration gradients observed in solution are simply explained by basic diffusion (Newman, 2001). The ion diffusion profile is strongly dependent on the tissue geometry meaning different formulae must be used to calculate fluxes. In the simplest case of planar diffusion, the following equation is used (Newman, 2001):

$$J = c u z F g (\Delta V / \Delta x)$$

Where J is the ion flux ($\text{mol m}^2 \text{s}^{-1}$); c is ion concentration (mol m^{-3}); u is the ion mobility (m s^{-1} per Newton mol^{-1}); z is the ion's valence; F is the Faraday number (96500 C mol^{-1}); g is a factor found from the measured Nernst slope for the electrode during calibration; dV is the voltage difference measured by the electrometer between the two positions (V); Δx is the distance between two positions (m).

For cylindrical geometry (e.g. roots) the radius of the cylinder (r) should be taken into account. This is done by replacing Δx in the equation above with:

$$\Delta x = r^2 [1/(r+x) - 1/(r+x+\Delta x)].$$

For spherical geometry (e.g. vacuoles and protoplasts) Δx is replaced with:

$$\Delta x = r \ln[(r+x+\Delta x)/(r+x)].$$

2.5.2 MIFE setup

A variety of MIFE configurations are available for measuring different types of tissues. For measurement of root fluxes (Figure 2.2) we used a conventional stereo microscope (ELeitz Wetzlar, Germany) mounted on its side (so the optical path was horizontal) with a MMT-5 micromanipulator (Narishige, Tokyo, Japan) used to position up to 3 microelectrodes with tips 1-2 μm apart 50 μm vertically above the root surface. The plant root was located horizontally in a 6mL chamber which was attached to a 3-dimensional stepper motor-driven, hydraulic micromanipulator (WR-88 Narishige, Tokyo, Japan) that was used to move the root vertically between 50 μm and 100 μm from the electrode tips. Roots must be mounted horizontally in order to bath the root and provide easy access for the electrodes lowered from above.

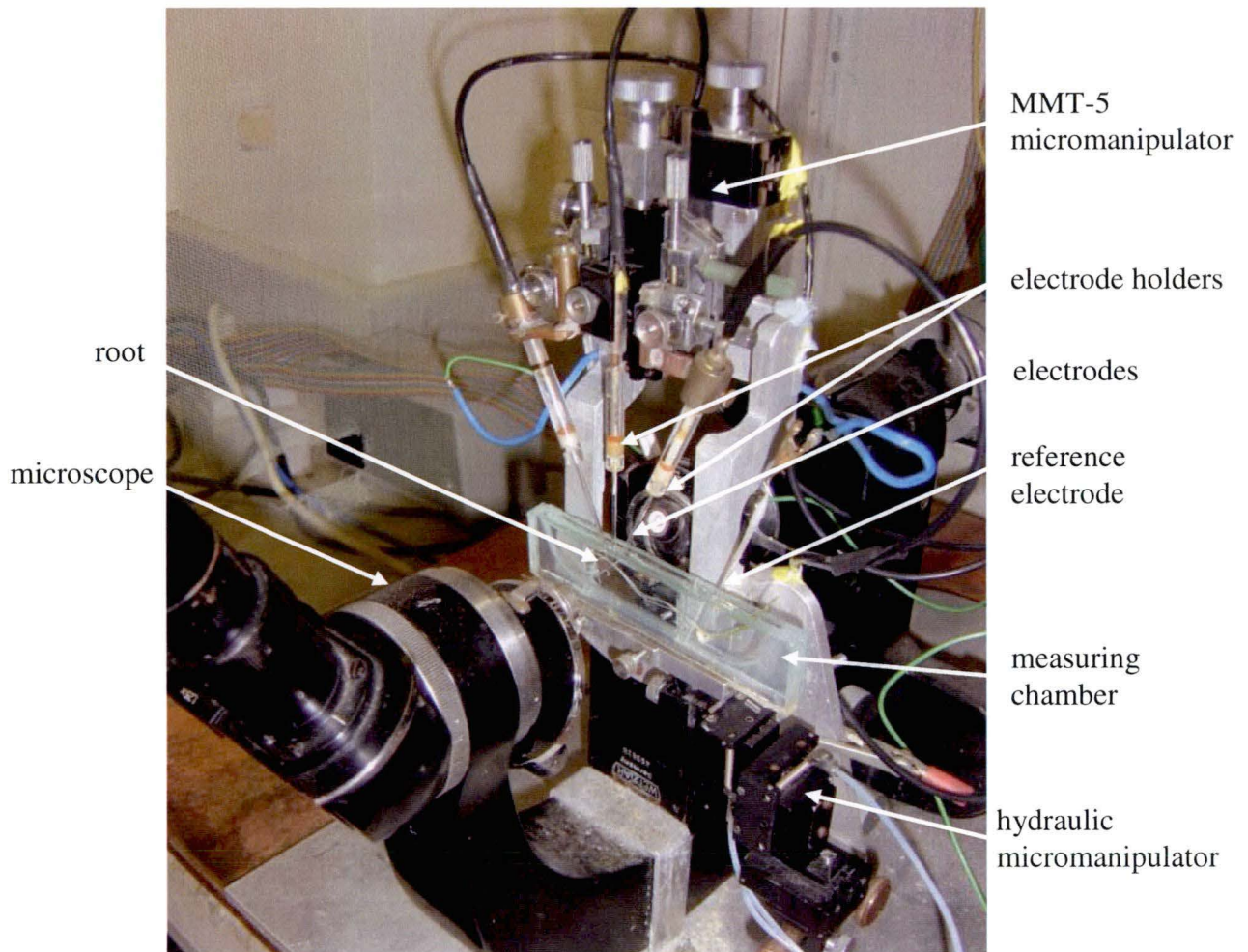


Figure 2.2. MIFE setup for measuring root fluxes.

For measurement of vacuolar fluxes (Figure 2.3) the MIFE hardware was set up around an inverted microscope (Olympus IX-50), with a one dimensional stepper motor hydraulic micromanipulator (MHW-4 Narishige, Tokyo Japan) which was used to move the electrode horizontally between 10 μm and 55 μm from the vacuole surface. The electrode was positioned and held with a MMT-5 micromanipulator (Narishige, Tokyo, Japan) and WI 64-0918 electrode holders (SDR Clinical Technology, Middle Cove, Australia) respectively. This setup allowed fine positioning of up to three electrode tips near the vacuole surface, although only one

channel was used. Additional flexibility in electrode positioning was achieved by mounting the manipulator ensemble on a Narishige MX-1 mechanical micromanipulator.

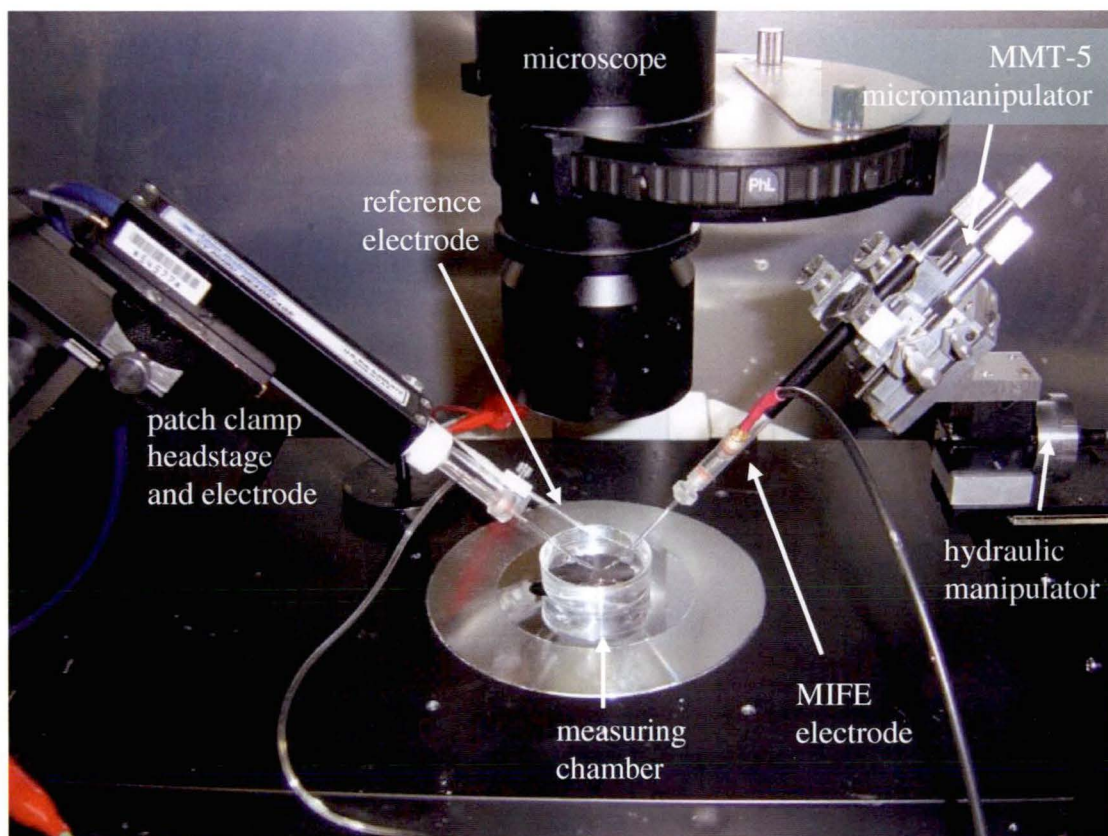


Figure 2.3. MIFE setup for measuring vacuoles on the right hand side. Patch clamp setup on the left hand side. For impalement measurements the patch headstage was replaced by an electrode and holder connected to the MIFE system.

The DOS-operated software CHART (University of Tasmania, Hobart, Australia) in conjunction with an analogue to digital interface card (DAS08) was used to control data acquisition and allow automated and interactive real-time control of the amplifier configuration and the micromanipulator while the data is being collected and written to disk. The CHART software is also used to calculate an average manipulator file,

which is used in flux calculations. It is necessary to input the specimen radius and the distance from the specimen surface to position 1 for this calculation. Flux calculations were performed automatically by the MFLUX software (University of Tasmania, Hobart, Australia) from the data and log files. In experiments measuring vacuolar flux, multiple vacuoles of different radii were measured so it was necessary to record the radius of each individual vacuole and later in a spreadsheet make a correction for the difference in radius from the generic radius entered for flux calculations (see appendix 3).

2.5.3 Microelectrode fabrication

Ion-selective microelectrode fabrication is the most crucial step of MIFE measurements. Microelectrode fabrication was as has been described previously (Shabala *et al.*, 1997; Shabala, 2000; Shabala and Knowles, 2002). Microelectrode blanks were made from 1.5 mm (OD) non-filamented borosilicate glass capillaries (GC 150-10, CDR Clinical Technology, Middle Cove, Australia). The blanks were pulled to a final tip diameter less than 1 μm using a custom built vertical pipette puller and oven dried at 225 °C After at least four hours (in practise the next morning) the electrodes were covered by a steel lid and after 10-15 min, 40-50 μL of tributylchlorosilane (90796, Fluka Chemicals, Busch, Switzerland) was injected under the lid. Ten minutes later the lid was removed and electrode blanks were baked a further 30 min at 225 °C to ensure complete drying. Silanisation causes the surface of the electrode blanks to become hydrophobic, so the hydrophobic LIX will be drawn into the tip of the prepared microelectrode by capillarity. Dried and cooled electrode blanks were stored in a closed container for up to six weeks.

A filling capillary was made by dipping a wide tipped (30-50 μm) glass micro-capillary (pulled from GC 100-10, CDR Clinical Technology, Middle Cove, Australia) into a stock container of LIX so that it drew a 1mm column into the electrode tip. This filling electrode was mounted horizontally on a three dimensional micromanipulator. A silanised microelectrode blank was mounted horizontally opposite the filling capillary with the tip in the field of view of a stereo microscope. The microelectrode tip was broken to 2-3 μm diameter with a blunt glass capillary (mounted next to the filling capillary) and then back filled with an appropriate back-filling solution (Table 2.1) using a syringe with a thin metal needle (MF34G-5, WPI, Sarasota, USA) avoiding bubble formation. Immediately after back-filling, the microelectrode tip was front-filled with the corresponding LIX (Table 2.1) by moving the filling electrode to just touch the microelectrode until the column of LIX was 100-200 μm long. The prepared microelectrodes were stored with their tips in experimental solution until mounted in the MIFE setup (most LIX remain stable for >8-10 hours). Most of the prepared microelectrodes can be used immediately after preparation, while others (eg. H^+ and Cl^-) need some conditioning time ($\sim 1\text{h}$) to ensure a stable response.

Table 2.1. Commercially available liquid ionophores (LIX) and the appropriate backfilling solutions used for preparation of ion selective microelectrodes.

Ion	Liquid ionophore (LIX)	Backfilling solution
K ⁺	Potassium ionophore I - cocktail A (Fluka 60031)	500 mM KCl
H ⁺	Hydrogen ionophore II – cocktail A (Fluka 95297)	15 mM NaCl, 40 mM KH ₂ PO ₄ (pH 6.0 with NaOH)
Ca ²⁺	Calcium ionophore I – cocktail A (Sigma I-1772)	500 mM CaCl ₂
Mg ²⁺	Magnesium ionophore I – cocktail A (Fluka 63048)	500 mM MgCl ₂
Cl ⁻	Chloride ionophore I – cocktail A (Fluka 24902)	500 mM KCl
Na ⁺	Sodium ionophore II – cocktail A (Fluka 71178)	500 mM NaCl

2.5.4 Microelectrode calibration and characteristics

Electrodes were calibrated before and after experimentation against a set of three standards with a series of concentrations covering the expected range of the relevant ion. Electrodes with calibrated Nernst slopes less than 50 mV per decade for monovalent ions and 25 mV per decade for divalent ions, or with correlation coefficients less than 0.999 were discarded. The ionic strength of solutions affects the calculated intercept of ion selective electrodes in the calibration file, therefore for experiments with high ionic strength solutions, microelectrodes were calibrated in a background of the dominant ions.

The electrode resistance is a critical factor influencing key electrode characteristics such as signal to noise ratio and microelectrode responsiveness. The resistance of the prepared microelectrodes was typically 1-3 GΩ, though Cl⁻ electrodes were much

higher and required special fabrication (see Chapter 4 materials and methods for detail). Electrode resistance increases as tip diameter decreases and LIX length increases, though tip diameter has a much greater influence. As electrode resistance increases so does electrode noise, limiting the size of flux that can be detected. Sensitivity can be improved by increasing the travel range of the electrode (making voltage changes larger) or by increasing electrode tip diameter. Electrode resistance and LIX length also influence how rapidly the electrode responds to changes in concentration. For accurate flux calculations the voltage must stabilise rapidly. From practical experience, stabilisation was achieved faster if the LIX column length was relatively short and tip diameter maximised. However this increased the likelihood of a gradual leak of LIX out of the tip and the electrode losing its selectivity. The best compromise was achieved by optimising the amount of silane used for electrode fabrication, the amount of LIX used for electrode filling and tip width.

2.6 Patch Clamp

The patch clamp is an electrophysiological technique that enables the measurement or control of voltage and current across a plant membrane attached to a small glass capillary. With careful control of the composition of pipette and bath solutions patch clamp allows the specific characteristics of channels, such as voltage dependence, selectivity, conductance and gating, to be determined. Depending on the patch configuration the responses of whole cells, whole organelles or individual channels can be measured. A clean membrane is essential for successful attachment of a patch so the vacuoles patched in this study were released immediately before patching (see Chapters 5 & 6 for details).

2.6.1 The gigohm seal

The single most important prerequisite for successful patch clamping is a very high resistance seal between the patch electrode and the membrane being clamped. With a high seal resistance ($>1\text{ G}\Omega$) and low pipette resistance ($<10\text{ M}\Omega$) most of the current measured is flowing through the membrane. To achieve a gigohm seal a fire-polished pipette is gently placed against the membrane surface and gentle suction applied. It was found that the type of glass of the capillaries used to make the pipette had a large influence on the rate of successful seal formation. Greatest success was obtained with World Precision Instruments Kwik-Fil 1B150F-4 (Sarasota, Florida, USA) (1.5mm outer diameter). Pipettes were either pulled on a two stage Narishige puller (PP-830, Narishige, Japan) with a 5mm initial pull and 10 seconds between pulls and polished with a MF 830 microforge (Narishige, Japan) or in three steps on a Brown/Flaming model P-97 puller (Sutter Instruments Co, Novato, CA) and polished on a LPZ 101 microforge (List Medical, Germany).

The resistance of the seal was measured within the Clampex 8 software by applying a square wave test pulse of 5-10mV amplitude, measuring the change in current and then calculating the resistance by $R=V/I$. During this test pulse, other parameters were compensated for such as capacitance and series resistance (see below). Throughout an experiment the seal was regularly tested to ensure that it remained intact. Application of a mild negative voltage (-60 mV) during seal formation often increased success rate.

2.6.2 Patch configurations

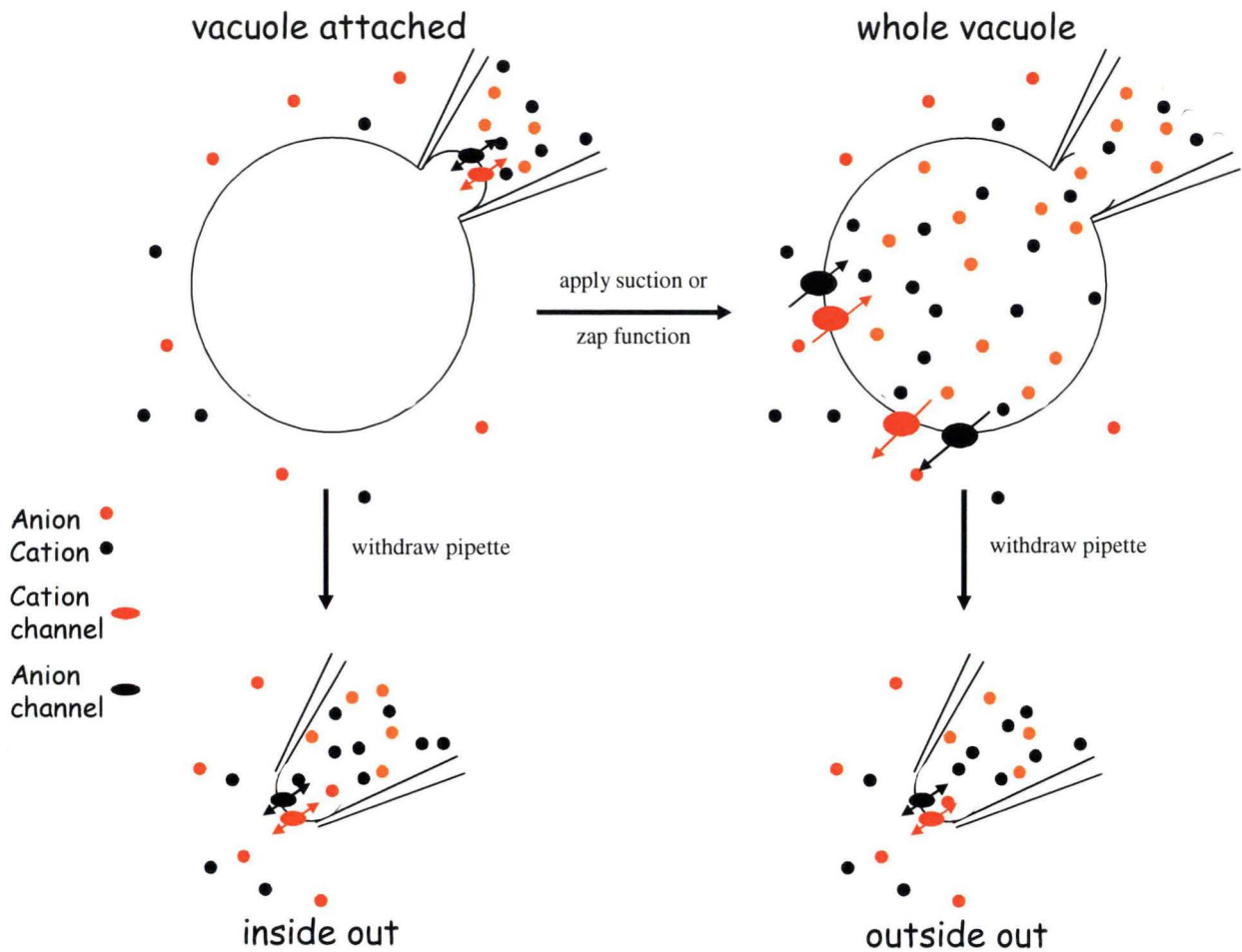


Figure 2.4. Patch clamp configurations.

Once a stable seal has been established on an intact vacuole this is referred to as vacuole attached (Figure 2.4). From this position the pipette can be withdrawn causing a small membrane patch to form across the pipette tip with the vacuolar side facing outwards, this is referred to as an inside out patch. Alternatively from vacuole attached, application of transient strong suction, often combined with a current pulse (via the ‘zap’ function), causes the membrane at the tip of the pipette to break and the

seal form around the outside of the pipette so that the pipette solution is continuous with the vacuolar solution, this is referred to as whole vacuole. From the whole vacuole configuration the pipette can be withdrawn causing a small membrane patch to form across the pipette tip with the cytosolic side facing outwards, this is referred to as an outside out patch. Inside out, outside out and cell attached patches can be used to examine the electrochemical characteristics of individual membrane channels because they may contain anywhere between zero and ten in the membrane patch. Careful selection of applied voltages and pipette and bath solutions allows the activation of individual channels. The whole vacuolar configuration is useful to study the combined response of all channels that open under the specific voltage protocol and pipette and bath solutions. When recording in whole vacuole configuration time must be allowed for perfusion of the pipette solution to fully displace the native vacuolar solution.

Once a suitable patch has been achieved the patch amplifier can be used in a number of different modes: voltage clamp, where voltage is controlled and current measured; current clamp where current is controlled and current measured or simply tracking both voltage and current. The most common mode, and that used in all experiments in this thesis is voltage clamp. When a voltage is applied (V_p) to the membrane, opening of channels will create a membrane current (I_i) that will then alter the actual voltage applied to the membrane and that measured by the amplifier (V_m). In order to maintain the applied membrane voltage and to estimate I_i , an operational amplifier generates an output feedback current (I_f) proportional the difference of its two input signals V_p and V_m . V_p is continuously adjusted so that I_i is equal and opposite to I_f .

2.6.3 Junction potentials and pipette offset

Between any two dissimilar conductors an electrical potential, known as the junction potential, will be created. In patch clamping the largest junction potentials occur at the junction formed between the silver chloride wire in contact with the pipette solution and at the junction between the pipette solution and the bath solution. In order to accurately know the voltage applied to the membrane whilst patch clamping, it is necessary to first correct these junction potentials to zero using the pipette offset on the patch amplifier when the pipette is held in the bath solution. However once a seal is established then the junction potential between the pipette and bath is eliminated so that an error equal and opposite to the pipette tip junction potential is incorporated into the holding potential applied by the patch amplifier. This error was corrected by subtracting the original pipette liquid-liquid junction potential from the amplifier holding potential. The liquid junction potential was estimated with JPCalc, part of the Clampex 8 software (Axon Instruments, Foster City, CA, USA), which uses the generalised Henderson equation to calculate the junction potential.

2.6.4 Capacitance and series resistance

Accurate measurement of current and voltage during voltage clamp measurements is complicated by capacitance and series resistance. Series resistance (R_s) is made up of the other resistances between the patch electrodes in series with the actual membrane resistance (the access resistance of the pipette, the bath and pipette solutions and the agar bridge in the reference electrode). These other resistances cause a discrepancy between the measured voltage and the actual applied membrane voltage which is equal to $I \times R_s$. When the measured current is very small (such as in inside out or outside out patches) then the error is inconsequential. However it becomes

significant when large currents are measured, often in whole vacuole configurations. In whole vacuole mode, series resistance was compensated by means of the compensation circuit of the patch-clamp amplifier. Capacitance in the system causes rapidly attenuating spikes in current measured after application of a voltage that masks the actual current across the membrane and causes the inaccurate application of voltage across the membrane. The capacitance consists of the membrane (C_m), pipette (C_t , transmural) and stray capacitance (such as microscope, stand, bath, etc.). The largest of these components is the membrane capacitance when operating in whole cell mode and this must be compensated by adjustments in the amplifier settings whilst applying the test pulse. The pipette capacitance is also compensated by amplifier settings and stray capacitance minimised by using small bath volumes. The pipette capacitance can be minimised through application of sylguard™ or paraffin wax to the tip, however we found it unnecessary for our experiments. R_s and C_m can change during experiments so was monitored and compensated between protocols. The measured C_m was recorded for each experiment to allow calculation of current density. 1 pF was estimated as approximately 100 μm^2 membrane area.

2.6.5 Data acquisition

Current measurements were performed using an Axopatch 200A or 200B integrating Patch-Clamp amplifier (Axon Instruments, Foster City, CA, USA). Vacuoles were located in a custom built chamber consisting of a circular Teflon ring with a glass coverslip attached to the base with Sylguard. Prior to an experiment the coverslip was carefully cleaned with 100% ethanol, rinsed in distilled water and dried with compressed air. The chamber was then filled with experimental solution and

vacuoles were transferred. The reference AgCl electrode was connected to the bath by a 3% agar bridge filled with 100 mM KCl.

Vacuolar ion currents were measured under voltage clamp conditions using two different recording modes: whole vacuole and outside out (cytosol side facing bath) patches. Voltage sign convention was cytosol *minus* vacuole. The records were filtered at 10 kHz by a low pass Bessel filter and digitized using either a Digidata 1200 or 1320 interface (Axon instruments, Foster City, CA, USA). Whole vacuole SV currents were evoked by a series of 0.6-1.2 s pulses from -100 to +200 mV in 20 mV increments. Single channel I/V curves were obtained from cytosol out patches by applying to a protocol of 50ms ramps from -200 to +200mV from a voltage holding potential of 50-70mV where only 1-2 channels were open at a time.

2.6.6 Data analysis

Whole cell currents

I/V curves from whole vacuoles were determined using the Clampfit 8 software (Axon instruments, Foster City, CA, USA). The activation and deactivation kinetics of the whole vacuolar currents were fitted to 2nd order Hodgkin-Huxley kinetics, yielding characteristic activation time, τ_{act} and deactivation time τ_{deact} . Channel density was calculated by dividing the whole vacuole current at 200 mV (almost all channels open) by the single channel conductance at 200mV and the surface area of the vacuole ($1\text{pF} \sim 100\text{ }\mu\text{m}^2$). The relative open probability versus voltage was calculated by dividing the whole vacuole current at any given voltage by the single channel current at the same voltage. This was then normalised to 1 (maximum open probability) for each individual vacuole. The mean open probability versus voltage was then calculated for a number of individual vacuoles.

Single channel currents

Single channel I/V curves were obtained directly from the current measured in ramp protocols and were corrected for the leak and capacitance simply by subtracting the averaged responses where no channels opened. Many individual I/V curves were averaged to produce a representative trace.

Chapter 3: Morphological responses to Al^{3+} and amelioration by Ca^{2+} , Mg^{2+} and silicate

3.1 Introduction

Changes in root length are the most obvious and most commonly reported effect of Al toxicity, and the mechanisms which confer the ability to maintain root elongation and division in the presence of Al have been the main focus of most studies of Al tolerance. Maintenance of root elongation is of course essential, because without the capacity to elongate a plant cannot grow a root system to scavenge the nutrients it requires for growth and reproduction. However root length is not the only feature of plant roots significant in productivity. Root hair growth and development is also essential for plant growth and productivity of crops because they dramatically increase the surface area of the roots for nutrient uptake. Al is highly toxic to root hair growth even at very low concentrations (Jones *et al.*, 1995) and so must have serious effects on nutrient uptake and plant yields.

In maize, Al caused a highly variable effect on the relative uptake of a range of nutrients. The most pronounced effects on macronutrients were reduced uptake of Ca and Mg across all cultivars, although there was significant correlation with Al tolerance, the more tolerant species having higher uptake than sensitive (Mariano and Keltjens, 2005). It is unclear whether higher nutrient uptake in tolerant cultivars is related to greater development of the root system, greater tolerance of uptake mechanisms or greater tolerance of root hairs. Some evidence for the latter is suggested by experiments in *Arabidopsis*. Al exposure generally causes cessation of root hair growth and prolonged elevation in root hair tip localised $[Ca^{2+}]_{cyt}$ in wildtype

and Al sensitive *Arabidopsis*, although these elevations could occur up to 15 minutes after the cessation of root growth and in 32% of root hairs growth stopped without any change in $[Ca^{2+}]_{cyt}$ (Jones *et al.*, 1998a). In contrast Al resistant mutants showed little root hair inhibition and no changes in $[Ca^{2+}]_{cyt}$ were observed (Jones *et al.*, 1998a).

The ability of ET8 to maintain higher root growth rates and better overall plant nutrition and productivity in the presence of Al compared with ES8 is well documented (Ryan *et al.*, 1995b), however no study was found comparing the tolerance of ET8 and ES8 root hairs to Al toxicity. The tolerance mechanism of the Alt-1 locus is thought to be restricted specifically to malate release in the elongation zone, so it has been presumed that no difference in the tolerance of root hair growth and development would be found.

There has also been little research on the effect of ameliorants on root hair morphology or their potential interactions with tolerance mechanisms. Ca, Mg and silicate are the most commonly mentioned solution ameliorants mentioned in the literature. Mg and Ca seem to have similar efficacy in amelioration though some suggest that one is more effective than the other. Specifically in soybean it has been shown that Mg^{2+} is more effective than Ca^{2+} because of enhanced citrate efflux (Silva *et al.*, 2001). Consequently it seems possible that there may be significant interaction between specific ameliorants and cultivars.

The purpose of this chapter was to determine whether ET8 and ES8 display similar toxicity to Al in root hair growth and nutrient acquisition, and whether there were any interactions between ameliorant, Al treatment and cultivar for root morphological characteristics.

3.2 Materials and methods

3.2.1 Morphological changes of ET8 and ES8 with exposure to Al from germination and amelioration by Ca, Mg and silicate

The near isogenic wheat (*Triticum aestivum* L.) lines, ET8 (Al-tolerant) and ES8 (Al-sensitive) were grown for 4 days on floating mesh in plastic containers with 100 mL aerated 200 μ M $CaCl_2$ solution adjusted to pH 4.5 with HCl. Solutions were refreshed after three days. The experimental design was a 2x2x4 factorial examining (i) the effect of genotype (ET8 and ES8), (ii) Al to cause ~30% growth inhibition (6 μ M Al for ET8 and 2 μ M for ES8) and (iii) ameliorants (1 mM $MgCl_2$, 1 mM $CaCl_2$ or 1 mM $NaSiO_4$) on root growth and morphology. The experimental design was a randomised complete block design with three replicates. The design also included external controls of three replicates of each cultivar grown at pH 5.5 without Al or an ameliorant present for which means and standard errors were calculated. Dependent parameters measured were: length of root and shoot; root diameter at the meristem, elongation zone and mature region; root hair length, diameter, and density; length of the mature root hair zone; solution pH and malate concentration. Total root hair surface area in mm^2 was calculated by:

$$RHSA = RHL \times T \times \Pi \times D \times LRHZ \times 10^6$$

Where RHSA is root hair surface area (μm^2); RHL is root hair length (μm); T is diameter (μm); Π is pi; D is density (hairs /mm) and LHRz is length of root hair zone (mm). Root to shoot ratio was also calculated. Statistically significant interactions were quantified by analysis of variance using the general linear models package of SPSS. To compare means, Fischers LSDs were calculated. Where root hairs were not present the values for root hair length, diameter, density and surface area and the

length of the root hair zone were treated as missing data points in the analysis. Unless otherwise indicated results described as significant are below or equal to the 0.05 probability level and where given as LSD values are at $p=0.05$.

3.2.2 Malate measurement

At the time of morphology assessment, 5 mL of solution was taken from each container and kept in the freezer for later determination of malate. The free concentration of malate in solution was estimated enzymatically using the change in absorbance after reaction with malic dehydrogenase (MDH) and nicotinamide adenine dinucleotide (NAD) (Gutmann and Wahlfeld, 1974). A number of basic solutions are required:

(1) Hydrazine buffer: Dissolve 11.4 g glycine and 25 ml hydrazine hydrate in 20 mL water (~pH 9.0) and make up to 300 mL with water.

(2) NAD: Dissolve 30 mg mL NAD in 1 mL water and store at 4°C. Prepared fresh for each experiment.

(3) MDH: As supplied, enzyme suspension in 3.2 M $(NH_4)_2SO_4$ at >1100 U/mg.

A standard curve was constructed by adding 0.68 mL of control malate solution to a spectrophotometer cuvette plus 0.75 mL hydrazine buffer and 50 μ L NAD. The cuvette was mixed with a pipette and the absorbance zeroed at 340 nm in an absorbance spectrometer. 5 μ L MDH was added and the increase in absorbance (Δ ABS) measured at 340 nm after the reaction had gone to completion was plotted against the known malate concentrations to produce a standard curve. Samples were then assayed and malate concentrations calculated from the standard curve.

3.2.3 Effect of low silicate levels on growth and fluxes from the elongation zone in ES8

ES8 plants were grown as above in a simple 100 μ M $CaCl_2$, 100 μ M KCl , 100 μ M $NaCl$ solution at pH 4.5, with addition of either or both 25 μ M $NaSiO_4$ and 2.5 μ M $AlCl_3$. After 4 days root and shoot length and fluxes of Ca^{2+} and K^+ from the elongation zone were measured. For flux measurements a single seedling was removed from the solution and placed into the measuring chamber filled with the solution taken from the pot the seedling was grown in. Net ion fluxes of Ca^{2+} and K^+ were estimated by measuring the ion gradients in the unstirred layers near the root surface using the MIFE technique (Newman *et al.*, 1987; Shabala *et al.*, 1997). Details on fabrication and calibration of ion selective microelectrodes were described in Chapter 2. The electrodes were positioned 1 mm proximal from the meristem (visible by the shape and size of cells), in the centre of the elongation zone.

3.2.4 Root hair morphology and nutrient acquisition after 24 hr exposure to Al

ET8 and ES8 were grown for 3 days on floating mesh in plastic containers with 0.5 L of aerated solution containing 0.1mM $CaNO_3$, 0.1 mM $MgSO_4$, 0.1 mM KCl and 0.1 mM NH_4NO_3 . The pH of the solution after 3 days of growth was approximately pH 4.0. After three days the solutions were exchanged with the same basic solution adjusted to pH 4.0 with HCl and including 10, 25, 50 or 100 μ M $AlCl_3$. After 24 hours the changes in root hair density, root hair length, diameter and density and fluxes from the root hair zone were measured.

Net fluxes of H^+ , K^+ and Cl^- were measured from the mature root zone essentially as described above. The only modification used in this study was that the Cl^- electrode tip was made 8-10 μ m (compared with 2-3 μ m for K^+ and H^+) to improve

responsiveness, minimise electrode drift and minimise resistance. MIFE measurements were made from the root hair zone where the root hairs had just reached their mature length. A minimum of 5 replicates were made for each cultivar at each $AlCl_3$ concentration.

3.3 Results

3.3.1 Effects of Al exposure, cultivar and amelioration by Ca^{2+} , Mg^{2+} and silicate on wheat root and shoot characteristics

There was no significant three way interaction between, Al, ameliorant and cultivar for root length, however there was a significant interaction between Al and ameliorant. Exposure to Al significantly reduced root elongation (Table 3.1). Ameliorants Ca^{2+} , Mg^{2+} and SiO_4^- all significantly improved root growth compared to the low pH control and the increase was significantly higher with Ca and Mg (Table 3.1). Al did not have a significant effect on root length in the presence of any of the ameliorants. No significant effects were observed between the two cultivars, ET8 and ES8. The root length of external controls (pH 5.5) were for ET8 $69.7 \text{ mm} \pm 0.37$ ($n = 3$) and ES8 $61.3 \text{ mm} \pm 0.77$ ($n = 3$).

Table 3.1. Effect of Al exposure and amelioration on root length in wheat. Data are means for ET8 and ES8 cultivars. Al treatments (+Al) were from germination at a concentration to reduce root elongation by 30% (2 μ M ES8 and 6 μ M ET8). The ameliorants were 1 mM $CaCl_2$, 1 mM $MgCl_2$ or 1 mM $NaSiO_4$. All solutions pH 4.5.

Al	Ameliorant	Mean root length (mm)
-Al	no ameliorant	30.6 ^c
	Ca^{2+}	72.7 ^a
	Mg^{2+}	67.0 ^a
	SiO_4^-	41.3 ^b
+Al	no ameliorant	21.2 ^d
	Ca^{2+}	68.8 ^a
	Mg^{2+}	70.3 ^a
	SiO_4^-	37.2 ^b
LSD (p = 0.05)		6.0

There was no significant three way interaction between, Al, ameliorant and cultivar for shoot length, however a significant interaction was observed between cultivar and Al (Table 3.2). A small but significant increase in shoot length was observed in ES8 in response to Al, but not in ET8. Shoot length was also significantly increased by Ca and Mg amelioration for all Al treatments and in both cultivars (Table 3.3). The shoot length of external controls (pH 5.5) were for ET8 37.7 mm \pm 2.9 (n = 3) and ES8 33.0 mm \pm 1.0 (n = 3).

Table 3.2. Effect of Al exposure and cultivar on shoot length in wheat. Data are means for all ameliorants. Al treatments (+Al) were from germination at a concentration to reduce root elongation by 30% (2 μ M ES8 and 6 μ M ET8). All solutions pH 4.5.

Al	Cultivar	Mean shoot length (mm)
-Al	ES8	33.1 ^b
	ET8	35.5 ^{ab}
+Al	ES8	36.5 ^a
	ET8	34.7 ^{ab}
LSD (p = 0.05)		2.8

Table 3.3. Effect of ameliorant on shoot length in wheat. Data are means for all cultivars and Al treatments. The ameliorants were 1 mM $CaCl_2$, 1 mM $MgCl_2$ or 1 mM $NaSiO_4$. All solutions pH 4.5.

Ameliorant	Mean shoot length (mm)
no ameliorant	31.2 ^b
Ca^{2+}	37.8 ^a
Mg^{2+}	38.4 ^a
SiO_4^-	32.4 ^b
LSD (p = 0.05)	2.8

There was no significant three way interaction between, Al, ameliorant and cultivar for root to shoot ratio, however there was a significant interaction between cultivar and ameliorant. Essentially it reflects the effects of ameliorants on root length because the ameliorants increase root length much more than shoot length. Treatment with Ca, Mg or silicate significantly increased the root to shoot ratio for both Al treatments. There was also a small difference in response to Ca between the two cultivars with ES8 showing a significantly greater ratio than ET8. The root:shoot ratios of external controls (pH 5.5) were for ET8 1.87 ± 0.14 (n = 3) and ES8 1.86 ± 0.07 (n = 3).

Table 3.4. Effect of ameliorant and cultivar on root to shoot ratio in wheat. Data are means for all cultivars and Al treatments. The ameliorants were 1 mM $CaCl_2$, 1 mM $MgCl_2$ or 1 mM $NaSiO_4$. All solutions pH 4.5.

Ameliorant	Cultivar	Root:shoot ratio
no ameliorant	ES8	0.81 ^d
	ET8	0.85 ^d
Ca^{2+}	ES8	2.01 ^a
	ET8	1.78 ^b
Mg^{2+}	ES8	1.85 ^{ab}
	ET8	1.75 ^b
SiO_4^-	ES8	1.14 ^c
	ET8	1.30 ^c
LSD (p = 0.05)		0.18

There was a significant three way interaction between Al, ameliorant and cultivar between meristem diameter, elongation zone diameter and mature zone diameter. At the meristem a significant increase in diameter was only observed in ES8 in response to silicate, Al and silicate and Al together (Table 3.5). In the elongation zone Al significantly increased the root diameter of both ET8 and ES8 though ES8 was significantly larger again than ET8 (Table 3.5). In the absence and presence of Al there were no significant changes in diameter with Ca or Mg amelioration (Table 3.5). With silicate however, in the absence of Al, the elongation zone diameter increased significantly in both ET8 and ES8 and once again the increase in diameter was significantly larger in ES8 than ET8 (Table 3.5). In addition to silicate, Al did not significantly change the diameter of ET8, but it significantly increased the diameter of ES8 (Table 3.5). In the mature zone a significant increase in diameter was only observed with four treatments; ET8 or ES8 with silicate and no Al, ET8 with Al and ET8 with Al and silicate (Table 3.5). The root diameters of external controls (pH 5.5) were for ET8: meristem $295.8 \mu\text{m} \pm 4.2$ ($n = 3$), elongation $445.8 \mu\text{m} \pm 11.0$ ($n = 3$), mature 516.7 ± 8.3 ($n = 3$); and for ES8 meristem $266.7 \mu\text{m} \pm 8.3$ ($n = 3$), elongation $437.5 \mu\text{m} \pm 12.5$ ($n = 3$), mature $508.3 \mu\text{m} \pm 22.0$ ($n = 3$).

Table 3.5. Effect of Al exposure, amelioration and cultivar on root diameter at the meristem, elongation zone and mature zone in wheat. Al treatments (+Al) were from germination at a concentration to reduce root elongation by 30% (2 μ M ES8 and 6 μ M ET8). The ameliorants were 1 mM $CaCl_2$, 1 mM $MgCl_2$ or 1 mM $NaSiO_4$. All solutions pH 4.5.

Al	Ameliorant	Cultivar	Meristem diameter (μm)	Elongation zone diameter (μm)	Mature zone diameter (μm)
-Al	no ameliorant	ES8	246 ^d	454 ^f	548 ^{bc}
		ET8	291 ^{abc}	475 ^{ef}	515 ^c
	Ca ²⁺	ES8	270 ^{bcd}	488 ^{ef}	517 ^c
		ET8	275 ^{bcd}	492 ^{ef}	521 ^{bc}
	Mg ²⁺	ES8	275 ^{bcd}	479 ^{ef}	504 ^c
		ET8	275 ^{bcd}	442 ^f	525 ^{bc}
	SiO ₄ ⁻	ES8	308 ^{ab}	663 ^b	625 ^a
		ET8	279 ^{bcd}	575 ^{cd}	579 ^b
+Al	no ameliorant	ES8	325 ^a	758 ^a	558 ^{bc}
		ET8	267 ^{cd}	583 ^c	579 ^b
	Ca ²⁺	ES8	258 ^{cd}	492 ^{ef}	542 ^{bc}
		ET8	267 ^{cd}	471 ^f	537 ^{bc}
	Mg ²⁺	ES8	267 ^{cd}	527 ^{de}	529 ^{bc}
		ET8	258 ^{cd}	483 ^{ef}	558 ^{bc}
	SiO ₄ ⁻	ES8	325 ^a	783 ^a	558 ^{bc}
		ET8	275 ^{bcd}	600 ^{bc}	667 ^{bc}
LSD (p = 0.05)			39	54	59

At low silicate concentrations in the solution amelioration was still observed. After four days 2.5 μ M Al significantly reduced root length, shoot length and root:shoot ratio (Figure 3.1). Inclusion of 25 μ M $NaSiO_4$ with Al significantly increased all parameters back to control levels. Silicate alone did not significantly affect growth parameters. These observations of root growth were paralleled by Ca^{2+} and K^+ fluxes from the root elongation zone. Ca^{2+} influx and K^+ efflux were both significantly reduced by Al exposure and restored to control values by the inclusion of silicate (Figure 3.2). Fluxes were measured for silicon amelioration alone as the mechanism of amelioration is significantly different to Ca and Mg (see discussion).

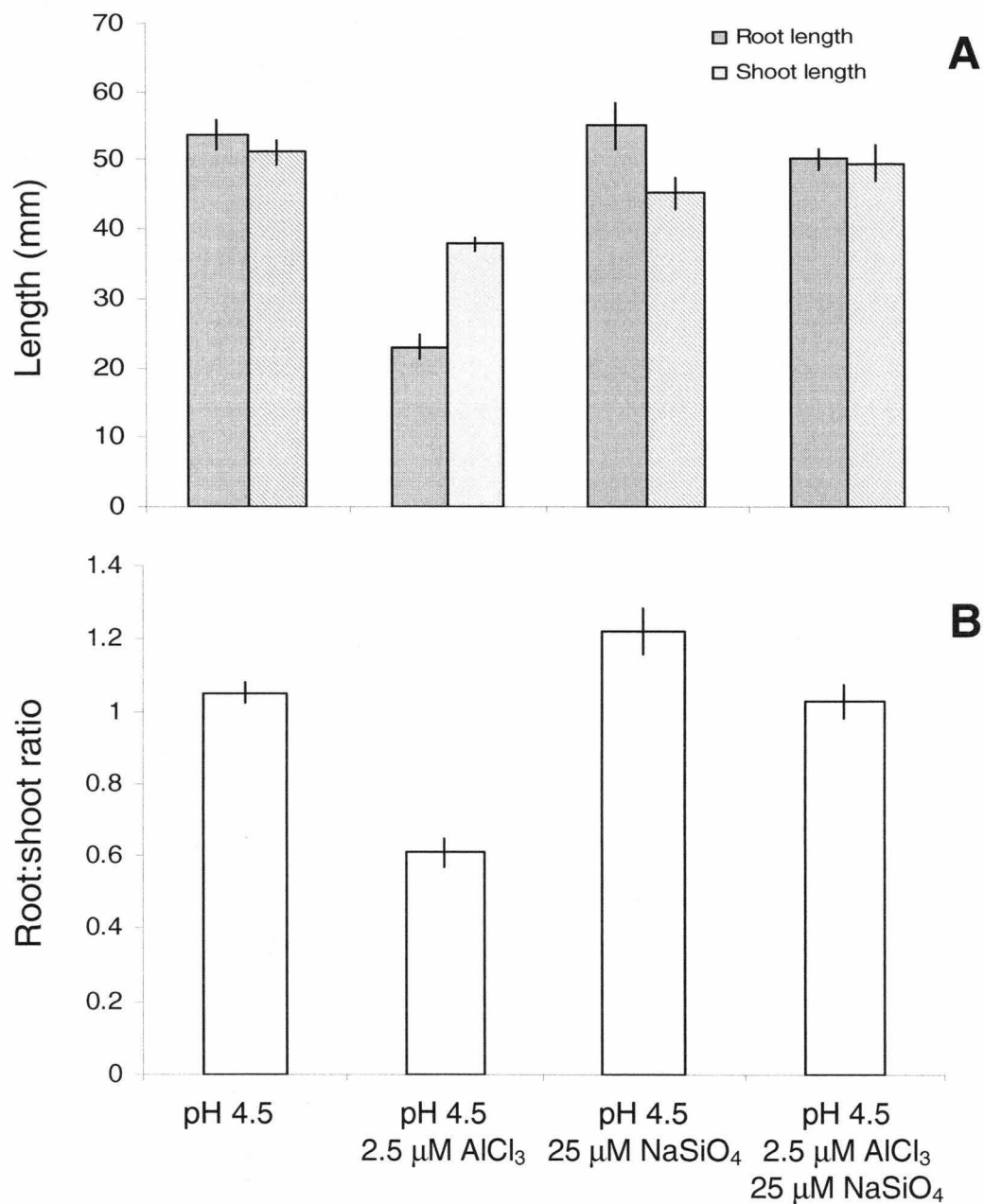


Figure 3.1. Effect of Al and amelioration by low concentrations of silicate from germination on root and shoot growth in ES8. Data are means \pm SEM (n = 6-8).

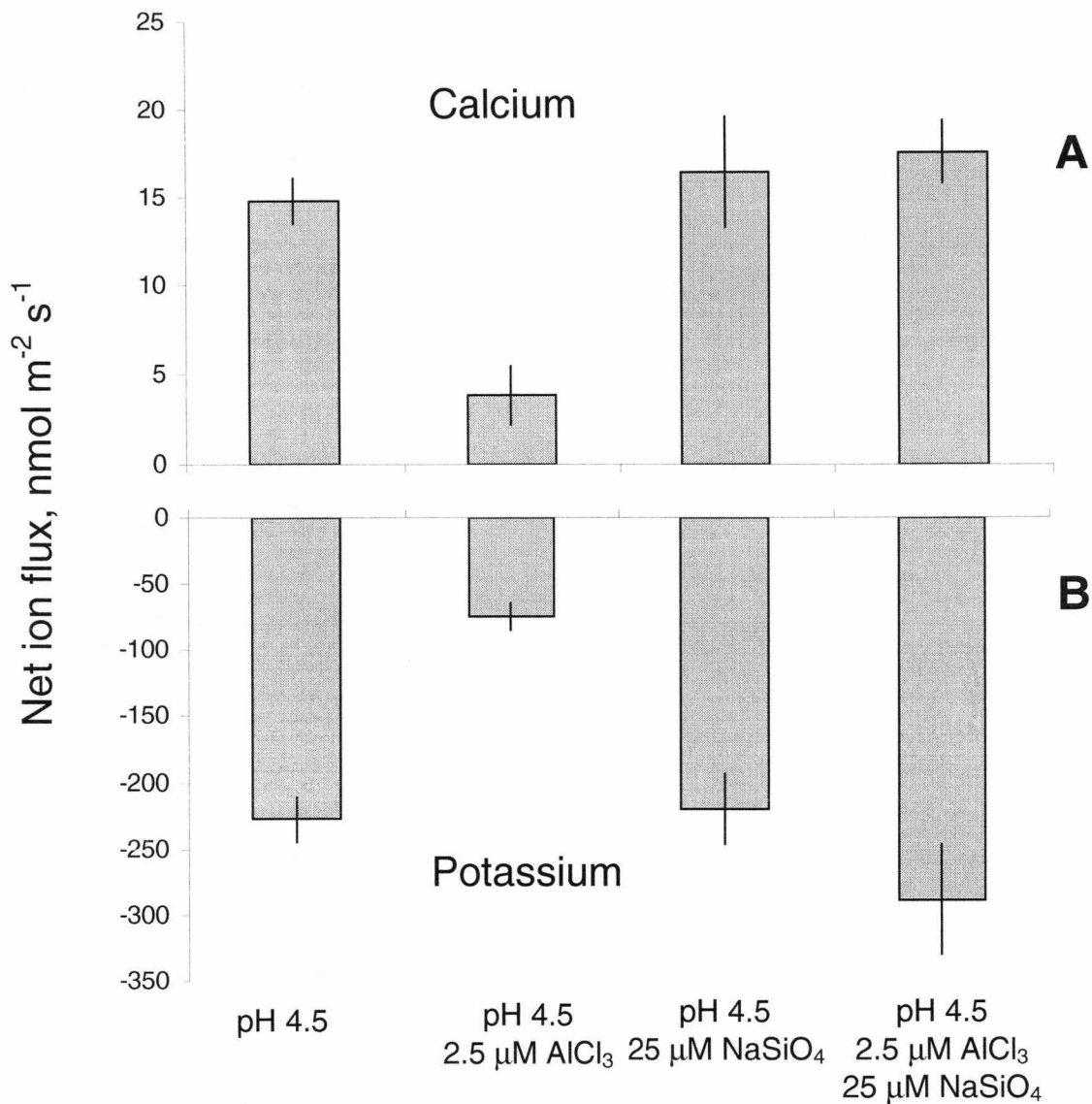


Figure 3.2. Effect of Al and amelioration by low concentrations of silicate from germination on Ca^{2+} and K^{+} fluxes from the elongation zone in ES8. Data are means \pm SEM ($n = 6-8$).

3.3.2 Effects of Al exposure, cultivar and amelioration by Ca²⁺, Mg²⁺ and silicate on root hair morphology

There was a significant three way interaction between Al, ameliorant and cultivar for root hair length. No root hairs were observed in ES8 exposed to Al, whereas root hair length significantly increased in ET8 exposed to Al (Table 3.6). In the absence of Al, Ca significantly increased root hair length in both ET8 and Mg significantly decreased root hair length in ES8. No root hairs were observed in ES8 treated with silicate. Ca and Mg both restored root hair length in Al treated ES8, and the Al plus Mg treatment was significantly higher than just Mg alone. In Al treated ET8, Mg caused a significant decrease in root hair length. Again for Al treated ES8 no root hairs were observed with silicate treatment. The root hair length of external controls (pH 5.5) was much longer than all other treatments. External controls (pH 5.5) for root hair length were for ET8 $320\ \mu\text{m} \pm 9.5$ ($n = 3$) and ES8 $306\ \mu\text{m} \pm 26.4$ ($n = 3$). Data are means \pm SEM. Active cytoplasmic streaming was observed in all treatments without Al, except silicate, and was also observed in the presence of Ca²⁺ and Al³⁺.

Table 3.6. Effect of Al exposure, amelioration and cultivar on root hair length in wheat. Al treatments (+Al) were from germination at a concentration to reduce root elongation by 30% (2 μ M ES8 and 6 μ M ET8). The ameliorants were 1 mM $CaCl_2$, 1 mM $MgCl_2$ or 1 mM $NaSiO_4$. All solutions pH 4.5.

Al	Ameliorant	Cultivar	Root hair length (μ m)
-Al	no ameliorant	ES8	128 ^{cd}
		ET8	106 ^{de}
	Ca ²⁺	ES8	147 ^{bc}
		ET8	151 ^{bc}
	Mg ²⁺	ES8	65 ^f
		ET8	71 ^{ef}
	SiO ₄ ⁻	ES8	-
		ET8	103 ^{de}
+Al	no ameliorant	ES8	-
		ET8	172 ^{ab}
	Ca ²⁺	ES8	140 ^c
		ET8	197 ^a
	Mg ²⁺	ES8	140 ^c
		ET8	106 ^{de}
	SiO ₄ ⁻	ES8	-
		ET8	106 ^{de}
LSD (p < 0.05)			30.5

There was a significant effect of cultivar, Al and ameliorant on root hair diameter, but no significant interactions. Root hair diameter was significantly thicker in ET8 ($13.53 \mu\text{m} \pm 0.26$, $n=24$) than ES8 ($11.70 \mu\text{m} \pm 0.33$, $n=13$) (Data are means, \pm SEM). Root hair diameter was significantly thinner after Al treatment ($12.32 \mu\text{m} \pm 0.30$, $n=18$) than without ($13.27 \mu\text{m} \pm 0.28$, $n=21$). Ca and Mg both significantly decreased root hair diameter, though Ca was significantly thinner than Mg (Table 3.7) The root hair diameters of external controls (pH 5.5) were for ET8 $10.1 \mu\text{m} \pm 0.7$ ($n = 3$) and ES8 $10.4 \mu\text{m} \pm 0.3$ ($n = 3$).

Table 3.7. Effect of ameliorant on root hair diameter in wheat. Data are means for all cultivars and Al treatments. The ameliorants were 1 mM CaCl_2 , 1 mM MgCl_2 or 1 mM NaSiO_4 . All solutions pH 4.5.

Ameliorant	Root hair diameter (μm)
no ameliorant	14.3 ^b
Ca^{2+}	11.0 ^c
Mg^{2+}	12.3 ^c
SiO_4^-	15.4 ^a
LSD ($p = 0.05$)	0.9

There was a significant interaction between Al and ameliorant for root hair density. There was a significant decrease in root hair density only for plants treated with Al and silicate (Table 3.8). It is important to remember that no root hairs were produced in ES8 with Al, silicate or Al plus silicate treatment (and consequently these were treated as missing data points), so the means for these treatments are from ET8 only. So Al does actually reduce root hair density in ES8 compared with ET8.

Table 3.8. Effect of Al exposure and amelioration on root hair density in wheat. Data are means for ET8 and ES8 cultivars. Al treatments (+Al) were from germination at a concentration to reduce root elongation by 30% (2 μ M ES8 and 6 μ M ET8). The ameliorants were 1 mM $CaCl_2$, 1 mM $MgCl_2$ or 1 mM $NaSiO_4$. All solutions pH 4.5.

Al	Ameliorant	Root hair density (#/mm)
-Al	no ameliorant	9.9 ^{bc}
	Ca^{2+}	10.8 ^{ac}
	Mg^{2+}	9.0 ^c
	SiO_4^-	12.7 ^a
+Al	no ameliorant	10.4 ^{bc}
	Ca^{2+}	11.6 ^{ab}
	Mg^{2+}	10.3 ^{bc}
	SiO_4^-	6.4 ^d
LSD (p = 0.05)		2.1

There was also a significant interaction between cultivar and ameliorant for root hair density (Table 3.9). This again simply shows that root hairs are not produced by ES8 in the presence of silicate.

Table 3.9. Effect of ameliorant and cultivar on root hair density in wheat. Data are means for all cultivars and Al treatments. The ameliorants were 1 mM $CaCl_2$, 1 mM $MgCl_2$ or 1 mM $NaSiO_4$. All solutions pH 4.5.

Ameliorant	Cultivar	Root hair density (#/mm)
no ameliorant	ES8	11.3 ^{ab}
	ET8	9.5 ^{bc}
Ca^{2+}	ES8	11.7 ^a
	ET8	10.7 ^{abc}
Mg^{2+}	ES8	8.9 ^c
	ET8	10.5 ^{ac}
SiO_4^-	ES8	-
	ET8	9.5 ^{bc}
LSD (p = 0.05)		2.1

For the length of the root hair zone, there were significant treatment effects for Al and ameliorant, but no significant interactions. Al significantly decreased the length of root hair zone compared with no Al ($36.1\text{ mm} \pm 1.2$, $n=18$; $33.6\text{ mm} \pm 1.3$, $n=21$ respectively). All ameliorants significantly increased the length of the root hair zone in the order silicate<<Mg<Ca (Table 3.10).

Table 3.10. Effect of ameliorant on length of the root hair zone in wheat. Data are means for all cultivars and Al treatments. The ameliorants were 1 mM $CaCl_2$, 1 mM $MgCl_2$ or 1 mM $NaSiO_4$. All solutions pH 4.5.

Ameliorant	Root hair zone length (mm)
no ameliorant	13.1 ^d
Ca^{2+}	53.0 ^a
Mg^{2+}	41.0 ^b
SiO_4^-	19.6 ^c
LSD ($p = 0.05$)	4.6

There was a significant three way interaction between cultivar, Al and ameliorant for the calculated total root hair surface area. The root hair surface area was not significantly reduced by Al in ET8 however it was completely abolished in ES8 (Table 3.11). Ca significantly increased root hair surface area in the presence and absence of Al, though the effect was significantly higher in Al treated ET8 compared with ES8 (Table 3.11). Additionally, combined Ca and Al treatment significantly increased ET8 and decreased ES8 root hair surface area compared with Ca alone (Table 3.11). Mg significantly increased the root hair surface area in ET8 without Al and in both ET8 and ES8 with Al (Table 3.11). Silicate completely abolished root hair growth in ES8 in the presence and absence of Al, whereas in ET8 it was significantly increased by silicate in the absence of Al (Table 3.11).

Table 3.11. Effect of Al exposure, amelioration and cultivar on total root hair surface area in wheat. Al treatments (+Al) were from germination at a concentration to reduce root elongation by 30% (2 μ M ES8 and 6 μ M ET8). The ameliorants were 1 mM $CaCl_2$, 1 mM $MgCl_2$ or 1 mM $NaSiO_4$. All solutions pH 4.5.

Al	Ameliorant	Cultivar	Root hair surface area (mm ²)
-Al	no ameliorant	ES8	0.80 ^{gh}
		ET8	0.74 ^h
	Ca ²⁺	ES8	3.53 ^{ab}
		ET8	2.89 ^c
	Mg ²⁺	ES8	0.88 ^{fg}
		ET8	1.48 ^{eg}
	SiO ₄ ⁻	ES8	-
		ET8	1.67 ^e
+Al	no ameliorant	ES8	-
		ET8	2.65 ^{cd}
	Ca ²⁺	ES8	2.65 ^{cd}
		ET8	3.76 ^a
	Mg ²⁺	ES8	1.98 ^{de}
		ET8	1.60 ^{ef}
	SiO ₄ ⁻	ES8	-
		ET8	0.43 ^h
LSD (p < 0.05)			0.72

3.3.3 Effects of 24 hr Al exposure on root hair morphology and fluxes from the root hair zone in ET8 and ES8

In four day old plants, 24 hr treatment with Al significantly increased root hair length in both ET8 and ES8 (Figure 3.3). The only significant difference between ET8 and ES8 in root hair length was observed at 100 μM Al where ET8 was greater (Figure 3.3). However root hair density was significantly higher in ET8 than ES8 for all Al treatments. Root hair density even increased in ET8 with Al^{3+} application up to 25 μM , after which it declined. This apparent tolerance of ET8 root hairs was reflected in fluxes of K^+ , H^+ and Cl^- from the root hair zone (Figure 3.4). Compared with control, fluxes of H^+ , K^+ and Cl^- were maintained in ET8 up to 25 μM $AlCl_3$, above which they declined. In comparison the fluxes in ES8 declined in all Al treatments and even reversed at high Al concentrations. The net fluxes in ET8 and ES8 control were roughly 50 $nmol\ m^{-2}s^{-1}$ K^+ influx, 120 $nmol\ m^{-2}s^{-1}$ H^+ efflux and 40 $nmol\ m^{-2}s^{-1}$ Cl^- influx.

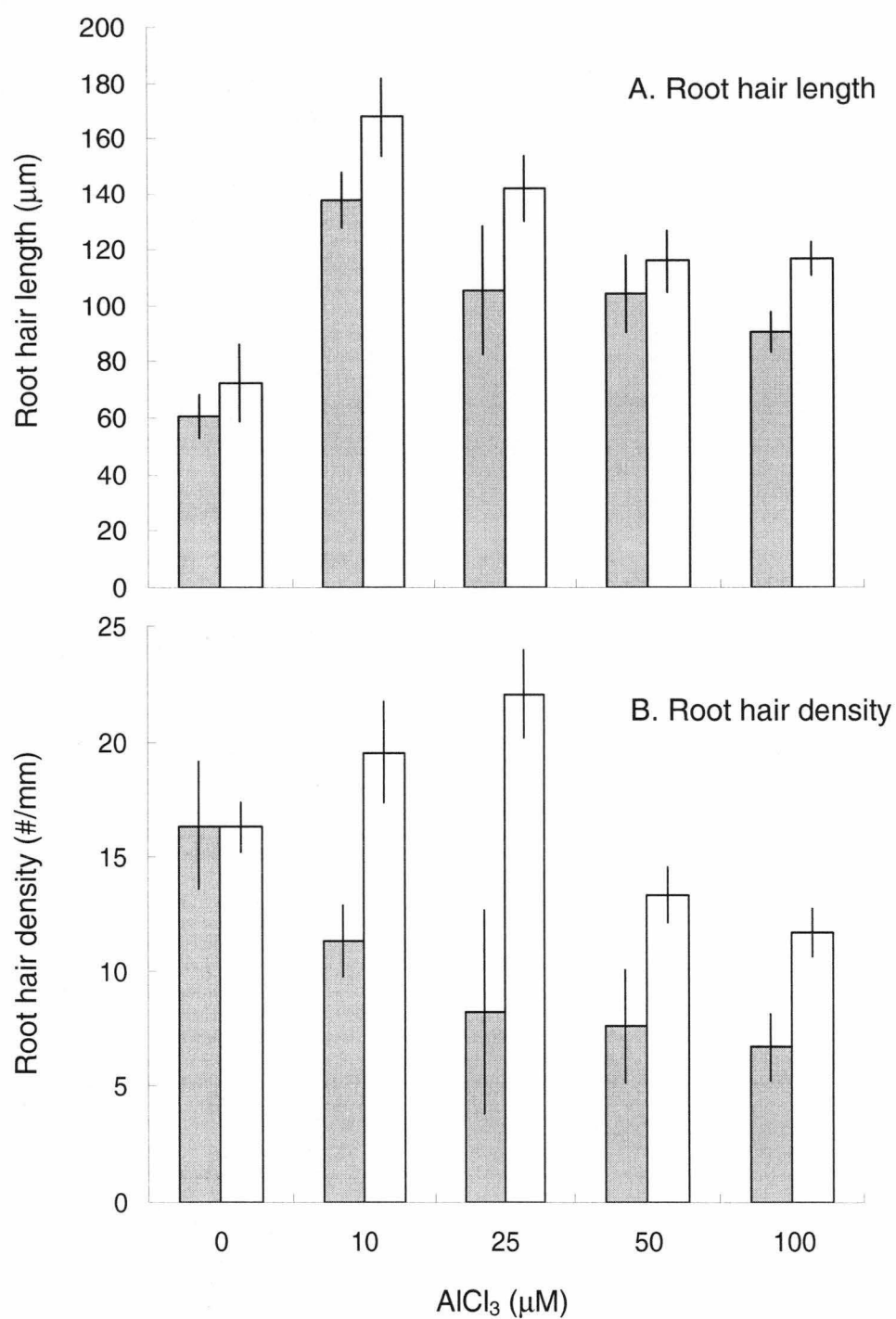


Figure 3.3. Root hair length and density measured in the mature root hair zone following a 24 h treatment with different Al^{3+} concentrations. Results are shown for ET8 (open bars) and ES8 (closed bars). Error bars are \pm SEM ($n = 5$ to 11).

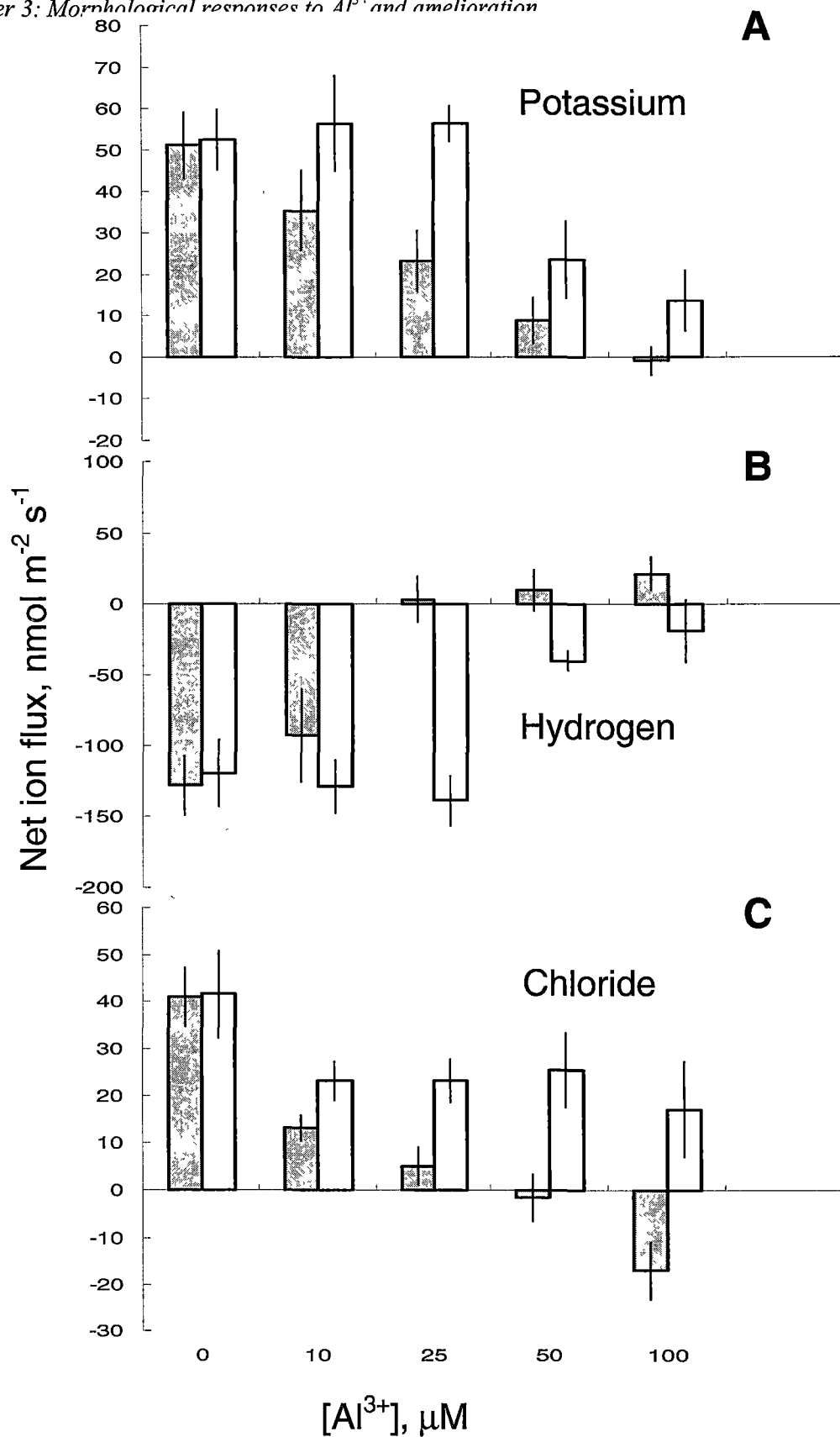


Figure 3.4. Net ion fluxes measured mature root hair zone following a 24 h treatment with different Al^{3+} concentrations. Results are shown for ET8 (open bars) and ES8 (closed bars). Error bars are \pm SEM ($n = 5$ to 12).

3.4 Discussion

3.4.1 Effects of Al exposure, cultivar and amelioration by Ca^{2+} , Mg^{2+} and silicate on wheat root and shoot characteristics

It is well established that ET8 and ES8 differ significantly in tolerance of root elongation in the presence of the same concentration of Al, but it is interesting to examine the effects of Al that cause equal inhibition of root elongation. This allows the determination of other aspects of plant growth that show differential tolerance between the two cultivars and allows determination of significant interactions between the two cultivars and ameliorants. The lack of a significant effect between ET8 and ES8 root lengths in the presence of Al (Table 3.1) shows that the Al concentrations selected for each cultivar (ES8 2 μ M and ET8 6 μ M) were appropriate to reduce root elongation equally. Whilst the root length showed no difference, elongation zone root diameter in the presence of Al was significantly higher in ES8 than ET8 suggesting this may be a more sensitive indicator of tolerance (Table 3.5). Meristem and elongation zone diameter both increased significantly in both cultivars with Al treatment. This increase of diameter is indicative of the disorganisation of cellulose micro fibrils that causes cellular expansion in all directions rather than linearly and may be responsible in part for reduction of root elongation (Blancaflor *et al.*, 1998; Sivaguru *et al.*, 1999). However, in this instance, alteration of cellular expansion, observed by increased root tip diameter, is not the most important factor in root elongation because there was no significant difference between ET8 and ES8 root length in the presence of Al or silicate. The small increase in shoot length observed in ES8 in the presence of Al (Table 3.2) was unexpected and remains unexplained at this stage.

3.4.2 Amelioration by Ca^{2+} , Mg^{2+} and silicate

Significant amelioration of root elongation by all ameliorants was observed for all Al treatments and cultivars. Geochem (Parker *et al.*, 1987) calculations suggest that 1 mM $MgCl_2$ or $CaCl_2$ only reduces Al^{3+} activity by ~25%. It is likely that this reduction in Al^{3+} activity is not the main explanation of amelioration by Ca or Mg because root and shoot growth were restored to that of the external, high pH controls (Table 3.1; Table 3.3). It seems Mg and Ca must also ameliorate H^+ toxicity. Whilst no significant differences were observed between Mg and Ca amelioration of root length, root hair growth in both Al free and Al treated solutions was commonly lower with Mg than Ca (Table 3.6; Table 3.10; Table 3.11). Rather than implying a different root hair amelioration mechanism for Ca and Mg this is probably simply a reflection that high Mg concentrations will reduce Ca^{2+} uptake in the root hair tip and consequently elongation rate will be reduced (Demidchik *et al.*, 2002).

Interestingly there was no significant interaction between cultivar and ameliorants. Previous research has suggested that Mg can be more effective than Ca by enhancing organic acid efflux (Silva *et al.*, 2001), so it might be expected that Mg ameliorants would provide better protection for ET8 than ES8 because it has greater capacity for malate efflux (Delhaize *et al.*, 1993 b). However higher malate release in Mg treatments was not observed. Unfortunately the differences in malate efflux could not be directly examined from the bulk solution malate concentration, because in all solutions malate was below the limits of detection. The similar efficacy of Mg and Ca to ameliorate low pH and Al suggest that a similar mechanism is operating in both. The mechanisms most likely involved include reduced Al binding to the membrane surface (Jones and Kochian, 1997) and improved Ca and Mg nutrition which are often deficient in low pH soils.

In contrast, the mechanism of silicate amelioration must be vastly different because amelioration was only observed in root length (Table 3.1). Silicate actually reduced root hair growth in ET8 and completely abolished it in ES8 (Table 3.6). Because silicate is negatively charged it will not reduce Al^{3+} activity at the membrane through decreased membrane surface charge. Various mechanisms for silicate induced amelioration have been suggested including release of phenolics, and internal and external Al complexing (Hodson and Sangster, 1999; Kidd *et al.*, 2001). As for Ca and Mg, silicate appears ameliorate at both low pH and Al, because at high concentrations root length significantly increased in the absence of Al and was not significantly reduced by the inclusion of Al with silicate (Table 3.1). The $NaSiO_4$ concentrations used were selected on the basis of other values used in the literature, where SiO_4 was presumed to not affect Al^{3+} activity because it did not affect malate exudation (Cocker *et al.*, 1998b). However it is unclear what the real effect of SiO_4 on Al^{3+} activity in solution is because Geochem (Parker *et al.*, 1987) could not complete the calculations for my high $NaSiO_4$ solutions. All inputs were checked thoroughly for mistakes, but the same error occurred each time. In low silicate solutions, which others claim to have no effect on Al activity in solution, activity was actually reduced by 90% (Parker, *et al.*, 1987). At low concentrations silicate ameliorated Al suppression of root growth, but did not significantly increase root length in the absence of Al (Figure 3.1). In order to see if low silicate concentrations significantly affected membrane transport processes, Ca^{2+} and K^+ fluxes were measured from the elongation zone (Figure 3.2). Silicate did not significantly alter the fluxes of Ca^{2+} or K^+ in the absence of Al, but it did restore fluxes to control levels in Al treated plants. Essentially these changes in flux seem to reflect the root elongation rate rather than any mechanism of amelioration. Clearly more work is required to clarify the

mechanism of silicate induced amelioration and even simply its effect on Al in solution.

3.4.3 Interaction of Al and cultivar on wheat root hair development

It is clear that ET8 and ES8 root hairs differ markedly in their tolerance of Al because Al concentrations that equally inhibit root length completely abolish root hair development in ES8, significantly increase root hair length and surface area in ET8 (Table 3.6 & Table 3.11). Similarly in 24 hr exposure to Al, once root hairs have already developed, ET8 root hairs were more tolerant than ES8 (Figure 3.3). MIFE experiments measuring the fluxes of K^+ , H^+ and Cl^- from the mature root hair zone showed significantly higher tolerance of fluxes to Al in ET8 than ES8 (Figure 3.4). Under control conditions there was a net influx of K^+ and Cl^- and efflux of H^+ . Maintenance of K^+ and Cl^- influx is essential for turgor regulation and consequently root hair elongation, possibly explaining why root hair growth was better in ET8 than ES8 in all Al treatments. In ES8 at Al concentrations where roots still have a significant density of root hairs, fluxes are reduced and even reversed, suggesting that the differences in fluxes cannot simply be explained by changes in root hair density (Figures 3.3 & 3.4). This suggests that there is some greater tolerance of transport mechanisms in ET8. At the low solution K^+ concentration of these experiments the majority of K^+ uptake will be active, mediated by H^+/K^+ symporters (Maathuis and Sanders, 1996; Santa-Maria *et al.*, 2000), it has also been suggested that the K^+ channel AKT1 may contribute (Very and Sentenac, 2003) though membrane potential suggests this is quite unlikely. The maintenance of H^+ efflux in ET8, but not ES8, in the presence of Al suggests that maintenance of H^+ ATPase activity may be part of the tolerance mechanism in root hairs to reduce acidification of the cytoplasm and to

maintain the proton gradient for K^+ uptake. Chloride uptake is also dependent upon a H^+/Cl^- symporter that has a stoichiometry of between 1:1 and 1:4 (Mistrik and Ullrich, 1996).

One possible hypothesis for the difference in root hair tolerance between the two wheat isogenic lines is that higher release of malate from ET8 increases solution malate concentration that confers tolerance. However in all treatments solution malate was less than 500 nm, which will have negligible effect on free Al^{3+} activity. It is possible that it may still be a malate effect if malate released from the root apex is retained in the cell walls and is still effective to reduce Al activity in the root region where root hairs are expanding. However this seems unlikely because significant differences were also observed in 24 hr treatment in which root hairs were already developed prior to Al treatment. It seems more likely therefore that the difference between ET8 and ES8 root hair tolerance is either expressed at the root hairs themselves or through differential production of hormones from the root tip under Al stress. The interaction between auxin transport and ethylene sensitivity is critical in root hair growth, and exogenous blockers that inhibit auxin transport reduce root hair length and density in *Arabidopsis* (Rahman *et al.*, 2002). Importantly in maize it has been shown that basipetal transport of exogenous IAA is decreased more in sensitive than tolerant cultivars (Kollmeier *et al.*, 2000). Whether ET8 and ES8 differ in their capacity to transport auxin in the presence of Al is unknown. To the best of my knowledge there are no reports suggesting malate exudation can occur from the root hairs. My data provides circumstantial evidence to support this, as net K^+ flux moves towards efflux more in ES8 than ET8 (Figure 3.4. Net ion fluxes measured mature root hair zone following a 24 h treatment with different Al^{3+} concentrations. Results

are shown for ET8 (open bars) and ES8 (closed bars). Error bars are \pm SEM (n = 5 to 12).).

The difference between ET8 and ES8 root hairs in tolerance to Al is highly surprising because it implies there may be more differences between ET8 and ES8 than simply Al tolerance mechanisms at the root tip. Future research should explore whether or not these differences are due to tolerance expressed at the root hair or at the root tip and whether there are any other differences between ET8 and ES8 which could contribute to greater tolerance of root hairs.

In summary, Mg^{2+} , Ca^{2+} , and to a lesser extent silicate all significantly ameliorate Al toxicity. The use of these ameliorants in management of acidic soils should be investigated further because Mg^{2+} and Ca^{2+} particularly, restored root growth to that of high pH controls. My data suggests that the mechanisms of amelioration by Mg^{2+} and Ca^{2+} are essentially similar, but SiO_4 amelioration is radically different and should be investigated further. The most significant finding of this chapter is that ET8 root hair growth and root hair zone nutrient acquisition show higher tolerance for Al than ES8. This appears contrary to the presumption that the only difference in tolerance between ET8 and ES8 is expressed only at the root apex. Further research is required to assess if it is in fact due to differences expressed at the root hairs or the apex via hormones or malate retention.

Chapter 4: Effect of Al^{3+} on membrane potential and ion fluxes at the root apex¹

4.1 Introduction

Significant variation in Al tolerance can exist within some plant species such as maize and wheat, and the mechanisms responsible for this variation have attracted considerable interest over the past 40 years. Many studies have described an Al-activated efflux of organic anions from the roots of a range of species and evidence from some of these indicate that the organic anions protect the plants from Al by chelating the harmful cations to form non-toxic complexes (Delhaize and Ryan, 1995; Ma *et al.*, 2001; Ryan *et al.*, 2001). Wheat provides some of the most compelling evidence for this hypothesis since much of the data was collected on a pair of near-isogenic lines, ET8 and ES8, that differ in Al tolerance at a single genetic locus (Delhaize *et al.*, 1993a; Delhaize *et al.*, 1993b; Ryan *et al.*, 1995b, a). Aluminium rapidly activates a large and sustained efflux of malate from the root apices of the Al-tolerant ET8. This response shows a saturating dependence on external Al concentration whereas the responses with several other trivalent cations tested (eg. La^{3+} and Ga^{3+}) were significantly smaller (Ryan *et al.*, 1995a; Kataoka *et al.*, 2002b). By contrast, the efflux of malate from the Al-sensitive ES8 genotype is small or absent. The gene associated with Al-induced malate release in wheat was recently isolated by Sasaki *et al.* (2004). The gene, designated *ALMT1*, encodes a membrane protein that facilitates an Al-activated malate efflux when expressed in tobacco, rice, barley and *Xenopus* oocytes (Delhaize *et al.*, 2004; Sasaki *et al.*, 2004).

¹ The contents of this chapter have already been published: Wherrett T., Ryan P.R., Delhaize E., Shabala S. (2005) Effect of aluminium on membrane potential and ion fluxes at the apices of wheat roots *Functional Plant Biology* **32**(3):199-208

The magnitude of the electrical potential difference across a plant-cell membrane (V_m) is a function of a diffusion potential and the activity of energy-dependent transport systems on the plasma membrane such as H^+ -ATPase which pumps H^+ out of the cell. The movement of ions across a cell membrane will affect V_m unless they are exquisitely balanced by the movement of other ions to maintain electroneutrality. Aluminium has the potential to affect V_m by directly interacting with the membrane to alter its structure and fluidity (Chen *et al.*, 1991), by blocking Ca^{2+} and K^+ channels (Ding *et al.*, 1993; Pineros and Tester, 1993; Gassmann and Schroeder, 1994) or by inhibiting the H^+ -ATPase in the plasma membrane (Ahn *et al.*, 2002). The Al-dependent release of malate anions from the roots of Al-tolerant wheat plants will depolarise those cells unless the flow of charge is balanced by the movement of other ions. Several studies have now demonstrated that the Al-activated malate efflux is accompanied by K^+ efflux and it has been proposed that this can account for electroneutrality (Ryan *et al.*, 1995a; Osawa and Matsumoto, 2002). However, all these studies used excised root apices and relatively short treatment times and it remains unclear whether a similar response operates in intact roots and whether it is sustained over long periods of Al exposure. We can predict that V_m in the root apices of Al-tolerant and Al-sensitive wheat will be affected differently by Al because Al-activated malate and K^+ efflux occur only from tolerant plants. However, it is difficult to predict how large these changes will be because they depend on membrane conductance and how rapidly the flow of balancing ions is initiated.

Although the effect of Al treatment on the V_m of root cells has been measured in a variety of species (Kinraide, 1988; Miyasaka *et al.*, 1989; Lindberg *et al.*, 1991; Olivetti *et al.*, 1995; Sasaki *et al.*, 1995; Lindberg and Strid, 1997; Papernik and Kochian, 1997; Takabatake and Shimmen, 1997; Pavlovkin and Mistrik, 1999) only

two studies have directly compared Al-tolerant and sensitive genotypes of wheat and the results from these are not consistent with one another. One study found that Al hyperpolarized the membrane in both genotypes (Lindberg and Strid, 1997) while the other found that Al depolarised the cells in Al-tolerant cultivars, but not Al sensitive cultivars (Papernik and Kochian, 1997).

In order to better understand the physiology of Al tolerance I have used near-isogenic wheat lines that differ in Al tolerance (ET8 and ES8) to investigate the effects of Al on root-cell V_m and measure the net ion fluxes that might contribute to the observed changes in V_m . These lines are over 99% identical to one another (Delhaize *et al.*, 1993b; Delhaize and Ryan, 1995) so any differences that are observed between them are almost certainly associated with the mechanism of Al tolerance and not due to some non-specific difference between the genotypes. My results show that the Al-tolerant and sensitive genotypes respond differently to Al and provide the first kinetics of Al-activated efflux of K^+ from intact wheat plants.

4.2 Materials and Methods

4.2.1 Plant materials

The near isogenic wheat (*Triticum aestivum* L.) lines, ET8 (Al-tolerant) and ES8 (Al-sensitive) were grown for 3-4 days on floating mesh in plastic containers with 0.5 L of aerated solution (control solution for ion flux measurements) containing 0.1mM $CaNO_3$, 0.1 mM $MgSO_4$, 0.1 mM KCl and 0.1 mM NH_4NO_3 . The pH of the solution after 4 days of growth was approximately pH 4.0.

4.2.2 Spatial distribution of malate efflux in ET8

The apical 3.0mm of 4 day old ET8 roots was excised and further divided into 0-1mm, 1-2mm and 2-3mm segments for analysis of malate efflux. Fifteen apices were collected for each measurement, and three replicates were made. Analysis of malate efflux was made essentially as described in chapter 3.3 except efflux was measured from the excised root sections as in Ryan *et al.* (1995a). Briefly, excised segments were transferred to a sterile 5 ml sample tube with 0.2 mM CaCl_2 , pH 4.3. Segments were gently rinsed with the same solution, then 1.0 mL of solution was added to each tube. The tubes were sealed with parafilm and transferred to a shaker (70 rpm). After 30 min the solution was discarded and replaced with 1 mL of 0.2 mM CaCl_2 , 50 μM AlCl_3 , pH 4.3. After a further 2 hr on the shaker the malate concentration in solution was measured as described in chapter 3.3.

4.2.3 Effects of Al on membrane potential

The roots of an intact wheat plant were mounted in a measuring chamber such that the roots were gently secured in a horizontal position with silicon grease and small plastic blocks. The plant was allowed to stabilize for 40-60 min while control solution (0.2 mM CaCl_2 , 2 mM NaCl , pH 4.3) flowed through the chamber. Measurements of the electrical potential difference (V_m) across the root-cell membranes were made at two positions along the root. One position was in the elongation zone (1 mm from the meristem) which was within the region of tissue previously found to release malate and K^+ . The other position was >10 mm farther back from the root cap and outside the region responsible for malate and K^+ efflux. The borosilicate glass microelectrodes (Clark Electromedical Instruments, Reading, UK) were filled with 2 M KCl, connected to an electrometer (FD 223, World Precision Instruments, Sarasota, FL

USA) via a Ag-AgCl half-cell and inserted into the root tissue with a manually operated micromanipulator (Narishige, Japan). V_m was monitored continually on a chart recorder. To minimise the difficulties associated with variable unstirred layers (Walker *et al.*, 1979), the solution flow-rate across the root surface was maintained constant during an experiment at approximately 4.0 mm s^{-1} . Once a stable measurement of V_m was obtained the same solution containing $50 \text{ }\mu\text{M AlCl}_3$ was flowed into the chamber. Measurements were also made from a number of plants using the same experimental protocol as for the non-invasive ion flux measurements.

4.2.4 Non-invasive ion flux measurements

Net ion fluxes were estimated by measuring the ion gradients in the unstirred layers near the root surface using the MIFE technique (Newman *et al.*, 1987; Shabala *et al.*, 1997). Details on fabrication and calibration of H^+ , K^+ , and Cl^- ion selective microelectrodes were as described previously in the general materials and methods. The only modification used in this study was that the Cl^- electrode tip was made 8-10 μm (compared with 2-3 μm for K^+ and H^+) to improve the responsiveness and to minimise electrode drift.

4.2.5 Short-term effects of Al on ion fluxes

Plants were transferred to fresh solution and selected seedlings had their root caps removed as described previously (Shabala *et al.*, 1997) to avoid the confounding effects of gravitropism on root curvature and ion fluxes (Weisenseel *et al.*, 1992; Shabala and Knowles, 2002). Roots were then placed horizontally in the measuring chamber filled with fresh solution and plants were left to equilibrate for up to 1 h. Elongation rate was measured prior to measurement to ensure root cap removal had

not affected growth. Fluxes of K^+ , H^+ and Cl^- were measured for 40 minutes in control (minus Al) and then for 2 h after addition of 50 μM $AlCl_3$. Measurements were made at two positions near the root apex, which is the region associated with the Al-activated efflux of malate and K^+ . One position was at the meristem clearly visible under a light microscope by the cubic shape of the cells (approximately 0.5 mm from the root tip) and the other position was 1 mm further back, in the elongation zone. The electrodes were moved from one position on the root to the other (meristem and elongation zone) every 2 minutes, with a 90 s measurement period at each position. A minimum of 6 replicate measurements were made for each ion and each genotype.

4.2.6 Long-term effects of Al on ion fluxes

Seedlings were grown in nutrient solution for 3 d and then 0, 10, 25 or 50 μM $AlCl_3$ was added (pH 4.0 adjusted with HCl). After 24 h a single seedling was removed from the solution and placed into the measuring chamber as described above. MIFE measurements were made in the same regions of the root as described above. A minimum of 6 replicates were made for each cultivar at each $AlCl_3$ concentration.

4.2.7 Effect of exogenous malate on K^+ fluxes

ET8 seedlings were prepared as for short term fluxes (4.2.5). K^+ fluxes were measured from the elongation zone for 5 min before 100 μM malate was added to solution. K^+ fluxes were measured for a further 15 min. 6 replicates were performed.

4.3 Results

4.3.1 Effect of Al on root growth and malate efflux

Root growth of the ET8 and ES8 near-isogenic lines was similar in the absence of Al. However, elongation of the Al-sensitive ES8 was inhibited by 24h treatment of 10 μM AlCl_3 whereas ET8 still showed some elongation in 10, 25 and 50 μM AlCl_3 (Figure 4.1).

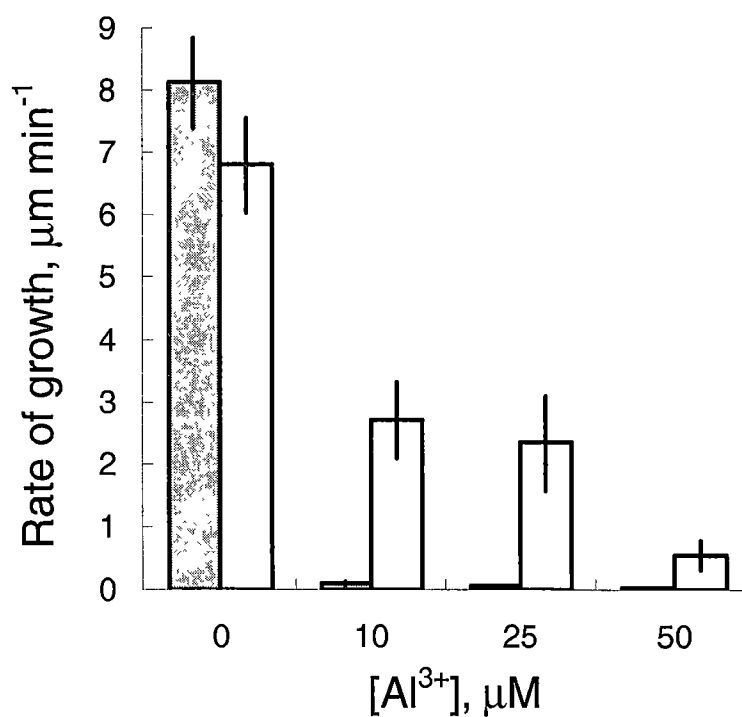


Figure 4.1. Effect of Al^{3+} on root growth of ET8 (open bars) and ES8 (closed bars) wheat lines. Mean root growth rates after 1 d treatment in a range of Al^{3+} concentrations are shown. Errors are \pm SEM ($n = 10-12$).

The spatial variation of Al-activated malate efflux from Al-tolerant wheat roots was also investigated by excising millimetre lengths of ET8 roots at the root apex and treating them with 50 μM AlCl_3 . The greatest malate efflux occurred 1-2 mm from the root tip, which incorporated the elongation zone (Figure 4.2). Efflux from the 0-1 mm and 2-3 mm sections were significantly lower (Figure 4.2). No malate efflux was detected from root tissues excised 10 mm back from the root apex (data not shown), which is consistent with previous reports (Ryan *et al.*, 1995a).

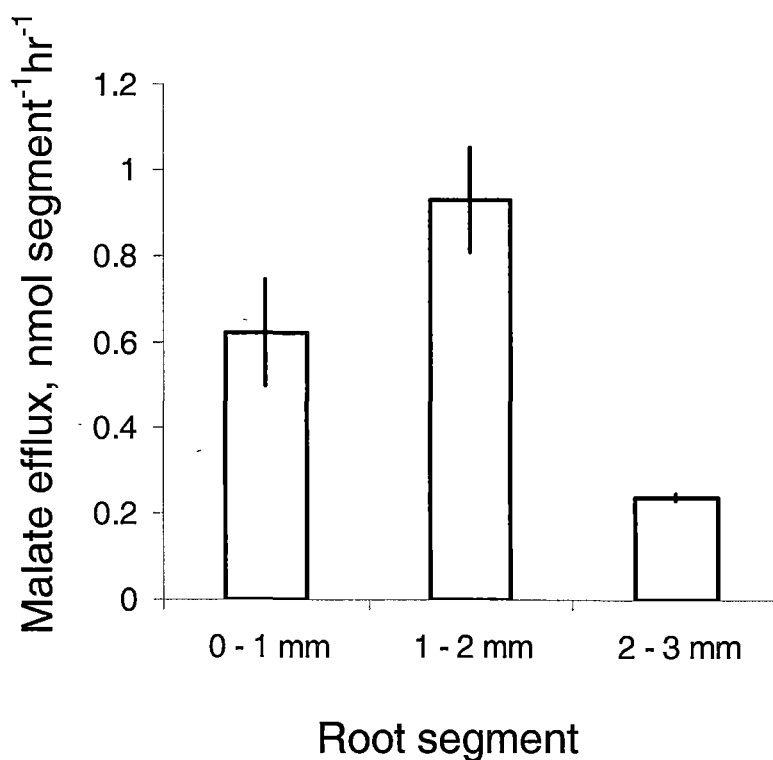


Figure 4.2. Spatial distribution of malate efflux from the terminal 3.0mm of ET8 apices in response to addition of 50 μM Al^{3+} . Errors are \pm SEM ($n = 3$)²

² The data in this figure was collected in collaboration with Peter Ryan and Emmanuel Delhaize

4.3.2 Effect of Al on root-cell V_m

The magnitude of the electrical potential difference across the root-cell membranes (V_m) in control solution was -112 ± 2.7 mV (SE, $n = 35$) at the elongation zone and -156.4 ± 3.9 mV (SE, $n = 20$) in the mature cells (> 10 mm farther back). No differences were detected between ET8 and ES8 prior to addition of Al^{3+} (data not shown). Addition of $50 \mu M AlCl_3$ induced a complex change in V_m at the root apex, but a pattern emerged that could be described by three distinct phases (Figure 4.3).

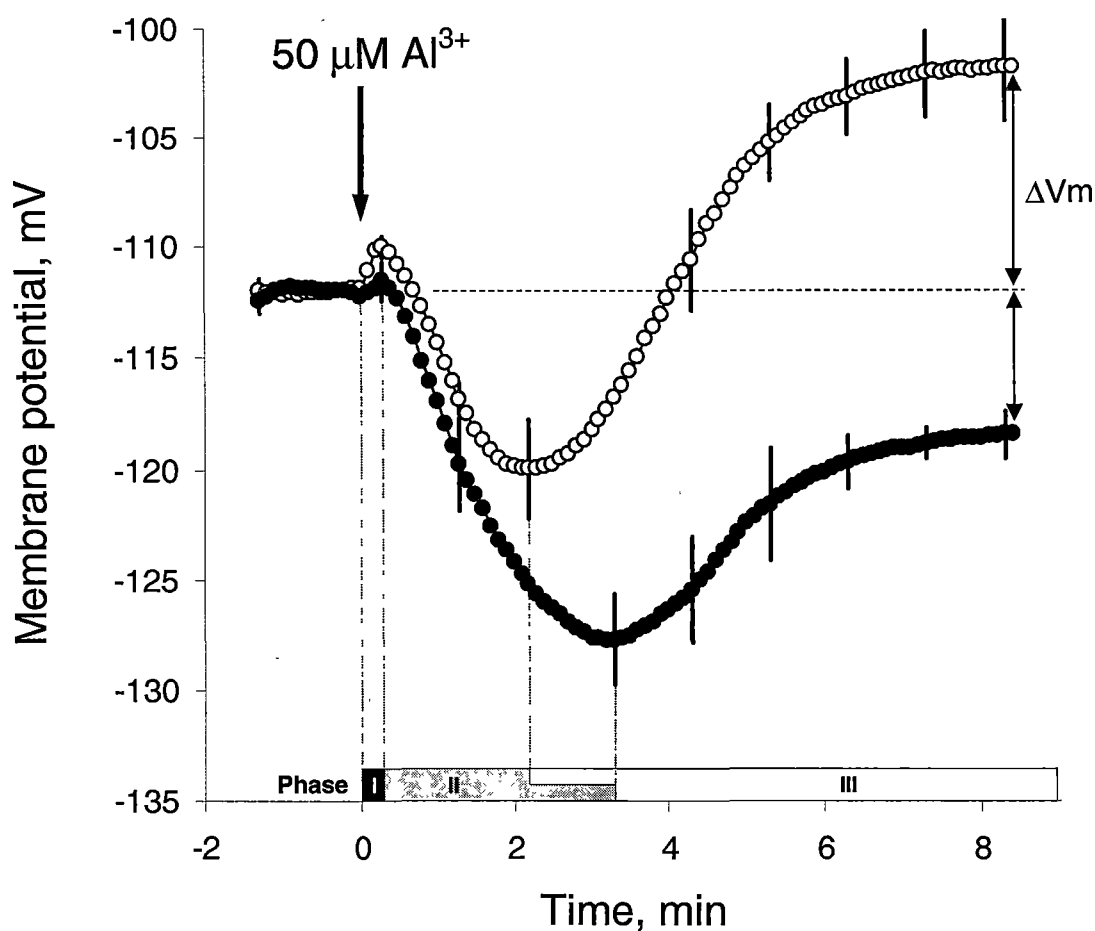


Figure 4.3. Average response of V_m to Al measured at the elongation zone in ET8 (open symbols) and ES8 (closed symbols) plants. At 0 min, 50 μM AlCl_3 was added and the response of V_m could be described by three separate phases (see text). Phase III ΔV_m was measured at 8.4 min as indicated by the arrows. The maximum hyperpolarisation of phase II was significantly smaller and earlier ($p < 0.01$) in ET8 (2.2 min ± 0.17) than ES8 (3.3 min ± 0.29). Error bars are \pm SEM ($n = 6$ to 7).³

³ The data in this figure was collected in collaboration with Peter Ryan and Emmanuel Delhaize

In most cases a small transient depolarisation (less negative) was observed immediately after adding Al, designated phase I. This was followed by a hyperpolarisation (more negative) lasting 2-4min (phase II). Finally, a slower depolarisation continued for up to 12 min and this was designated as phase III. The magnitudes of the changes in phase I were similar in ET8 and ES8, but the hyperpolarisation in phase II was significantly smaller and peaked sooner ($p < 0.01$) and the depolarisation in phase III was significantly ($p < 0.01$) larger in ET8 (Figure 4.3). This resulted in the final V_m for ET8 plants being more positive than the pre-Al values whereas the final V_m in ES8 was slightly more negative than the pre-Al values (Figure 4.3). The difference between final ET8 and ES8 V_m was significant at $p < 0.01$. Similar changes in V_m were observed when experiments were repeated using the same protocol as used in the MIFE experiments (data not shown). When roots were exposed to the same concentration of a different trivalent cation La^{3+} , the V_m at the root apex became 25-30 mV more negative in both genotypes after 3-10 min ($\Delta V_m = -25.7 \pm 3.5$ for ET8; $\Delta V_m = -30.5 \pm 5.1$ for ES8, where errors are SE for $n = 11-15$). In contrast, the addition of $AlCl_3$ or $LaCl_3$ caused little or no change in V_m in the more mature cells 10 mm or more farther back ($\Delta V_m = -2.6 \pm 1.9$ for $AlCl_3$; $\Delta V_m = -6.9 \pm 1.9$ for $LaCl_3$, where errors are SE for $n = 12-14$).

4.3.3 Effect of Al on net ion fluxes

The net fluxes of K^+ , H^+ and Cl^- were measured at two positions near the root apex, the meristem and the elongation zone. In the absence of Al, the pattern of fluxes for these three ions was similar to those previously reported for root apices (Newman *et al.*, 1987; Ryan *et al.*, 1990; Kochian *et al.*, 1991; Shabala *et al.*, 1997; Shabala and

Knowles, 2002; Shabala, 2003). This can be summarised as a net efflux of K^+ of between 100 and 400 $\text{nmol m}^{-2} \text{s}^{-1}$, a larger influx of H^+ of between 500 and 1000 $\text{nmol m}^{-2} \text{s}^{-1}$ and a small Cl^- influx of about 40 $\text{nmol m}^{-2} \text{s}^{-1}$ (Figs. 4-7). Although fluxes at the two positions were qualitatively similar the net fluxes were larger at the elongation zone than the meristem. Addition of 50 μM Al to the bathing solution induced immediate changes in the K^+ and H^+ fluxes at the elongation zone, but the two genotypes responded differently (Figure 4.4).

In the Al-tolerant ET8, Al induced a rapid increase in K^+ efflux from ET8 (peak ~8 min) that gradually returned to oscillate around control levels (Figure 4.4A). In contrast, Al induced a rapid and sustained reduction in net K^+ efflux at the elongation zone of Al-sensitive ES8, which became significantly smaller than ET8 (Figure 4.4A). Although the stimulation of K^+ efflux by Al in ET8 was not maintained, after 24h the K^+ efflux of ET8 was still greater than ES8 (Figure 4.6A). This difference between the genotypes was not detected when fluxes were measured from the root meristem, where Al^{3+} reduced K^+ efflux in both ES8 and ET8 (Figure 4.5A & Figure 4.7A).

Furthermore, Al caused a rapid and sustained increase in H^+ influx in ET8 at the elongation zone, whereas for ES8, H^+ influx was reduced for at least 40 min before recovering to control levels (Figure 4.4). These differences between ET8 and ES8 were still apparent after 24 h treatment at all the Al concentrations tested (Figure 4.6B). Once again, the changes in H^+ fluxes were detected at the elongation zone, but not at the meristem where influx transiently increased in both genotypes (Figure 4.5B). Interestingly, a difference was detected between ET8 and ES8 at the meristem after 24hrs where H^+ influx was higher in ET8 than ES8 at all concentrations measured (Figure 4.7B).

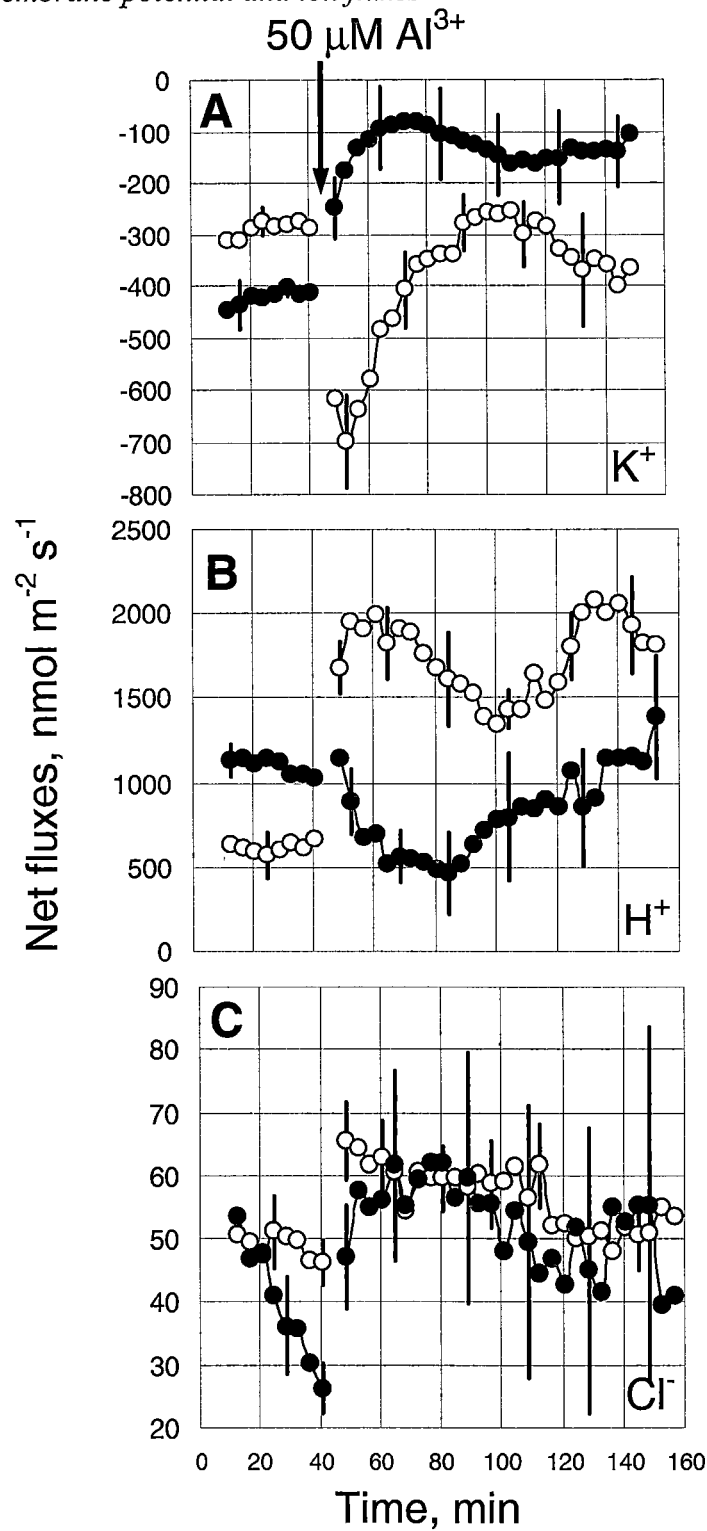


Figure 4.4. Transient responses of ion fluxes to Al measured at the elongation zone. Potassium fluxes are shown in (A), H^+ in (B) and Cl^- in (C). Data show the responses collected on ET8 plants (open symbols) and ES8 plants (closed symbols) after $50 \mu\text{M Al}$ was added as shown. Positive values are defined as influxes and negative values as effluxes. Error bars are $\pm \text{SEM}$ ($n = 6$ to 8).

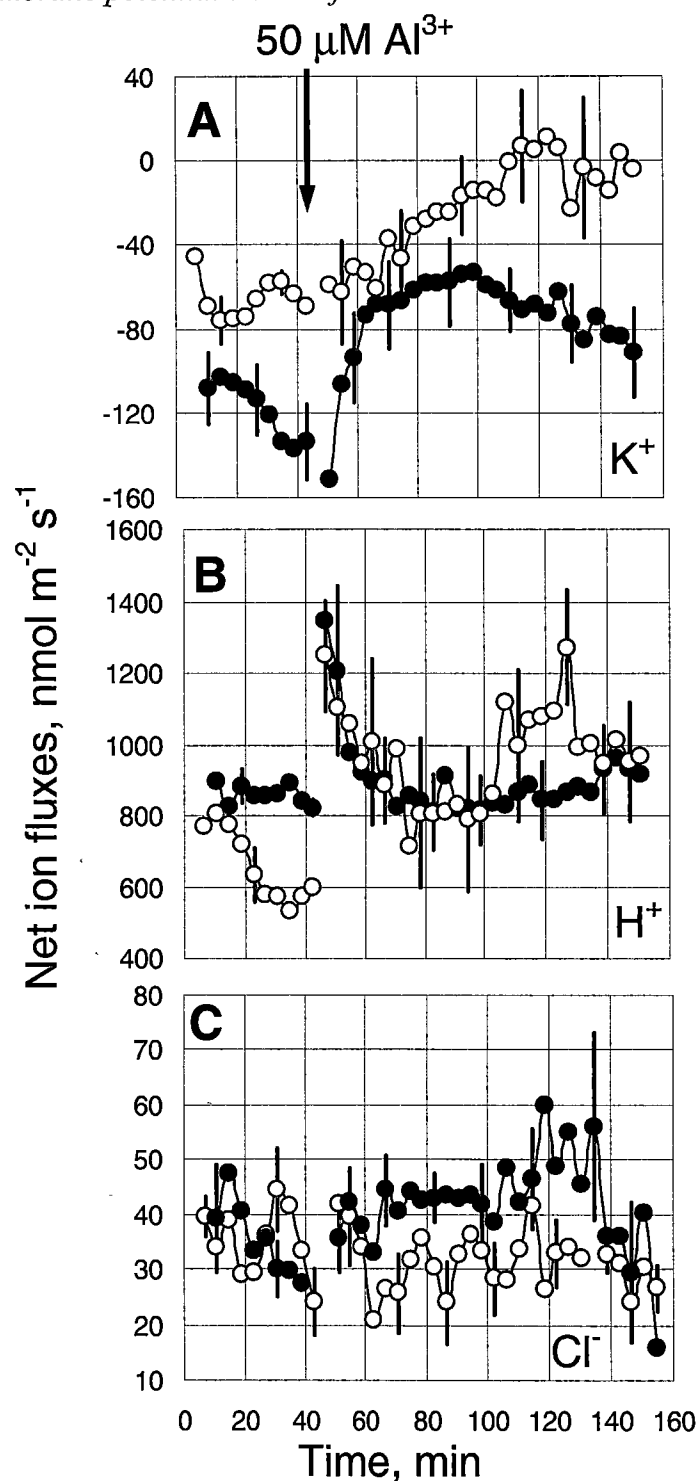


Figure 4.5. Transient responses of ion fluxes to Al measured at the root meristem.

Potassium fluxes are shown in (A), H^+ in (B) and Cl^- in (C). Data show the responses collected on ET8 plants (open symbols) and ES8 plants (closed symbols) after $50 \mu\text{M Al}$ was added as shown. Positive values are defined as influxes and negative values as effluxes. Error bars are $\pm \text{SEM}$ ($n = 6$ to 8).

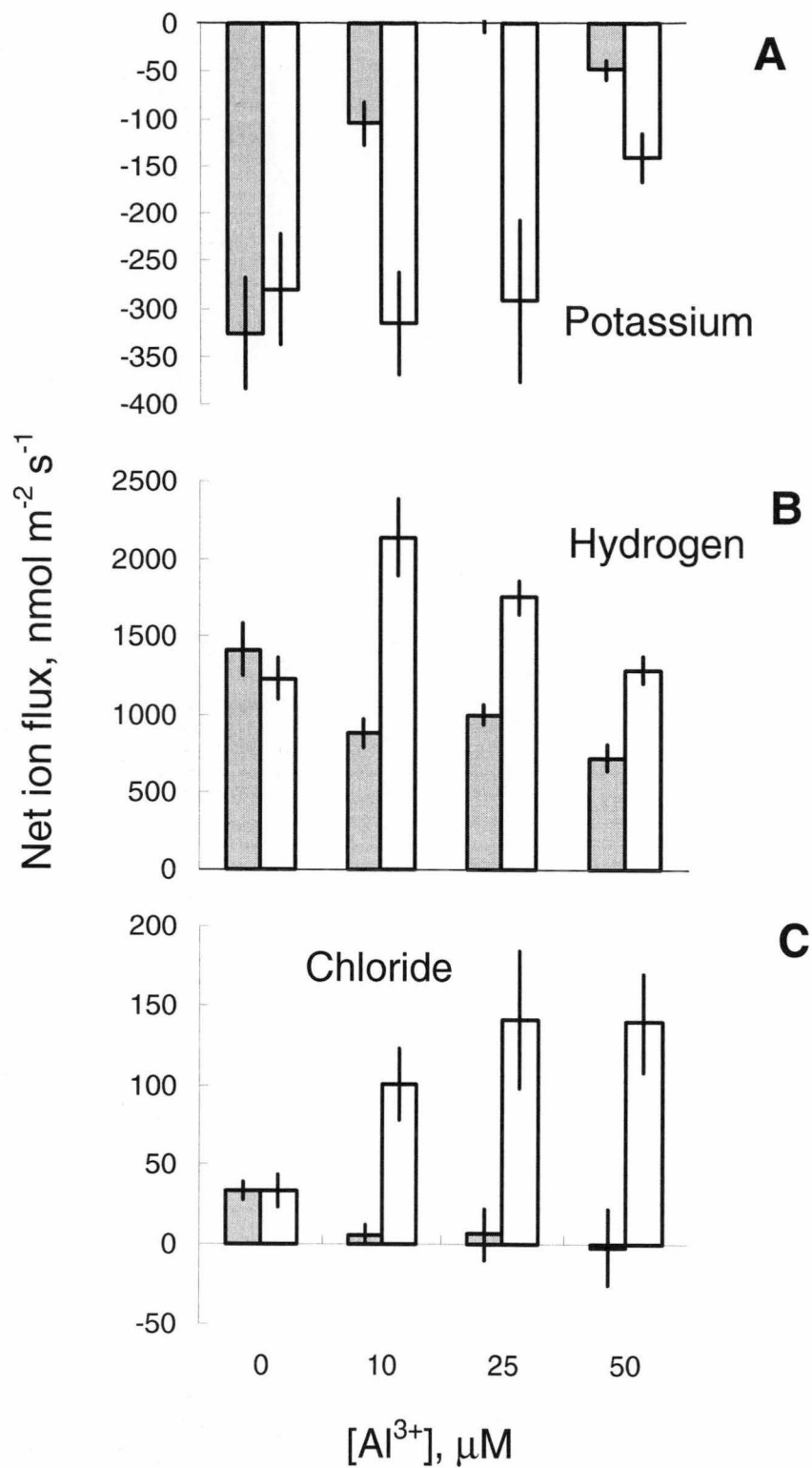


Figure 4.6. Net ion fluxes measured at the elongation zone following a 24 h treatment with different Al^{3+} concentrations. Results are shown for ET8 (open bars) and ES8 (closed bars). Error bars are \pm SEM (n = 6 to 8).

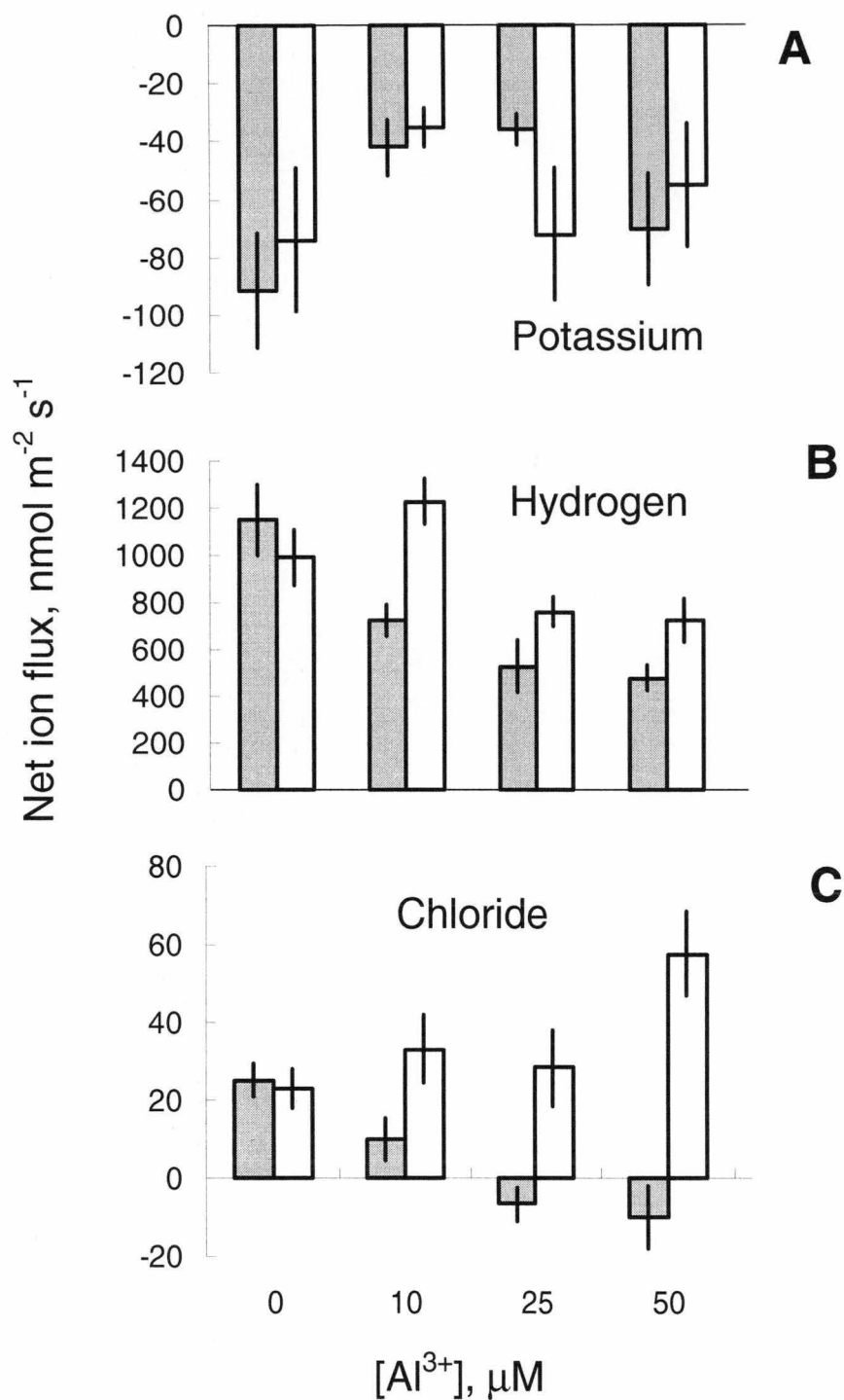


Figure 4.7. Net ion fluxes measured at the root meristem following a 24 h treatment with different Al^{3+} concentrations. Results are shown for ET8 (open bars) and ES8 (closed bars). Error bars are \pm SEM ($n = 6$ to 8).

Net Cl^- fluxes were relatively small, but a small increase in Cl^- influx was discernible after Al addition in both cultivars at the elongation zone (Figure 4.4C), but not at the meristem (Figure 4.5C). Following a 24 h treatment Cl^- influx at the elongation zone ceased in ES8 at all Al concentrations tested, while for ET8 net Cl^- influx increased (Figure 4.6C). As for H^+ , differences were observed between cultivars after 24h, where Cl^- influx increased in ET8, but decreased and became efflux in ES8 (Figure 4.7C).

4.3.4 Effect of exogenous malate on K^+ fluxes

There was no significant effect of exogenous malate application on K^+ fluxes from the elongation zone in ET8 seedlings (data not shown).

4.4 Discussion

4.4.1 Membrane potential and malate efflux

Aluminium has been shown to interact with a number of plant membrane transport processes that could affect V_m . The effect of Al on root-cell V_m has been measured previously in a range of species and experimental conditions to investigate Al toxicity. However, no consensus has emerged that describes a general response of V_m to Al treatment. This study measured the effect of Al on V_m in a pair of near-isogenic lines of wheat that differ in Al tolerance. Although the response of V_m was complex, a pattern emerged that is generally consistent with the report of Papernik and Kochian (1997) for wheat and with Olivetti *et al.* (1995) for snapbean. Specifically, it was shown that an Al-dependent depolarisation (phase III; Figure 4.3) occurred in the Al-tolerant genotype, but not in the sensitive near-isogenic line and that it was

triggered by Al, but not La. This supports the hypothesis that depolarisation is specifically associated with Al activated malate efflux because the activation of malate efflux by La is significantly smaller than by Al (Ryan *et al.*, 1995b; Kataoka *et al.*, 2002a; Kataoka *et al.*, 2002b). My results differ from those of Papernik and Kochian (1997) in three aspects: first, an additional hyperpolarisation (phase II) preceded the depolarisation described in both studies. The reasons for this may be differences in experimental conditions since the rate of solution flow was considerably faster in my study. Second, the Al-dependent depolarisation occurred at the elongation zone (1-2 mm from the apex), but not 10 mm from the apex. Third, the effects of the anion channel blocker anthracene-9-carboxylate (A-9-C) on V_m could not be repeated. Papernik and Kochian (1997) reported that pre-treating roots with A-9-C had no effect on the Al-dependent changes of V_m and therefore concluded that the efflux of malate anions was not responsible for the observed depolarisations in Al-tolerant plants. However it was found that exposure of roots to similar concentrations of A-9-C depolarised the cell membranes even in the absence of Al (data not shown). Interestingly, the Al-tolerance mechanism in snapbean is believed to be similar to wheat, in that Al activates the release of an organic anion (citrate) from the roots (Miyasaka *et al.*, 1991). The physiology of these responses in wheat and snapbean are consistent with a model whereby the Al-activated efflux of organic anions from ET8 is involved, at least in part, with the observed depolarisations in this Al-tolerant genotype. The inhibition of the plasma membrane H^+ -ATPase by Al (Ahn *et al.*, 2002) is another interaction that could depolarise cells if it leads to a decrease in H^+ efflux. Nevertheless, this is unlikely to explain the results here because the depolarisations were observed only in the Al tolerant plants, and not in the sensitive plants that are presumably subject to greater stress. Additionally an increase in H^+

flux, which would be expected with inhibition of H^+ ATPase, occurs in ET8 and not ES8. Reasons for this increase are discussed later.

4.4.2 Al effects on root fluxes

To resolve some of these issues and to investigate how Al affects the transport of inorganic ions I measured the net fluxes of K^+ , H^+ and Cl^- at the elongation and meristematic zones. In the absence of Al, the sum of these three fluxes is not zero. For example, by adding average values for the K^+ , H^+ and Cl^- fluxes near the elongation zone (approximately -400, 1000 and 40 $nmol\ m^{-2}s^{-1}$ respectively; Figure 4.6), a net influx of cations (bath solution 0.1 mM $CaNO_3$, 0.1 mM $MgSO_4$, 0.1 mM KCl and 0.1 mM NH_4NO_3) of approximately 640 $nmol\ m^{-2}s^{-1}$ is predicted. This imbalance is partly explained by the movement of other ions not examined here. It is also well established that an inward current does occur at root apices when placed in a conducting medium (Scott, 1962; Miller and Gow, 1989; Ryan *et al.*, 1992; Weisenseel *et al.*, 1992). The net influx of ions in one region of the root might be balanced by the efflux of ions from a neighbouring region, forming current loops through the tissue and medium. Figure 4.4A shows that Al stimulates K^+ efflux from intact Al-tolerant wheat roots which provides independent support for previous studies using excised root apices Ryan *et al.* (1995a). It also provides the first direct evidence that this difference between ET8 and ES8 is sustained for many hours even if root growth is significantly inhibited in both genotypes. The difference between genotypes was apparent only in the elongation zone and not in the position at the meristem (Figure 4.4A). Importantly, maximum malate efflux occurred from the region 1-2mm from the root tip (Figure 4.2), which corresponds to the measurements made at the elongation zone in this experiment. The terminal 0-1mm segment showed a smaller, but significant

release of malate as well (Figure 4.2), however this did not induce similar changes in ion fluxes at the meristem to those observed at the elongation zone. The terminal 0-1mm segments include tissues from the root cap, apical meristem, distal transition zone and elongation zone. It is likely that malate release occurred from regions where ion fluxes were not measured such as the elongation zone or root cap.

Based on the MIFE data, I can also conclude that the model proposed by Olivetti *et al.* (1995) to explain the Al-dependent depolarisations in snapbean (blockage of outward K^+ channels) is unlikely to be occurring in wheat because the depolarisations in ET8 are associated with a transient increase in K^+ efflux (Figure 4.4), not a decrease as would be predicted from that model. Furthermore, the hyperpolarisation of ES8 is associated with a decrease in K^+ efflux.

The magnitude and timing of V_m changes and ion fluxes are critical in understanding the sequence of events by which Al affects membrane potential and ion fluxes in tolerance and toxicity responses. The general similarity of the phases in ET8 and ES8 (Figure 4.3) suggests that there are both common and divergent effects on membrane potential and fluxes in the elongation zone in these cultivars. It is likely that the blockage of Ca^{2+} channels contributes to the hyperpolarisation observed in phase II because Al and La caused this response in both genotypes (Figure 4.3) and both these cations are known to be potent antagonists Ca^{2+} channels (Ding *et al.*, 1993; Pineros and Tester, 1993). However, in ET8, the magnitude of phase II was smaller, the peak earlier and the depolarisation of phase III greater than ES8 (Fig 3.) which is consistent with a model whereby the depolarisation in ET8 is due to a rapid efflux of malate in response to Al exposure. Ryan *et al* (1997b) report that Al activated an immediate inward rectifying current in 20% of the ET8 protoplasts measured. Therefore, in an intact ET8 root, Al^{3+} will induce an almost immediate

efflux in malate, which will increase over the next few minutes because more channels are activated. Importantly, my data also shows that K^+ efflux peaks about 8 minutes after exposure to Al, once significant depolarisation has already occurred in ET8 (Figs. 3 & 4). Additionally application of exogenous malate did not alter K^+ efflux from the elongation of ET8 seedlings, suggesting that malate does not activate a glutamate K^+ channel (Sivaguru *et al.*, 2003b), or at least that it does not alter K^+ flux in the absence of a change in V_m . These findings are consistent with an alternative model, which invokes no direct interaction between Al and the K^+ channels, but simply proposes that the stimulation of K^+ efflux is triggered by the membrane depolarisation caused by organic anion efflux. Similar activation of the potassium outward rectifier (KORC) is observed in guard cells (MacRobbie, 1998).

Another model for the relationship between malate and K^+ efflux in wheat was recently presented by Osawa and Matsumoto (2002). They proposed that Al can trigger K^+ efflux in the Al-tolerant cultivar Atlas independently of malate release and, conversely, that K^+ efflux is not a requirement for Al-activated malate efflux. This means that for this alternative model to be correct, the Al-activated malate and K^+ efflux should be encoded by very closely located genes. Because their model was developed on the results from inhibitors that have non-specific interactions and no kinetics of either malate or K^+ efflux were measured, these results require further validation.

Aluminium also caused significant changes in the net H^+ fluxes. The ET8 genotype showed a rapid increase in H^+ influx whereas a decrease was observed in ES8 at the meristem (Figure 4.4B). This was also maintained after 24 hours at the elongation zone and also at the meristem (Figure 4.6B and Figure 4.7B). I suggest two factors that may contribute to this response: (i) the maintenance of a greater Cl^- influx

in the ET8 uptake (discussed later), and (ii) an 'apparent' H^+ influx that will be generated by the association of H^+ when the divalent malate²⁻ anions are released into the acidic bathing solution. Assuming that at each malate²⁻ anion released becomes associated with a single H^+ (pK_{as} 3.4 and 5.1, external pH 4.0) the apparent H^+ influx will be equivalent to $210 \text{ nmol m}^{-2}\text{s}^{-1}$ (assumes a malate efflux of 0.93 nmol h^{-1} from the 1-2mm segment; Figure 4.2). Yet this represents only 20 % of the observed increase in H^+ influx observed indicating that other mechanisms must also be involved. The increase in H^+ influx may also contribute to the observed depolarisation of ET8. Interestingly these results are contrary to what would be expected if Al inhibition of H^+ ATPase is important in toxicity, as has been suggested previously (Ahn *et al.*, 2001). Inhibition of H^+ ATPase would result in a net increase in H^+ influx and presumably this would be higher in the sensitive cultivar. Recent work by Ahn *et al.* (2004) has shown activation of H^+ ATPase in ET8 and suppression in ES8. However my data shows that H^+ influx is increased in ET8 rather than ES8. Further work needs to be done to explain this paradox.

The net Cl^- fluxes in the short-term experiments were modest compared to the changes in K^+ and H^+ fluxes and no genotypic differences were observed (Figs. 4C & 6C). However after 24 h treatments, differences between the genotypes did emerge. Chloride uptake by ET8 at the elongation zone increased in a dose dependent manner compared to the minus-Al controls after 24 h whereas it was strongly inhibited in ES8 (Figure 4.6). It can be expected that ES8 plants will experience more stress than the ET8 plants, particularly at the lower Al concentrations. At $50 \mu\text{M}$ Al this difference would be reduced because the root growth of both genotypes is severely inhibited but, even here, Cl^- influx was significantly greater in ET8 than ES8 and compared to the ET8 control (Figs. 6 & 7). The maintenance of a higher Cl^- influx by ET8 could help

balance the loss of malate anions along with the K^+ efflux. Furthermore, it could account for some of the stimulation in H^+ uptake found in ET8 because Cl^- uptake requires a symport with H^+ (Sanders, 1980; Reid and Walker, 1984). In the longer term, Cl^- uptake might also be required to maintain cell turgor for root growth since the sustained efflux of malate and K^+ from these cells would tend to reduce the cellular osmotic potential. It is also interesting to note that these differences were present in both the elongation and meristematic zones.

The combination of standard electrophysiological methods with the non-invasive MIFE technique has enabled the testing and verification of a specific hypothesis previously based on excised root tissue to provide further insight into the mechanism of Al tolerance in wheat. Furthermore, the high spatial resolution of the MIFE technique has made it possible to show spatial variation in the magnitude of the Al-activated responses occurring at the root apex. The differences in the mechanisms of malate exudation identified in this chapter have been commonly used to explain the difference between ET8 and ES8 in Ca^{2+} homeostasis after addition of Al. However no studies have been found that examine if this is due to differences in malate exudation or the actual channels involved in homeostasis.

Chapter 5: Effect of Al^{3+} on slow vacuolar channels and their involvement in Al induced $[Ca^{2+}]_{cyt}$ elevation⁴

5.1 Introduction

Despite aluminium (Al) toxicity being the most significant constraint to plant growth in acid soils, the primary mechanism of Al toxicity remains unclear (Barcelo and Poschenrieder, 2002). Disruption of Ca homeostasis has been suggested as a primary trigger of Al toxicity (Rengel and Zhang, 2003). A sustained elevation of cytosolic Ca^{2+} in response to Al has been demonstrated in a number of different plant species (Jones *et al.*, 1998a; Zhang and Rengel, 1999; Ma *et al.*, 2002), potentially interfering with the normal cytosolic Ca^{2+} signalling and disrupting Ca^{2+} dependent metabolic processes.

Recently it has been shown that in intact apical root cells, Al induces a larger and faster increase in cytosolic Ca^{2+} activity in ES8 than ET8, which was correlated with Al induced growth inhibition (Zhang and Rengel, 1999). This supports the possible involvement of raised $[Ca^{2+}]_{cyt}$ in Al toxicity, yet the source and mechanism of Al-induced Ca^{2+} rise is unknown.

Experiments in BY2 tobacco cells have suggested that Al stimulates elevated $[Ca^{2+}]_{cyt}$ by production of O_2^- which opens a ROS activated Ca channel (Kawano *et al.*, 2003). Further experiments by the same authors with tobacco expressing the *Arabidopsis* two pore channel (AtTPC1) suggested that the ROS activated Ca channel is in fact the TPC1 channel (Kawano *et al.*, 2004a). The authors concluded that TPC1 is likely to be expressed in the plasma membrane (Kawano *et al.*, 2003; Kawano *et al.*, 2004a). However, recent experiments on *Arabidopsis* mutants lacking and over

⁴ The contents of this chapter have already been published: Wherrett T., Shabala S., Pottosin I. (2005) Different properties of SV channels in root vacuoles from near isogenic Al-tolerant and Al-sensitive wheat cultivars *FEBS Letters* **579**(30):6890-689

expressing TPC1 have explicitly demonstrated that this channel is actually present in the tonoplast, not the plasma membrane. Moreover, these studies have shown that TPC1 is identical to the ubiquitous slow vacuolar (SV channel) and is involved in Ca^{2+} signalling (Peiter *et al.*, 2005). This calls for further study of the involvement of the SV channel in Al induced signalling, toxicity and tolerance.

5.2 Materials and Methods

5.2.1 Plant material and isolation of vacuoles

Wheat (*Triticum aestivum* L.) seedlings of cultivars ET8 and ES8 were germinated in a floating mesh on aerated 500mL solutions of 0.2mM $CaCl_2$, pH 4.5. After 4-5 days, protoplasts were isolated from the terminal 2-3mm of roots of 27 different plants as has been described in the general materials and methods. For experiments examining pre-treatment of Al, the growth solution was replaced with fresh solution containing 14 μ M $AlCl_3$ 24 hours prior to isolation. Isolated protoplasts were held on ice until required.

A small aliquot (~5 μ L) of isolated protoplasts were transferred into the patch chamber containing standard bath solution (see below). Protoplasts were allowed to adhere to the bottom of the chamber, solution was flushed and then plasma membranes were ruptured to release vacuoles by application of a strong suction pulse with a used patch electrode. Immediately after this the electrode was substituted for a fresh one filled the appropriate pipette solution (see below), the vacuole was sealed against its tip and patch clamp measurements were initiated. Occasionally vacuoles

were spontaneously released from protoplasts in the chamber, these could be patched immediately with higher success rate.

5.2.2 Experimental solutions

The standard bath solution contained (in mM): 100 KCl, 2 CaCl₂, 15 HEPES, adjusted to pH 7.5 with KOH. The standard pipette solution contained (in mM): 100 KCl, 2 CaCl₂, 15 MES, adjusted to pH 5.0 with KOH. For experiments where Al was included in the vacuole pipette, 30 or 144 μ M AlCl₃ was added to the standard pipette solution from a stock of 10 mM AlCl₃ in 0.1 mM HCl resulting in a final free concentration of 0.3 or 1.4 μ M Al³⁺ according to Geochem (Parker *et al.*, 1987). Osmolality of all solutions was adjusted to 450mOsm with sorbitol using a cryoscopic osmometer (Osmomat 030, Gonotec, Germany).

5.2.3 Patch-clamp protocols and analyses

Fabrication of patch pipettes was as described in the general materials and methods using the P-97 puller. Current measurements were performed using an Axopatch 200A integrating Patch-Clamp amplifier (Axon Instruments, Foster City, CA, USA). Vacuolar ion currents were measured under voltage clamp conditions using two different recording modes: whole vacuole and cytosol out patches. Voltage sign convention was cytosol *minus* vacuole. In whole vacuole mode, membrane capacitance and access resistance were measured, and access resistance was compensated by means of compensation circuit of patch-clamp amplifier. Whole vacuole SV currents were evoked by a series of 0.6-1.2 s pulses from -100 to +200 mV in 20 mV increments. Relative open probability and channel density were

calculated as outlined in the general materials and methods. Activation time course was fitted to 2nd order Hodgkin-Huxley kinetics, yielding characteristic activation time, τ_{act} . Single channel I/V curves were obtained from cytosol out patches by applying to a protocol of 50 ms ramps from -200 to +200 mV from a voltage holding potential of 50-70 mV where only 1-2 channels were open at a time.

5.3 Results

5.3.1 Direct effects of Al on SV channels in ET8 and ES8

In ET8, but not ES8, 1.4 μ M free vacuolar Al^{3+} (pH 5.0) slowed the activation kinetics of SV channels (Figure 5.1) and caused approximately a 20 mV increase in the activation threshold, thereby reducing open probability by almost one order of magnitude at physiological potentials (Figure 5.2). This indicates cultivar specific (ET8 only) stabilisation by Al of the closed states vs open state of SV similar to the effect of vacuolar Ca^{2+} , yet at much lower concentration (1.4 μ M Al^{3+} compared with 10 mM Ca^{2+}) (data not shown).

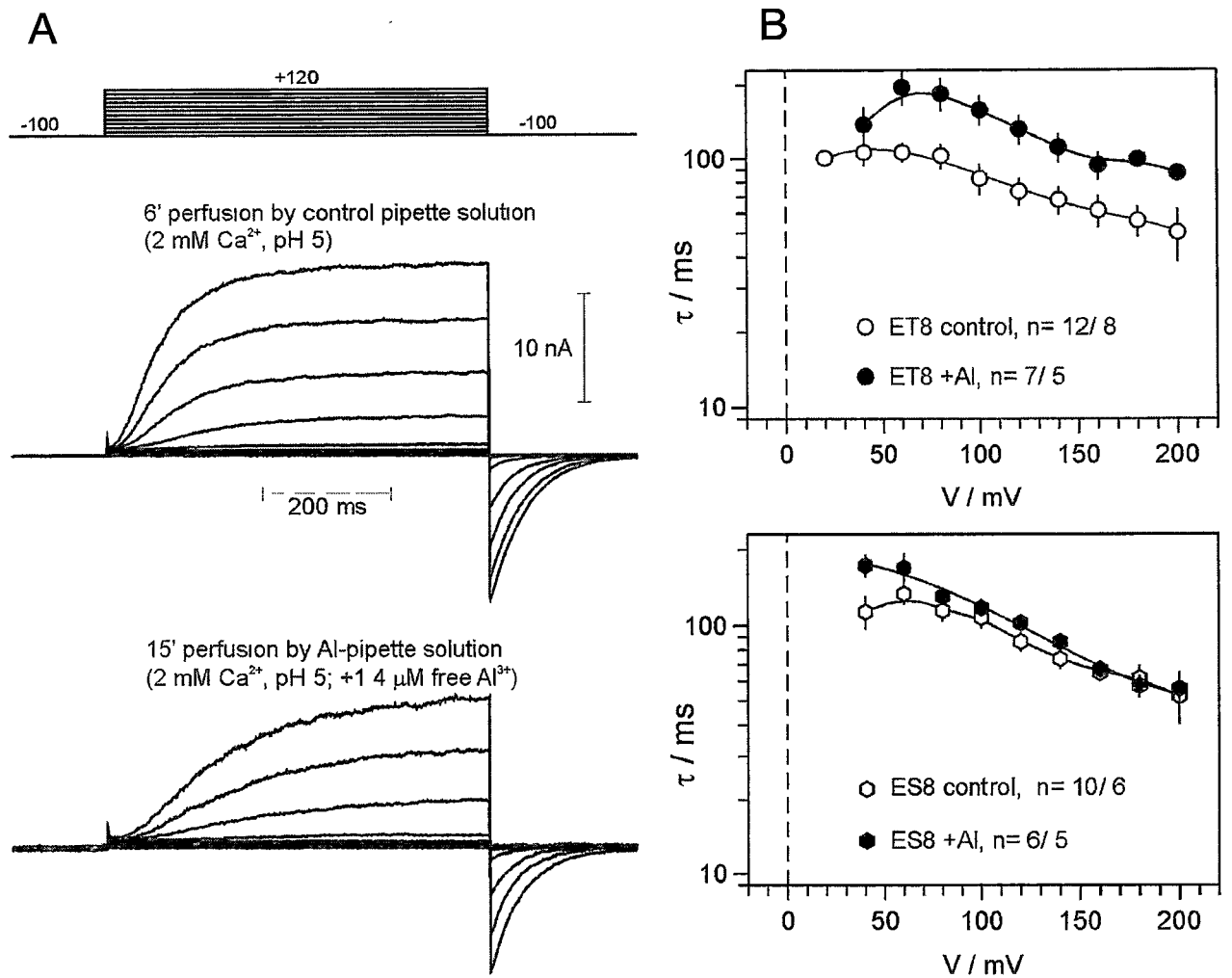


Figure 5.1. Effect of Al on the activation of SV currents. (A) An example of SV current recording in ET8 vacuole. The same vacuole was first internally perfused with a control solution, and then with a new pipette containing 1.4 μ M free Al^{3+} . (B) Mean (\pm SD) values of characteristic activation time as a function of voltage show that addition of 1.4 μ M free Al^{3+} slowed the activation of SV significantly only in ET8 vacuoles. n = 12/ 8 indicates 12 vacuoles patched from 8 independent protoplast isolations.

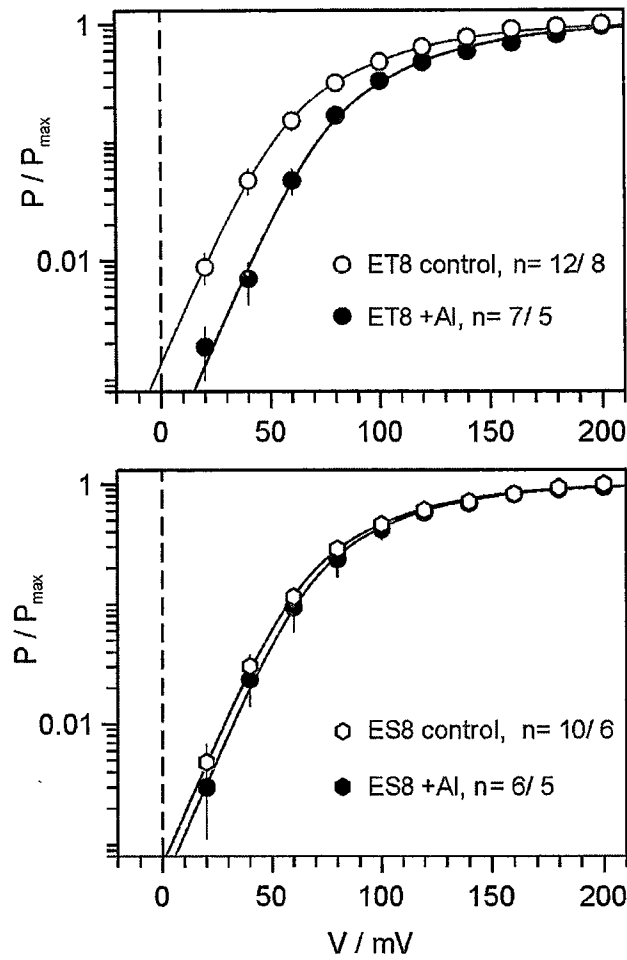


Figure 5.2. Modulation of the SV channel voltage dependence by vacuolar Al^{3+} in ET8 and ES8. Mean (\pm SD, $n=4-8$) of open probability as a function of voltage. Free vacuolar Al^{3+} concentration was $1.4 \mu M$. Lines are best fits to a sequential two closed states- one open state (C2-C1-O) model (Pottosin *et al.*, 2004). $n = 12/8$ indicates 12 vacuoles patched from 8 independent protoplast isolations.

There was no effect of vacuolar Al^{3+} on deactivation kinetics in either ET8 or ES8, but the deactivation was approximately two times faster in ES8 across the whole voltage range (Figure 5.3).

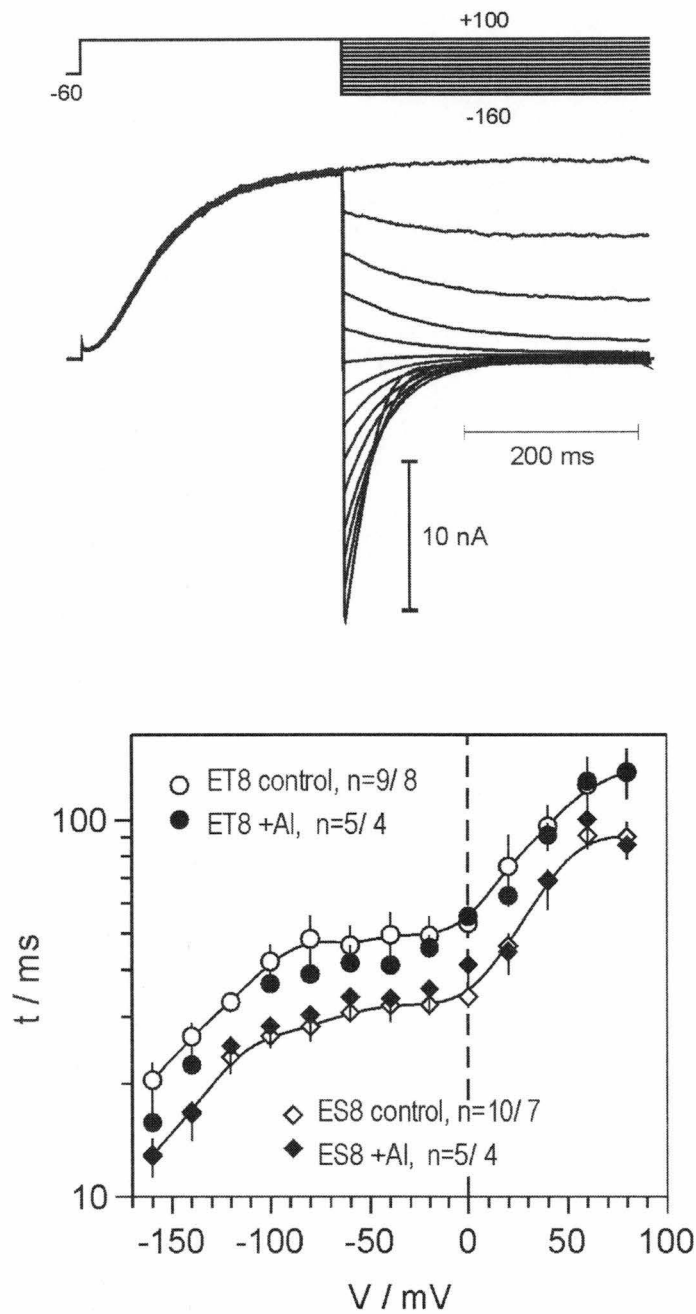


Figure 5.3. Effect of Al^{3+} on deactivation kinetics of SV current. (A) Voltage protocol to evoke tail currents and typical current response of ET8. (B) Tail currents were fitted to mono-exponential function, yielding characteristic times for deactivation (t). Free vacuolar Al^{3+} concentration was $1.4 \mu M$

Al^{3+} (free concentration of 0.3 and 1.4 μM at pH 5.0) applied from luminal side of an excised patch reduced current through a single open SV channel both in ET8 and ES8. The block was voltage-dependent, with only cytosol directed negative currents being affected (Figure 5.4), suggesting that the binding site for Al^{3+} within the SV channel pore is located at some electric distance from the membrane surface. However the block was only partial at large negative potentials, which implies that Al^{3+} can permeate the pore.

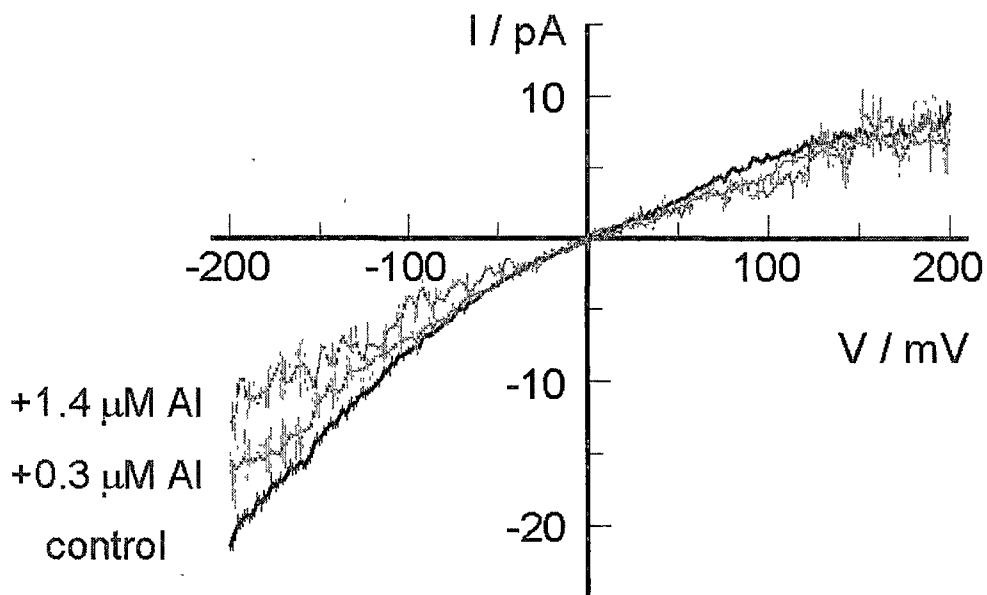


Figure 5.4 Effect of Al^{3+} on single channel I/V curve from ES8. Mean (\pm SD, control $n=32$, 0.3 μM Al $n=11$, 1.4 μM Al $n=6$).

5.3.2 Long-term effects of Al on SV channel in ET8 and ES8

The SV channel density, obtained by dividing the whole vacuole current at large positive voltage (+200 mV) through single channel current at this voltage, was significantly higher in control ES8 than ET8 (47.7 ± 5.3 mV ($n=19$) and 63.0 ± 7.5 mV ($n=14$) SV channels per $100\mu m^2$ of membrane surface), and not altered significantly ($P > 0.05$) after 24 hour pre-treatment with $14 \mu M$ $AlCl_3$. However, analysis of the SV channel voltage dependence, measured immediately after achieving of the whole vacuole configuration, revealed a substantial difference between ET8 and ES8. Whilst the voltage dependence for SV channels in ET8 was similar to that for untreated plants, SV channels in ES8 displayed a substantially lower threshold for voltage activation (Figure 5.5) (more than one order of magnitude difference in open probability at physiological potentials). Perfusion of the vacuole by control pipette solution over 5-6 minutes completely abolished this shift of voltage dependence. With untreated plants, both ET8 and ES8, I observed a similar trend (an increase of the activation threshold with time), yet these shifts were much smaller in magnitude (<10 mV, results not shown). Perfusion of the vacuole by control pipette solution over 5-6 min completely abolished this shift in voltage dependence. Even though the increase in open probability was significant statistically, this data must be treated as preliminary as only a small number of vacuoles were successfully patched (ET8 $n=3$, ES8 $n=4$).

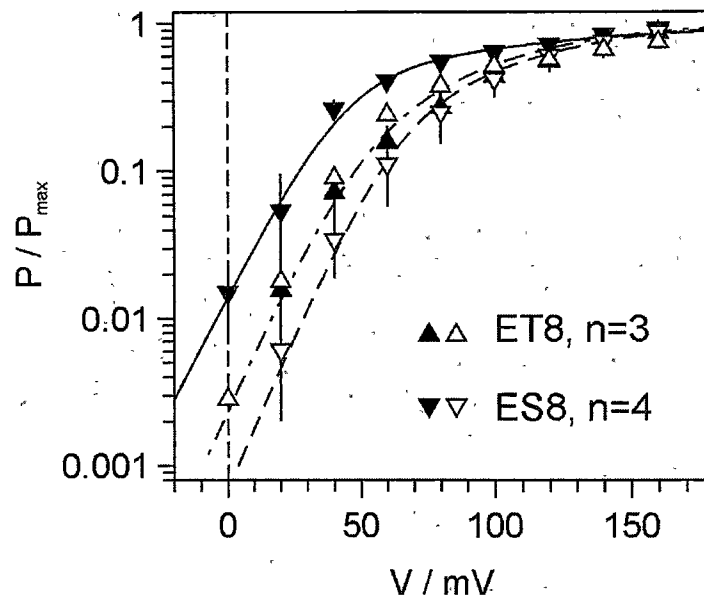


Figure 5.5 Long term (24 h) effects of $14 \mu M$ free Al^{3+} on SV channels in ET8 and ES8 plants. Filled symbols represent the voltage dependence of the SV channels immediately after obtaining of whole vacuole configuration; open symbols are for voltage-dependence after 5-6 min of vacuole perfusion with a control pipette solution. For a comparison, steady state voltage dependence in control conditions for ET8 (dashed-dotted line) and ES8 (dashed line) were replotted from Figure 5.2.

5.4 Discussion

5.4.1 Genetics of ET8 and ES8

ET8 and ES8 wheat cultivars have been used as a model system to study Al tolerance as they only differ at a single genetic locus (Delhaize *et al.*, 1993b; Ryan *et al.*, 1995b, a). Very strong evidence has been presented to support the hypothesis of Al activated malate efflux as the only mechanism conferring the difference in Al tolerance between ET8 and ES8 (Ryan *et al.*, 1995b, a; Ryan *et al.*, 1997b; Zhang *et al.*, 2001; Sasaki *et al.*, 2003; Delhaize *et al.*, 2004; Sasaki *et al.*, 2004) and was attributed to the level of expression of *ALMT1* gene (Sasaki *et al.*, 2003; Delhaize *et al.*, 2004; Sasaki *et al.*, 2004). Consequently the vast majority of research in wheat, especially with these genotypes, has focussed on this mechanism. However my data shows that ET8 and ES8 also differ in their SV channel density (even in the absence of Al treatment) and SV channel properties after exposure to vacuolar Al^{3+} . This questions the assumption that the *Alt1* locus controls only the expression of the plasma membrane malate channel as previously believed.

5.4.2 SV channel properties in ET8 and ES8

SV channels in wheat root vacuoles display landmark characteristics of SV channels (Ward and Schroeder, 1994; Allen and Sanders, 1996, 1997): they activate with steep voltage dependence at positive (cytosol minus vacuole) voltages and show a characteristic delay in activation time course, implying the involvement of at least two closed states (Pottosin *et al.*, 2004). Under conditions of this study (100 mM K^+ , 2 mM Ca^{2+}) the unitary conductance of wheat SV channels was 66 pS, typical for SV channels at these conditions (Schulz-Lessdorf and Hedrich, 1995). Although the basic

characteristics of SV channels in ET8 and ES8 cultivars were similar, quantitatively significant differences were observed in deactivation kinetics (Figure 5.3). Also, the activation kinetics of SV in ET8 and ES8 were equal under control conditions, but was selectively slowed by micromolar Al^{3+} in ET8, but not in ES8 vacuoles (Figure 5.1). Furthermore, SV channel open probability was decreased in ET8, but not in ES8 (Figure 5.1), indicating cultivar specific stabilisation of the closed states of SV in ET8. These observed differences in functional characteristics of SV channels between genotypes may be attributed to either alteration of the respective gene or to complex regulation of the SV channels, especially Ca- dependent and Ca-independent phosphorylation-dephosphorylation of the channel protein (Bethke and Jones, 1997). Significantly my finding of higher channel density in ES8 than ET8 may contribute to the faster and higher elevation of $[Ca^{2+}]_{cyt}$ in ES8.

5.4.3 SV channels, Ca^{2+} signalling and Al tolerance

Al induced elevations in $[Ca^{2+}]_{cyt}$ have been shown to correlate well with reduction in root growth in both wheat and rye (Zhang and Rengel, 1999; Ma *et al.*, 2002). Moreover, it has been shown that the increase in $[Ca]_{cyt}$ is faster and higher in Al-sensitive ES8 than Al-tolerant ET8 (Zhang and Rengel, 1999). This difference was explained by malate exudation in ET8 reducing Al^{3+} activity at the plasma membrane and therefore the response in $[Ca^{2+}]_{cyt}$. The specific mechanism of Al-induced Ca^{2+} elevation remains unknown. Both intra- and extracellular sources of Ca^{2+} have been suggested; with the depolarisation activated cation channel (DACC) considered the most likely route for extracellular Ca^{2+} (Rengel and Zhang, 2003). However, my recent results have shown prolonged and substantial Al-induced depolarisation in ET8

and not ES8 (Werrett *et al.*, 2005). This questions the involvement of DACC in Al-induced Ca^{2+} signalling because significant depolarisation is only observed in ET8 that has a smaller increase in cytosolic Ca (Zhang and Rengel, 1999). More likely Ca^{2+} is released from an internal store via some signalling pathway. The SV channel is a likely candidate for this process.

The SV channel is permeable to both mono- and divalent cations and is activated by positive vacuolar voltage as well as cytosolic Ca^{2+} (Ward and Schroeder, 1994; Schulzlessdorf and Hedrich, 1995; Allen and Sanders, 1996, 1997; Pottosin *et al.*, 2001; Pottosin *et al.*, 2004). The latter feature makes SV channel the most likely candidate for Ca^{2+} -induced Ca^{2+} release from the tonoplast (Pottosin *et al.*, 1997; Bewell *et al.*, 1999; Pei *et al.*, 1999; Sanders *et al.*, 2002; Pottosin *et al.*, 2004). The importance of SV channels in Ca^{2+} signalling has been clearly demonstrated in recent experiments with *Arabidopsis* mutants. The SV channel has been identified as a product of TPC1 gene, encoding double-pore Ca channel (Peiter *et al.*, 2005). Knock-out *Arabidopsis* mutants showed altered Ca^{2+} signalling (no stomatal closure in response to high external Ca) and reduced repression of germination and $[Ca^{2+}]_{cyt}$ elevation in response to exogenous ABA. Importantly, elevated ABA is one of the early responses to Al (Kasai *et al.*, 1993; Shen *et al.*, 2004a), and it has been noted that trivalent ion toxicities bear some resemblance to ABA response (Rock and Quatrano, 1996; Pei *et al.*, 2000; Murata *et al.*, 2001).

Mediation of Al-induced cytosolic Ca^{2+} signalling by SV channels has been directly investigated by Kawano and co-authors in tobacco BY-2 cell cultures (Kawano *et al.*, 2003; Kawano *et al.*, 2004a; Kawano *et al.*, 2004b; Lin *et al.*, 2005). Similarly to intact wheat apices they observed that Al increases $[Ca^{2+}]_{cyt}$, which the authors suggest is stimulated by superoxide production (Kawano *et al.*, 2003).

However they observed significant differences in the timing and duration of $[Ca^{2+}]_{\text{cyt}}$ elevation compared with wheat and higher Al concentrations in tobacco actually reduced the increase in $[Ca^{2+}]_{\text{cyt}}$ (Zhang and Rengel, 1999; Kawano *et al.*, 2003; Kawano *et al.*, 2004a). One of the possible reasons may be species-specificity (tobacco suspension cells vs intact wheat roots). Geochem calculations (Parker *et al.*, 1987), when applied to the experimental solutions used by Kawano and co-authors, showed that for all the $AlCl_3$ concentrations added to solution (0.1-40 mM $AlCl_3$) the actual free Al^{3+} concentration in their experiments was negligibly small ($4.99\text{-}5.07 \times 10^{-10}$ M Al^{3+} free activity, $3.24\text{-}5.22 \times 10^{-9}$ M Al^{3+} free concentration) and there was negligible change in the concentration of Al complexes. Experiments with Al by Jones *et al.* (1998b) also in tobacco BY-2 cells, where pH and speciation were carefully controlled, actually observed a decrease in $[Ca^{2+}]_{\text{cyt}}$. This casts some serious doubt on validity of the above results and raises the question of what is actually inducing the response they observe.

Irrespective of the problems with Al speciation incurred by Kawano and co-authors, their experiments with transformed tobacco clearly showed that $[Ca^{2+}]_{\text{cyt}}$ increases in response to reactive oxygen species (ROS), with the response being higher in cells over expressing TPC1 and reduced by co-suppression of this gene (Kawano *et al.*, 2003; Kawano *et al.*, 2004a). Again, ROS production has been identified as a very early response to Al (Boscolo *et al.*, 2003; Yamamoto *et al.*, 2003). The SV channel is also believed to promote Ca^{2+} -induced Ca^{2+} release (Carpaneto *et al.*, 2001). This evidence strongly suggests that SV channels are involved in Al induced Ca^{2+} elevation, which may be signalled by ABA, ROS or Ca^{2+} .

5.4.4 Possible signalling pathway

The precise signalling pathway requires further elucidation, however a plausible mechanism may be suggested. Exposure to Al^{3+} causes production of ROS (Cakmak and Horst, 1991; Boscolo *et al.*, 2003; Yamamoto *et al.*, 2003) and ABA (Kasai *et al.*, 1993; Shen *et al.*, 2004a) that induce opening of SV channels, causing elevation of $[Ca^{2+}]_{cyt}$. The latter promotes further SV channel opening via CICR mechanism (Bewell *et al.*, 1999). The combination of elevated ROS and $[Ca^{2+}]_{cyt}$ will precipitate further toxic effects. The greater SV channel density in ES8 compared with ET8 contributes to the faster and higher elevation of $[Ca^{2+}]_{cyt}$ in ES8.

5.4.5 Impact of SV channel properties on Al tolerance

In the short term, Al^{3+} causes the cytosolic Ca^{2+} rise without crossing the plasma membrane (Zhang and Rengel, 1999), but in the longer term Al^{3+} is taken up into the cytoplasm and vacuole (Rengel and Reid, 1997; Taylor *et al.*, 2000), therefore its effects on the intracellular Ca-channels should be considered. Reduced open probability of SV channels by vacuolar Al^{3+} in Al-tolerant ET8 cultivar may have a number of significant benefits. Firstly, as deduced from the single channel I/V curves (Figure 5.5), Al^{3+} is permeable in SV channels, so Al^{3+} induced closure of the SV channels (Figure 5.1 and Figure 5.2) may aid sequestering Al in the vacuole. The involvement of vacuolar sequestering in Al tolerance is supported by observations from a tolerant maize variety that only exhibits transient inhibition by Al (Vázquez *et al.*, 1999). From 4 hrs of exposure, increased Al was observed in the vacuole; and after 24 hr root elongation was restored (Vázquez *et al.*, 1999). Al was not detected in the cell wall and higher vacuolar concentrations were measured (Vázquez *et al.*,

1999). Secondly, it may also help to lower the elevation in cytosolic Ca^{2+} due to a decreased release of Ca^{2+} via SV channels.

Finally, long-term exposure to Al^{3+} increased open probability of SV channels in ES8, but not in ET8. No change in ET8 open probability in response to Al pre-treatment may reflect a difference in Al response mechanisms or a lower concentration of Al due to malate chelation. The increase of open probability in ES8 was quickly lost suggesting low molecular weight regulatory factors were rapidly washed out by vacuole perfusion with a standard solution (Figure 5.4). Physiologically this is highly significant because more SV channels are open at physiological tonoplast potentials, contributing to the sustained elevation of cytoplasmic Ca^{2+} in ES8. The number of successful patches obtained was quite low for a study comparing two cultivars; however the large shift in open probability (more than one order of magnitude at physiological potentials) gives confidence that further experiments will confirm the observation. The nature of these regulatory factors is a subject for further investigation. It would also be interesting to investigate whether this long term response is specific to Al^{3+} toxicity or a general stress response.

In conclusion it is obvious that ET8 and ES8 differ in more than just Al induced malate efflux (Ryan *et al.*, 1995b, a; Ryan *et al.*, 1997b; Zhang *et al.*, 2001; Sasaki *et al.*, 2003; Sasaki *et al.*, 2004) thus questioning the idea of Alt1 locus only controlling expression of the plasma membrane malate channel (Sasaki *et al.*, 2003; Delhaize *et al.*, 2004; Sasaki *et al.*, 2004). Differential channel density and regulation of SV channels in ES8 and ET8 by Al^{3+} , either directly (inhibition in ET8) or indirectly (increased open probability in ES8) may contribute to different Ca^{2+} responses in these cultivars, and consequently to Al-tolerance. This may be particularly relevant in

the difference between ET8 and ES8 root hair tolerance noted in chapter 3. In order to determine conclusively whether or not the difference in SV channels are inherited on the Alt-1 locus it would be necessary to see if this co-segregates with malate exudation. Further work is warranted to determine the long-term implications of these SV channel differences and the exact signalling pathway involved.

Chapter 6: Second messengers and Ca^{2+} signalling in Al toxicity and tolerance

6.1 Introduction

Al induced elevations in $[\text{Ca}^{2+}]_{\text{cyt}}$ have been shown to correlate well with inhibition of root growth in both wheat and rye (Zhang and Rengel, 1999; Ma *et al.*, 2002). Moreover, it has been shown that the increase in $[\text{Ca}]_{\text{cyt}}$ is faster and higher in Al-sensitive ES8 than Al-tolerant ET8 (Zhang and Rengel, 1999). This difference was explained by malate exudation in ET8 reducing Al^{3+} activity at the plasma membrane and therefore the response in $[\text{Ca}^{2+}]_{\text{cyt}}$. The specific mechanism of Al-induced Ca^{2+} elevation remains unknown. As shown in the previous chapter, the SV channel and vacuole are likely sources of Ca^{2+} for the Al induced elevation in $[\text{Ca}^{2+}]_{\text{cyt}}$. The precise signalling pathway requires further elucidation, however it is thought to involve Al^{3+} induced production of ROS (Cakmak and Horst, 1991; Boscolo *et al.*, 2003; Yamamoto *et al.*, 2003) and possibly ABA (Kasai *et al.*, 1993; Shen *et al.*, 2004a) that elevates $[\text{Ca}^{2+}]_{\text{cyt}}$, possibly through opening of SV channels. Elevated $[\text{Ca}^{2+}]_{\text{cyt}}$ promotes further SV channel opening via a calcium-induced calcium release (CICR) mechanism (Bewell *et al.*, 1999). The combination of elevated ROS and $[\text{Ca}^{2+}]_{\text{cyt}}$ will precipitate further toxic effects.

The SV channel is permeable to both mono- and divalent cations and is activated by positive vacuolar voltage as well as cytosolic Ca^{2+} (Ward and Schroeder, 1994; Schulzlessdorf and Hedrich, 1995; Allen and Sanders, 1996, 1997; Pottosin *et al.*, 2001; Pottosin *et al.*, 2004). The latter feature makes the SV channel the most likely candidate for Ca^{2+} -induced Ca^{2+} release from the tonoplast (Pottosin *et al.*, 1997;

Bewell *et al.*, 1999; Pei *et al.*, 1999; Carpaneto *et al.*, 2001; Sanders *et al.*, 2002; Pottosin *et al.*, 2004). The actual capacity of SV to be involved in CICR has been questioned because significant increases in open probability were only observed at vacuolar:cytosol Ca^{2+} ratios that favour movement from the cytoplasm to the vacuole (Pottosin *et al.*, 1997). However, subsequently it has been shown that the open probability of SV channels is strongly modulated by cytosolic and vacuolar concentrations of a number of ions and other compounds; and the SV channel still remains the prime candidate for involvement in CICR. SV open probability is increased by cytosolic Mg, some suggest that Mg^{2+} activates SV enough that it opens at physiological potentials and $[\text{Ca}^{2+}]_{\text{cyt}}$ capable of CICR (Carpaneto *et al.*, 2001). Calmodulin and calcineurin have also been shown to modulate SV activity in a complex manner probably involving a number of different phosphorylated states (Allen and Sanders, 1995; Bethke and Jones, 1997).

Second messengers that are known to elicit elevated $[\text{Ca}^{2+}]_{\text{cyt}}$ and have been implied in Al toxicity include ABA (Kasai *et al.*, 1993; Shen *et al.*, 2004a; Peiter *et al.*, 2005), reactive oxygen species (ROS) (Boscolo *et al.*, 2003; Kawano *et al.*, 2003; Yamamoto *et al.*, 2003; Kawano *et al.*, 2004a), Ca^{2+} (Pottosin *et al.*, 1997; Bewell *et al.*, 1999; Pei *et al.*, 1999; Carpaneto *et al.*, 2001; Sanders *et al.*, 2002; Pottosin *et al.*, 2004), and IP_3 (Allen *et al.*, 1995; Muir and Sanders, 1997; Taylor and Laude, 2002; Martinez-Estevez *et al.*, 2003; Vermassen *et al.*, 2004).

The purpose of this chapter was to examine the SV to participate in Ca^{2+} release, to identify signalling molecules capable of eliciting vacuolar Ca^{2+} release and to determine if any of the differences in SV channels discovered in Chapter 5 influence Ca^{2+} signalling and Al tolerance.

6.2 Materials and Methods

6.2.1 Plant material and vacuole isolation

Red beets were used as a model system to study the possible involvement of SV channels and second messengers in Al induced changes in homeostasis. Red beet was selected because vacuole isolation is both rapid and simple and a large amount of research on SV has already been conducted in red beet. Fresh red beets were purchased from the local market. Osmolality of juice squeezed from the roots ranged from 500-650 mOsm, measured using a vapour pressure osmometer (Wescor, Vapro 5520, Utah, USA). Accordingly, the bath solution (100 mM KCl plus 1mM HEPES, adjusted to pH 7.4 with KOH) osmolality was adjusted with sorbitol so that it was 20-50 mOsm hyperosmotic to that of the red beet used for each experiment. Vacuoles were released by incubating slices of red beet root in the standard bath solution for five minutes before fine forceps were used to tear the slices apart. Under the microscope 10-20 vacuoles were selected in 6 μL of the isolating medium and transferred to the experimental chamber containing 1.5 mL of fresh bath solution. Vacuoles of a diameter 40–60 μm were selected for measurement.

Wheat (*Triticum aestivum* L.) seedlings of cultivars ET8 and ES8 were germinated in a floating mesh on aerated 500mL solutions of 0.2 mM CaCl_2 , pH 4.5. After 4-5 days, protoplasts were isolated from the terminal 2-3 mm of roots of 27 different plants essentially as has been described in the general materials and methods, but with one modification, all Ca^{2+} was removed from the final gradients to minimise contamination of the bath solution. Isolated protoplasts were held on ice until required. A small aliquot ($\sim 5\mu\text{L}$) of isolated protoplasts were transferred into the experimental chamber containing 0.75 mL of lysis solution (100 mM KCl and 1mM

HEPES, adjusted to pH 7.4 with KOH). Vacuoles were spontaneously released from the protoplasts and then 0.75 mL of solution (100mM KCl and 1mM HEPES, adjusted to pH 7.4 with KOH, adjusted with sorbitol to 300 mOsm) was added to the bath so the final osmolality was roughly isotonic. The osmolality of the wheat roots was previously measured as 250-260 mOsm in root sap released by pulping and centrifuging approximately 30 roots of 5 day old plants (Wescor, Vapro 5520, Utah, USA). Vacuoles of a diameter 40–60 μm were selected for measurement.

6.2.2 Intravacuolar ion activities and concentration

SV channel activity is significantly modulated by both intravacuolar and cytosolic ion activities. However, one of the problems of the research attempting to determine the physiological function of SV is that the intravacuolar concentration of ions, particularly Ca^{2+} remains uncertain, and it is not known how the native vacuolar solution affects SV open probability and voltage dependence. The use of multibarrelled microelectrodes is the standard electrophysiological technique for measuring intracellular ion activities. Multibarrelled electrodes include barrels for ion selective resins and one barrel for membrane potential measurement allowing this to be subtracted from raw potential measurements and a correction in calculated ion activity to be made. Unfortunately this technique was not available in our laboratory, meaning adaptations and additional calculations were made to calculate the intravacuolar ion activities. Liquid junction potential (LJP) and membrane potential (V_m) both cause a change in the raw voltage of each ion selective electrode and consequently cause inaccuracies in the calculation of ion activity. The effects of liquid junction potential (LJP) and membrane potential (V_m) were accounted for by measurement and addition of the respective mean LJP and V_m for each experiment to

the raw voltage values and recalculating the actual activity using the calibration data of each electrode (see appendix 2). Concurrent to all measurements of V_m and ion activity, Ca^{2+} fluxes were measured (as described below) with a second electrode positioned on the opposite side of the vacuole at a distance of 20 μm from the vacuole surface, which showed that the impalement was leaky if large Ca^{2+} fluxes were observed. All measurements were made on freshly isolated red beet vacuoles held in the standard bath solution.

For membrane potential, filamented borosilicate glass microelectrodes (Harvard Apparatus GC150F-10, Kent, UK) were filled with 1 M KCl, connected to the MIFE system and inserted into individual vacuoles with a manually operated micromanipulator (Narishige, Japan) at an angle of approximately 60° to horizontal. Voltage was continuously monitored and recorded by the MIFE system.

LJP was measured by observing the change in voltage observed when electrodes filled with the standard backfilling solution for each different ion (see general materials and methods) were transferred from a simple 50 mM KCl salt solution (pH 5.5) to one with 50 mM malic acid, adjusted to pH 5.5 with KOH. The only modification of backfilling solutions was the addition of 1 M KCl to the H^+ backfilling solution.

Microelectrodes for intravacuolar ion activities were prepared essentially as for MIFE electrodes (see general materials and methods) except that they were pulled on a two stage puller (Narishige PP-830, Japan) to the smallest diameter that still allowed back filling. These electrodes were then dried, silanised and filled as for MIFE electrodes except they were silanised for 40 min. An issue for some ionophores is their selectivity for other ions. K, H and Ca LIXs are highly selective for their specific ion, however reduced selectivity is observed in Mg LIX against Ca^{2+} (Knowles and

Shabala, 2004) and Na LIX against K^+ (Carden *et al.*, 2001; Chen *et al.*, 2005). Consequently K^+ and Ca^{2+} activities were measured before Na^+ and Mg^{2+} respectively so the selectivity of the LIXs could be determined in the background of expected intravacuolar activities. The voltage of ion selective microelectrodes is also affected by the ionic strength of the solutions, so the major osmoticants (K^+ and Na^+) were determined first and included in calibration solutions. Ion activity or concentration were estimated for K^+ , Na^+ , Ca^{2+} , Mg^{2+} and H^+ in that order. For intravacuolar activity the ion selective microelectrodes were connected to the MIFE system and inserted into individual vacuoles with a manually operated micromanipulator (Narishige, Japan) at an angle of approximately 60° to horizontal as for membrane potential measurements.

K, Ca and Mg LIX were successfully used for impalement and measurement of intravacuolar ion activity. K electrodes were calibrated in the background of 60 mM NaCl and Ca electrodes in the background of 115 mM KCl and 60mM NaCl. Mg^{2+} electrodes were calibrated in a background of 115 mM KCl and 60mM NaCl and 200 μM CaCl_2 . The Mg^{2+} activity was measured for a number of vacuoles without correction for vacuolar Ca^{2+} activity to determine a rough activity. A range of 5-11 mM Mg^{2+} was measured. The sensitivity of the Mg electrode to 150-350 μM CaCl_2 was determined in the background of 115 mM KCl, 60 mM NaCl and MgCl_2 concentrations of 1, 5, 10, 20 and 40 mM. At and above 5 mM MgCl_2 there was no significant change in electrode voltage due to changes in $[\text{CaCl}_2]$ so there was no need to make additional corrections for the poor selectivity of the Mg LIX. The Na LIX is highly sensitive to K^+ and could not be calibrated in the background of 115mM KCl. Instead, Na^+ concentration was estimated by squeezing juice from red beet, centrifuging at 200g and then measuring the sap Na^+ concentration with a Na filter on

a flame photometer (EEL flame photometer, Evans Electroselenium Ltd., Essex, UK). The majority of solution collected will be from the vacuole and will be mostly free Na because no chemical extraction or digestion was used. The H^+ LIX could not be successfully used to measure intravacuolar pH, because the H^+ LIX would not fill electrodes unless the tips were made wider. Even if impalements were achieved with no significant increase in Ca^{2+} flux, there was very little voltage shift. Sometimes vesicles formed within the electrode opening were visible and every H^+ electrode when removed from the vacuole could not be recalibrated.

Intravacuolar Ca^{2+} activity was also independently estimated by measuring the Ca^{2+} flux reversal at increasing Ca^{2+} concentrations (see below).

6.2.3 Vacuolar Ca fluxes

Net Ca^{2+} fluxes were estimated by measuring the ion gradients in the unstirred layers near the vacuole surface using the MIFE technique (Newman *et al.*, 1987; Shabala *et al.*, 1997). Fabrication and calibration of Ca^{2+} ion selective microelectrodes were as has been described in the general materials and methods except that they were calibrated in the background of 100 mM K^+ to account for the effect of bath ionic strength. The MIFE electrode was positioned 10 μm from the vacuole surface and moved back and forth 50 μm in a horizontal plane to avoid any confounding effects of background fluxes from the glass. For every individual measurement of Ca^{2+} flux from the vacuole, the background flux was measured immediately adjacent to the vacuole and later subtracted to give the real flux. Because many vacuoles were measured for each experiment, the diameter of every vacuole was measured to later calculate flux (Appendix 3). The change in Ca^{2+} flux was used to both estimate the intravacuolar ion concentration and to examine the effect of various second

messengers on vacuolar Ca^{2+} release. For each experiment the control flux from a number of vacuoles was measured before the compound, or combination of compounds were added and the changes in Ca^{2+} flux measured. Red beet vacuoles, which are much easier to isolate, were used to screen responses before the most relevant second messengers were tested on ET8 and ES8 to determine their potential role in $[\text{Ca}^{2+}]_{\text{cyt}}$ elevation. The statistical significance of changes in Ca^{2+} flux in red beet vacuoles was analysed by a one way analysis of variance using SPSS and means were compared using Duncan's multiple range test.

Intravacuolar $[\text{Ca}^{2+}]$ was estimated by measuring the external concentration at which Ca^{2+} flux reversal occurred. Additional CaCl_2 was added to the chamber so that fluxes were measured at background Ca^{2+} contamination ($3.5 \mu\text{M}$ measured by MIFE) plus an additional 0, 20, 50, 70, 100, 150 and $250 \mu\text{M}$ CaCl_2 . The intravacuolar $[\text{Ca}^{2+}]$ was calculated by using the Nernst equation. It was assumed that at the bath $[\text{Ca}^{2+}]$ where no Ca^{2+} flux occurred, the Nernst potential was equal to the measured membrane potential (-4.1 mV) and the nernst equation could be solved for the intravacuolar activity.

Nernst equation:
$$V_{\text{eq.}} = \frac{RT}{zF} \ln \left(\frac{[\text{X}]_{\text{out}}}{[\text{X}]_{\text{in}}} \right)$$

Where: $V_{\text{Eq.}}$ is the equilibrium potential (Nernst potential) for a give ion
 R is the universal gas constant ($8.314 \text{ J.K}^{-1}.\text{mol}^{-1}$).
 T is the temperature in Kelvin ($\text{K} = ^\circ\text{C} + 273.15$).
 z is the valence of the ionic species.
 F is the Faraday's constant (96485 C.mol^{-1}).
 $[\text{X}]_{\text{out}}$ is the concentration of the ionic species X in the extracellular fluid.
 $[\text{X}]_{\text{in}}$ is the concentration of the ionic species X in the intracellular fluid.

6.2.4 Patch clamp

Patch clamp was used to examine SV channel activity with intravacuolar ionic activities mimicking native solutions and to see the effects on SV channels of compounds that were identified from the MIFE studies. Fabrication of patch pipettes was as described in the general materials and methods. Current measurements were performed using an Axopatch 200B integrating Patch-Clamp amplifier (Axon Instruments, Foster City, CA, USA). Vacuolar ion currents were measured under voltage clamp conditions in the cytosol out configuration. Single channel currents were evoked by a series of 0.6-1.2 s pulses from -100 to +180 mV in 20 mV increments. Ramps of 50 ms duration between -200 to +200 mV from a holding of 50-70 mV were performed to determine single channel IV curves. Relative open probability was calculated as outlined in the general materials and methods.

The effect of the measured intravacuolar ionic activities on modulation of SV channel activity by intravacuolar Ca^{2+} and cytosolic Ca^{2+} and Mg^{2+} was examined in cytosol out patches. The basic pipette solution was 62mM NaCl, 125 mM KCl, 8 mM Mg, 200 μ M CaCl_2 , adjusted to pH 7.0. The basic bath solution was 100 mM KCl, 2mM CaCl_2 , 10 mM HEPES adjusted to pH 7.4. For experiments looking at the modulation of SV activity by vacuolar Ca^{2+} the basic pipette solution was adjusted to include 0 (2mM EGTA) or 500 μ M CaCl_2 . For the experiments examining cytosolic Mg^{2+} and Ca^{2+} modulation of SV activity the bath solution was altered to also include 0.1 μ M Ca^{2+} , 1.5 mM MgCl_2 ; 20 μ M Ca^{2+} , 1.5 mM MgCl_2 ; 0.1 μ M Ca^{2+} , 0.5 mM MgCl_2 ; or 20 μ M Ca^{2+} , 0.5 mM MgCl_2 .

Unfortunately at the time of experiments examining the effect of second messengers on SV activity, the available red beet were displaying a low level of SV activity and rapid run down during experiments so it is only possible to present some representative traces for H_2O_2 here. The pipette solution was 100 mM KCl, 2 mM EGTA adjusted to pH 7.0 with KOH and 640 mOsm with sorbitol. The basic bath solution was 100 mM KCl, 1.5 mM MgCl_2 , 1 mM HEPES adjusted to pH 7.4 with KOH and 640 mOsm with sorbitol. To this bath solution 1 mM H_2O_2 was added to determine the effects on SV activity.

6.2.5 *Arabidopsis* morphology

The importance of SV channel density in Al toxicity was investigated in growth experiments of *Arabidopsis* mutants varying in TPC1 expression. Wildtype (Columbia), TPC1 under expressing (*tpc 1-2*) and TPC1 over expressing (TPC1 5-6 and TPC1 10-20) mutants were grown on agar plates in the presence and absence of Al.

The agar growth solution was specially formulated to give a free Al^{3+} activity that reduced the root growth of wildtype Columbia by approximately 20%. The growth media was prepared from a number of stocks:

- 1) RGS solution (“Rabby Growth Solution”), 20 mM KNO_3 , 8 mM CaCl_2 , 8 mM MgSO_4 , 0.1 mM KH_2PO_4 , 46.1 μM H_3BO_3 , 1.6 μM $\text{ZnSO}_4 \cdot 6\text{H}_2\text{O}$ and 0.784 μM $\text{CuCl}_2 \cdot 2\text{H}_2\text{O}$.
- 2) 20 mM $\text{AlCl}_3 \cdot 6\text{H}_2\text{O}$ in 0.1 mM HCl.
- 3) 200 mM succinic acid adjusted to pH 4.9 with NaOH.

To prepare the media required for 20-30 plates, 200mL of 2% agar (w/v) and 2% sucrose (w/v) in distilled water (adjusted to pH 4.9 with HCl), 100 mL of distilled water and 132 mL of RGS (in a 500 mL schott bottle) were sterilised in an autoclave. The solutions were allowed to cool to 60-80°C. 10 mL of 0.2 μ M filtered succinic acid stock was added to the RGS solution and the volume made up to 200mL with sterile water. The sterilised agar was added to this to make a final volume of 400mL. To one preparation 0.2 μ M filtered $AlCl_3$ stock was added to give a final concentration of 500 μ M $AlCl_3$. The final concentration of the growth media was 6.6 mM KNO_3 , 2.64 mM $CaCl_2$, 2.64 mM $MgSO_4$, 33 μ M KH_2PO_4 , 15.21 μ M H_3BO_3 0.53 μ M $ZnSO_4 \cdot 6H_2O$, 0.26 μ M $CuCl_2 \cdot 2H_2O$, 5 mM succinic acid, pH 4.9, 1% agar (w/v), 1% sucrose (w/v) and 0 or 500 μ M $AlCl_3$. The media was then poured into large plastic petri plates in a laminar flow and allowed to cool before *Arabidopsis* seeds were planted.

Arabidopsis seeds were sterilised in 30% bleach (v/v), 0.1% triton solution for 10 min in a 1.5 mL Eppendorf tube. Seeds were then centrifuged, supernatant poured off and rinsed in 1 mL sterilised distilled water six times before plating. Seeds were suspended in approximately 0.1mL of sterile distilled water and transferred to media plates with sterilised yellow tips, whose ends had been cut to allow single seeds to pass. 15-20 seeds were evenly spaced in a line across each plate; three replicate plates of each treatment and *Arabidopsis* genotype were planted. Plates were sealed with Parafilm™ and placed vertically under a fluorescent tube. Root lengths were recorded and photos taken after 5 days.

6.3 Results

6.3.1 Intravacuolar ionic composition

Accounting for the effects of LJP (Ca electrode 1.275 mV, K 1.375 mV, Mg 6.6 mV), V_m (-4.22 mV) and ionophore selectivity, the following intravacuolar ion activities were calculated: 116.6 ± 1.1 mM K^+ (SEM, $n = 8$); 196.0 ± 18.0 μ M Ca^{2+} (SEM, $n = 7$); 8.3 ± 0.7 mM Mg^{2+} (SEM, $n = 7$). Ca^{2+} flux reversal occurs at approximately 207 μ M Ca^{2+} in the bath (Figure 6.1). The intravacuolar Ca^{2+} concentration was calculated independently from the flux reversal, as approximately 243 μ M.

Ca^{2+} fluxes were significantly inhibited by 100 μ M zinc, suggesting a significant component of the flux measured may be through SV channels (Figure 6.1A).

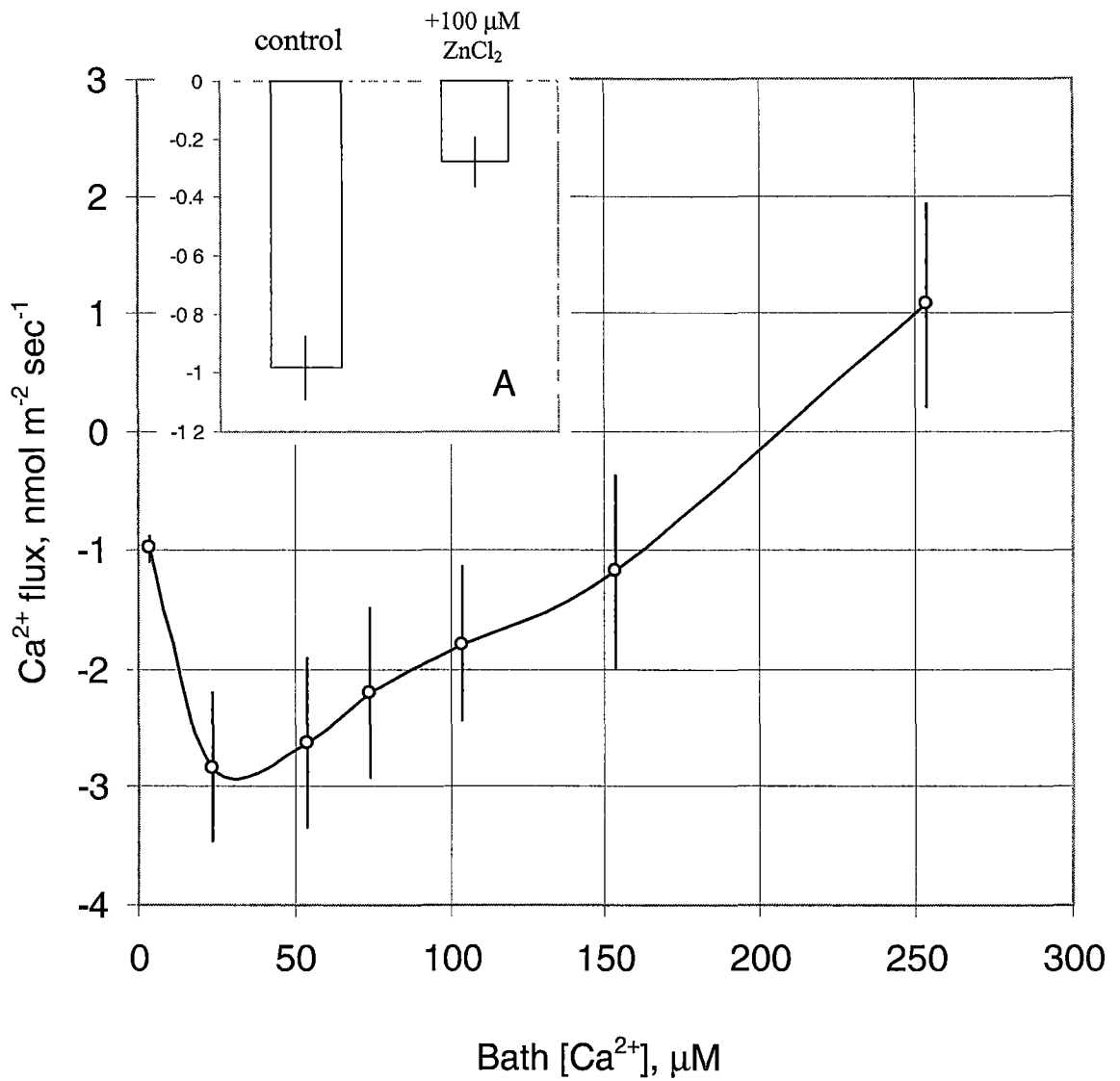


Figure 6.1. Red beet vacuolar Ca^{2+} fluxes in standard bath solution (100 mM KCl 1 mM HEPES, pH 7.4) in response to changing bath Ca^{2+} concentration. Data are mean \pm SEM (n = 6-19). Negative values indicate efflux. The reversal point of efflux to influx suggests a vacuolar Ca^{2+} concentration of around 243 μM. A. Inhibition of Ca flux by Zn (standard bath solution without additional Ca^{2+}), suggesting a significant proportion of flux may be through SV channels. Data is mean \pm SEM (n = 7-8).

6.3.2 SV activity under native vacuolar ion activities

With the background of the measured vacuolar ion activities, SV open probability was not significantly altered by changes of 0 – 500 μM vacuolar Ca^{2+} activity (Figure 6.2). In absence of Ca^{2+} 62 mM Na^+ decreased open probability more than the equivalent concentration of K^+ (Figure 6.2 A), but it ameliorated the inhibitory effect of 500 μM Ca^{2+} .

In vacuole out patches cytosolic Ca and Mg significantly increased SV open probability (Figure 6.3 A). In the cell attached mode 1.5 mM Mg also significantly increased SV open probability (Figure 6.3 B). 20 μM Ca^{2+} only increased SV open probability at high cytosolic Mg^{2+} activities.

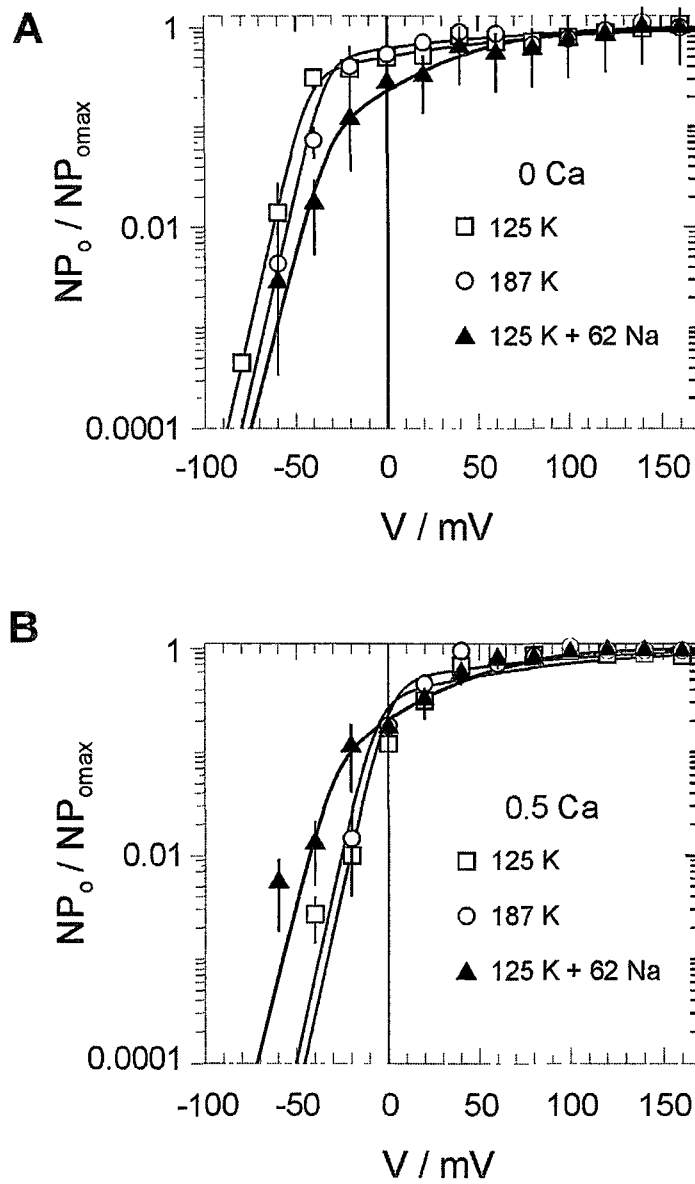


Figure 6.2. Effect of vacuolar Na^+ on the SV channel voltage dependence at $0 \mu\text{M}$ CaCl_2 (A) and $500 \mu\text{M}$ CaCl_2 (B). Data from excised patches, at least 3 replicates for each condition are presented as mean \pm SD. Curves are best fits for a three state lineal scheme (C2-C1-O), where transition between two closed states (C2 and C1) and channel opening (C1-O transition) are described by two Boltzmann functions.⁵

⁵ The data in this figure was collected in collaboration with Vadim Perez

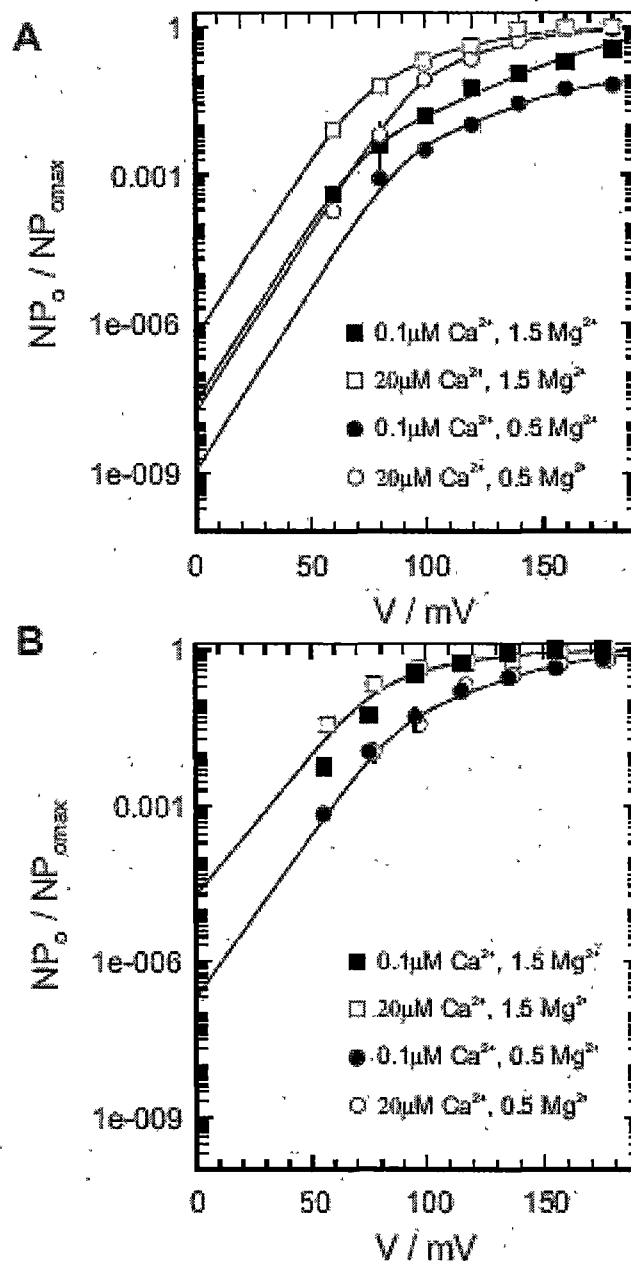


Figure 6.3. Modulation of the SV channel voltage dependence by cytosolic Ca^{2+} and Mg^{2+} in vacuole attached and outside out configurations. A. Open probability of SV channel in isolated cytosol out patches. B. Open probability of SV channel in vacuole attached patches. Data are mean (\pm SD, $n=4-8$).⁶

⁶ The data in this figure was collected in collaboration with Vadim Perez

6.3.3 Ca^{2+} currents in red beet vacuoles

The effect of all chemicals and second messengers tested on Ca^{2+} fluxes in red beet (30 combinations in total) are summarised in Table 6.1. Significant ($p < 0.01$) increases in Ca^{2+} efflux were observed with 1.5 mM Mg^{2+} , 100 μM cAMP, 10 μM ATP, 5 and 10 μM Ca^{2+} and 50 μM ATP. A significant ($p < 0.01$) decrease in Ca^{2+} efflux was observed with 1 mM and 100 μM H_2O_2 treatment. Figures Figure 6.3- Figure 6.7 summarise the important data in graphical formats.

Table 6.1. Effect of various compounds on Ca^{2+} flux from SV vacuoles. Data are means ($n = 5-60$). Significant differences ($p < 0.01$) from the mean, as calculated by Duncans multiple range (SPSS), are indicated by asterisks.

Treatment	Mean Ca^{2+} flux ($\text{nmol m}^{-2} \text{s}^{-1}$)
Control	-0.866
100 μM CaM	-0.879
200 μM CaM	-1.332*
1.5 mM Mg	-1.428*
100 μM cAMP	-1.475*
100 μM cAMP/ CaM	-1.602*
100 μM cAMP/CaM/ATP	-1.460*
10 μM cGMP	-0.860
10 μM cGMP, 100 μM CaM	-0.940
10 μM cGMP, 100 μM CaM, 1 mM Mg	-1.035
100 μM cGMP/CaM	-1.012
10 μM ATP	-1.472*
10 μM ATP, 100 μM CaM	-0.848
100 μM ATP	-0.810
100 μM ATP/CaM	-0.848
2 μM IP3	-0.697
2 μM IP3, 100 μM CaM	-0.860
2 μM IP3, 100 μM CaM, 1mM Mg	-0.995
10 μM IP3	-0.820
10 μM IP3, 100 μM CaM	-1.128
10 μM IP3, 100 μM CaM, 1 mM Mg	-1.009
5 μM Ca	-2.457*
10 μM Ca	-2.634*
10 μM Ca, 100 μM CaM	-2.608*
1 mM H_2O_2	-0.073*
0.1 mM H_2O_2	-0.123*
10 μM ABA	-0.731
10 μM ABA, 2 μM IP3	-0.782
50 μM ABA	-1.274*
50 μM ABA, 2 μM IP3	-1.354*

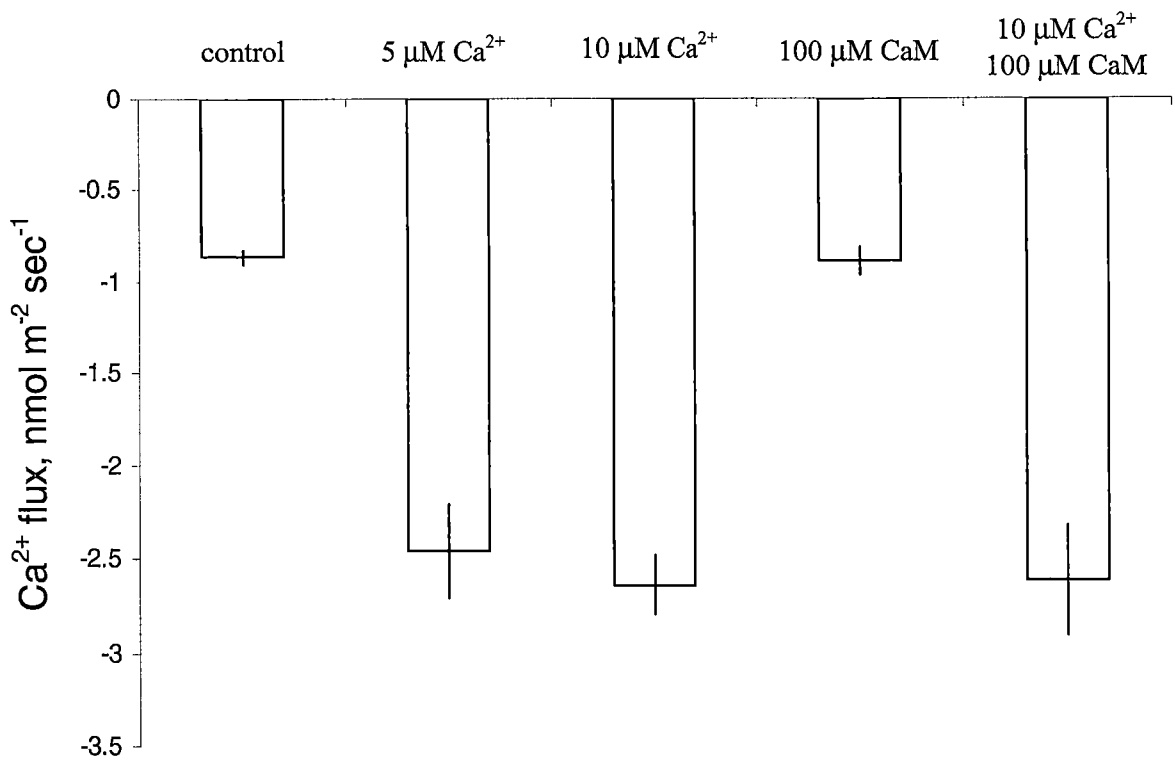


Figure 6.4. Ca^{2+} efflux induced by low bath Ca^{2+} concentrations and calmodulin (CaM) in red beet vacuoles. Control treatment was the standard bath solution (100 mM KCl, 1 mM HEPES, pH 7.4). Data are mean \pm SEM (n = 8-60).

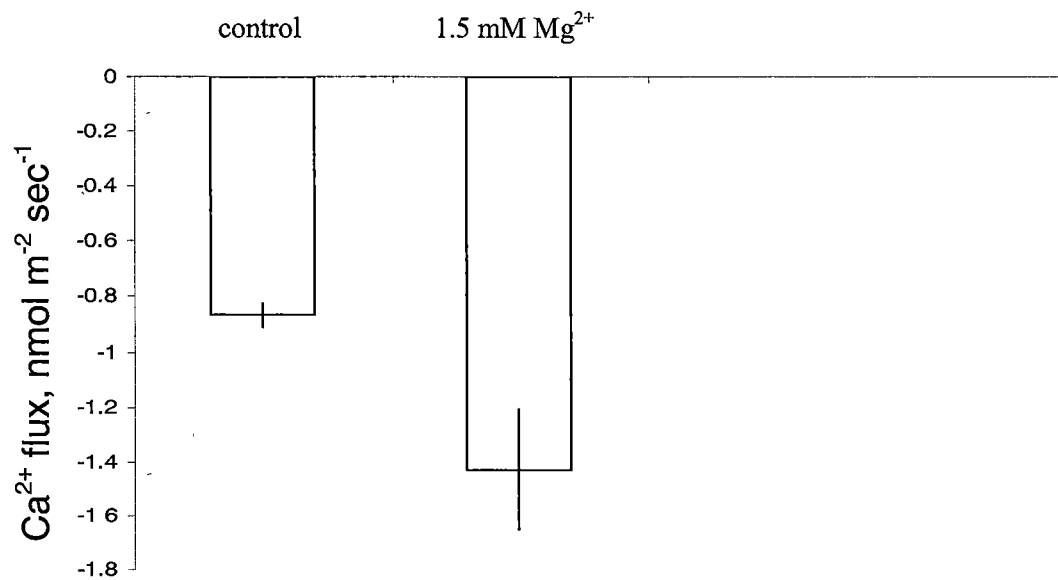


Figure 6.5. Ca^{2+} efflux induced by bath Mg^{2+} in red beet vacuoles. Control treatment was the standard bath solution (100 mM KCl, 1 mM HEPES, pH 7.4). Data are mean \pm SEM (n = 9-60).

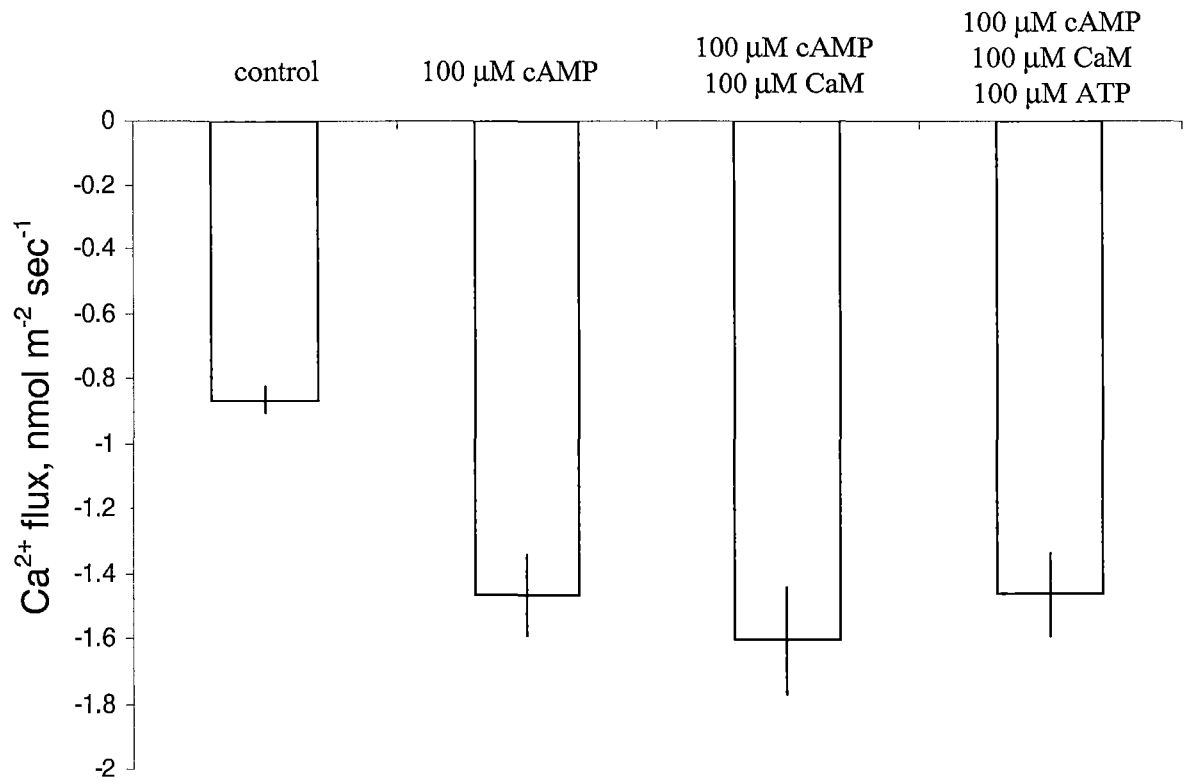


Figure 6.6. Ca^{2+} efflux induced by bath cAMP alone and in combination with calmodulin (CaM) and ATP in red beet vacuoles. Control treatment was the standard bath solution (100 mM KCl, 1 mM HEPES, pH 7.4). Data are mean \pm SEM (n = 10-60).

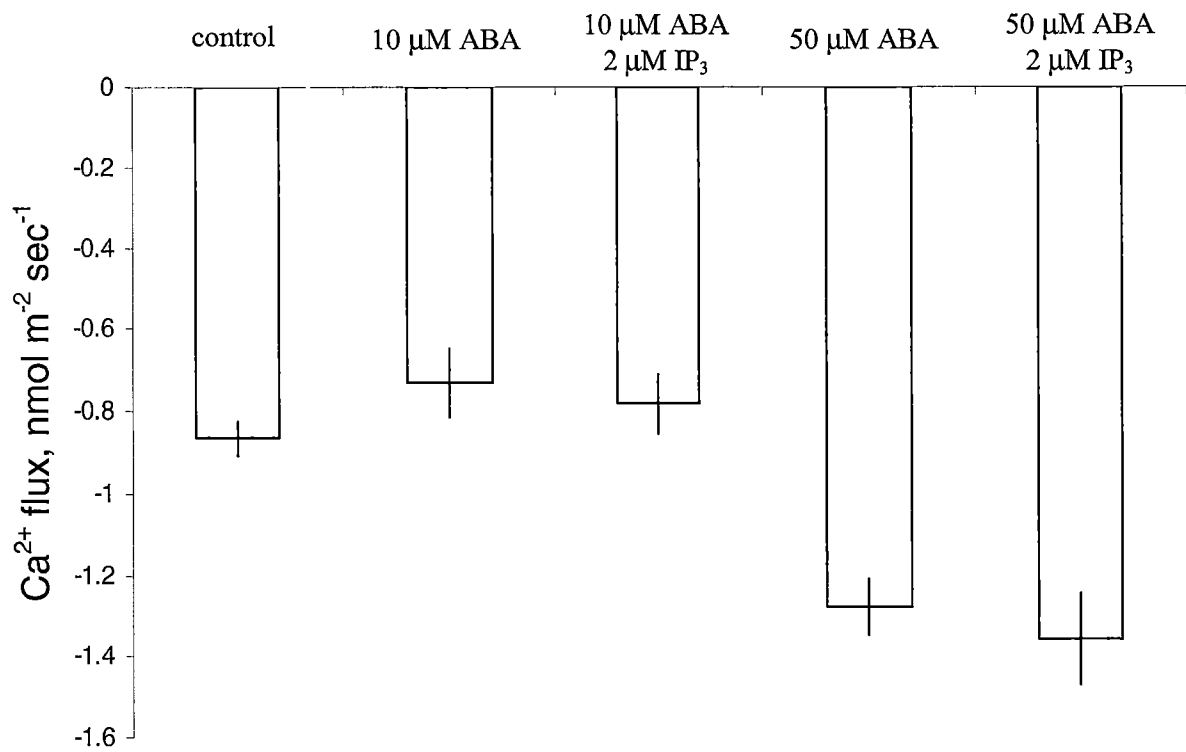


Figure 6.7. Ca^{2+} efflux induced by bath ABA alone and in combination with inositol triphosphate (IP_3) in red beet vacuoles. Control treatment was the standard bath solution (100 mM KCl, 1 mM HEPES, pH 7.4). Data are mean \pm SEM (n = 5-60).

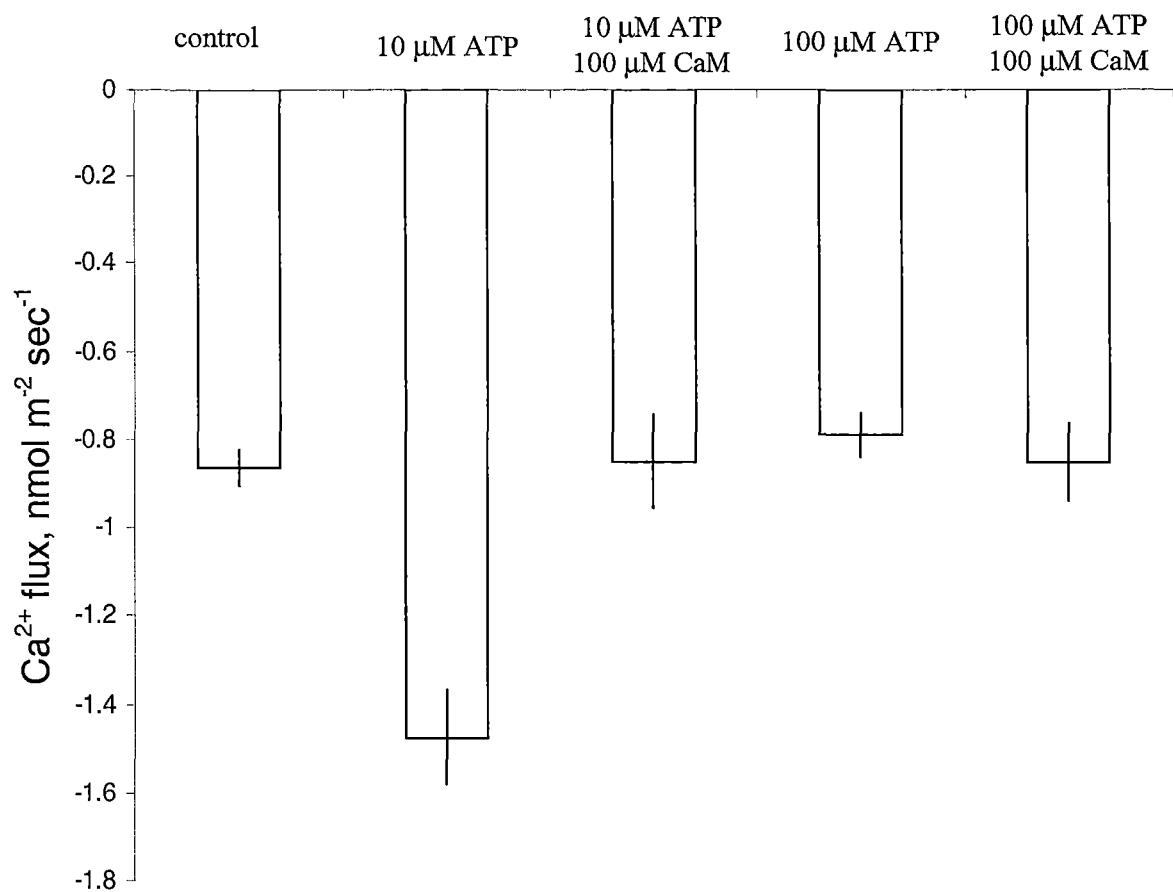


Figure 6.8. Ca^{2+} efflux induced by bath ATP alone and in combination with calmodulin (CaM) in red beet vacuoles. Control treatment was the standard bath solution (100 mM KCl, 1 mM HEPES, pH 7.4). Data are mean \pm SEM (n = 12-60).

6.3.4 Ca^{2+} currents in ET8 and ES8 wheat vacuoles

Second messengers identified from MIFE fluxes with red beet vacuoles were examined on ET8 and ES8. Ca^{2+} efflux in wheat is significantly higher from ES8 than ET8 vacuoles (Figure 6.8). ABA and IP_3 independently and in combination increased Ca^{2+} efflux, whereas cAMP did not significantly alter fluxes. In all treatments the flux of ES8 was higher than that of ET8.

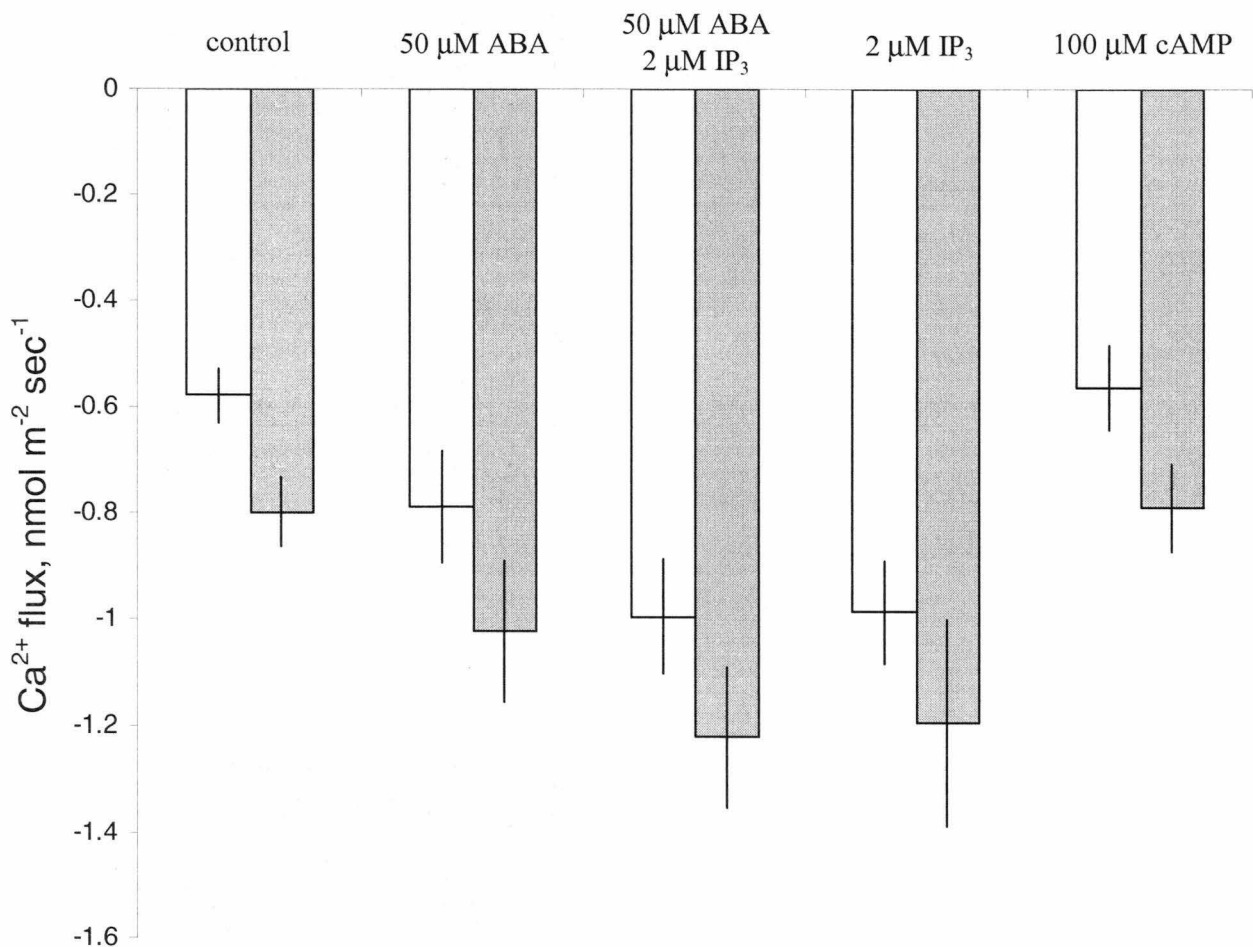


Figure 6.9. Ca^{2+} efflux in ET8 and ES8 induced by bath ABA, IP_3 and cAMP. Control treatment was the standard bath solution (100 mM KCl 1 mM HEPES, pH 7.4). Data are mean \pm SEM (n = 5-9)

6.3.5 Effects of second messengers on red beet SV activity

Because of the problem of SV run down and the absence of SV currents at the time of measurement only a representative trace of the effect of H_2O_2 on SV activity can be given here. Addition of 1mM H_2O_2 to the bath inhibits SV and increases the leak current (Figure 6.10).

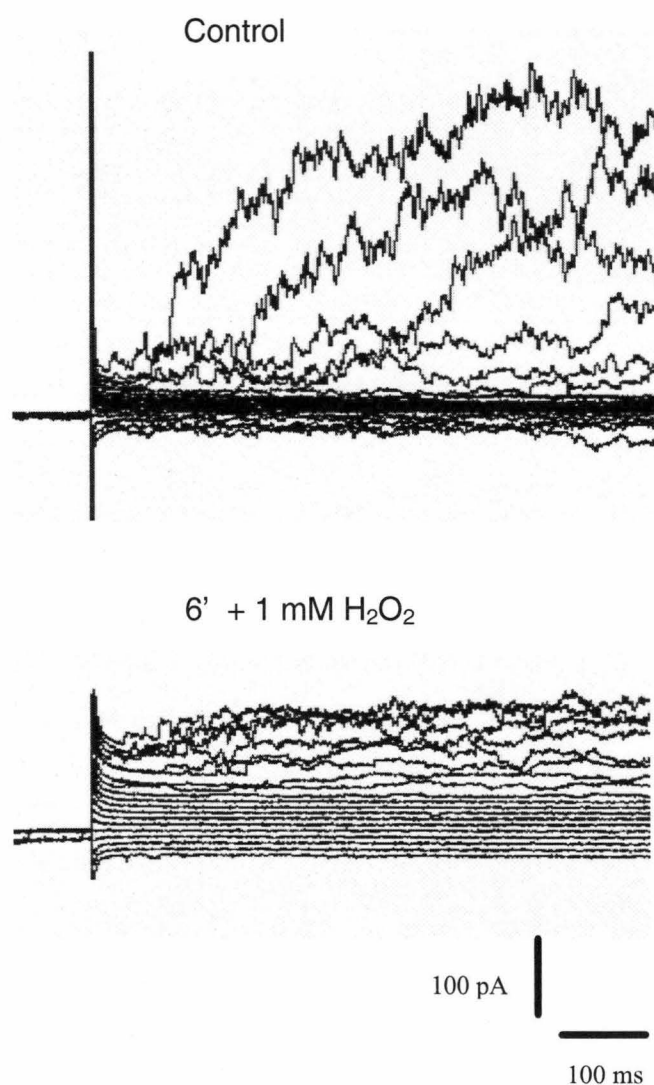


Figure 6.10. Representative traces of large outside out vacuoles showing inhibition of SV currents and increase of leak by 1 mM H_2O_2 .

6.3.6 Growth experiments of *Arabidopsis* mutants

The *Arabidopsis* mutants selected differ in the expression of TPC1 that encodes the SV channel. In the absence of Al, all *Arabidopsis* mutants had significantly lower root elongation than the wild type Columbia, with the *Arabidopsis* mutant *tpc 1-2* (under expressing TPC1) the lowest (Figure 6.9). However the elongation of Al treated plants relative to control was much higher in *tpc 1-2* plants than Columbia or the other mutants. Relative root length was slightly lower in TPC1 over expressors TPC1 5-6 and TPC1 10-21 than Columbia.

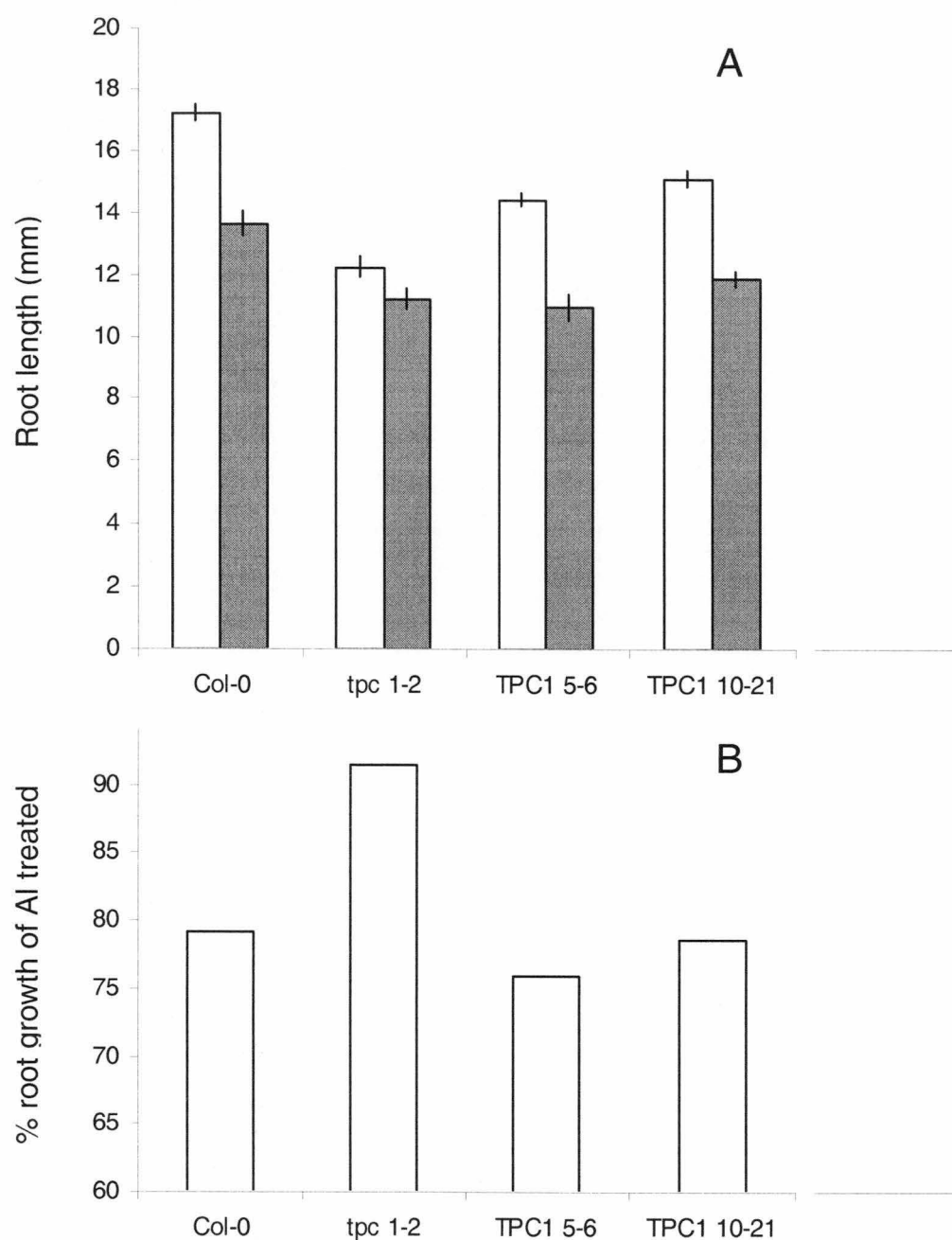


Figure 6.11. Effect of Al on root length in *Arabidopsis* wildtype Columbia (Col-0) and TPC-1 under expressor (*tpc 1-2*) and over expressors (TPC1 5-6 and TPC1 10-21). A. Data are mean root length \pm SEM ($n = 26-38$) for Al free (open columns) and 500 μM AlCl_3 (closed columns). B. Percentage root length of Al treated compared to control.

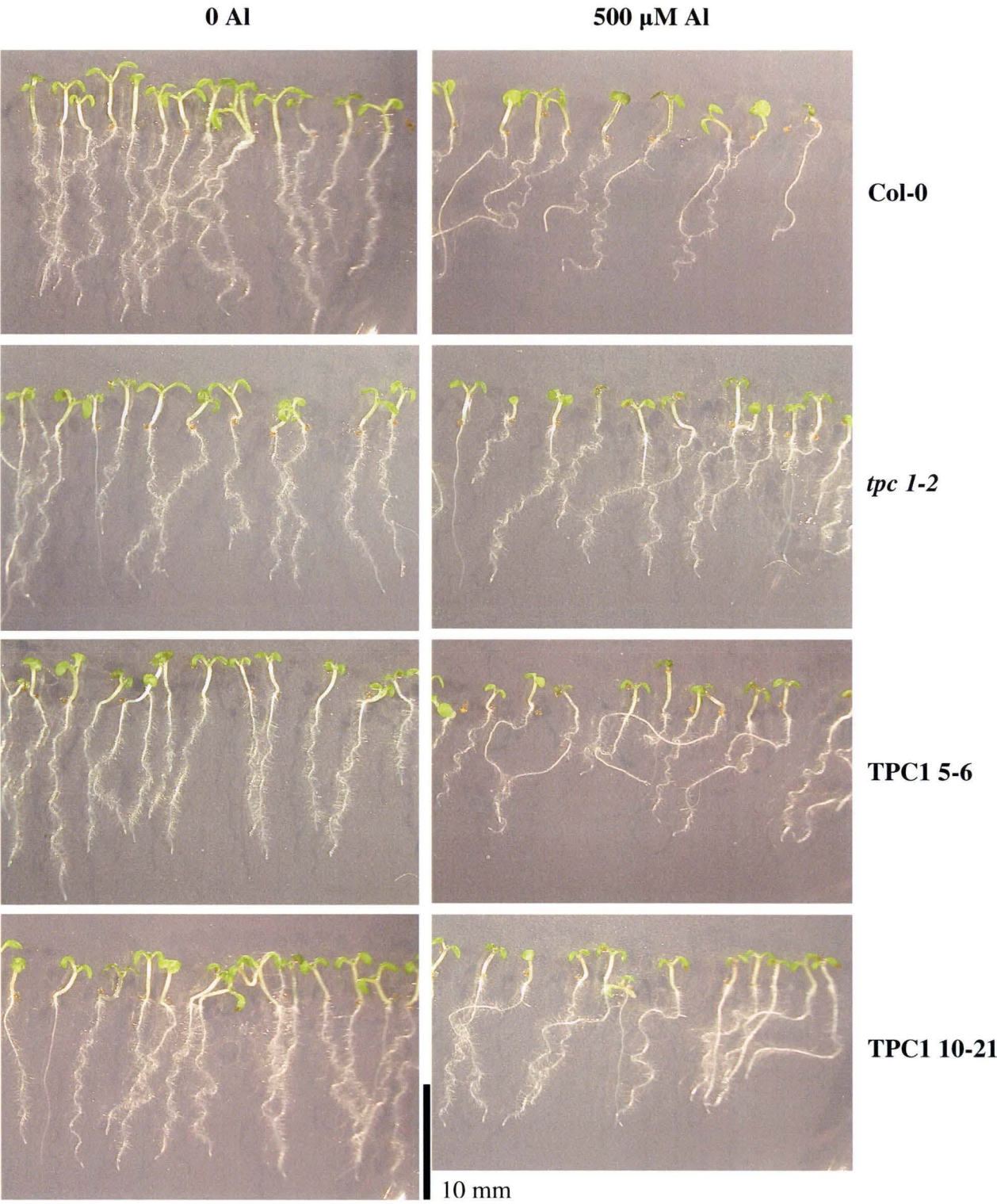


Figure 6.12. Photographs of *Arabidopsis* mutants and their response to Al treatment.

6.4 Discussion

6.4.1 Capacity of SV to mediate Ca^{2+} flux at physiological potentials

The estimation of intravacuolar Ca^{2+} via the flux reversal and ion selective micro electrode concur that the $[\text{Ca}^{2+}]_{\text{vac}}$ activity was around 190-250 μM . This is much lower than the activities commonly reported in the literature. This discrepancy may be due to artefacts created by various experimental techniques. Fluorescent dyes are frequently used, but problems loading, interference of the cell wall and unknown effects all create artefacts. Impalement can have problems of leaking and blockage. However the use of Ca^{2+} flux reversal should have minimal artefacts as the vacuole remains intact. The concurrence of flux reversals and impalement gives confidence to these measurements. The low value of $[\text{Ca}^{2+}]_{\text{vac}}$ suggests that with the native ionic composition we may expect the activity of the SV channel to be higher than previously expected. However patch experiments performed in conjunction with these MIFE experiments show that with solutions mimicking the native vacuolar ionic composition of red beet SV channel open probability is not affected by changes in $[\text{Ca}^{2+}]_{\text{vac}}$ (Figure 6.2). It was found that this was caused by the high Na^+ concentration, which seems to act as a natural buffer of SV activity to $[\text{Ca}^{2+}]_{\text{vac}}$ maintaining SV at a low open probability. The effect of vacuolar Na^+ on the SV channel voltage dependence is stronger than is expected from the surface charge theory (Figure 6.2 A) (Pottosin *et al.*, 2005). Red beet is highly salt tolerant and can accumulate very high concentrations of Na^+ , the measurement of 60 mM is higher than the vacuolar concentrations reported for other species (Greenway and Munns, 1980), so such strong buffering of SV activity would not be expected in other species. It would be nice to develop another Na LIX that is selective only for Na^+ , which

would allow our crude measurements to be confirmed and the Na^+ activity to be reliably determined in other plant species.

6.4.2 Screening elicitors of vacuolar Ca^{2+} flux with red beet vacuoles

Measuring the effect of various chemicals and second messengers on Ca^{2+} fluxes from vacuoles using the MIFE system proved to be a viable technique. However the very small fluxes were at the limit of the MIFE system to detect. This meant that extreme care had to be taken to standardise the distance the electrode was placed from each sample, control treatments had to be performed for each group of vacuoles to ensure normal fluxes and the electrical noise of the system had to be absolutely minimised.

Elevated $[\text{Ca}^{2+}]_{\text{cyt}}$ signals many different growth and developmental processes and it has become clear that specificity of Ca^{2+} signalling involves the complex interaction of location and timing of Ca^{2+} concentration changes, as well as the involvement of Ca^{2+} sensor molecules (Luan *et al.*, 2002). Ca^{2+} sensors are commonly proteins that change their conformation when bound with Ca^{2+} and become physiologically ‘active’ or ‘inactive’. In this way calcium sensors act synergistically with Ca^{2+} to monitor and interpret temporal and spatial changes in Ca^{2+} . Calmodulin (CaM) and calcineurin (a calmodulin dependent type 2B protein phosphatase) are two Ca^{2+} sensors that have been shown to influence SV channel activity. Even within these two calcium sensors there are a number of plant isoforms that seem to have different biological function, although the specific function of many remain unknown (Lee *et al.*, 2000).

Calmodulin inhibitors and certain chemicals that phosphorylate SV have been shown to decrease activity (Schulzlessdorf and Hedrich, 1995; Bethke and Jones, 1997).

Exogenous application of plant isoforms of CaM, but not bovine CaM, can restore the

activity of SV decreased by CaM inhibitors (Weiser *et al.*, 1991; Bethke and Jones, 1994). Low levels of calcineurin in the presence of CaM restored phosphorylated SV activity by dephosphorylation, but individually neither effected activity (Bethke and Jones, 1997). A high level of calcineurin has been shown to inhibit SV activity (Allen and Sanders, 1995). Exogenous application of spinach CaM was shown to increase SV sensitivity to Ca^{2+} (Weiser *et al.*, 1991).

Unfortunately at this time calcineurin (from bovine brain) cannot be imported into Australia because of quarantine against Bovine Spongiform Encephalopathy (Mad Cow Disease). So it was not possible to test the effect of calcineurin, in combination with CaM or any Ca^{2+} second messengers. Additionally, no plant calmodulin isoforms were available commercially and they could not be sourced elsewhere, so only the effect of Bovine calmodulin could be examined.

In the literature there are no reports of CaM increasing SV activity except in the presence of another elicitor or restoring activity lost because of a CaM inhibitor. This has prompted the suggestion that endogenous CaM is tightly bound with SV in patch preparations (Bethke and Jones, 1997). Interestingly my results concurred with these observations at 100 μM CaM, but at 200 μM CaM increased Ca^{2+} efflux was observed (Table 6.1). This may reflect an increase in CaM binding to the SV channel above the level of endogenous CaM. Addition of exogenous CaM at 100 μM did not significantly affect the flux in response to any second messengers, except it prevented the increase in Ca^{2+} efflux induced by 10 μM ATP. It would be very useful for future research to examine the effect of various CaM isoforms, in conjunction with calcineurin and other second messengers, on the fluxes of Ca^{2+} from vacuoles and SV channel activity. CaM isoforms have been shown to have diverse effects on CaM dependent enzymes and calcineurin (Lee *et al.*, 2000).

Mg in the bath increased Ca^{2+} efflux (Table 6.1), confirming patch experiments showing that cytosolic Mg^{2+} activation of SV (Pei *et al.*, 1999; Carpaneto *et al.*, 2001) (Figure 6.3) does result in increased flux through SV at physiological potentials. However Mg^{2+} did not significantly alter the fluxes observed with any second messengers (Table 6.1).

A number of common second messengers, some of which have already been implicated in Al toxicity, were tested to see which elicited Ca^{2+} flux from red beet vacuoles. No effects alone or in combination with any other chemicals were observed for cGMP or IP_3 . The result for IP_3 is in contrast to patch clamp data that showed an IP_3 induced activation of currents from vacuoles (Scanlon *et al.*, 1996; Taylor and Laude, 2002). Both 5 μM and 10 μM Ca^{2+} significantly increased Ca^{2+} flux as would be expected in CICR through SV and potentially an IP_3 gated channel also.

Interestingly, cAMP significantly increased Ca^{2+} efflux (Table 6.1). It is known that cAMP is involved in the tolerance mechanism of ET8, being required for the activation of an Al induced K^+ permeable plasma membrane channel (Zhang *et al.*, 2001). The response of cAMP to Al exposure in ET8 and ES8 is unknown.

The effect of ATP on Ca^{2+} fluxes was variable, a significant increase was only observed at 10 μM ATP and not 100 μM . In the presence of 100 μM CaM, no significant increase in flux was observed, suggesting CaM may affect ATP binding. Patch clamp data has suggested at 200 μM ATP, SV channel activity decreases because of phosphorylation, though in the same series of experiments 2 mM ATP activated SV, possibly through enhanced activation of a protein kinase (Bethke and Jones, 1997). Physiological ATP concentrations reported in the literature are 200 μM to 2 mM (Roberts *et al.*, 1985; Wu and Assmann, 1995) and although ATP is generally considered in metabolism, its potential role as a signalling compound at low

concentrations was demonstrated recently (Demidchik *et al.*, 2003a). It is also possible that 10 μM ATP might have energised the voltage-ATPase and altered Ca^{2+} flux via other gradients. This hypothesis could be examined in future research by the use of a non hydrolysed analogue of ATP.

The response of Ca^{2+} fluxes to ABA is important in the mechanism of both AI and other abiotic stress induced elevation of $[\text{Ca}^{2+}]_{\text{cyt}}$. Significant efflux only occurred at high levels of ABA indicating a threshold of response (Table 6.1). Practically this means that small fluctuations will not induce an increase in $[\text{Ca}^{2+}]_{\text{cyt}}$ unless this threshold is met. Exogenous application of peroxide significantly reduced Ca^{2+} efflux from red beet vacuoles (Table 6.1) and decreased SV opening (Figure 6.10). An increase Ca fluxes from vacuoles was predicted by Kawano *et al.* (2003; 2004a) who observed that peroxide induced an increase in $[\text{Ca}^{2+}]_{\text{cyt}}$ that correlated with expression of TPC1. My results in conjunction with theirs suggests that peroxide applied exogenously to intact cells may stimulate SV channel Ca^{2+} release by some downstream messenger rather than directly interacting with the channel itself.

6.4.3 Vacuolar Ca^{2+} fluxes in ET8 and ES8

In Chapter 5, it was suggested that the difference in SV channel density and electrophysiological properties between ES8 and ET8 may result in differences of Ca^{2+} flux and $[\text{Ca}^{2+}]_{\text{cyt}}$. This hypothesis was confirmed because Ca^{2+} flux was significantly higher in ES8 in controls and all other treatments than ET8 (Figure 6.9). Interestingly in both wheat cultivars, no response was observed to addition of cAMP, however a significant increase in fluxes did occur with IP_3 (Figure 6.9). The reason for this difference from red beet vacuoles is unknown. ABA and ABA with IP_3 also increased Ca^{2+} efflux. No differences were observed between ET8 and ES8 in the

magnitude of response to these second messengers (Figure 6.9). This implies that the difference between ET8 and ES8 in Ca^{2+} signalling and $[\text{Ca}^{2+}]_{\text{cyt}}$ in response to Al, presuming it is elicited by either ABA or IP_3 , is due to the difference in density and Al^{3+} activity at the plasma membrane surface.

6.4.4 SV channel density affects tolerance to Al

To examine whether or not differences in SV channel density without differences in electrophysiological properties could influence Al tolerance, growth of *Arabidopsis* mutants over and under expressing the TPC1 gene in the presence and absence of Al were compared. Root elongation was reduced in all TPC1 mutants in the absence of Al and Al reduced root elongation in all mutants (Figure 6.11 & 6.12). However, the relative reduction in root elongation was greatest with over expression of SV (TPC1 5-6 and TPC1 20-21) and least with under expression of SV (*tpc 1-2*) (Figure 6.11). This conclusively demonstrates that SV channel density plays a role in Al tolerance, and will contribute in part to the difference in tolerance between ET8 and ES8. The differences in SV channel properties shown in Chapter 5 may accentuate the difference in tolerance. This difference may be more important in the tolerance of root hairs of ET8 compared to ES8 (Chapter 3) where malate exudation does not occur.

Chapter 7: General Discussion

Through the detailed study of two near isogenic wheat cultivars, this project has significantly increased the understanding of the physiology of Al toxicity and tolerance. By examining the effects of Al on the root hair zone (Chapter 3.4.3) and differences in SV channel properties (Chapter 5.4) it has been clearly demonstrated that the difference in tolerance between ET8 and ES8 is more complex than the simple expression of the Al activated malate channel. All previous research on these cultivars has focussed on the root apex and malate exudation, and a gene encoded on the ALT1 locus has recently been shown to encode a plasma membrane activated malate channel (Sasaki *et al.*, 2003). So it was surprising to find that ET8 also showed a higher tolerance in both root hair growth and in nutrient uptake. This difference may be attributed to either tolerance mechanisms expressed directly at the root hairs or those expressed in the root apex. Tolerance mechanisms expressed directly at the root hair could include the differences observed in SV channel properties at the root apex. This could be tested by examining the SV channel properties of root hair vacuoles from ET8 and ES8. Tolerance mechanisms expressed at the root apex may affect root hair growth through hormones or the retention of malate in the cell wall. Future research should focus on determining the cause for the observed difference in root hair tolerance.

Significant differences in SV channel properties between ET8 and ES8 which affect Ca^{2+} homeostasis and response to Al have also been demonstrated. SV channel density was shown to be higher in ES8 than ET8 (Chapter 5.4.2) and the importance for Ca^{2+} homeostasis and Al tolerance confirmed by Ca^{2+} flux measurements in wheat (Chapter 6.4.3) and growth experiments with *Arabidopsis* mutants (Chapter 6.4.4) respectively. *Arabidopsis* mutants that under expressed TPC1, resulting in lower SV

density, had better relative root elongation in the presence of Al than wildtype (Columbia) and over expressing mutants. Furthermore it was shown that after 24 hr exposure to Al, the open probability was significantly increased in ES8 by some unidentified low molecular weight compound. The nature of this compound should be identified by future research. It is suggested that these differences in ET8 and ES8 SV channel properties contribute to the lower elevation of cytosolic Ca^{2+} and consequently higher Al tolerance of ET8 (Chapter 5.4). To demonstrate unequivocally that the differences in SV channel are inherited on the ALT-1 locus a full genetic study examining co-segregation with Al tolerance is necessary. Given the extreme difficulty encountered in successfully patching wheat root apex vacuoles, this would be a major undertaking.

It is widely reported that Al exposure results in elevated cytosolic Ca^{2+} activity and some have suggested that this is directly related to the primary Al toxicity (Rengel and Zhang, 2003). The nature of the pathway and the source of Ca^{2+} (intracellular or extracellular) had not previously been clarified. This study has shown from the characterisation of membrane potential changes in response to Al in ET8 and ES8, that an extracellular source for Ca^{2+} is unlikely, except possibly through a non selective cation channel (NSCC). Further work is needed to determine whether there is an effect of Al on NSCC. Given that an external source of Ca^{2+} was unlikely, this project then examined the possible role of a wide range of second messengers in eliciting Ca^{2+} efflux from vacuoles using the MIFE™ system (Chapter 6.4). This proved to be a useful technique to screen potential elicitors on red beet vacuoles before specifically examining the effect of some specifically affected by ET8 and ES8.

Whilst these differences between ET8 and ES8 highlight that Al tolerance is influenced by more than just Al induced malate efflux, the significance of malate efflux should not be under emphasised. This project has clarified the changes in membrane potential in ET8 and ES8 in response to Al (Chapter 4.3.2). Whilst the response was complex and multiphasic, it was shown that membrane depolarisation, associated with malate efflux, was observed in ET8 but not ES8. Real time Al activated K^+ efflux from intact ET8 wheat roots was been shown for the first time and the possible involvement of Cl^- in charge balance after 24h was also shown (Chapter 4.3.3).

A more complete model than those in Chapter 2 (Ryan *et al.*, 2001; Rengel and Zhang, 2003) can now be presented.

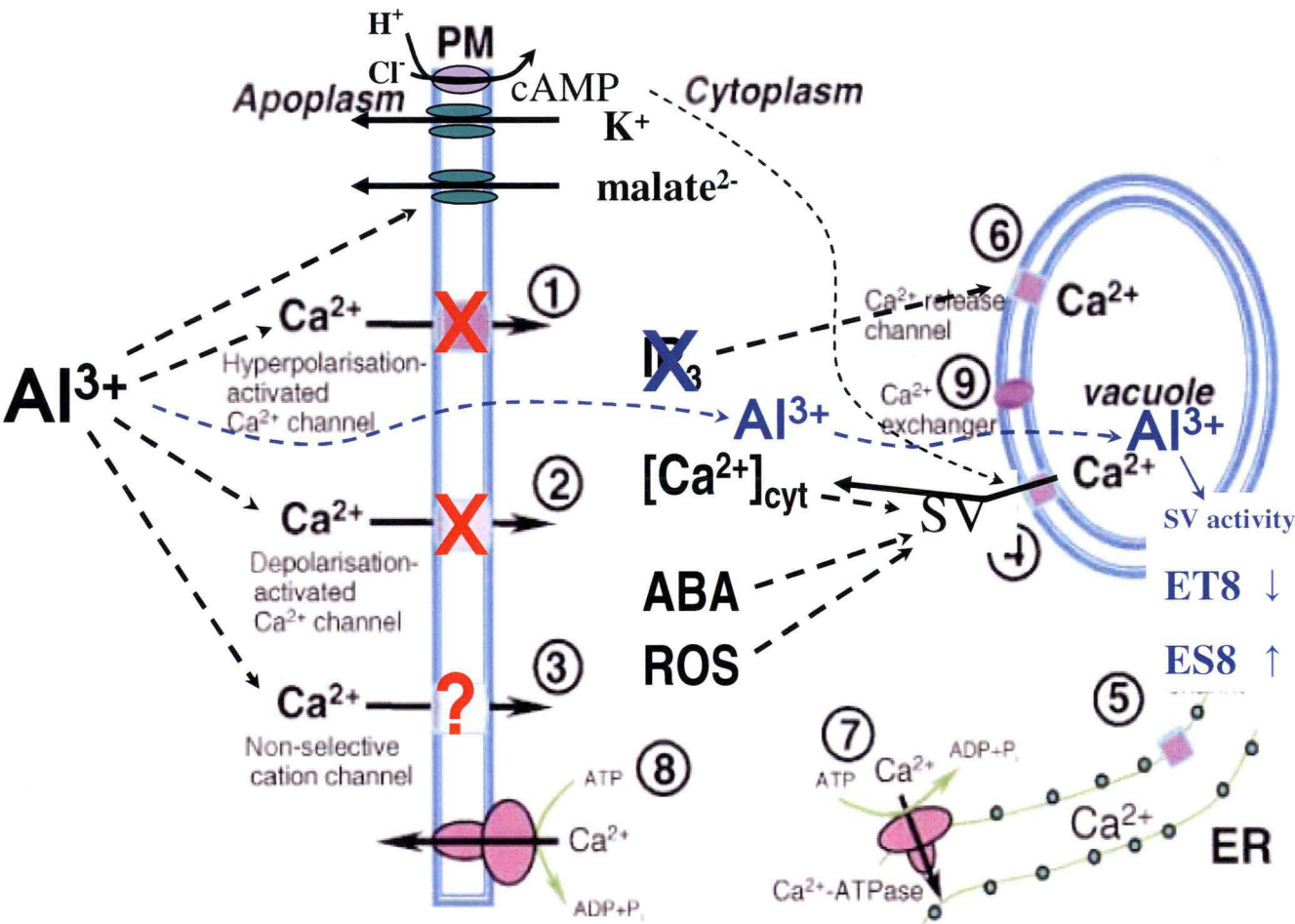


Figure 7.1. Proposed model of response of ET8 and ES8 apical cells to Al exposure.

Adapted from (Rengel and Zhang, 2003).

The following scenario is suggested:

Aluminium binds to the plasma membrane or malate activated channel and in ET8 activates the opening of the malate permeable channel. Malate efflux occurs and the depolarisation activates K^+ efflux to charge balance. In the longer term Cl^- influx also contributes to charge balance and the maintenance of turgor for elongation. Enhanced Ca^{2+} influx into the cytoplasm does not occur across the plasma membrane because HACC is inhibited by Al^{3+} , DACC cannot be involved or else higher $[Ca^{2+}]_{cyt}$ elevation would occur in ET8 and it is most likely that NSCC is blocked by Al^{3+} . If it is not blocked then this will contribute to the difference between ET8 and ES8 because hyperpolarisation in ES8 would increase flux through NSCC. Rather, Al induced $[Ca^{2+}]_{cyt}$ elevation, is signalled from internal stores by IP_3 , ABA or ROS which activate the vacuole IP_3 channel (IP_3 only) and either the SV channel or another Ca^{2+} channel. The increase in cytoplasmic Ca^{2+} increases SV activity, thereby further increasing $[Ca^{2+}]_{cyt}$. This initial elevation in Ca^{2+} is faster and higher in ES8 than ET8 because of the higher density of SV channels in ES8 and because actual Al exposure is higher.

In the longer term (indicated by blue arrows), Al crosses the plasma membrane, binding IP_3 and reducing its activity before being sequestered in the vacuole. ET8 SV channel activity is reduced by Al^{3+} in the vacuole, thereby reducing the leak of Al^{3+} back into the cytoplasm and also decreasing the elevation of $[Ca^{2+}]_{cyt}$. In ES8 the production of an unidentified low molecular weight compound significantly increases SV channel activity therefore increasing the leak of Al^{3+} into the cytoplasm and maintaining high $[Ca^{2+}]_{cyt}$.

The research outcomes of this study may contribute, in the longer term, to the sustainable management of acidic soils. A more complete understanding of plant

physiology is essential to techniques involving plant breeding, genetic engineering and even more basic ameliorative techniques. This project has only briefly examined amelioration of Al toxicity by ameliorants in solution. It confirms the previous findings that Ca^{2+} , Mg^{2+} and silicate can effectively ameliorate Al toxicity and significantly Ca^{2+} and Mg^{2+} can also ameliorate H^+ toxicity. To some it may seem antiquated, but arresting soils acidification, building the soil properties and assisting plant growth through ameliorants must play a key role in the long term sustainable management of acid soils. The author looks forward eagerly to the day where our understanding allows us to manage acid soils and Aluminium toxicity more sustainably.

References

- Ahn SJ, Rengel Z and Matsumoto H (2004) Aluminum-induced plasma membrane surface potential and H⁺-ATPase activity in near-isogenic wheat lines differing in tolerance to aluminium. *New Phytologist* **162**:71-79
- Ahn SJ, Sivaguru M, Chung GC, Rengel Z and Matsumoto H (2002) Aluminium-induced growth inhibition is associated with impaired efflux and influx of H⁺ across the plasma membrane in root apices of squash (*Cucurbita pepo*). *Journal of Experimental Botany* **53**:1959-1966
- Ahn SJ, Sivaguru M, Osawa H, Chung GC and Matsumoto H (2001) Aluminum inhibits the H⁺-ATPase activity by permanently altering the plasma membrane surface potentials in squash roots. *Plant Physiology* **126**:1381-1390
- Alcamo J and Bartnicki J (1988) Atmospheric models and acidification - summary and conclusions of the warsaw-ii meeting on atmospheric computations to assess acidification in europe. *Water Air and Soil Pollution* **40**:1-7
- Allen GJ, Muir SR and Sanders D (1995) Release of Ca²⁺ from individual plant vacuoles by both INSP(3) and cyclic ADP-ribose. *Science* **268**:735-737
- Allen GJ and Sanders D (1995) Calcineurin, a type 2b protein phosphatase, modulates the Ca²⁺-permeable slow vacuolar ion-channel of stomatal guard-cells. *Plant Cell* **7**:1473-1483
- Allen GJ and Sanders D (1996) Control of ionic currents in guard cell vacuoles by cytosolic and luminal calcium. *Plant Journal* **10**:1055-1069

References

- Allen GJ and Sanders D (1997) Vacuolar ion channels of higher plants. *In Advances in botanical research incorporating advances in plant pathology*, vol 25, Vol 25, pp 217-252
- Baier AC, Somers DJ and Gustafson JP (1995) Aluminum tolerance in wheat - correlating hydroponic evaluations with field and soil performances. *Plant Breeding* **114**:291-296
- Barcelo J and Poschenrieder C (2002) Fast root growth responses, root exudates, and internal detoxification as clues to the mechanisms of aluminium toxicity and resistance: A review. *Environmental and Experimental Botany* **48**:75-92
- Basu U, Godbold D and Taylor GJ (1994) Aluminum resistance in triticum-aestivum associated with enhanced exudation of malate. *Journal of Plant Physiology* **144**:747-753
- Bethke PC and Jones RL (1994) Ca^{2+} -calmodulin modulates ion-channel activity in storage protein vacuoles of barley aleurone cells. *Plant Cell* **6**:277-285
- Bethke PC and Jones RL (1997) Reversible protein phosphorylation regulates the activity of the slow-vacuolar ion channel. *Plant Journal* **11**:1227-1235
- Bewell MA, Maathuis FJM, Allen GJ and Sanders D (1999) Calcium-induced calcium release mediated by a voltage-activated cation channel in vacuolar vesicles from red beet. *Febs Letters* **458**:41-44
- Bhuja P, McLachlan K, Stephens J and Taylor G (2004) Accumulation of 1,3-beta-d-glucans, in response to aluminum and cytosolic calcium in *Triticum aestivum*. *Plant and Cell Physiology* **45**:543-549

References

- Birchall JD (1992) The interrelationship between silicon and aluminum in the biological effects of aluminum. *Ciba Foundation Symposia* **169**:50-68
- Blamey FPC, Nishizawa NK and Yoshimura E (2004) Timing, magnitude, and location of initial soluble aluminum injuries to mungbean roots. *Soil Science and Plant Nutrition* **50**:67-76
- Blancaflor EB, Jones DL and Gilroy S (1998) Alterations in the cytoskeleton accompany aluminum-induced growth inhibition and morphological changes in primary roots of maize. *Plant Physiology* **118**:159-172
- Bolan NS, Hedley MJ and White RE (1991) Processes of soil acidification during nitrogen cycling with emphasis on legume based pastures. *Plant and Soil* **134**:53-63
- Boscolo PRS, Menossi M and Jorge RA (2003) Aluminum-induced oxidative stress in maize. *Phytochemistry* **62**:181-189
- Britez RM, Watanabe T, Jansen S, Reissmann CB and Osaki M (2002) The relationship between aluminium and silicon accumulation in leaves of *Faramea marginata* (Rubiaceae). *New Phytologist* **156**:437-444
- Cakmak I and Horst WJ (1991) Effect of aluminum on lipid-peroxidation, superoxide-dismutase, catalase, and peroxidase-activities in root-tips of soybean (*Glycine max*). *Physiologia Plantarum* **83**:463-468
- Carden DE, Diamond D and Miller AJ (2001) An improved Na⁺-selective microelectrode for intracellular measurements in plant cells. *Journal of Experimental Botany* **52**:1353-1359

References

- Carpaneto A, Cantu AM and Gambale F (2001) Effects of cytoplasmic Mg^{2+} on slowly activating channels in isolated vacuoles of *Beta vulgaris*. *Planta* **213**:457-468
- Chen JP, Sucoff EI and Stadelmann EJ (1991) Aluminum and temperature alteration of cell-membrane permeability of *Quercus rubra*. *Plant Physiology* **96**:644-649
- Chen Z, Newman I, Zhou M, Mendham N, Zhang G and Shabala S (2005) Screening plants for salt tolerance by measuring K^{+} flux: A case study for barley. *Plant Cell and Environment* **28**:1230-1246
- Ciamporova M (2000) Diverse responses of root cell structure to aluminium stress. *Plant and Soil* **226**:113-116
- Ciamporova M (2002) Morphological and structural responses of plant roots to aluminium at organ, tissue, and cellular levels. *Biologia Plantarum* **45**:161-171
- Cocker KM, Evans DE and Hodson MJ (1998a) The amelioration of aluminium toxicity by silicon in higher plants: Solution chemistry or an in plants mechanism? *Physiologia Plantarum* **104**:608-614
- Cocker KM, Evans DE and Hodson MJ (1998b) The amelioration of aluminium toxicity by silicon in wheat (*Triticum aestivum* L.): Malate exudation as evidence for an *in planta* mechanism. *Planta* **204**:318-323
- Cocker KM, Hodson MJ, Evans DE and Sangster AG (1997) Interaction between silicon and aluminum in *Triticum aestivum* L. (cv. Celtic). *Israel Journal of Plant Sciences* **45**:285-292

References

Coventry DR and Slattery WJ (1991) Acidification of soil associated with lupins grown in a crop-rotation in north-eastern victoria. *Australian Journal of Agricultural Research* **42**:391-397

Crawford SA, Marshall AT and Wilkens S (1998) Localisation of aluminium in root apex cells of two australian perennial grasses by x-ray microanalysis. *Australian Journal of Plant Physiology* **25**:427-435

CSIRO (2004) Acid soils - a ticking time bomb? *In*. CSIRO Plant Industry Communication Group, Clayton South, Victoria

Darko E, Ambrus H, Stefanovits-Banyai E, Fodor J, Bakos F and Barnaba B (2004) Aluminium toxicity, al tolerance and oxidative stress in an al-sensitive wheat genotype and in al-tolerant lines developed by in vitro microspore selection. *Plant Science* **166**:583-591

Degenhardt J, Larsen PB, Howell SH and Kochian LV (1998) Aluminum resistance in the *Arabidopsis* mutant alr-104 is caused by an aluminum-induced increase in rhizosphere ph. *Plant Physiology* **117**:19-27

Delhaize E, Craig S, Beaton CD, Bennet RJ, Jagadish VC and Randall PJ (1993a) Aluminum tolerance in wheat (*Triticum aestivum* L.) .1. Uptake and distribution of aluminum in root apices. *Plant Physiology* **103**:685-693

Delhaize E, Higgins TJ and Randall PJ (1991) Aluminium tolerance in wheat: Analysis of polypeptides in the root apices of tolerant and sensitive genotypes. *In* RJ Wirght, VC Baligar, RP Murrman, eds, *Plant-soil interactions at low ph*. Kluwer Academic Publishers, Dordrecht, pp 1071-1079

References

- Delhaize E and Ryan PR (1995) Aluminum toxicity and tolerance in plants. *Plant Physiology* **107**:315-321
- Delhaize E, Ryan PR, Hebb DM, Yamamoto Y, Sasaki T and Matsumoto H (2004) Engineering high-level aluminum tolerance in barley with the ALMT1 gene. *Proceedings of the National Academy of Sciences of the United States of America* **101**:15249-15254
- Delhaize E, Ryan PR and Randall PJ (1993b) Aluminum tolerance in wheat (*Triticum aestivum* L.) .2. Aluminum-stimulated excretion of malic-acid from root apices. *Plant Physiology* **103**:695-702
- Demidchik V, Bowen HC, Maathuis FJM, Shabala SN, Tester MA, White PJ and Davies JM (2002) *Arabidopsis thaliana* root non-selective cation channels mediate calcium uptake and are involved in growth. *Plant Journal* **32**:799-808
- Demidchik V, Essah PA and Tester M (2004) Glutamate activates cation currents in the plasma membrane of *Arabidopsis* root cells. *Planta* **219**:167-175
- Demidchik V, Nichols C, Markiyan O, Dark A, Glover B and Davies J (2003a) Is ATP a signalling agent in plants? *Plant Physiology* **133**:456-461
- Demidchik V, Shabala SN, Coutts KB, Tester MA and Davies JM (2003b) Free oxygen radicals regulate plasma membrane Ca^{2+} and K^{+} -permeable channels in plant root cells. *Journal of Cell Science* **116**:81-88
- Dennison KL and Spalding EP (2000) Glutamate-gated calcium fluxes in *Arabidopsis*. *Plant Physiology* **124**:1511-1514

References

- Desikan R, Cheung MK, Bright J, Henson D, Hancock JT and Neill SJ (2004) ABA, hydrogen peroxide and nitric oxide signalling in stomatal guard cells. *Journal of Experimental Botany* **55**:205-212
- Devi SR, Yamamoto Y and Matsumoto H (2003) An intracellular mechanism of aluminum tolerance associated with high antioxidant status in cultured tobacco cells. *Journal of Inorganic Biochemistry* **97**:59-68
- Ding JP, Badot PM and Pickard BG (1993) Aluminum and hydrogen-ions inhibit a mechanosensory calcium-selective cation channel. *Australian Journal of Plant Physiology* **20**:771-778
- Dolling PJ (1995) Effect of lupins and location on soil acidification rates. *Australian Journal of Experimental Agriculture* **35**:753-763
- Exley C (2004) The pro-oxidant activity of aluminum. *Free Radical Biology and Medicine* **36**:380-387
- Exley C, Schneider C and Doucet FJ (2002) The reaction of aluminium with silicic acid in acidic solution: An important mechanism in controlling the biological availability of aluminium? *Coordination Chemistry Reviews* **228**:127-135
- Ezaki B, Katsuhara M, Kawamura M and Matsumoto H (2001) Different mechanisms of four aluminum (Al)-resistant transgenes for al toxicity in *Arabidopsis*. *Plant Physiology* **127**:918-927
- Falcke M (2004) Reading the patterns in living cells - the physics of Ca^{2+} signaling. *Advances in Physics* **53**:255-440

References

- Foreman J, Demidchik V, Bothwell JHF, Mylona P, Miedema H, Torres MA, Linstead P, Costa S, Brownlee C, Jones JDG, Davies JM and Dolan L (2003) Reactive oxygen species produced by NADPH oxidase regulate plant cell growth. *Nature* **422**:442-446
- Frantzios G, Galatis B and Apostolakos P (2000) Aluminium effects on microtubule organization in dividing root-tip cells of *Triticum turgidum*. I. Mitotic cells. *New Phytologist* **145**:211-224
- Frantzios G, Galatis B and Apostolakos P (2001) Aluminium effects on microtubule organization in dividing root-tip cells of *Triticum turgidum*. II. Cytokinetic cells. *Journal of Plant Research* **114**:157-170
- Fukuyama K, Sasaki T, Yamamoto Y and Matsumoto H (2005) Aluminum-induced secretion of organic acids is related to the expression of ALMT1 homologue in rye. *Plant and Cell Physiology* **46**:S158-S158
- Galloway JN (1989) Atmospheric acidification - projections for the future. *Ambio* **18**:161-166
- Gassmann W and Schroeder JI (1994) Inward-rectifying K⁺ channels in root hairs of wheat - a mechanism for aluminum-sensitive low-affinity K⁺ uptake and membrane-potential control. *Plant Physiology* **105**:1399-1408
- Goulding KWT, Bailey NJ, Bradbury NJ, Hargreaves P, Howe M, Murphy DV, Poulton PR and Willison TW (1998) Nitrogen deposition and its contribution to nitrogen cycling and associated soil processes. *New Phytologist* **139**:49-58

References

- Greenway H and Munns R (1980) Mechanisms of salt tolerance in non halophytes. *Annual Review of Plant Physiology* **31**:149-190
- Grenda A and Badora A (2001) The influence of aluminium and manganese toxicity in the soil on the bioaccumulation of Al and Mn in two cultivars of wheat (*Triticum aestivum* L.). In *Plant nutrition: Food security and sustainability of agro-ecosystems through basic and applied research. Fourteenth international plant nutrition colloquium, hannover, germany*,
- Gu Z, Huang C, Lu J, Qin J and He Z (1999) Techniques and efficacy of silicon fertiliser application in fluvo-aquic soils and paddy soils in rice-wheat rotation regions. *Jiangsu Agricultural Sciences* **3**
- Gunse B, Poschenrieder C and Barcelo J (2000) The role of ethylene metabolism in the short-term responses to aluminium by roots of two maize cultivars different in Al-resistance. *Environmental and Experimental Botany* **43**:73-81
- Gutmann I and Wahlfeld AW (1974) L-malate: Determination with malate dehydrogenase and NAD. In Burgmeyer, ed, *Methods of enzymatic analysis*, Vol 3. Academic Press, New York, pp 1585-1589
- Hamilton DWA, Hills A, Kohler B and Blatt MR (2000) Ca^{2+} channels at the plasma membrane of stomatal guard cells are activated by hyperpolarization and abscisic acid. *Proceedings of the National Academy of Sciences of the United States of America* **97**:4967-4972
- Hara T, Gu MH and Koyama H (1999) Ameliorative effect of silicon on aluminum injury in the rice plant. *Soil Science and Plant Nutrition* **45**:929-936

References

- Hattori T, Inanaga S, Tanimoto E, Lux A, Luxova M and Sugimoto Y (2003) Silicon-induced changes in viscoelastic properties of sorghum root cell walls. *Plant and Cell Physiology* **44**:743-749
- Hayes JE and Ma JF (2003) Al-induced efflux of organic acid anions is poorly associated with internal organic acid metabolism in triticales roots. *Journal of Experimental Botany* **54**:1753-1759
- Haynes RJ and Mokolobate MS (2001) Amelioration of al toxicity and p deficiency in acid soils by additions of organic residues: A critical review of the phenomenon and the mechanisms involved. *Nutrient Cycling in Agroecosystems* **59**:47-63
- He L and Jiang S (1999) Response of wheat to silicon-calcium fertilizer. *Soils and Fertilizers (Beijing)*
- Hetherington AM and Brownlee C (2004) The generation of Ca^{2+} signals in plants. *Annual Review of Plant Biology* **55**:401-427
- Hodson MJ and Evans DE (1995) Aluminium/silicon interactions in higher plants. *Journal of Experimental Botany* **46**:161-171
- Hodson MJ and Sangster AG (1999) Aluminium/silicon interactions in conifers. *Journal of Inorganic Biochemistry* **76**:89-98
- Hoekenga OA, Vision TJ, Shaff JE, Monforte AJ, Lee GP, Howell SH and Kochian LV (2003) Identification and characterization of aluminum tolerance loci in *Arabidopsis* (landsberg erecta x columbia) by quantitative trait locus mapping. A physiologically simple, but genetically complex trait. *Plant Physiology* **132**:936-948

References

- Horst WJ (1995) The role of the apoplast in aluminum toxicity and resistance of higher-plants - a review. *Zeitschrift Fur Pflanzenernahrung Und Bodenkunde* **158**:419-428
- Horst WJ, Asher CJ, Cakmak I, Szulkiewicz P and Wissemeier AH (1992) Short-term responses of soybean roots to aluminum. *Journal of Plant Physiology* **140**:174-178
- Horst WJ, Schmohl N, Kollmeier M, Baluska F and Sivaguru M (1999) Does aluminium affect root growth of maize through interaction with the cell wall - plasma membrane - cytoskeleton continuum? *Plant and Soil* **215**:163-174
- Hossain MT, Mori R, Soga K, Wakabayashi K, Kamisaka S, Fujii S, Yamamoto R and Hoson T (2002) Growth promotion and an increase in cell wall extensibility by silicon in rice and some other poaceae seedlings. *Journal of Plant Research* **115**
- Huang JW, Grunes DL and Kochian LV (1995) Aluminum and calcium-transport interactions in intact roots and root plasmalemma vesicles from aluminum-sensitive and tolerant wheat cultivars. *Plant and Soil* **171**:131-135
- Huang JWW, Grunes DL and Kochian LV (1992) Aluminum effects on the kinetics of calcium-uptake into cells of the wheat root apex - quantification of calcium fluxes using a calcium-selective vibrating microelectrode. *Planta* **188**:414-421
- Huang JWW, Pellet DM, Papernik LA and Kochian LV (1996) Aluminum interactions with voltage-dependent calcium transport in plasma membrane vesicles isolated from roots of aluminum-sensitive and -resistant wheat cultivars. *Plant Physiology* **110**:561-569

References

- Ishikawa S, Wagatsuma T and Ikarashi T (2003) Rapid changes in levels of mineral nutrients in root-tip cells following short-term exposure to aluminium. *Plant and Soil* **255**:245-251
- Ishikawa S, Wagatsuma T, Takano T, Tawaraya K and Oomata K (2001) The plasma membrane intactness of root-tip cells is a primary factor for al-tolerance in cultivars of five species. *Soil Science and Plant Nutrition* **47**:489-501
- Jones DL, Gilroy S, Larsen PB, Howell SH and Kochian LV (1998a) Effect of aluminum on cytoplasmic Ca^{2+} homeostasis in root hairs of *Arabidopsis thaliana* (L.). *Planta* **206**:378-387
- Jones DL and Kochian LV (1995) Aluminum inhibition of the inositol 1,4,5-trisphosphate signal-transduction pathway in wheat roots - a role in aluminum toxicity. *Plant Cell* **7**:1913-1922
- Jones DL and Kochian LV (1997) Aluminum interaction with plasma membrane lipids and enzyme metal binding sites and its potential role in al cytotoxicity. *Febs Letters* **400**:51-57
- Jones DL, Kochian LV and Gilroy S (1998b) Aluminum induces a decrease in cytosolic calcium concentration in by-2 tobacco cell cultures. *Plant Physiology* **116**:81-89
- Jones DL, Shaff JE and Kochian LV (1995) Role of calcium and other ions in directing root hair tip growth in limnobia-stolonifera. 1. Inhibition of tip growth by aluminum. *Planta* **197**:672-680

References

- Jorge RA, Menossi M and Arruda P (2001) Probing the role of calmodulin in al toxicity in maize. *Phytochemistry* **58**:415-422
- Kasai M, Sasaki M, Tanakamaru S, Yamamoto Y and Matsumoto H (1993) Possible involvement of abscisic-acid in increases in activities of 2 vacuolar H⁺-pumps in barley roots under aluminum stress. *Plant and Cell Physiology* **34**:1335-1338
- Kataoka T, Nakanishi T, Stekelenburg A, Delhaize E and Ryan PR (2002a) Malate efflux from al-tolerant wheat root treated with several trivalent cations. *Plant and Cell Physiology* **43**:S51-S51
- Kataoka T and Nakanishi TM (2001) Aluminium distribution in soybean root tip for a short time al treatment. *Journal of Plant Physiology* **158**:731-736
- Kataoka T, Stekelenburg A, Nakanishi TM, Delhaize E and Ryan PR (2002b) Several lanthanides activate malate efflux from roots of aluminium-tolerant wheat. *Plant Cell and Environment* **25**:453-460
- Kawano T, Kadono T, Fumoto K, Lapeyrie F, Kuse M, Isobe M, Furuichi T and Muto S (2004a) Aluminium as a specific inhibitor of plant tpc1 Ca²⁺ channels. *Biochemical and Biophysical Research Communications* **324**:40-45
- Kawano T, Kadono T, Furuichi T, Muto S and Lapeyrie F (2003) Aluminum-induced distortion in calcium signaling involving oxidative bursts and channel regulation in tobacco by-2 cells. *Biochemical and Biophysical Research Communications* **308**:35-42

References

- Kawano T, Lapeyrie F, Kadono T, Furuichi T and Muto S (2004b) Aluminum as a specific inhibitor of the reactive oxygen species-responsive calcium channels. *Plant and Cell Physiology* **45**:S173-S173
- Kidd PS, Llugany M, Poschenrieder C, Gunse B and Barcelo J (2001) The role of root exudates in aluminium resistance and silicon-induced amelioration of aluminium toxicity in three varieties of maize (*zea mays* l.). *Journal of Experimental Botany* **52**:1339-1352
- Kiegle E, Gilliam M, Haseloff J and Tester M (2000) Hyperpolarisation-activated calcium currents found only in cells from the elongation zone of *Arabidopsis thaliana* roots. *Plant Journal* **21**:225-229
- Kinraide TB (1988) Proton extrusion by wheat roots exhibiting severe aluminum toxicity symptoms. *Plant Physiology* **88**:418-423
- Kinraide TB (1991) Identity of the rhizotoxic aluminum species. *Plant and Soil* **134**:167-178
- Kinraide TB (1993) Aluminum enhancement of plant-growth in acid rooting media - a case of reciprocal alleviation of toxicity by 2 toxic cations. *Physiologia Plantarum* **88**:619-625
- Kinraide TB (1997) Reconsidering the rhizotoxicity of hydroxyl, sulphate, and fluoride complexes of aluminium. *Journal of Experimental Botany* **48**:1115-1124
- Kinraide TB (2001) Ion fluxes considered in terms of membrane-surface electrical potentials. *Australian Journal of Plant Physiology* **28**:605-616

References

- Kinraide TB (2004) Possible influence of cell walls upon ion concentrations at plasma membrane surfaces. Toward a comprehensive view of cell-surface electrical effects upon ion uptake, intoxication, and amelioration. *Plant Physiology* **136**:3804-3813
- Kinraide TB, Pedler JF and Parker DR (2004) Relative effectiveness of calcium and magnesium in the alleviation of rhizotoxicity in wheat induced by copper, zinc, aluminum, sodium, and low pH. *Plant and Soil* **259**:201-208
- Kinraide TB, Ryan PR and Kochian LV (1992) Interactive effects of Al^{3+} , H^{+} , and other cations on root elongation considered in terms of cell-surface electrical potential. *Plant Physiology* **99**:1461-1468
- Kinraide TB, Ryan PR and Kochian LV (1994) Al^{3+} - Ca^{2+} interactions in aluminum rhizotoxicity .2. Evaluating the Ca^{2+} -displacement hypothesis. *Planta* **192**:104-109
- Knowles A and Shabala S (2004) Overcoming the problem of non-ideal liquid ion exchanger selectivity in microelectrode ion flux measurements. *Journal of Membrane Biology* **202**:51-59
- Kobayashi Y, Yamamoto Y and Matsumoto H (2004) Studies on the mechanism of aluminum tolerance in pea (*Pisum sativum* L.) using aluminum-tolerant cultivar 'Alaska' and aluminum-sensitive cultivar 'Hyogo'. *Soil Science and Plant Nutrition* **50**:197-204
- Kochian LV (1995) Cellular mechanisms of aluminum toxicity and resistance in plants. *Annual Review of Plant Physiology and Plant Molecular Biology* **46**:237-260

References

- Kochian LV, Hoekenga OA and Pineros MA (2004) How do crop plants tolerate acid soils? - mechanisms of aluminum tolerance and phosphorous efficiency. *Annual Review of Plant Biology* **55**:459-493
- Kochian LV, Shaff JE and Ryan PR (1991) Microelectrode-based investigations into the relationship between Al toxicity and root-cell membrane transport processes. *Current Topics in Plant Biochemistry and Physiology* **10**:117-133
- Kollmeier M, Felle HH and Horst WJ (2000) Genotypical differences in aluminum resistance of maize are expressed in the distal part of the transition zone. Is reduced basipetal auxin flow involved in inhibition of root elongation by aluminum? *Plant Physiology* **122**:945-956
- Kretschmar RM, Hafner H, Bationo A and Marschener H (1991) Long- and short-term effects of crop residues on aluminium toxicity, phosphorus availability and growth of pearl millet in an acid sandy soil. *Plant and Soil* **136**:215-223
- Ktitorova IN and Skobeleva OV (1999) Changes in elastic properties of cell walls and some parameters of plant water relations in response to acidification of the medium. *Russian Journal of Plant Physiology* **46**:201-206
- Kuhn JM and Schroeder JI (2003) Impacts of altered RNA metabolism on abscisic acid signaling. *Current Opinion in Plant Biology* **6**:463-469
- Kwak JM, Mori IC, Pei ZM, Leonhardt N, Torres MA, Dangel JL, Bloom RE, Bodde S, Jones JDG and Schroeder JI (2003) NADPH oxidase *atrbohD* and *atrbohF* genes function in ROS-dependent ABA signaling in *Arabidopsis*. *Embo Journal* **22**:2623-2633

References

- Larsen PB, Degenhardt J, Tai CY, Stenzler LM, Howell SH and Kochian LV (1998) Aluminum-resistant *Arabidopsis* mutants that exhibit altered patterns of aluminum accumulation and organic acid release from roots. *Plant Physiology* **117**:9-18
- Lazof DB and Holland MJ (1999) Evaluation of the aluminium-induced root growth inhibition in isolation from low pH effects in *Glycine max*, *Pisum sativum* and *Phaseolus vulgaris*. *Australian Journal of Plant Physiology* **26**:147-157
- Lee SH, Johnson JD, Walsh MP, Van Lierop JE, Sutherland C, Xu AD, Snedden WA, Kosk-Kosicka D, Fromm H, Narayanan N and Cho MJ (2000) Differential regulation of Ca^{2+} /calmodulin-dependent enzymes by plant calmodulin isoforms and free Ca^{2+} concentration. *Biochemical Journal* **350**:299-306
- Liang YC, Yang CG and Shi HH (2001) Effects of silicon on growth and mineral composition of barley grown under toxic levels of aluminum. *Journal of Plant Nutrition* **24**:229-243
- Lin C, Yu YW, Kadono T, Iwata M, Umemura K, Furuichi T, Kuse M, Isobe M, Yamamoto Y, Matsumoto H, Yoshizuka K and Kawano T (2005) Action of aluminum, novel TPC1-type channel inhibitor, against salicylate-induced and cold-shock-induced calcium influx in tobacco by-2 cells. *Biochemical and Biophysical Research Communications* **332**:823-830
- Lindberg S and Strid H (1997) Aluminium induces rapid changes in cytosolic pH and free calcium and potassium concentrations in root protoplasts of wheat (*Triticum aestivum*). *Physiologia Plantarum* **99**:405-414
- Lindberg S, Szynekier K and Greger M (1991) Aluminum effects on transmembrane potential in cells of fibrous roots of sugar-beet. *Physiologia Plantarum* **83**:54-62

References

- Liu K and Luan S (2001) Internal aluminum block of plant inward K^+ channels. *Plant Cell* **13**:1453-1465
- Luan S, Kudia J, Rodriguez-Concepcion M, Yalovsky S and Gruissem W (2002) Calmodulins and calcineurin b-like proteins: Calcium sensors for specific signal response coupling in plants. *The PLant Cell*:S389-S400
- Ma JF, Hiradate S and Matsumoto H (1998) High aluminum resistance in buckwheat - ii. Oxalic acid detoxifies aluminum internally. *Plant Physiology* **117**:753-759
- Ma JF, Ryan PR and Delhaize E (2001) Aluminium tolerance in plants and the complexing role of organic acids. *Trends in Plant Science* **6**:273-278
- Ma QF, Rengel Z and Kuo J (2002) Aluminium toxicity in rye (*Secale cereale*): Root growth and dynamics of cytoplasmic Ca^{2+} in intact root tips. *Annals of Botany* **89**:241-244
- Ma Z and Miyasaka SC (1998) Oxalate exudation by taro in response to al. *Plant Physiology* **118**:861-865
- Maathuis F and Sanders D (1996) Mechanisms of potassium absorption by higher plant roots. *Physiologia Plantarum* **96**:158-168
- MacRobbie EAC (1998) Signal transduction and ion channels in guard cells. *Philosophical Transactions of the Royal Society of London Series B-Biological Sciences* **353**:1475-1488
- Mak DOD, McBride SMJ and Foskett JK (2003) Spontaneous channel activity of the inositol 1,4,5-trisphosphate (INSP(3)) receptor (INSP(3)r). Application of allosteric

References

modeling to calcium and INSP(3) regulation of INSP(3)r single-channel gating.

Journal of General Physiology **122**:583-603

Mangabeira P, Mushrifah I, Escaig F, Laffray D, Franca MGC and Galle P (1999)

Use of sims microscopy and electron probe x-ray microanalysis to study the subcellular localization of aluminium in *Vicia faba* roots cells. *Cellular and Molecular Biology* **45**:413-422

Mannion AM (1998) Global environmental change: The causes and consequences of disruption to biogeochemical cycles. *Geographical Journal* **164**:168-182

Mariano ED and Keltjens WG (2003) Evaluating the role of root citrate exudation as a mechanism of aluminium resistance in maize genotypes. *Plant and Soil* **256**:469-479

Mariano ED and Keltjens WG (2004) Variation for aluminum resistance among maize genotypes evaluated with three screening methods. *Communications in Soil Science and Plant Analysis* **35**:2617-2637

Mariano ED and Keltjens WG (2005) Long-term effects of aluminum exposure on nutrient uptake by maize genotypes differing in aluminum resistance. *Journal of Plant Nutrition* **28**:323-333

Marienfeld S, Schmohl N, Klein M, Schroder WH, Kuhn AJ and Horst WJ (2000)

Localisation of aluminium in root tips of zea mays and vicia faba. *Journal of Plant Physiology* **156**:666-671

Marschner H (1991) Mechanisms of adaptation of plants to acid soils. *Plant and Soil* **134**:1-20

References

- Martinez J, Feltl T, Scanlon CH, Lumsden PJ and Machackova I (2000) Subcellular localization of a high affinity binding site for d-myo-inositol 1,4,5-trisphosphate from *Chenopodium rubrum*. *Plant Physiology* **124**:475-483
- Martinez-Estevez M, Racagni-Di Palma G, Munoz-Sanchez JA, Brito-Argaez L, Loyola-Vargas VM and Hernandez-Sotomayor SMT (2003) Aluminium differentially modifies lipid metabolism from the phosphoinositide pathway in *Coffea arabica* cells. *Journal of Plant Physiology* **160**:1297-1303
- Massot N, Nicander B, Barcelo J, Poschenrieder C and Tillberg E (2002) A rapid increase in cytokinin levels and enhanced ethylene evolution precede Al^{3+} -induced inhibition of root growth in bean seedlings (*Phaseolus vulgaris* L.). *Plant Growth Regulation* **37**:105-112
- Matsumoto H (2000) Cell biology of aluminum toxicity and tolerance in higher plants. In *International review of cytology - a survey of cell biology*, vol 200, Vol 200. ACADEMIC PRESS INC, San Diego, pp 1-46
- Medvedev SS (2005) Calcium signaling system in plants. *Russian Journal of Plant Physiology* **52**:249-270
- Meriga B, Reddy BK, Rao KR, Reddy LA and Kishor PBK (2004) Aluminium-induced production of oxygen radicals, lipid peroxidation and DNA damage in seedlings of rice (*oryza sativa*). *Journal of Plant Physiology* **161**:63-68
- Miller AL and Gow NAR (1989) Correlation between profile of ion-current circulation and root development. *Physiologia Plantarum* **75**:102-108

References

- Mistrik I and Ullrich CI (1996) Mechanism of anion uptake in plant roots: Quantitative evaluation of H^+/NO_3^- and $H^+/H_2PO_4^-$ stoichiometries. *Plant Physiology and Biochemistry* **34**:629-636
- Miyasaka SC, Buta JG, Howell RK and Foy CD (1991) Mechanism of aluminum tolerance in snapbeans - root exudation of citric-acid. *Plant Physiology* **96**:737-743
- Miyasaka SC and Hawes MC (2001) Possible role of root border cells in detection and avoidance of aluminum toxicity. *Plant Physiology* **125**:1978-1987
- Miyasaka SC, Kochian LV, Shaff JE and Foy CD (1989) Mechanisms of aluminum tolerance in wheat - an investigation of genotypic differences in rhizosphere pH, K^+ , and H^+ transport, and root-cell membrane-potentials. *Plant Physiology* **91**:1188-1196
- Moody PW and Aitken RL (1997) Soil acidification under some tropical agricultural systems .1. Rates of acidification and contributing factors. *Australian Journal of Soil Research* **35**:163-173
- Mori IC, Kwak JM, Leonhardt N, Bloom R, Bodde S and Schroeder JI (2004) Reactive oxygen species regulation in ABA signaling in *Arabidopsis* guard cells. *Plant and Cell Physiology* **45**:S52-S52
- Morikawa CK and Saigusa M (2002) Si amelioration of Al toxicity in barley (*Hordeum vulgare* L.) growing in two andosols. *Plant and Soil* **240**:161-168
- Mueller-Roeber B and Pical C (2002) Inositol phospholipid metabolism in *Arabidopsis*. Characterized and putative isoforms of inositol phospholipid kinase and phosphoinositide-specific phospholipase c. *Plant Physiology* **130**:22-46

References

- Muir SR, Bewell MA, Sanders D and Allen GJ (1997) Ligand-gated Ca^{2+} channels and Ca^{2+} signalling in higher plants. *Journal of Experimental Botany* **48**:589-597
- Muir SR and Sanders D (1996) Pharmacology of Ca^{2+} release from red beet microsomes suggests the presence of ryanodine receptor homologs in higher plants. *Febs Letters* **395**:39-42
- Muir SR and Sanders D (1997) Inositol 1,4,5-trisphosphate-sensitive Ca^{2+} release across nonvacuolar membranes in cauliflower. *Plant Physiology* **114**:1511-1521
- Murata Y, Pei ZM, Mori IC and Schroeder J (2001) Absciscic acid activation of plasma membrane Ca^{2+} channels in guard cells requires cytosolic nad(p)h and is differentially disrupted upstream and downstream of reactive oxygen species production in abi1-1 and abi2-1 protein phosphatase 2c mutants. *Plant Cell* **13**:2513-2523
- Navazio L, Bewell MA, Siddiqua A, Dickinson GD, Galione A and Sanders D (2000) Calcium release from the endoplasmic reticulum of higher plants elicited by the NADP metabolite nicotinic acid adenine dinucleotide phosphate. *Proceedings of the National Academy of Sciences of the United States of America* **97**:8693-8698
- Navazio L, Mariani P and Sanders D (2001) Mobilization of Ca^{2+} by cyclic ADP-ribose from the endoplasmic reticulum of cauliflower florets. *Plant Physiology* **125**:2129-2138
- Newman IA (2001) Ion transport in roots: Measurement of fluxes using ion-selective microelectrodes to characterize transporter function. *Plant Cell and Environment* **24**:1-14

References

- Newman IA, Kochian LV, Grusak MA and Lucas WJ (1987) Fluxes of H^+ and K^+ in corn roots - characterization and stoichiometries using ion-selective microelectrodes. *Plant Physiology* **84**:1177-1184
- Noble AD, Zenneck I and Randall PJ (1996) Leaf litter ash alkalinity and neutralisation of soil acidity. *Plant and Soil* **179**:293-302
- Ochocka AM and Pawelczyk T (2003) Isozymes delta of phosphoinositide-specific phospholipase c and their role in signal transduction in the cell. *Acta Biochimica Polonica* **50**:1097-1110
- Olbe M and Sommarin M (1991) ATP-dependent Ca^{2+} transport in wheat root plasma-membrane vesicles. *Physiologia Plantarum* **83**:535-543
- Olbe M, Widell S and Sommarin M (1997) Active calcium transporters in isolated membranes of wheat root cells. *Journal of Experimental Botany* **48**:1767-1777
- Olivetti GP, Cumming JR and Etherton B (1995) Membrane-potential depolarization of root cap cells precedes aluminum tolerance in snapbean. *Plant Physiology* **109**:123-129
- Ono K, Yamamoto Y, Hachiya A and Matsumoto H (1995) Ono k, Yamamoto Y, Hachiya A, Matsumoto H (1995) Ssynergistic inhibition of growth by aluminum and iron of tobacco (*nicotiana tabacum* l.) cells in suspension culture. *Plant and Cell Physiology* **36**:115-125
- Osawa H and Matsumoto H (2002) Aluminium triggers malate-independent potassium release via ion channels from the root apex in wheat. *Planta* **215**:405-412

References

- Oteiza PI (1994) A mechanism for the stimulatory effect of aluminum on iron-induced lipid peroxidation. *Archives of Biochemistry and Biophysics* **308**:374-379
- Pan JW, Zhu MY and Chen H (2001) Aluminum-induced cell death in root-tip cells of barley. *Environmental and Experimental Botany* **46**:71-79
- Papernik LA and Kochian LV (1997) Aluminum tolerance in wheat: The possible involvement of electrical signals. *Plant Physiology* **114**:550-550
- Park KY, Jung JY, Park J, Hwang JU, Kim YW, Hwang I and Lee Y (2003) A role for phosphatidylinositol 3-phosphate in abscisic acid-induced reactive oxygen species generation in guard cells. *Plant Physiology* **132**:92-98
- Parker DR, Zelazny LW and Kinraide TB (1987) Improvements to the program geochem. *Soil Science Society of America Journal* **51**:488-491
- Pavlovkin J and Mistrik I (1999) Phytotoxic effect of aluminium on maize root membranes. *Biologia* **54**:473-479
- Pei ZM, Murata Y, Benning G, Thomine S, Klusener B, Allen GJ, Grill E and Schroeder JI (2000) Calcium channels activated by hydrogen peroxide mediate abscisic acid signalling in guard cells. *Nature* **406**:731-734
- Pei ZM, Ward JM and Schroeder JI (1999) Magnesium sensitizes slow vacuolar channels to physiological cytosolic calcium and inhibits fast vacuolar channels in fava bean guard cell vacuoles. *Plant Physiology* **121**:977-986

References

- Peiter E, Maathuis FJM, Mills LN, Knight H, Pelloux M, Hetherington AM and Sanders D (2005) The vacuolar Ca^{2+} -activated channel TPC1 regulates germination and stomatal movement. *Nature* **434**:404-408
- Pellet DM, Grunes DL and Kochian LV (1995) Organic-acid exudation as an aluminum-tolerance mechanism in maize (*Zea mays* L.). *Planta* **196**:788-795
- Pellet DM, Papernik LA, Jones DL, Darrah PR, Grunes DL and Kochian LV (1997) Involvement of multiple aluminium exclusion mechanisms in aluminium tolerance in wheat. *Plant and Soil* **192**:63-68
- Pellet DM, Papernik LA and Kochian LV (1996) Multiple aluminum-resistance mechanisms in wheat - roles of root apical phosphate and malate exudation. *Plant Physiology* **112**:591-597
- Peng XX, Yu L, Yang C and Liu YH (2003) Genotypic difference in aluminum resistance and oxalate exudation of buckwheat. *Journal of Plant Nutrition* **26**:1767-1777
- Pina-Chable ML and Hernandez-Sotomayor SMT (2001) Phospholipase c activity from *Catharanthus roseus* transformed roots: Aluminum effect. *Prostaglandins & Other Lipid Mediators* **65**:45-56
- Pineros M and Tester M (1993) Plasma-membrane Ca^{2+} channels in roots of higher-plants and their role in aluminum toxicity. *Plant and Soil* **156**:119-122
- Pineros M and Tester M (1995) Characterization of a voltage-dependent Ca^{2+} -selective channel from wheat roots. *Planta* **195**:478-488

References

- Pineros M and Tester M (1997) Calcium channels in higher plant cells: Selectivity, regulation and pharmacology. *Journal of Experimental Botany* **48**:551-577
- Pineros MA and Kochian LV (2001) A patch-clamp study on the physiology of aluminum toxicity and aluminum tolerance in maize. Identification and characterization of Al^{3+} -induced anion channels. *Plant Physiology* **125**:292-305
- Pineros MA, Magalhaes JV, Alves VMC and Kochian LV (2002) The physiology and biophysics of an aluminum tolerance mechanism based on root citrate exudation in maize. *Plant Physiology* **129**:1194-1206
- Pineros MA, Shaff JE, Manslank HS, Alves VMC and Kochian LV (2005) Aluminum resistance in maize cannot be solely explained by root organic acid exudation. A comparative physiological study. *Plant Physiology* **137**:231-241
- Plieth C (2005) Calcium: Just another regulator in the machinery of life? *Annals of Botany* **96**:1-8
- Plieth C, Sattelmacher B, Hansen UP and Knight MR (1999) Low-ph-mediated elevations in cytosolic calcium are inhibited by aluminium: A potential mechanism for aluminium toxicity. *Plant Journal* **18**:643-650
- Pottosin II, Dobrovinskaya OR and Muniz J (2001) Conduction of monovalent and divalent cations in the slow vacuolar channel. *Journal of Membrane Biology* **181**:55-65
- Pottosin II, Martinez-Estevéz M, Dobrovinskaya OR and Muniz J (2005) Regulation of the slow vacuolar channel by luminal potassium: Role of surface charge *Journal of Membrane Biology* **205**(2):103-111

References

- Pottosin, II, Martinez-Estevez M, Dobrovinskaya OR, Muniz J and Schoenknecht G (2004) Mechanism of luminal Ca^{2+} and Mg^{2+} action on the vacuolar slowly activating channels. *Planta* **219**:1057-1070
- Pottosin, II, Tikhonova LI, Hedrich R and Schonknecht G (1997) Slowly activating vacuolar channels can not mediate Ca^{2+} -induced Ca^{2+} release. *Plant Journal* **12**:1387-1398
- Rahman A, Hosokawa S, Oono Y, Amakawa T, Goto N and Tsurumi S (2002) Auxin and ethylene response interactions during *Arabidopsis* root hair development dissected by auxin influx modulators. *Plant Physiology* **130**:1908-1917
- Rahman MT, Kawamura K, Koyama H and Hara T (1998) Varietal differences in the growth of rice plants in response to aluminum and silicon. *Soil Science and Plant Nutrition* **44**:423-431
- Rahman MT, Koyama H and Hara T (1999) Effect of aluminum and silicon in solution on the growth of rice (*Oryza sativa* L.) suspension cells. *Soil Science and Plant Nutrition* **45**:693-700
- Reid RJ, Tester MA and Smith FA (1995) Calcium aluminum interactions in the cell-wall and plasma-membrane of chara. *Planta* **195**:362-368
- Reid RJ and Walker NA (1984) The energetics of Cl^- active transport in *Chara*. *Journal of Membrane Biology* **78**:157-162
- Rengel Z (1992) Disturbance of cell Ca^{2+} homeostasis as a primary trigger of al toxicity syndrome. *Plant Cell and Environment* **15**:931-938

References

- Rengel Z (1996) Tansley review no 89 - uptake of aluminium by plant cells. *New Phytologist* **134**:389-406
- Rengel Z, Pineros M and Tester M (1995) Transmembrane calcium fluxes during Al stress. *Plant and Soil* **171**:125-130
- Rengel Z and Reid RJ (1997) Uptake of al across the plasma membrane of plant cells. *Plant and Soil* **192**:31-35
- Rengel Z and Zhang WH (2003) Role of dynamics of intracellular calcium in aluminium-toxicity syndrome. *New Phytologist* **159**:295-314
- Richards KD, Schott EJ, Saharma YK, Davis KR and Gardner RC (1998) Aluminium induces oxidative stress genes in *Arabidopsis thaliana*. *Plant Physiology* **116**:409-418
- Ridley AM, Slattery WJ, Helyar KR and Cowling A (1990) The importance of the carbon-cycle to acidification of a grazed annual pasture. *Australian Journal of Experimental Agriculture* **30**:529-537
- Roberts JKM, Lane AN, Clark RA and Nieman RH (1985) Relationships between the rate of synthesis of ATP and the concentrations of reactants and products of ATP hydrolysis in maize root tips, determined by ^{31}P nuclear magnetic resonance. *Archives of Biochemistry and Biophysics* **240**:712-722
- Rock CD and Quatrano RS (1996) Lanthanide ions are agonists of transient gene expression in rice protoplasts and act in synergy with ABA to increase em gene expression. *Plant Cell Reports* **15**:371-376

References

- Ryan PR, Delhaize E and Jones DL (2001) Function and mechanism of organic anion exudation from plant roots. *Annual Review of Plant Physiology and Plant Molecular Biology* **52**:527-560
- Ryan PR, Delhaize E and Randall PJ (1995a) Characterization of Al-stimulated efflux of malate from the apices of Al-tolerant wheat roots. *Planta* **196**:103-110
- Ryan PR, Delhaize E and Randall PJ (1995b) Malate efflux from root apices and tolerance to aluminum are highly correlated in wheat. *Australian Journal of Plant Physiology* **22**:531-536
- Ryan PR, Ditomaso JM and Kochian LV (1993) Aluminum toxicity in roots - an investigation of spatial sensitivity and the role of the root cap. *Journal of Experimental Botany* **44**:437-446
- Ryan PR, Kinraide TB and Kochian LV (1994) Al^{3+} - Ca^{2+} interactions in aluminum rhizotoxicity .1. Inhibition of root-growth is not caused by reduction of calcium-uptake. *Planta* **192**:98-103
- Ryan PR and Kochian LV (1993) Interaction between aluminum toxicity and calcium-uptake at the root apex in near-isogenic lines of wheat (triticum-aestivum l) differing in aluminum tolerance. *Plant Physiology* **102**:975-982
- Ryan PR, Newman IA and Shields B (1990) Ion fluxes in corn roots measured by microelectrodes with ion-specific liquid membranes. *Journal of Membrane Science* **53**:59-69
- Ryan PR, Reid RJ and Smith FA (1997a) Direct evaluation of the Ca^{2+} -displacement hypothesis for Al toxicity. *Plant Physiology* **113**:1351-1357

References

- Ryan PR, Shaff JE and Kochian LV (1992) Aluminum toxicity in roots - correlation among ionic currents, ion fluxes, and root elongation in aluminum-sensitive and aluminum-tolerant wheat cultivars. *Plant Physiology* **99**:1193-1200
- Ryan PR, Skerrett M, Findlay GP, Delhaize E and Tyerman SD (1997b) Aluminum activates an anion channel in the apical cells of wheat roots. *Proceedings of the National Academy of Sciences of the United States of America* **94**:6547-6552
- Ryder M, Gerard F, Evans DE and Hodson MJ (2003) The use of root growth and modelling data to investigate amelioration of aluminium toxicity by silicon in picea abies seedlings. *Journal of Inorganic Biochemistry* **97**:52-58
- Samuels TD, Kucukakyuz K and Rincon-Zachary M (1997) Al partitioning patterns and root growth as related to Al sensitivity and Al tolerance in wheat *Plant Physiol.* **113**:527-534
- Sanders D (1980) The mechanism of Cl^- transport at the plasma membrane of *chara corallina*. *Journal of Membrane Biology* **53**:129-142
- Sanders D, Pelloux J, Brownlee C and Harper JF (2002) Calcium at the crossroads of signaling. *Plant Cell* **14**:S401-417
- Santa-Maria GE, Danna CH and Czibener C (2000) High-affinity potassium transport in barley roots. Ammonium -sensitive and -insensitive pathways. *Plant Physiology* **123**:297-306
- Sasaki M, Kasai M, Yamamoto Y and Matsumoto H (1995) Involvement of plasma-membrane potential in the tolerance mechanism of plant-roots to aluminum toxicity. *Plant and Soil* **171**:119-124

References

- Sasaki T, Yamamoto Y, Ezaki B, Katsuhara M, Ahn SJ, Ryan PR, Delhaize E and Matsumoto H (2004) A wheat gene encoding an aluminum-activated malate transporter. *Plant J* **37**:645-653
- Sasaki T, Yamamoto Y, Ezaki B, Katsuhara M, Ryan PR, Delhaize E and Matsumoto H (2003) A gene encoding an aluminum-activated malate transporter segregates with aluminum tolerance in wheat. *Plant and Cell Physiology* **44**:S84-S84
- Sathyanarayanan PV and Poovaiah BW (2004) Decoding Ca^{2+} signals in plants. *Critical Reviews in Plant Sciences* **23**:1-11
- Scanlon CH, Martinec J, Machackova I, Rolph CE and Lumsden PJ (1996) Identification and preliminary characterization of a Ca^{2+} -dependent high-affinity binding site for inositol-1,4,5-trisphosphate from chenopodium rubrum. *Plant Physiology* **110**:867-874
- Schachtman DP, Tyerman SD and Terry BR (1991) The K^+/Na^+ selectivity of a cation channel in the plasma-membrane of root-cells does not differ in salt-tolerant and salt-sensitive wheat species. *Plant Physiology* **97**:598-605
- Scholz-Starke J, Gambale F and Carpaneto A (2005) Modulation of plant ion channels by oxidizing and reducing agents. *Archives of Biochemistry and Biophysics* **434**:43-50
- Schulzlessdorf B and Hedrich R (1995) Protons and calcium modulate sv-type channels in the vacuolar-lysosomal compartment - channel interaction with calmodulin inhibitors. *Planta* **197**:655-671

References

- Schulz-Lessdorf B and Hedrich R (1995) Protons and calcium modulate sv-type channels in the vacuolar-lysosomal compartment - channel interaction with calmodulin inhibitors. *Planta* **197**:655-671
- Schuurkes J (1986) Atmospheric ammonium-sulfate deposition and its role in the acidification and nitrogen enrichment of poorly buffered aquatic systems. *Experientia* **42**:351-357
- Scott BIH (1962) Electricity in plants. *Scientific America* **136**:3-11
- Shabala S (2000) Ionic and osmotic components of salt stress specifically modulate net ion fluxes from bean leaf mesophyll. *Plant Cell and Environment* **23**:825-837
- Shabala S (2003) Physiological implications of ultradian oscillations in plant roots. *Plant and Soil* **255**:217-226
- Shabala S and Knowles A (2002) Rhythmic patterns of nutrient acquisition by wheat roots. *Functional Plant Biology* **29**:595-605
- Shabala SN, Newman IA and Morris J (1997) Oscillations in H⁺ and Ca²⁺ ion fluxes around the elongation region of corn roots and effects of external ph. *Plant Physiology* **113**:111-118
- Shen H, Ligaba A, Yamaguchi M, Osawa H, Shibata K, Yan XL and Matsumoto H (2004a) Effect of k-252a and abscisic acid on the efflux of citrate from soybean roots. *Journal of Experimental Botany* **55**:663-671
- Shen J, Tang C, Rengel Z and Zhang F (2004b) Root-induced acidification and excess cation uptake by n-2-fixing lupinus albus grown in phosphorus-deficient soil. *Plant and Soil* **260**:69-77

References

- Shen RF, Ma JF, Kyo M and Iwashita T (2002) Compartmentation of aluminium in leaves of an Al-accumulator, *fagopyrum esculentum* moench. *Planta* **215**:394-398
- Silva IR, Smyth TJ, Israel DW, Raper CD and Rufty TW (2001) Magnesium ameliorates aluminum rhizotoxicity in soybean by increasing citric acid production and exudation by roots. *Plant and Cell Physiology* **42**:546-554
- Simonovicova M, Huttova J, Mistrik I, Siroka B and Tamas L (2004a) Peroxidase mediated hydrogen peroxide production in barley roots grown under stress conditions. *Plant Growth Regulation* **44**:267-275
- Simonovicova M, Huttova J, Mistrik I, Siroka B and Tamas L (2004b) Root growth inhibition by aluminum is probably caused by cell death due to peroxidase-mediated hydrogen peroxide production. *Protoplasma* **224**:91-98
- Sivaguru M, Baluska F, Volkmann D, Felle HH and Horst WJ (1999) Impacts of aluminum on the cytoskeleton of the maize root apex. Short-term effects on the distal part of the transition zone. *Plant Physiology* **119**:1073-1082
- Sivaguru M, Ezaki B, He ZH, Tong HY, Osawa H, Baluska F, Volkmann D and Matsumoto H (2003a) Aluminum-induced gene expression and protein localization of a cell wall-associated receptor kinase in *Arabidopsis*. *Plant Physiology* **132**:2256-2266
- Sivaguru M, Pike S, Gassmann W and Baskin TI (2003b) Aluminum rapidly depolymerizes cortical microtubules and depolarizes the plasma membrane: Evidence that these responses are mediated by a glutamate receptor. *Plant and Cell Physiology* **44**:667-675

References

- Suwalsky M, Norris B, Kiss T and Zatta P (2002) Effects of Al(III) speciation on cell membranes and molecular models. *Coordination Chemistry Reviews* **228**:285-295
- Tabuchi A and Matsumoto H (2001) Changes in cell-wall properties of wheat (*Triticum aestivum*) roots during aluminum-induced growth inhibition. *Physiologia Plantarum* **112**:353-358
- Takabatake R and Shimmen T (1997) Inhibition of electrogenesis by aluminum in characean cells. *Plant and Cell Physiology* **38**:1264-1271
- Takita E, Koyama H and Hara T (1999) Organic acid metabolism in aluminum-phosphate utilizing cells of carrot (*Daucus carota* L.). *Plant and Cell Physiology* **40**:489-495
- Tamas L, Budikova S, Huttova J, Mistrik I, Simonovicova M and Siroka B (2005) Aluminum-induced cell death of barley-root border cells is correlated with peroxidase- and oxalate oxidase-mediated hydrogen peroxide production. *Plant Cell Reports* **24**:189-194
- Tamas L, Huttova J and Mistrik I (2003) Inhibition of Al-induced root elongation and enhancement of Al-induced peroxidase activity in Al-sensitive and Al-resistant barley cultivars are positively correlated. *Plant and Soil* **250**:193-200
- Tamas L, Simonovicova M, Huttova J and Mistrik I (2004) Aluminium stimulated hydrogen peroxide production of germinating barley seeds. *Environmental and Experimental Botany* **51**:281-288

References

- Tang C, Raphael C, Rengel Z and Bowden JW (2000) Understanding subsoil acidification: Effect of nitrogen transformation and nitrate leaching. *Australian Journal of Soil Research* **38**:837-849
- Tang Y, Garvin DF, Kochian LV, Sorrells ME and Carver BF (2002) Physiological genetics of aluminum tolerance in the wheat cultivar atlas 66. *Crop Science* **42**:1541-1546
- Taylor CW and Laude AJ (2002) IP₃ receptors and their regulation by calmodulin and cytosolic Ca²⁺. *Cell Calcium* **32**:321-334
- Taylor GJ, McDonald-Stephens JL, Hunter DB, Bertsch PM, Elmore D, Rengel Z and Reid RJ (2000) Direct measurement of aluminum uptake and distribution in single cells of *Chara corallina*. *Plant Physiology* **123**:987-996
- Vázquez MD (2002) Aluminum exclusion mechanism in root tips of maize (*Zea mays* L.): Lysigeny of aluminum hyperaccumulator cells. *Plant Biology* **4**:234-249
- Vázquez MD, Poschenrieder C, Corrales I and Barceló J (1999) Change in apoplastic aluminum during the initial growth response to aluminum by roots of a tolerant maize variety. *Plant Physiology* **119**:435-444
- Vermassen E, Parys JB and Mauger JP (2004) Subcellular distribution of the inositol 1,4,5-trisphosphate receptors: Functional relevance and molecular determinants. *Biology of the Cell* **96**:3-17
- Very AA and Sentenac H (2003) Molecular mechanisms and regulation of K⁺ transport in higher plants. *Annual Review of Plant Biology* **54**:575-603

References

- Vitorello VA and Haug A (1996) Short-term aluminium uptake by tobacco cells: Growth dependence and evidence for internalization in a discrete peripheral region. *Physiologia Plantarum* **97**:536-544
- von Uexkull HR and Mutert E (1995) Global extent, development and economic-impact of acid soils. *Plant and Soil* **171**:1-15
- Voundi Nkana JC, Tack FMG and Verloo MG (1998) Paper pulp as an amendment to a tropical acid soil: Effects on growth of rye grass. *Communications in Soil Science and Plant Analysis* **29**:1329-1340
- Vranova E, Inze D and Van Breusegem V (2002) Signal transduction during oxidative stress. *Journal of Experimental Botany* **53**:1227-1236
- Walker NA, Beilby MJ and Smith FA (1979) Amine uniport at the plasmalemma of charophyte cells. I. Vurrent-voltage curves, saturation kinetics and the effect of unstirred layers. *Journal of Membrane Biology* **49**:21-55
- Ward JM and Schroeder JI (1994) Calcium-activated K^+ channels and calcium-induced calcium-release by slow vacuolar ion channels in guard-cell vacuoles implicated in the control of stomatal closure. *Plant Cell* **6**:669-683
- Watanabe T and Osaki M (2002) Mechanisms of adaptation to high aluminum condition in native plant species growing in acid soils: A review. *Communications in Soil Science and Plant Analysis* **33**:1247-1260
- Wehr JB, Menzies NW and Blamey FPC (2003) Model studies on the role of citrate, malate and pectin esterification on the enzymatic degradation of Al- and ca-pectate

References

gels: Possible implications for Al-tolerance. *Plant Physiology and Biochemistry* **41**:1007-1010

Weisenseel MH, Becker HF and Ehlgötz JG (1992) Growth, gravitropism, and endogenous ion currents of cress roots (*Lepidium-sativum* L.) - measurements using a novel 3-dimensional recording probe. *Plant Physiology* **100**:16-25

Weiser T, Blum W and Bentrup FW (1991) Calmodulin regulates the Ca^{2+} -dependent slow-vacuolar ion channel in the tonoplast of *Chenopodium-rubrum* suspension cells. *Planta* **185**:440-442

Wenzl P, Chaves AL, Patino GM, Mayer JE and Rao IM (2002a) Aluminum stress stimulates the accumulation of organic acids in root apices of *Brachiaria* species. *Journal of Plant Nutrition and Soil Science-Zeitschrift Fur Pflanzenernahrung Und Bodenkunde* **165**:582-588

Wenzl P, Mancilla LI, Mayer JE, Albert R and Rao IM (2003) Simulating infertile acid soils with nutrient solutions: The effects on *Brachiaria* species. *Soil Science Society of America Journal* **67**:1457-1469

Wenzl P, Mayer JE and Rao IM (2002b) Aluminum stress. Inhibits accumulation of phosphorus in root apices of aluminum-sensitive but not aluminum-resistant *Brachiaria* cultivar. *Journal of Plant Nutrition* **25**:1821-1828

Wenzl P, Patino GM, Chaves AL, Mayer JE and Rao IM (2001) The high level of aluminum resistance in signalgrass is not associated with known mechanisms of external aluminum detoxification in root apices. *Plant Physiology* **125**:1473-1484

References

- Wherrett T, Ryan PR, Delhaize E and Shabala S (2005) Effect of aluminium on membrane potential and ion fluxes at the apices of wheat roots. *Functional Plant Biology* **32**:199-208
- Wilkinson S and Davies WJ (2002) ABA-based chemical signalling: The co-ordination of responses to stress in plants. *Plant Cell and Environment* **25**:195-210
- Wong MTF, Akyeampong E, Nortcliff S, Rao MR and R.S. S (1995) Initial responses of maize and beans to decreased concentration of monomeric inorganic aluminium with application of manure or tree prunings to an oxisol in burundi. *Plant and Soil* **171**
- Wu WH and Assmann SM (1995) Is ATP required for K⁺ channel activation in *vicia* guard cells? *Plant physiology* **107**:101-109
- Wymer CL, Bibikova TN and Gilroy S (1997) Cytoplasmic free calcium distributions during the development of root hairs of *Arabidopsis thaliana*. *Plant Journal* **12**:427-439
- Yamaguchi M, Sasaki T, Sivaguru M, Yamamoto Y, Osawa H, Ahn SJ and Matsumoto H (2005) Evidence for the plasma membrane localization of Al-activated malate transporter (ALMT1). *Plant and Cell Physiology* **46**:812-816
- Yamamoto Y, Hachiya A and Matsumoto H (1997) Oxidative damage to membranes by a combination of aluminum and iron in suspension-cultured tobacco cells. *Plant and Cell Physiology* **38**:1333-1339
- Yamamoto Y, Kobayashi Y, Devi SR, Rikiishi S and Matsumoto H (2003) Oxidative stress triggered by aluminum in plant roots. *Plant and Soil* **255**:239-243

References

Yamamoto Y, Kobayashi Y and Matsumoto H (2001) Lipid peroxidation is an early symptom triggered by aluminum, but not the primary cause of elongation inhibition in pea roots. *Plant Physiology* **125**:199-208

Yamamoto Y, Kobayashi Y, Rama Devi S, Rikiishi S and Matsumoto H (2002) Aluminium toxicity is associated with mitochondrial dysfunction and the production of reactive oxygen species in plant cells. *Plant physiology* **128**:65-74

Yang YH, Chen SM, Chen Z, Zhang HY, Shen HG, Hua ZC and Li N (1999) Silicon effects on aluminum toxicity to mungbean seedling growth. *Journal of Plant Nutrition* **22**:693-700

Yang ZM, Nian H, Sivaguru M, Tanakamaru S and Matsumoto H (2001) Characterization of aluminium-induced citrate secretion in aluminium-tolerant soybean (*Glycine max*) plants. *Physiologia Plantarum* **113**:64-71

Yang ZM, Sivaguru M, Horst WJ and Matsumoto H (2000) Aluminium tolerance is achieved by exudation of citric acid from roots of soybean (*Glycine max*). *Physiologia Plantarum* **110**:72-77

Yermiyahu U, Rytwo G, Brauer DK and Kinraide TB (1997) Binding and electrostatic attraction of lanthanum (La^{3+}) and aluminum (Al^{3+}) to wheat root plasma membranes. *Journal of Membrane Biology* **159**:239-252

Zhang WH and Rengel Z (1999) Aluminium induces an increase in cytoplasmic calcium in intact wheat root apical cells. *Australian Journal of Plant Physiology* **26**:401-409

References

- Zhang WH, Ryan PR and Tyerman SD (2001) Malate-permeable channels and cation channels activated by aluminum in the apical cells of wheat roots. *Plant Physiology* **125**:1459-1472
- Zhang XG, Jessop RS and Alter D (2003) Organic acid exudation associated with aluminium stress tolerance in triticale and wheat. *Australian Journal of Agricultural Research* **54**:979-985
- Zheng SJ, Ma JF and Matsumoto H (1998a) Continuous secretion of organic acids is related to aluminium resistance during relatively long-term exposure to aluminium stress. *Physiologia Plantarum* **103**:209-214
- Zheng SJ, Ma JF and Matsumoto H (1998b) High aluminum resistance in buckwheat - i. Al-induced specific secretion of oxalic acid from root tips. *Plant Physiology* **117**:745-751
- Zheng SJ, Yang JL, He YF, Yu XH, Zhang L, You JF, Shen RF and Matsumoto H (2005) Immobilization of aluminum with phosphorus in roots is associated with high aluminum resistance in buckwheat. *Plant Physiology* **138**:297-303
- Zhu MY, Ahn S and Matsumoto H (2003a) Inhibition of growth and development of root border cells in wheat by Al. *Physiologia Plantarum* **117**:359-367
- Zhu MYY, Pan JW, Wang LL, Gu Q and Huang CY (2003b) Mutation induced enhancement of Al tolerance in barley cell lines. *Plant Science* **164**:17-23
- Zoysa AKN, Loganathan P and Hedley MJ (1998) Effect of forms of nitrogen supply on mobilisation of phosphorus from a phosphate rock and acidification in the rhizosphere of tea. *Australian Journal of Soil Research* **36**:373-387

References

Zsoldos F, Vashegyi A, Bona L and Pecsvaradi A (2003a) Effects of silicon on growth and potassium transport in triticale and rye exposed to aluminium and nitrite stress. *Cereal Research Communications* **31**:379-386

Zsoldos F, Vashegyi A, Pecsvaradi A and Bona L (2003b) Influence of silicon on aluminium toxicity in common and durum wheats. *Agronomie* **23**:349-354

Appendix 1: Solutions for Protoplast isolation

Gradient 3:	500mM Sucrose	34.23g	
	5mM MES	0.196g	
	1mM CaCl ₂ ·2H ₂ O	0.030g	
	KOH	to	pH 6.0
	H ₂ O	to	200mL
			Store in frozen aliquots

Gradient 2:	400mM Sucrose	13.69g	
	100mM Sorbitol		1.820g
	5mM MES	0.098g	
	1mM CaCl ₂ ·2H ₂ O	0.015g	
	KOH	to	pH 6.0
	H ₂ O	to	100mL
			Store in frozen aliquots

Gradient 1:	500mM Sorbitol		91.084g
	5mM MES	0.976g	
	1mM CaCl ₂ ·2H ₂ O	0.147g	
	KOH	to pH	6.0
	H ₂ O	to	1000mL

Use 750mL G1 for prep. of solution A (below). Store remainder in frozen aliquots.

Solution A:			
Gradient 1			750mL
BSA 0.5% (Albumin Bovine)		3.75g	
PVP 0.5% (Polyvinylpyrrolidone)		3.75g	
1.0M HCl	to		pH 5.5

Use 250mL for enzyme solutions below. Store remainder frozen as 5mL aliquots.

Cellulase/Pectolyase Solution:			
Solution A		250mL	
Cellulase (RS) 0.8%	2g		
Pectolyase 0.8%	0.2g		
1.0N HCl	to	pH 5.5	
Slowly add enzyme to stirring solution			

Appendix 2: Correction of intravacuolar ion activities for liquid junction potential and Vm

$=V_m + LJP = 10^{(Em\ correction/slope)} = (correction\ factor) \cdot [Ca^{2+}]$							
	[Ca ²⁺]	slope	Vm	LJP	Em correctio	Correction factor	Real Activity
q1071241	133.86	-34.6	-4.22	1.275	-2.945	1.216509786	162.842
	162.56	-34.6	-4.22	1.275	-2.945	1.216509786	197.7558308
q2231144	130.9868	-21.12	-4.22	1.275	-2.945	1.378609567	180.5796556
q2221512							
	123.91	-24.34	-4.22	1.275	-2.945	1.321278135	163.7195737
q1071430	114.38	-25.92	-4.22	1.275	-2.945	1.299028942	148.5829304
q2231008	179.7358	-24.33	-4.22	1.275	-2.945	1.321429441	237.5081778
	212.6973	-24.33	-4.22	1.275	-2.945	1.321429441	281.0644743
	Ca ²⁺						
Mean	151.1614						196.0075204
SEM	13.39417						17.98784018
	K ⁺	slope	Vm	LJP	Em correctio	Correction factor	Real Activity
q2241138	102400.6	-43	-4.22	1.375	-2.845	1.164562472	119251.913
	102829.3	-43	-4.22	1.375	-2.845	1.164562472	119751.1951
q2231543	98696.12	-50.68	-4.22	1.375	-2.845	1.137985014	112314.7027
	98872.22	-50.68	-4.22	1.375	-2.845	1.137985014	112515.1094
	100977.4	-50.68	-4.22	1.375	-2.845	1.137985014	114910.7799
	101251	-50.68	-4.22	1.375	-2.845	1.137985014	115222.1426
q3011101	104277.5	-46.3	-4.22	1.375	-2.845	1.15198569	120126.1801
	102866.8	-46.3	-4.22	1.375	-2.845	1.15198569	118501.0896
	K ⁺						
Mean	101521.4						116574.139
SEM	697.6912						1140.233921
	Mg ²⁺	slope	Vm	LJP	Em correctio	Correction factor	Real Activity
q3021203	11369.01	-23.53	-4.22	6.6	2.38	0.79223227	9006.892642
	14165	-23.53	-4.22	6.6	2.38	0.79223227	11221.97011
	9282.37	-23.53	-4.22	6.6	2.38	0.79223227	7353.793058
q30111715	6516.29	-23.53	-4.22	6.6	2.38	0.79223227	5162.41522
	10546.9	-23.53	-4.22	6.6	2.38	0.79223227	8355.594531
	10573.87	-23.53	-4.22	6.6	2.38	0.79223227	8376.961035
	10445.03	-23.53	-4.22	6.6	2.38	0.79223227	8274.88983
	Mg ²⁺						
Mean	10414.07						8250.359489
SEM	866.011						686.0818249

The above values are calculations from a spread sheet to account for the membrane potential and liquid junction potential (LJP) for each vacuole. From the left the columns show, file name, intravacuolar activity calculated by MIFE (μM), Nernst slope of the electrode, membrane potential (Vm), LJP, voltage (Em) correction, correction factor and finally the real activity. The voltage correction was calculated by addition of Vm and LJP. The correction factor was calculated from the Nernst equation.

Correction Factor = 10^(Em cor/slope)

Appendix 3: Calculations to correct for individual vacuole size

dia (div)	r (μm)	Δx (actual)	Δx (calc)	Correction factor Δx(calc)/Δx(actual)
12	29.82	11.52136364	9.733870968	0.844854071
13.5	33.5475	12.75221739	9.733870968	0.763308111
12	29.82	11.52136364	9.733870968	0.844854071
9.5	23.6075	9.259529447	9.733870968	1.051227389
12	29.82	11.52136364	9.733870968	0.844854071
10.5	26.0925	10.19706897	9.733870968	0.954575379

dia (div) is the diameter measured on the microscope micrometer (1 dia = 4.97 μm)

The above values are calculations from a spread sheet, based on the Nernst equation below, and are designed to calculate a correction factor to multiply the fluxes calculated by Mflux from the generic radius entered (9.94 μm). Δx was calculated for generic radius, Δx(calc), and for the real vacuolar radius, Δx(actual). The correction factor for fluxes was given by Δx(calc)/ Δx(actual).

Nernst equation: $J = c u z F g (\Delta V/\Delta x)$

Where J is the ion flux (mol m² s⁻¹); c is ion concentration (mol m⁻³); u is the ion mobility (m s⁻¹ per Newton mol⁻¹); z is the ion's valence; F is the Faraday number (96500 C mol⁻¹); g is a factor found from the measured Nernst slope for the electrode during calibration; dV is the voltage difference measured by the electrometer between the two positions (V); Δx is the distance between two positions (m).

For spherical geometry (e.g. vacuoles and protoplasts) Δx is replaced with:

$$\Delta x = r \ln[(r+x+\Delta x)/(r+x)].$$